



Some pages of this thesis may have been removed for copyright restrictions.

If you have discovered material in AURA which is unlawful e.g. breaches copyright, (either yours or that of a third party) or any other law, including but not limited to those relating to patent, trademark, confidentiality, data protection, obscenity, defamation, libel, then please read our [Takedown Policy](#) and [contact the service](#) immediately

TITLE PAGE

Gold Mineralisation in the Caledonides of the British Isles with Special Reference to the
Dolgellau Gold-belt, North Wales and the Southern Uplands, Scotland.

VOL. 2

JONATHAN NADEN

Doctor of Philosophy

THE UNIVERSITY OF ASTON IN BIRMINGHAM

APRIL 1988

This copy of the Thesis has been supplied on the condition that anyone who consults it is understood to recognise that its copyright rests with its author and that no quotation from this thesis and no information derived from it may be published without the author's prior, written consent.

TABLE OF CONTENTS FOR
VOLUME 2

FIGURES AND TABLES FOR CHAPTER 2:

THE OCCURRENCE OF GOLD ASSOCIATED WITH THE CALEDONIDES OF THE BRITISH ISLES 15

Figure 2.1. Geographical distribution of gold occurrences in England, Wales and Southern Scotland.	16
Figure 2.2. Geographical distribution of gold occurrences in Northern Scotland.	17
Figure 2.3. Geographical distribution of gold occurrences in Ireland.	18
Figure 2.4. Geographical distribution of gold mines in the Dolgellau Gold-belt.....	19
Table 2.1. Table summarising the geological and mineralogical details of gold mineralisation in the Dolgellau Gold-belt.	20
Figure 2.5. General geology surrounding Ogofau Mine, Dyfed, South Wales.	
Figure 2.6. General geology associated with the Helmsdale placer gold deposit with approximate localities of recorded gold occurrences.	23
Table 2.2. Minor occurrences of gold in Scotland.	24
Figure 2.7. General geology associated with the Gold Mines River placer gold deposit with approximate localities of recorded gold occurrences.	25

FIGURES FOR CHAPTER 3:

THE GENERAL GEOLOGY OF THE HARLECH DOME 26

Figure 3.1. Stratigraphy of the Harlech Dome.	27
Figure 3.2. General geology of the Harlech Dome.	28
Figure 3.3. Outcrop of the Rhobell Fawr Volcanic Group and the western margin of the Aran Volacanic Group.....	29
Figure 3.4. Titanium versus zirconium scattergram for the intrusive rocks of the Harlech Dome.	30
Figure 3.5. General geochemistry of the intrusive rocks.	31
Figure 3.6. Main structural features of the Harlech Dome.	32
Figure 3.7. Rose diagram showing the spatial relationship between the minor faults, quartz veins and dykes in the Harlech Dome.....	33
Figure 3.8. Geology surrounding the Coed-y-Brenin porphyry copper deposit	34

Figure 3.9. Geology surrounding the Glasdir copper body.....	35
FIGURES, PLATES AND TABLES FOR CHAPTER 4:	
THE GEOLOGY, MINERALOGY AND MINERAL CHEMISTRY OF CLOGAU MINE.....	36
Figure 4.1. Geology surrounding Clogau Mine.	37
Figure 4.2. Sample location map, and general geology of No. 4 Level, Clogau Mine.....	38
Figure 4.3. Schematic map of the geology of the ore shoot on No. 4 Level, Clogau Mine.....	39
Plate 4.1. Bismuth tellurides and carbonate infilling fractures in quartz.....	40
Plate 4.2. Sericite laths included in galena.....	40
Plate 4.3. Thin veinlet of graphite in quartz with associated arsenopyrite locally altering to limonite, and gold.....	41
Plate 4.4. Small rutile grains in shale inclusion	41
Plate 4.5. Galena replacing cobaltite and pyrrhotine.....	42
Plate 4.6. Crossed nicols view of plate 4.5 showing the presence of arsenopyrite and bismuthinite	42
Plate 4.7. Euhedral cubes and rhombs of cobaltite locally cemented by chalcopyrite.....	43
Plate 4.8. Thin chalcopyrite vein in a micro-fracture in quartz.	43
Plate 4.9. Pyrrhotine and chalcopyrite intergrown exhibiting mutual grain boundaries.....	44
Plate 4.10. Porous zoned pyrite replacing pyrrhotine.....	44
Plate 4.11. Triple point grain boundaries in tellurbismuth.....	45
Plate 4.12. Careous grain boundaries within tellurbismuth.....	45
Plate 4.13. Small galena inclusions forming along cleavage in tellurbismuth.....	46
Plate 4.14. Myrmekitic intergrowth of galena and tellurbismuth	46
Plate 4.15. Galena rim on tetradyomite.....	47
Plate 4.16. Careous boundary between tellurbismuth and tetradyomite	47

Plate 4.17. Fingerprint intergrowth at the margin between tetradyomite and quartz.....	48
Plate 4.18. Discrete galena grains in tellurbismuth.	48
Plate 4.19. Galena replacing tellurbismuth along cleavage	49
Plate 4.20. Small isolated grain of altaite in tellurbismuth.....	49
Plate 4.21. Altaite grain with small inclusion of native gold in tellurbismuth.	50
Plate 4.22. Galena and altaite replacing tellurbismuth along cleavage.....	50
Plate 4.23a. Galena and hessite in tellurbismuth.....	51
Plate 4.23b. Crossed polars view of figure 4.23a.....	51
Plate 4.24. Line of small hessite inclusions forming along a dissolution surface on tellurbismuth.....	52
Plate 4.25. Small isolated grain of native gold in tellurbismuth.....	52
Plate 4.26. Galena replacing pyrrhotine along grain boundaries.....	53
Plate 4.27. Cluster of ragged tetradyomite laths and wehrlite in galena	53
Plate 4.28 Skeletal wehrlite, native bismuth and bismuthinite replacing galena.	54
Plate 4.29. Skeletal wehrlite replacing galena along cleavage	54
Plate 4.30. Small hessite grain in galena associated with cleavage.	55
Plate 4.31. Native gold and ?Hedleyite in galena.....	55
Plate 4.32. Native bismuth forming along cleavage in galena.....	56
Plate 4.33. Bismuthinite in galena.....	56
Plate 4.34. Veinlets of native gold in quartz.....	57
Plate 4.35. Gold cementing and replacing pyrite in quartz	57
Plate 4.36. Veinlet of native gold in galena.....	58
Plate 4.37. Stiboiluzonite inclusions in galena.....	58
Plate 4.38. Tetrahedrite in a vug in quartz.	59
Plate 4.39. Pyrrhotine altering to pyrite and marcasite.	59
Plate 4.40. Covellite replacing galena	60
Plate 4.41. Arsenopyrite altering to limonite.	60

Table 4.3 Analytical details of electron probe micro-analyses.....	61
Figure 4.4. Line concentration profile across a cobaltite grain showing the variations in major element chemistry.....	63
Figure 4.5. Line concentration profile across a cobaltite grain showing the variations in minor element chemistry.....	63
Table 4.5. Summary Statistics of the major and minor element chemistry of tellurbismuth.....	64
Figure 4.6a. Histogram of the distribution of lead in tellurbismuth.....	65
Figure 4.6b. Histogram of the distribution of bismuth in tellurbismuth.....	65
Figure 4.6c. Histogram of the distribution of sulphur in tellurbismuth.....	66
Figure 4.6d. Histogram of the distribution of tellurium in tellurbismuth.....	66
Figure 4.6e. Histogram of the distribution of antimony in tellurbismuth.....	67
Figure 4.6f. Histogram of the distribution of cadmium in tellurbismuth.....	67
Figure 4.6g. Histogram of the distribution of silver in tellurbismuth.....	68
Table 4.6. Correlation matrix for the major and minor elements in tellurbismuth.....	69
Table 4.7. Summary statistics of the major and minor element chemical data for Tetradyomite.....	69
Figure 4.7. X-Y plot showing the variation of the molar ratios of Bi, Te, S, Sb and Cd in tetradyomite.....	70
Figure 4.8. X-Y plots of the molar ratios $(\text{Bi}+\text{Pb})/(\text{Te}+\text{Cd}+\text{Sb})$ and $\text{S}/(\text{Te}+\text{Cd}+\text{Sb})$ versus Total wt%.....	70
Table 4.8. Correlation matrix for the major and minor elements in tetradyomite.....	71
Figure 4.9a. Histogram showing the distribution of lead in tetradyomite.....	72
Figure 4.9b. Histogram showing the distribution of bismuth in tetradyomite.....	72
Figure 4.9c. Histogram showing the distribution of sulphur in tetradyomite.....	73
Figure 4.9d. Histogram showing the distribution of tellurium in tetradyomite.....	73
Figure 4.9e. Histogram showing the distribution of antimony in tetradyomite.....	74
Figure 4.9f. Histogram showing the distribution of cadmium in tetradyomite.....	74
Figure 4.9g. Histogram showing the distribution of silver in tetradyomite.....	75

Table 4.9. Summary statistics for the major and minor elements in galena	76
Figure 4.10a. Line concentration profile across a tetradyomite-galena-tellurbismuth intergrowth, showing the variation in antimony concentration between different minerals.....	77
Figure 4.10b. Line concentration profile across a galena-tellurbismuth intergrowth, showing the variation in antimony concentration between the two minerals.....	77
Figure 4.11. Histogram of the distribution of tellurium in galena from the tellurbismuth-dominated assemblage.....	78
Figure 4.12. Histogram of the distribution of bismuth in galena from the tellurbismuth-dominated assemblage.....	78
Table 4.10. Correlation matrix for major and minor element chemistry in galena from the tellurbismuth-dominated telluride assemblage.....	79
Table 4.11. Summary statistics for the major and minor element concentrations in the fingerprint intergrowths.	79
Figure 4.13. Box plots showing the statistical variation of antimony between tellurbismuth, tetradyomite, galena and the fingerprint intergrowths.....	80
Figure 4.14. Box plots showing the statistical variation of cadmium between tellurbismuth, tetradyomite, galena and the fingerprint intergrowths.....	80
Figure 4.15. Box plots showing the statistical variation of silver between tellurbismuth, tetradyomite, galena and the fingerprint intergrowths.....	81
Table 4.12. Summary statistics for the major and minor element concentrations in galena from the sulphide-dominated telluride assemblage.....	82
Figure 4.16. Histograms comparing the distribution of tellurium in galena between the two telluride assemblages.....	83
Figure 4.17. Histograms comparing the distribution of silver in galena between the two telluride assemblages.....	84
Figure 4.18. Histograms comparing the distribution of cadmium in galena between the two telluride assemblages.....	85
Figure 4.19. Histograms comparing the distribution of bismuth in galena between the two telluride assemblages.....	86
Table 4.13. Correlation matrix for the major and minor elements in galena from the sulphide-dominated telluride assemblage.....	87

Table 4.14a. Analyses of the minor tellurides, bismuthinite, and native bismuth from No. 4 Level.....	88
Table 4.14b. Analyses of the sulphosalts in BM kingsbury (K2).....	89
Figure 4.20. Histogram of the fineness of gold from No. 4 Level.....	90
Figure 4.21. Histogram of the fineness of placer gold from the Hirgwm river.....	90
Table 4.15. Summary statistics of fineness of native gold from No. 4 Level Clogau Mine, placer gold from the Hirgwm river, and the gold-bearing samples from the British Museum (Natural History) and the National Museum of Wales.....	91
Table 4.16. Fineness of gold in gold-bearing samples loaned from the British Museum (Natural History) and the National Museum of Wales.	91
Figure 4.22. Line concentration profiles across a tellurbismuth-galena intergrowth showing the variation in major "cation" (Bi, Pb), "anion" (Te, S) and minor element (Sb, Cd) chemistries.....	92
Figure 4.23. Line concentration profile across a tellurbismuth-galena-tetradymite intergrowth showing the variation in major "cation" (Bi, Pb), "anion" (Te, S) and minor element (Sb, Cd) chemistries.....	93
Figure 4.24. Line concentration profiles illustrating the variation in major "cation" (Bi, Pb) and "anion" (Te, S) chemistries.....	94
FIGURES AND TABLES FOR CHAPTER 5:	
CONDITIONS OF ORE FORMATION AT CLOGAU MINE.....	95
Table 5.1. Comparison of Gibbs Free energy between data calculated in this thesis and that by Barton and Skinner (1979).....	96
Table 5.2. Sulphidation and telluridation reactions investigated.	97
Figure 5.1.a Activity of tellurium plot for the telluridation of various compositions of electrum.....	98
Figure 5.1b. Activity of tellurium-activity sulphur plot showing the method of calculation of tellurium activity in equilibrium with hessite and electrum.....	99
Figure 5.2. Temperature-activity grid for the telluridation reactions.....	100
Figure 5.3. Temperature-activity grid for the sulphidation reactions	101
Figure 5.4. Mineral stability fields at 350°C and 1 atmosphere.	102
Figure 5.5. Mineral stability fields at 300°C and 1 atmosphere.	103

Figure 5.6. Mineral stability fields at 250°C and 1 atmosphere.....	104
Figure 5.7. Mineral stability fields at 200°C and 1 atmosphere.....	105
Figure 5.8. Diagrammatic illustration of the stability ranges of the observed phases at Clogau Mine.....	106
Table 5.3. Comparison of theoretically stable and unstable assemblages with actually observed assemblages.....	107

FIGURES FOR CHAPTER 7:

THE GEOLOGY AND MINERALISATION OF THE SOUTHERN UPLANDS.....

Figure 7.1. Fault bounded tracts and greywacke formations of the Southern Uplands.....	109
Figure 7.2. Geology of the Leadhills-Wanlockhead mining district.....	110
Figure 7.3. Distribution of arsenic-antimony mineralisation in the Southern Uplands.....	111
Figure 7.4. Geology surrounding the Black Stockarton Moor sub-volcanic complex.....	112
Figure 7.5. Geology of the Cu-Fe-As-Mo mineralisation at Caingarroch Bay.....	113
Figure 7.6. Geology of the Fe-Co-Ni mineralisation at Talnوتر.....	114
Figure 7.7. Geology of the gold mineralisation at the Fore Burn Igneous Complex.....	115
Figure 7.8. Geology of the gold mineralisation at the margin of the Loch Doon granitoid Complex.....	116
Figure 7.9. Relationship between structure intrusives and mineralisation.....	117

FIGURES, PLATES AND TABLES FOR CHAPTER 8:

MORPHOLOGICAL, PETROLOGICAL AND COMPOSITIONAL OF THE SOUTHERN UPLANDS PLACER GOLD; METHODOLOGY.....

Table 8.1. List of morphological characteristics of the Southern Uplands placer gold.....	119
--	-----

Plates 8.1a to 8.1d SEM electronmicrographs of placer gold collected from the Hirgwm river, Bontddu, North Wales, 1km downstream form Clogau mine. These grains are used to illustrate the morphological characteristic of a glazed surface.....	120
Plates 8.1e to 8.1h SEM electronmicrographs of placer gold collected from the River Mawddach by T.A. Readwin	121
Plates 8.2a to 8.2d SEM electronmicrographs showing the morphological features of lode gold dissolved from quartz using hydrofluoric acid.....	122
Plates 8.3a to 8.3d SEM electronmicrographs of placer gold grains from the Southern Uplands which illustrate the macro-morphological feature of grains that preserve most of their original crystalline features.....	123
Plates 8.4a to 8.4d SEM electronmicrographs of placer gold grains from the Southern Uplands that are used to illustrate the macro morphological feature of deformed crystalline texture.....	124
Plates 8.5a to 8.5d SEM electronmicrographs of placer gold grains from the Southern Uplands that are used to illustrate the macro-morphological feature of irregularly shaped gold grains.....	125
Plates 8.6a to 8.6d SEM electronmicrographs of placer gold from the Southern Uplands that illustrates the macro-morphological feature subrounded and folded placer goldgrains.	126
Plates 8.7a to 8.7d SEM electronmicrographs of placer gold from the Southern Uplands that are used to illustrate the macro-morphological feature of placer gold grains with a generally elongate shape.	127
Plates 8.8a to 8.8d SEM electronmicrographs of placer gold grains from the Southern Uplands which illustrate the macro-morphological feature of placer gold that is "nugget"-shaped.	128
Plates 8.9a to 8.9d SEM electronmicrographs of placer gold from the Southern Uplands that illustrate placer gold that exhibits the macro-morphological feature of flake-shaped grains.....	129
Plates 8.10a to 8.10d SEM electronmicrographs of placer gold grains from the Southern Uplands that are used to illustrate the micro-morphological feature of a smooth unworn surface at high magnification.	130
Plates 8.11a to 8.11c SEM electronmicrographs of placer gold from the Southern Uplands that illustrate the micro-morphological feature of original inclusions.....	131

Plates 8.12a to 8.12b SEM electronmicrographs of placer gold grains from the Southern Uplands that illustrate the micro-morphological feature of an irregular surface at high magnification.....	132
Plates 8.13a to 8.13d SEM electronmicrographs of placer gold grains that show the micro-morphological feature of trapped mineral grains.	133
Plates 8.14a to 8.14d SEM electronmicrographs of placer gold grains from the Southern Uplands that exhibit the micro-morphological feature of a flaky surface at high magnification.....	134
Plates 8.15a to 8.15d SEM electronmicrographs of placer gold grains from the Southern Uplands that exhibit the micro-morphological features of a surface that is generally smooth and worn at high magnification, and has random scratches on it.	135
Plates 8.16a to 8.16d SEM electronmicrographs of placer gold grains from the Southern Uplands that show the micro-morphological feature of the formation of a dough like surface texture at high magnification.....	136
Plates 8.17a to 8.17d SEM electronmicrographs of placer gold grains from the Southern Uplands which exhibit the micro-morphological feature of a porous surface at high magnification.....	137
Table 8.2. Relationship between macro- and micro-morphological characteristics.	138

FIGURES, PLATES AND TABLES FOR CHAPTER 9:

MORPHOLOGICAL, PETROLOGICAL AND COMPOSITIONAL DATA FOR THE SOUTHERN UPLANDS PLACER GOLD.....	139
Figure 9.1. Map showing the geology and the distribution of placer gold in the Loch Doon-Glenkens area.....	140
Figure 9.2. Map showing the geology and the distribution of placer gold in the Abington-Biggar-Moffat area.	141
Figure 9.3. Histogram showing the distribution of macro-morphological characteristics of the Loch Doon-Glenkens placer gold.....	142
Figure 9.4. Histogram showing the distribution of micro-morphological characteristics of the Loch Doon-Glenkens placer gold.....	142
Figure 9.5. Geographical distribution of macro-morphological characteristics for the Loch Doon-Glenkens placer gold.	143

Figure 9.6. Geographical distribution of micro-morphological characteristics for the Loch Doon-Glenkens placer gold.	144
Figure 9.7. Geographical distribution of placer gold preserving original morphological features.....	145
Figure 9.8. Histogram showing the surface fineness distribution (from semi-quantitative energy dispersive analysis) of placer gold from the Loch Doon-Glenkens area.....	146
Figure 9.9. Geographical distribution of the surface fineness of placer gold from the Loch Doon-Glenkens area.	147
Plate 9.1. Backscattered electron image and X-ray (Ag_{La}) map of a silver-rich vein in a heterogeneous placer gold grain (sample no. C35).	148
Plate 9.2. Photomicrograph of a thin incomplete gold enrichment rim on a placer gold grain.....	149
Plate 9.3. Backscattered electron image and X-ray (Bi_{Mo}) map of a native bismuth inclusion in a placer gold grain (sample no. C303).	150
Table 1. Summary statistics of the fineness of the Loch Doon-Glenkens placer gold.....	151
Figure 9.10. Histogram showing the core fineness distribution (from EPMA analysis) of placer gold from the Loch Doon-Glenkens area.....	151
Figure 9.11. Geographical distribution of the core fineness of placer gold from the Loch Doon-Glenkens area.	152
Figure 9.12a. Line concentration profile showing the variation in silver content in placer gold from pan concentrate C18.....	153
Figure 9.12b. Line concentration profile showing the variation in silver content in placer gold from pan concentrate C22.....	153
Figure 9.12c. Line concentration profile showing the variation in silver content in placer gold from pan concentrate C22.....	154
Figure 9.12d. Line concentration profile showing the variation in silver content in placer gold from pan concentrate C35.....	154
Figure 9.12e. Line concentration profile showing the variation in silver content in placer gold from pan concentrate C37.....	155
Figure 9.13. Annealing history limits for the heterogeneous placer gold from the Loch Doon-Glenkens area.....	156

Figure 9.14. Histogram of the distribution of macro-morphological characteristics of the Abington-Biggar-Moffat placer gold.	157
Figure 9.15. Histogram of the distribution of micro-morphological characteristics of the Abington-Biggar-Moffat placer gold.	157
Figure 9.16. Geographical distribution of macro-morphological characteristics for the Abington-Biggar-Moffat placer gold.	158
Figure 9.17. Geographical distribution of micro-morphological characteristics for the Loch Doon-Glenkens placer gold.	159
Figure 9.18. Histogram of the distribution of the surface fineness of the Abington-Biggar-Moffat placer gold.	160
Table 9.2. Summary statistics of the core fineness of the Abington-Biggar-Moffat placer gold.	160
Figure 9.19. Histogram of the distribution of the core fineness of the Abington-Biggar-Moffat placer gold.	161
Figure 9.20. Geographical distribution of the core fineness of the placer gold from the Abington-Biggar-Moffat area.....	162
Figure 9.21. Histogram showing the frequency distribution of the macro-morphological characteristics of placer gold from the Loch Doon-Glenkens and the Abington-Biggar-Moffat areas.....	163
Figure 9.22. Histogram of the morphological characteristics of placer gold with finneness <950.....	163
Figure 9.23. Histogram of the morphological characteristics of placer gold with finneness >950.....	164
APPENDICES.	
Appendix 1a. Calculation of thermochemical data.....	165
Appendix 1b. Thermochemical Data.	174
Appendix 2. Sample preparation techniques of the Southern Uplands placer gold for SEM and EPMA analyses.	189
Appendix 3. Method employed for the calculation of the annealing history limits for heterogeneous placer gold.	192
Appendix 4a. Sample details for the material from Clogau Mine and Dogellau Gold-belt.	196
Appendix 4b. Mineralogical data for chapter 4.	200

Appendix 5. Southern Uplands placer gold data.....	223
--	-----

FIGURES AND TABLES FOR
CHAPTER 2:

**THE OCCURRENCE OF GOLD
MINERALISATION IN THE
CALEDONIDES OF THE BRITISH
ISLES.**

Figure 2.1. Geographical distribution of gold occurrences in England, Wales and Southern Scotland.



Figure 2.2. Geographical distribution of gold occurrences in Northern Scotland (after Gallagher *et al.*, 1971).



Figure 2.3. Geographical distribution of gold occurrences in Ireland (after Jackson, 1979).



Figure 2.4. Geographical distribution of gold mines in the Dolgellau Gold-belt (after Bottrell *et al.*, (1988).



Table 2.1. Table summarising the geological and mineralogical details of gold mineralisation in the Dolgellau Gold-belt (compiled from Andrew, 1910; Archer, 1959; Gilbey, 1969 and Morrison 1975).

MINES	GRID REF.	STRIKE/ DIP	GEOLOGY	MINERALOGY	ASSAYS (PPM)	PRODUCTION FIGURES TONNES (ORE)	Kg (GOLD)	AVERAGE GRADE (PPM)
								(PPM)
Panorama (four veins)	SH629164 320/90 320/90 320/90 330/45 W	All four veins are within the Vgra Flags, and are generally sub-parallel to bedding		Well mineralised with mainly chalcopyrite and pyrrhotine.	—	—	—	—
Cae-Gwlan	330/80 W	Southern end of the vein is in the Pen-Rhos Shales it then crosses the Vgra Flags and enters the Clogau Shales where it terminates against the Lyn-Bodyn Fault.		Poorly mineralised with chalcopyrite ± pyrite	—	—	—	—
Farchynys	320/90	Vein is confined to the Pen-Rhos Shales		Vein contains only quartz	9	—	—	—
Bwlch-Coch - Uchaf	330/-	Vein occurs on the eastern side of the Lynn-Bodyn Fault in Vgra Flags, and is in contact with a 'greenstone' sill		Poorly mineralised with chalcopyrite and minor pyrite	—	—	—	—
Heilo-d-Uchaf	325/80 W	Probably a continuation of 4. It branches and has a 'banded' appearance due to wallrock inclusions		Only patchily mineralised with Chalcoocite and pyrite	Gold by assay	—	—	—
Hendrefardon	SH671201 330/85 W	Confined to the Gammian Flags, runs parallel and cross cuts an intrusion		Poorly mineralised with pyrite	—	—	—	—
West Vgra / Nant-Goch	325/90	The vein runs along the contact between the Vgra Flags and a greenstone intrusion		Abundant Chalcoocite, pyrite, Pyrrhotite ± galena.	15	—	—	—
Vgra	SH663192 210/70 S 280/75 N	Comprises of two intersecting veins 30m apart, connected by ledgers and cross veins		Mainly chalcoocite, pyrite and a trace of gold	15	—	—	—
Clogau / St. David's	SH676201 (Au mine) SH679198 (Cu mine)	There are a number of veins that have been worked in the Clogau St David's mine System All of them are in the Clogau Shales, which have been intruded by greenstone sills		The ore minerals are mainly chalcoocite and pyrrhotine with minor amounts of galena tellurides & gold	East Clogau 27 West Clogau 26	To 1862 1862-1907 254,750	110 224 820	3.2.
Bryn-y-Groes	310 -	Vein is confined to the Vgra Flags, and is associated w/in a greenstone intrusion		Poorly Mineralised with small amounts of chalcoocite and pyrite, and a trace of Gold	—	—	—	—
Brynnifron		Vein is confined to the Vgra Flags, but it is not associated with any greenstone intrusions		Poorly mineralised	—	—	—	—
Gareth Gell	SH688201	Vein is confined to the Vgra Flags		Chalcoocite, pyrite ± sphalerite and Galena	3 - 15	To 1862. 26	0.1	6
Cambrian	SH692195	Vein is confined to the Vgra Flags		Poorly mineralised with galena chalcoocite & Sphalerite Although gold has been found n slate	Sph conc 9183	—	—	—
Prince of Wales (A)	SH701196	The A and B veins are in the Pen Rhos Shales and the C vein is in the Vgra Flags, but at its Eastern extremity it crosses into the Pen Rhos Shales		All the veins are well mineralised with sphalerite, galena ± chalcoocite pyrite & pyrrhotine	A Sph conc 2081 B 12 C Gr conc 245	20 — — 67	1.8 — — 2.5	90 — — 37
Princess Alice (B)								
Moe Sp. (C)	SH704201							

Table 2.1. Continued.

MINES	GRID REF.	STRIKE/ DIP	GEOLOGY	MINERALOGY	ASSAYS (PPM)	PRODUCTION FIGURES TONNES (ORE)	KG (GOLD)	AVERAGE GRADE (PPM)
Cassallgwm / Union	SH709215	300/90	Vein traverses both the Vigras Flags and The Clogau Shales, with greenstone intrusions at intervals along its length	Poorly mineralised with sphalerite, galena and chalcopyrite	—	1893.4	—	—
Cefn Coch	SH717231	315/-	vein outcrops at the Clogau Shales - Gamin Flags boundary. Greenstone sills occur at intervals along its length and form one or both wall	Well mineralised with sphalerite, galena ± chalcopyrite and pyrite	—	1906	62 0.8	1.8 —
Berthlwyd	SH722235		Continuation of the Cefn Coch mine, mainly produced lead and zinc	Well mineralised with pyrite, galena, sphalerite and a trace of gold	Gn & Sp conc 9.2-11.2	—	—	—
Cae-Mawr	SH726225	255/40 S	Confined to the Pen Rhos Shales	Poorly mineralised with chalcopyrite.	1.4-1.7	1891	10	0.03 3
Glasdir	SH742224		Intrusive Breccia pipe, emplaced within the Ffestiniog Flags	Pyrite, marcasite, arsenopyrite, minor sphalerite and chalcopyrite	Cu conc 30	13077 1.2% Cu in ore (Cu conc.)	—	—
Ffridd Goch	SH747244	355/70 E	Confined to the lower part of the Ffestiniog Flags At the southern end associated with a greenstone intrusion	Poorly mineralised with pyrite and chalcopyrite	—	1896-1902 110	—	5 30
Cwmnant Hyll (2 veins)	SH751245	265/- 205/-	Confined to the lower part of the Ffestiniog Flags, associated with a greenstone intrusion	Poorly mineralised with pyrite and chalcopyrite, and trace of gold	—	—	—	—
Dol-y-Frwyngog	SH747256	335/90	Vein confined to Pen Rhos Shales, associated with greenstone Intrusion	Chalcopyrite and pyrite	1.6-2.3 9-14 14	317	4.7	1.6
Cefn Deuddwr	SH735263	345/65 N	Vein confined to Vigras Flags, and associated with several greenstones along its length	Chalcopyrite ± galena	—	6	0.2	40
Tyddyn-Gwriadys	SH735266	305/70 N	Vein is in the Clogau Shales, and cross cuts several greenstones	Argentiferous galena, sphalerite, pyrite arsenopyrite, and a trace of gold.	153.0-163.0 (Ag) 6-16 (Au)	—	0.2	—
Cwm Helsian	SH742282	260/70N	Two sets of veins the eastern vein is in the Vigras Flags and the western is in the Penrhos Shales	Quartz, pyrite, chalcopyrite, sphalerite argeniferous galena and trace of gold	EAST 5-29 picked galena 490	1849-1905 616 pre 1849 304	9.3 3.5	20
Gwynfynydd	SH736282	290 70N	Number of parallel and companion lobes in the Clogau Shales and the Vigras Flags the lobes are terminated against the Trawsfynydd Fault	Galena, sphalerite, pyrite and chalcopyrite Gold is only found at vein shale intersections	WEST 1.44% Ag 8-15 Au	— 51	0.4	8
Castell carn Dochan	SH850307	315	The lode is in Shales ashes and lavas of Ordovician age	Galena, sphalerite, chalcopyrite and pyrite	p/re 1865 35.56 1855-1866 27.31	4.6 11.5	13	4

Figure 2.5. General geology surrounding Ogofau Mine, Dyfed, south Wales (after Steed *et al.*, 1976).



Figure 2.6. General geology associated with the Helmsdale placer gold deposit with approximate localities of recorded gold occurrences (compiled using Geological Survey Map [Sutherland Sheet] and from occurrences cited in MacLaren, 1902).



Table 2.2 Minor occurrences of gold in Scotland (compiled from Lindsay, 1867).

1. Perthshire:
 - Breadlebane - Nugget weighing 60g.
 - Tyndrum - Gold associated with vein quartz.
 - Upper Strathearn - Placer gold occurring in streams draining into the northern and southern ends of Loch Earn.
 - Glenalmond - Placer gold occurring in the Glenquich and other valleys in the Grampians.
2. Forfarshire: Clova district - ?Placer gold.
3. Aberdeenshire: River Dee -
 - Placer gold.
 - Braemar - ?Placer gold.
 - Invercauld - Placer gold.
4. Argyllshire Dunoon - Placer gold

Figure 2.7. General geology associated with the Gold Mines River placer gold deposit with approximate localities of recorded gold occurrences (after Macardle and Warren, 1987).



FIGURES AND TABLES FOR
CHAPTER 3:

**THE GENERAL GEOLOGY OF
THE HARLECH DOME.**

Figure 3.1. Stratigraphy of the Harlech Dome (after Allen and Jackson, 1985).

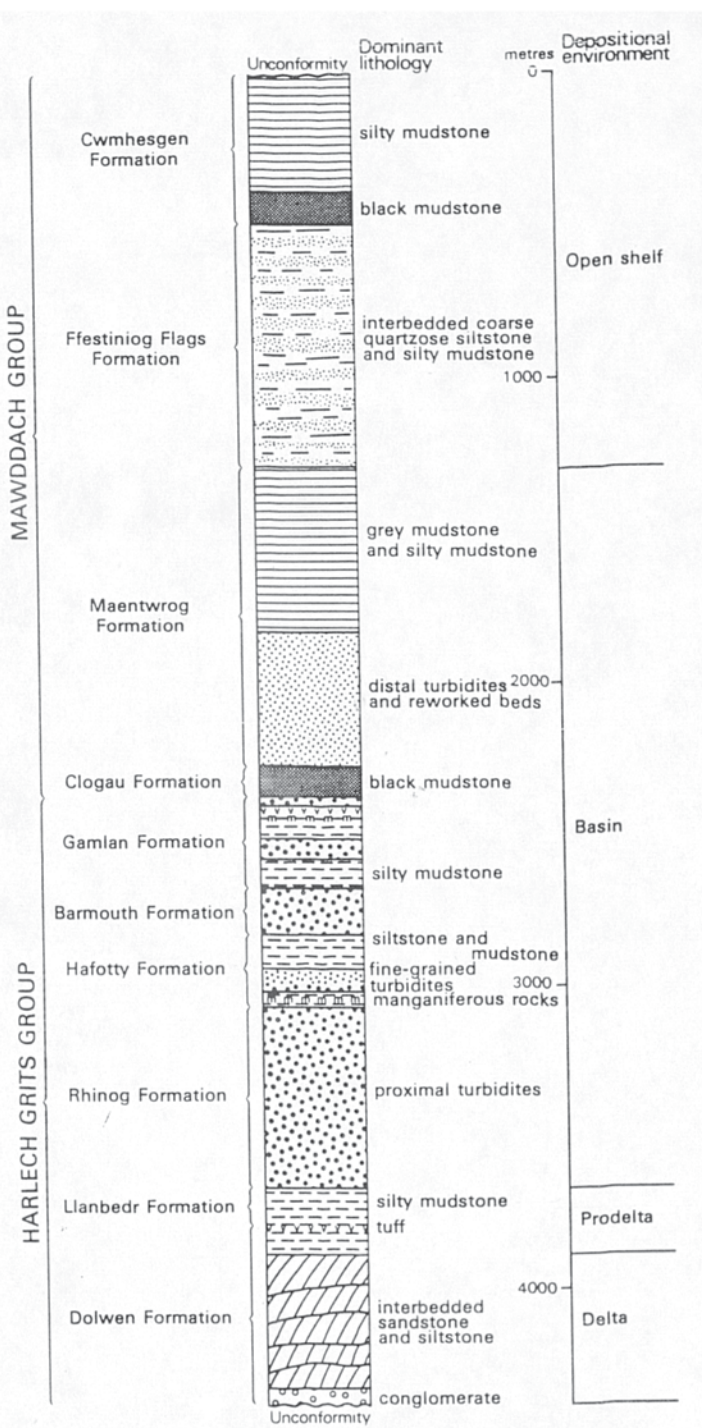


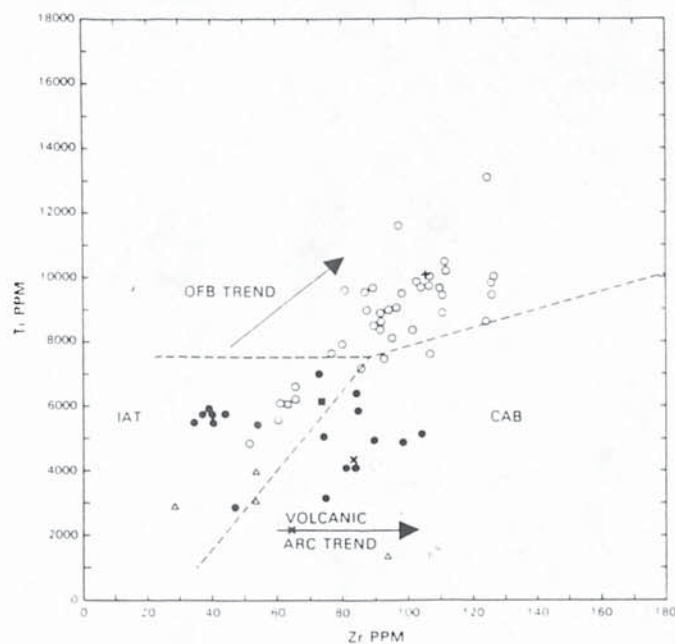
Figure 3.2. General geology of the Harlech Dome (after Allen and Jackson, 1985).



Figure 3.3. Outcrop of the Rhobell Fawr Volcanic Group, and the western margin of the Aran Volacanic Group Stratigraphy of the Harlech Dome (after Allen and Jackson, 1985).



Figure 3.4. Titanium versus zirconium scattergram for the intrusive rocks (after Allen and Jackson, 1985).



- △ Coed y Brenin basic intrusions.
- Ophiitic dolerite intrusions of the SW Arans (Dunkley, 1978).
- Dolerites from the Moel y Llan and Cerniau intrusive complexes Rhobell Fawr (Kokelaar, 1977)
- + Average dolerite intrusion into Ordovician rocks around the Harlech Dome (Allen et al 1976)
- Average albitised dolerite intrusion into Cambrian (Allen et al. 1976)
- Field boundaries and trends for ocean floor basalts (OFB) and volcanic arc basalts - island arc tholeites (IAT) and calc-alkaline basalts (CAB) from Garcia (1978) after Pearce and Cann (1973)
- Dykes Low-Ti dolerite
- ✗ Minor concordant intrusions Low-Ti dolerite

Figure 3.5. General geochemistry of the intrusive rocks of the Harlech Dome (after Allen and Jackson, 1985).

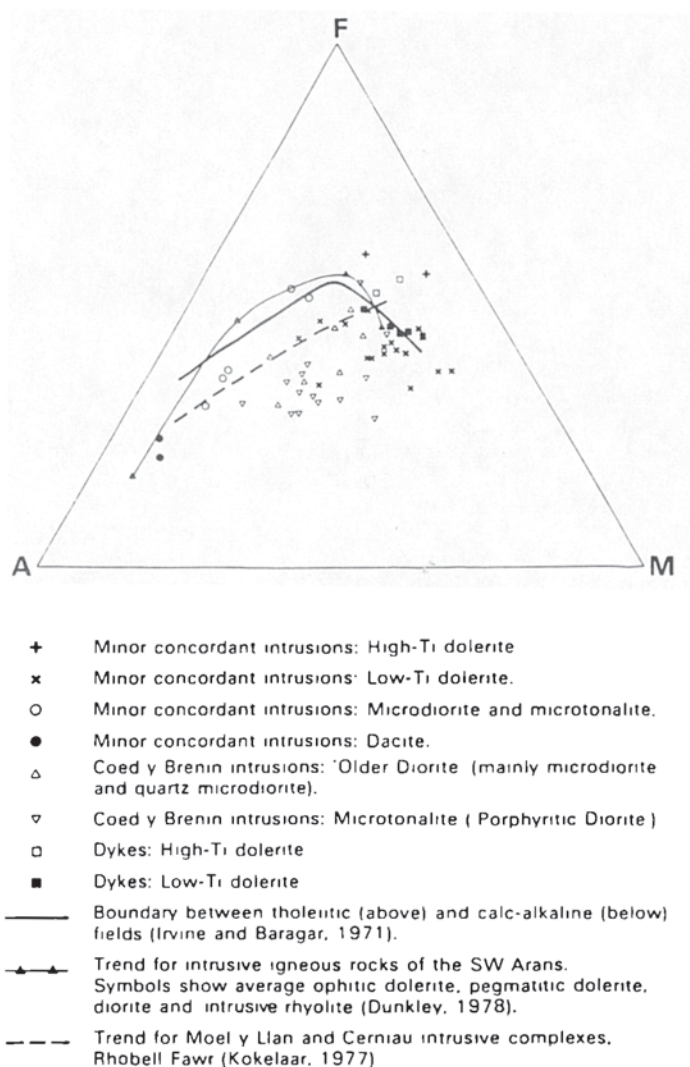


Figure 3.6. Main structural features of the Harlech Dome (after Allen and Jackson, 1985).



Figure 3.7. Rose diagram showing the spatial relationship between the minor faults, quartz veins and dykes in the Harlech Dome Stratigraphy of the Harlech Dome (after Allen and Jackson, 1985).

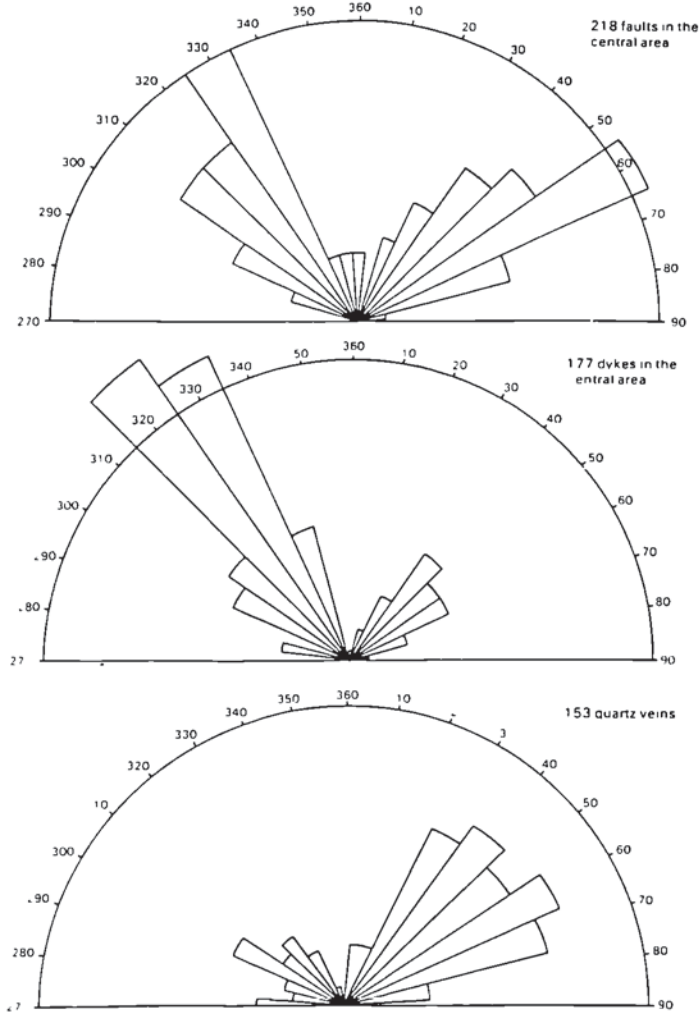


Figure 3.8. Geology surrounding the Coed-y-Brenin porphyry copper deposit (after Allen and Jackson, 1985).



Figure 3.9. Geology surrounding the Glasdir copper body (after Allen and Easterbrook, 1978).



FIGURES, TABLES AND PLATES
FOR CHAPTER 4:

**THE GEOLOGY, MINERALOGY
AND MINERAL CHEMISTRY OF
CLOGAU MINE.**

Figure 4.1. Geology surrounding Clogau Mine (after Allen and Jackson, 1985).



Figure 4.2. Sample location map.

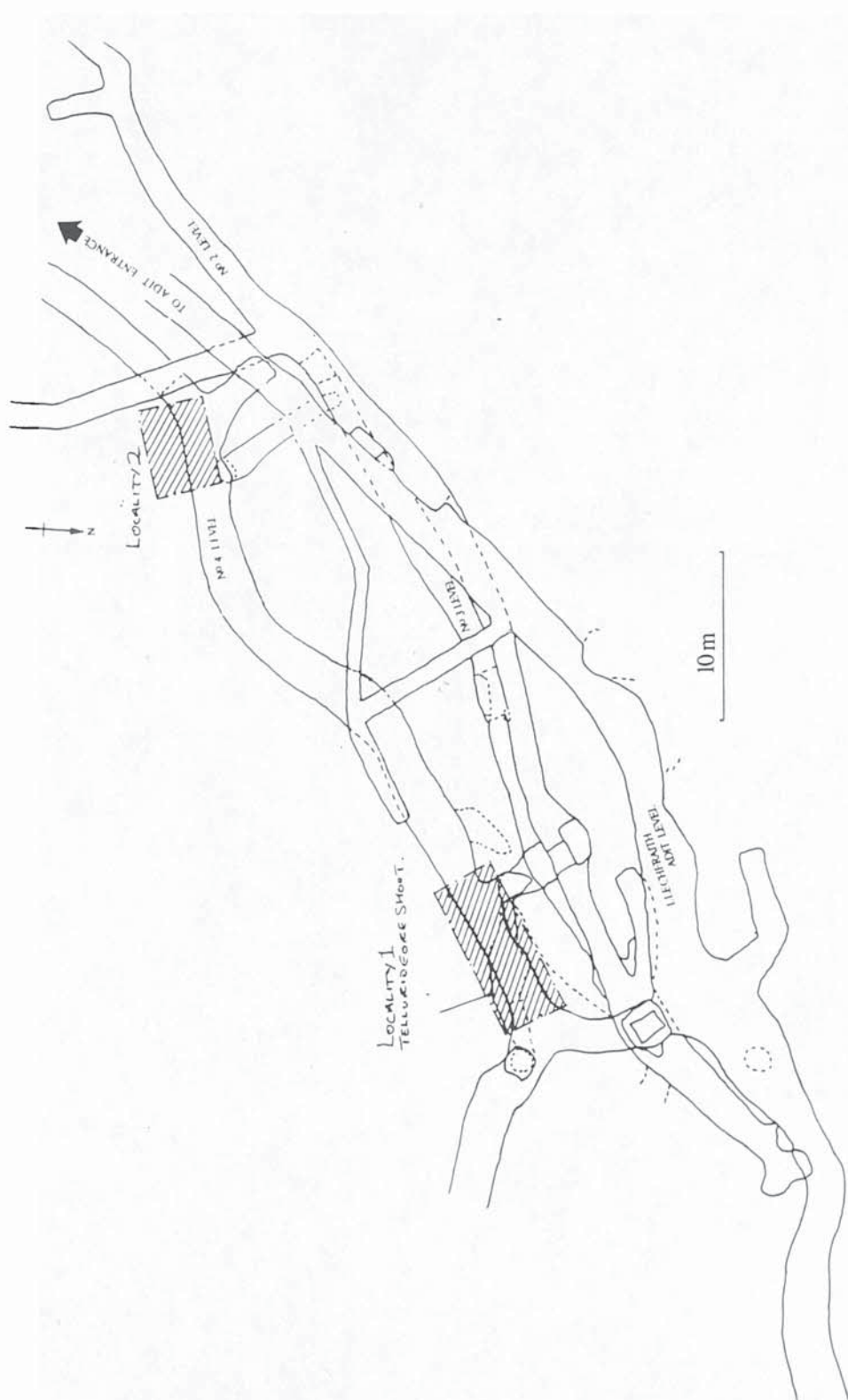


Figure 4.3. Schematic map of the geology of the ore shoot on No. 4 Level, Clogau Mine.

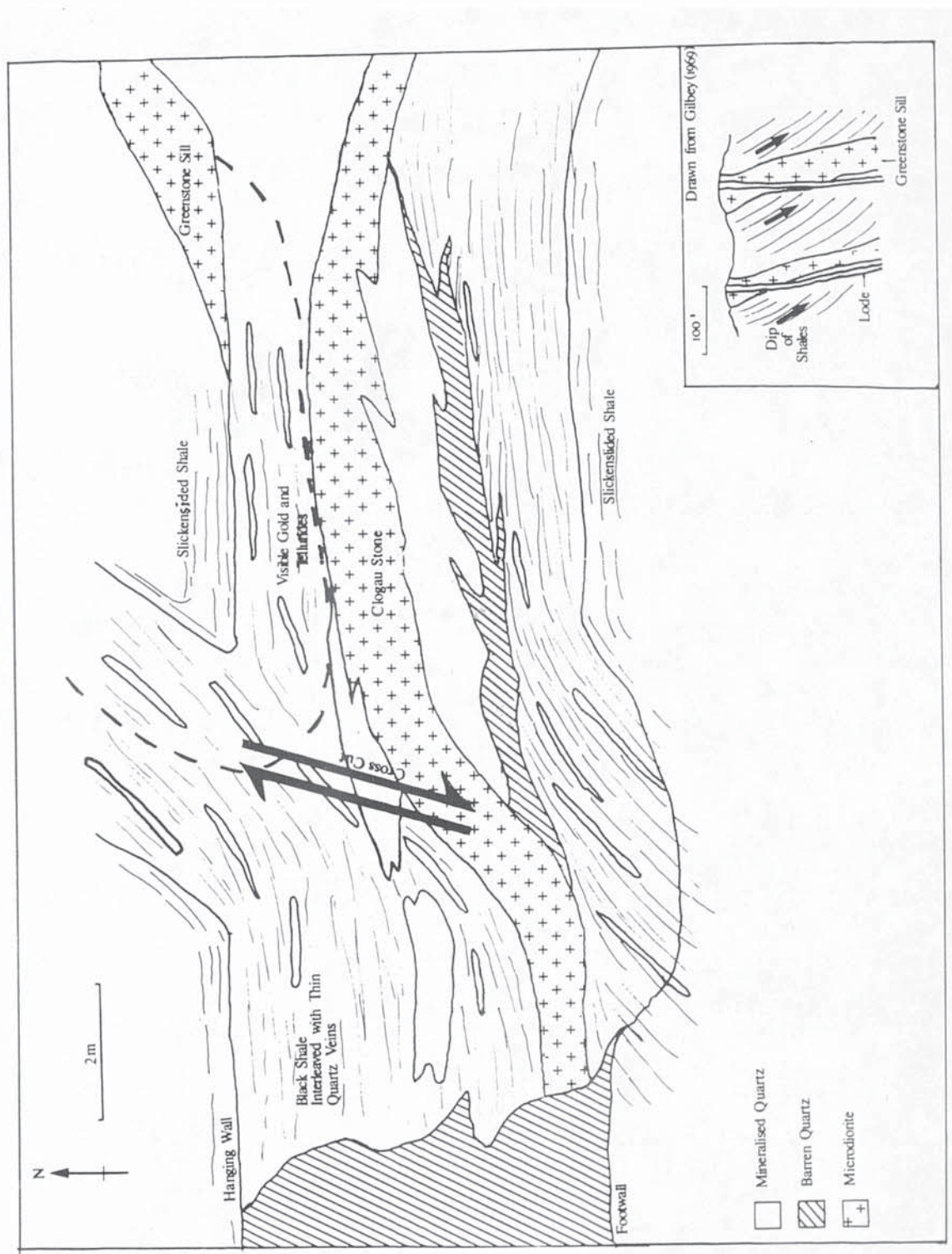


Plate 4.1. Bismuth tellurides (Bt) and carbonate (Ca) infilling fractures in quartz (air, PPL, sample number: JN 1).

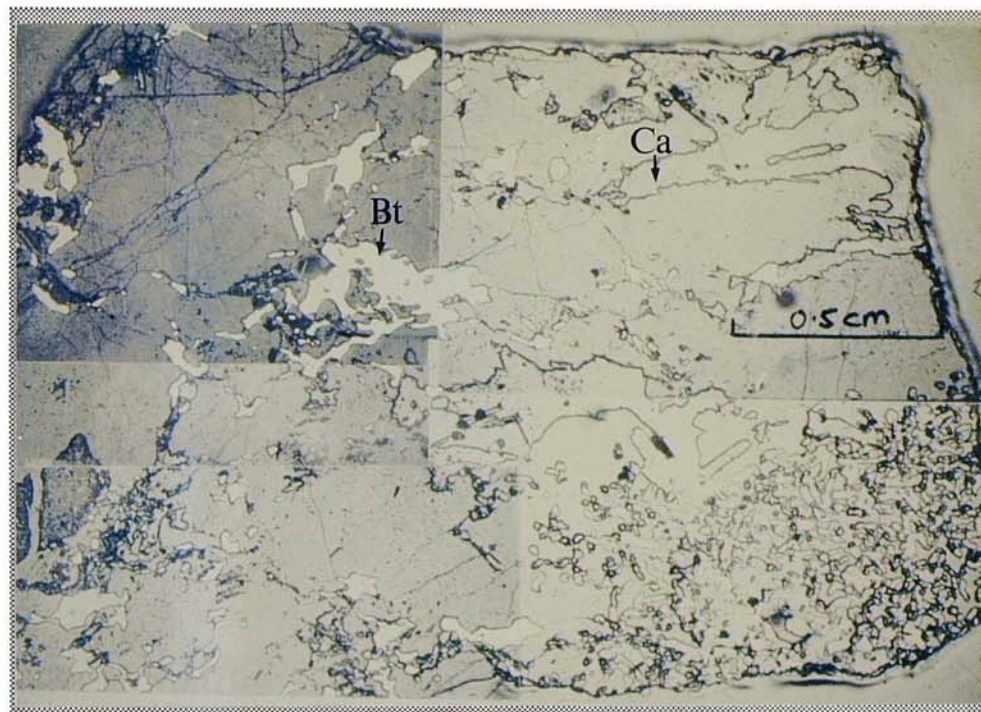


Plate 4.2. Sericite laths (sc) included in galena (mid-grey). The brown-grey phase in galena is pyrrhotine (po) (field of view 225 μ m, oil immersion, PPL, sample number: K3).

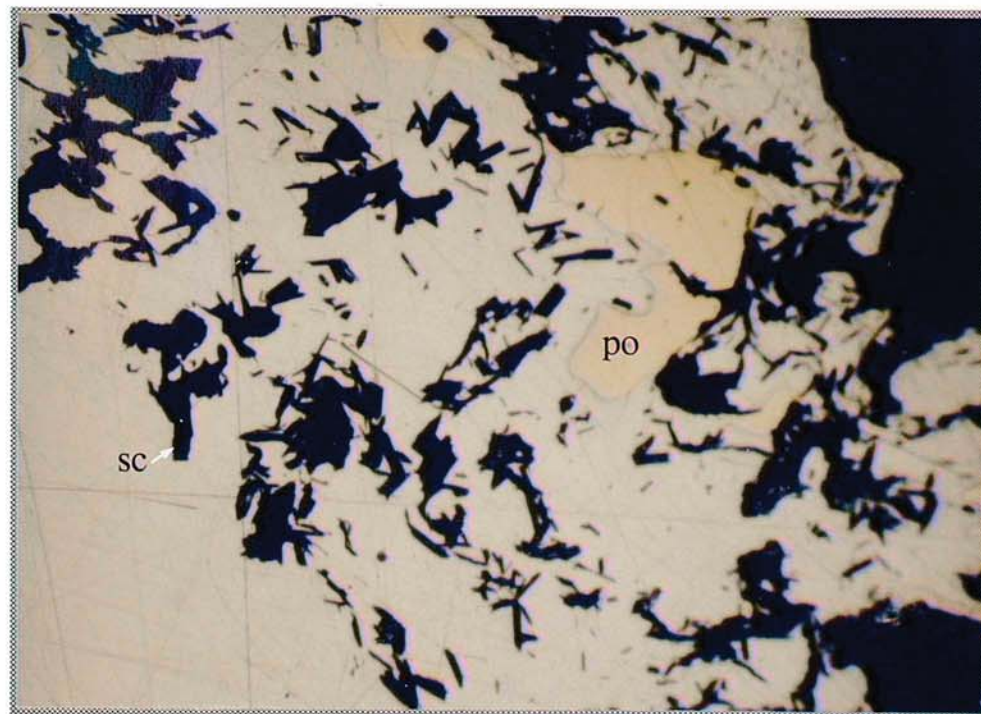


Plate 4.3. Thin veinlet of graphite (gr) in quartz (transluscent to black) with associated arsenopyrite (as) which has locally altered to limonite (Im). Note the native gold (Au) associated with the graphite veinlet (field of view 560 μ m, oil immersion, PPL, sample number: K2).

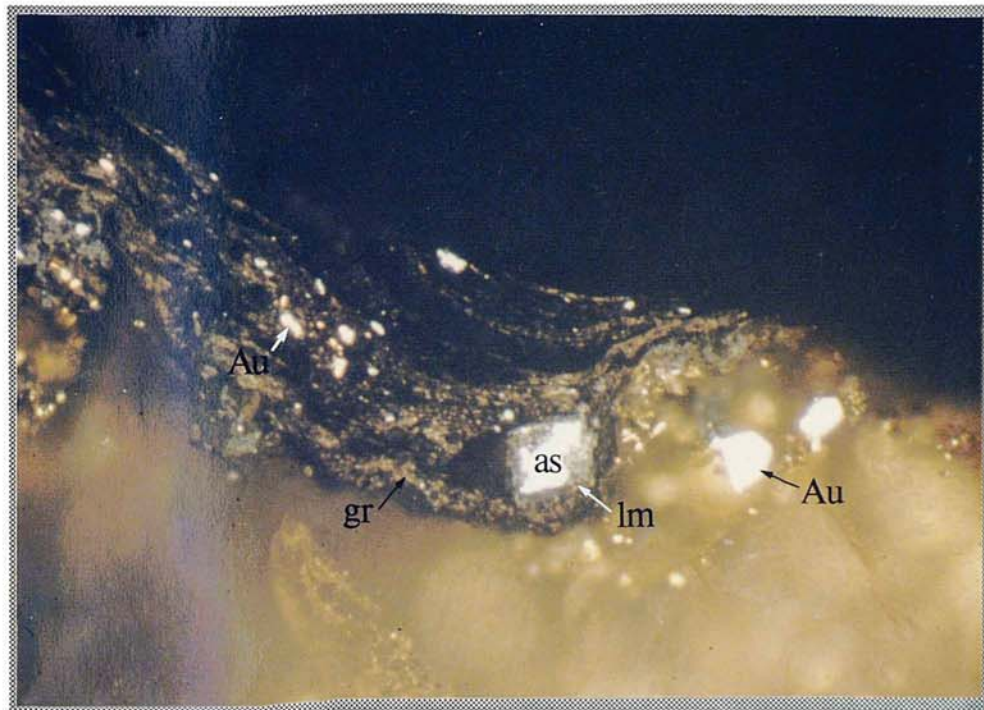


Plate 4.4. Small rutile grains (rt) in shale inclusion (field of view 1125 μ m, air, PPL, sample number: SB 128 B).



Plate 4.5. Galena (gn) replacing cobaltite (cb) and pyrrhotine (po) (field of view 560 μ m, air, PPL, sample number: JN 12).

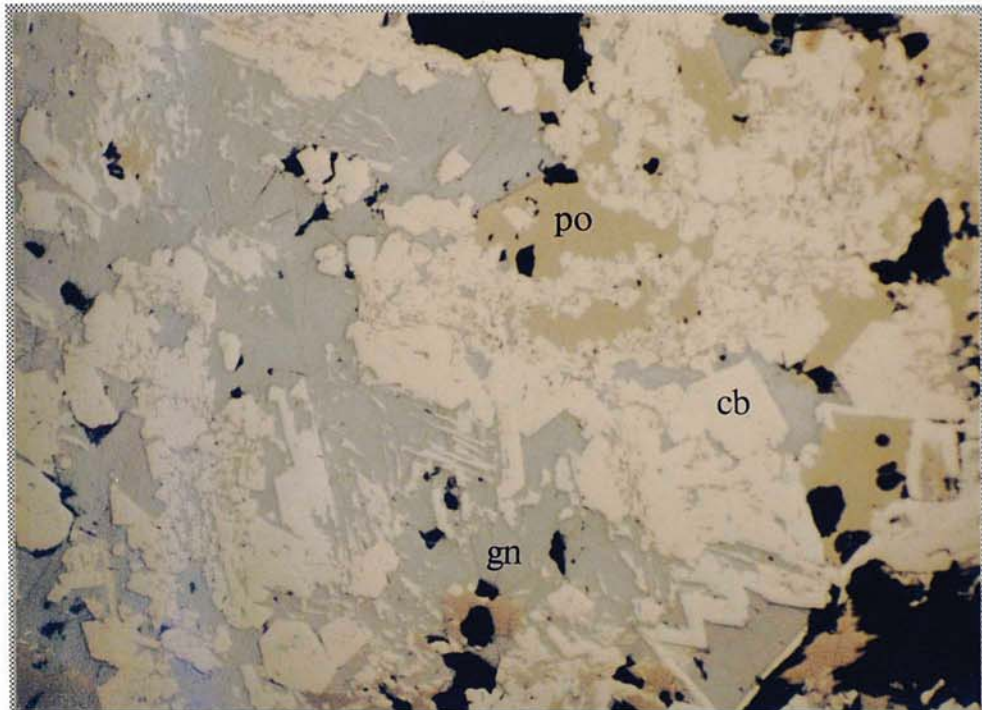


Plate 4.6. Crossed nicols view of plate 4.5. Note that in addition to galena, cobaltite and pyrrhotine; arsenopyrite (as), showing blue anisotropy colours, and bismutinite (bs), exhibiting grey-white anisotropy colours are also present (field of view 1125 μ m, air, crossed nicols, sample number: JN 12).

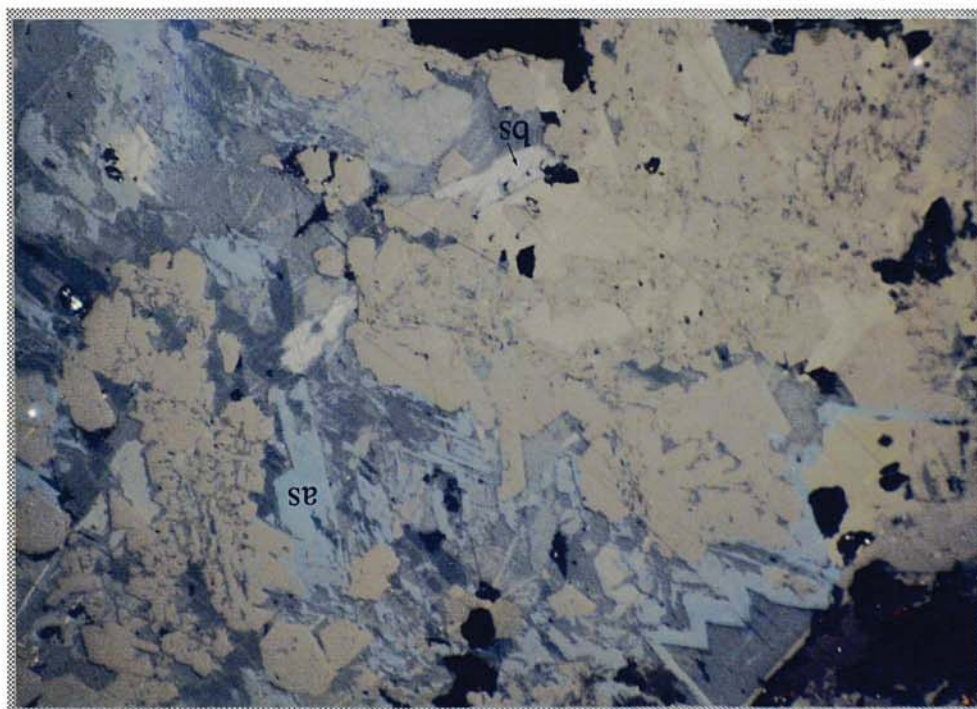


Plate 4.7. Euhedral cubes and rhombs of cobaltite (cb) locally cemented by chalcopyrite (cp) (field of view 1125 μ m, air, PPL, sample number: SB 128 COB).

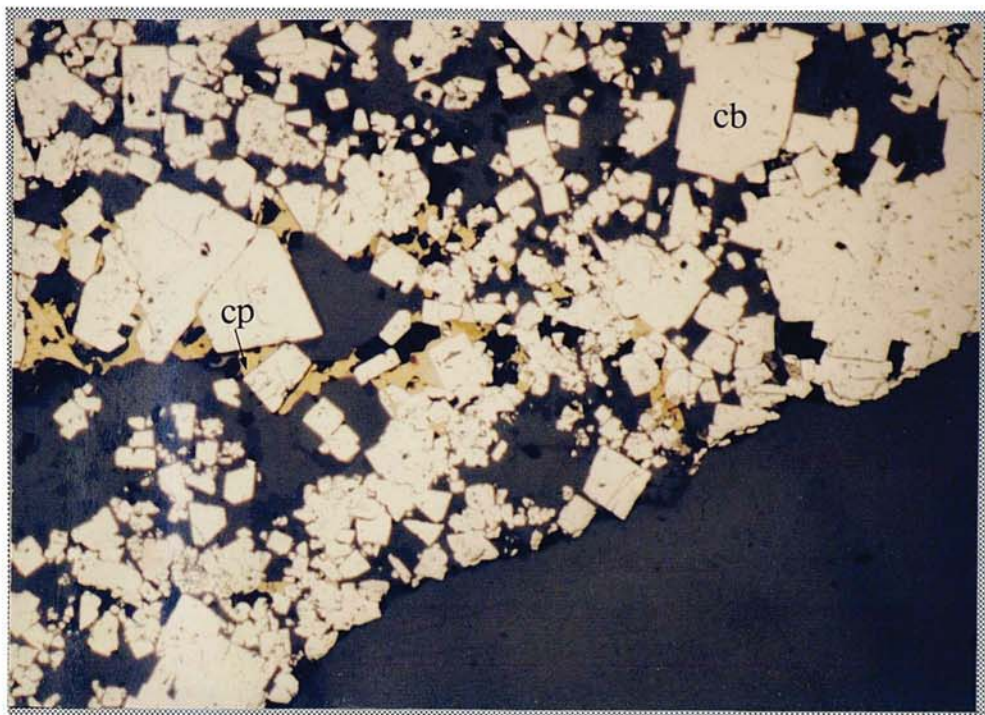


Plate 4.8. Thin chalcopyrite (cp) vein in a micro-fracture in quartz. Note how the chalcopyrite vein follows the contact between quartz and a shale ribbon (poorly polished area) (field of view 1125 μ m, air, PPL, sample number: SB 128 B).

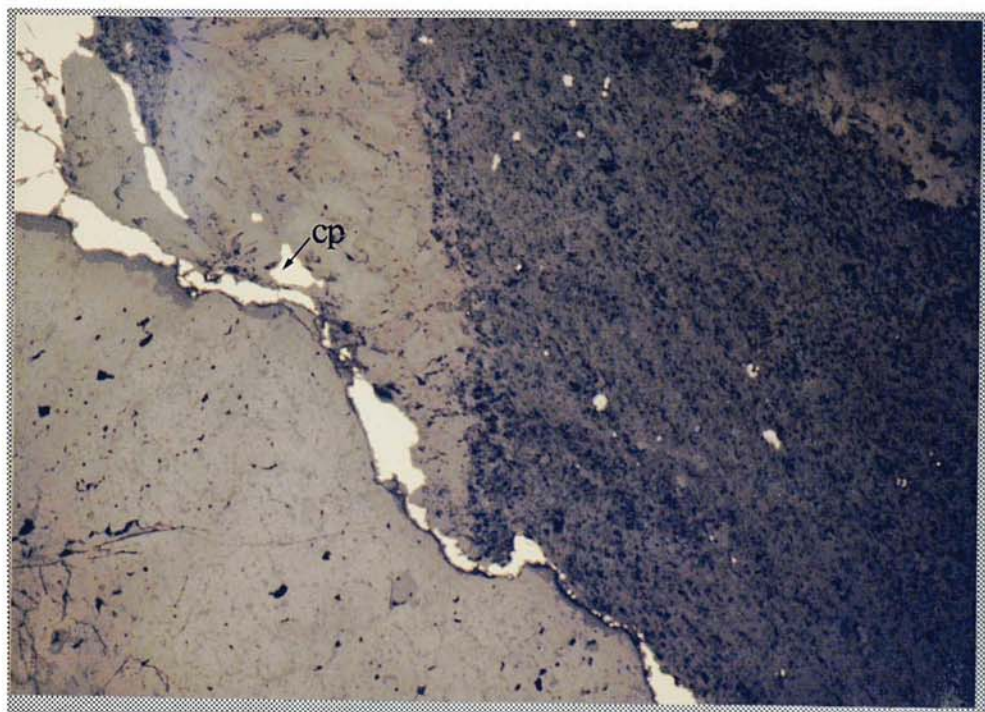


Plate 4.9. Intergrowth of pyrrhotine (po) and chalcopyrite (cp) exhibiting mutual grain boundaries (field of view 1125 μ m, air, PPL, sample number: SB 128 B).

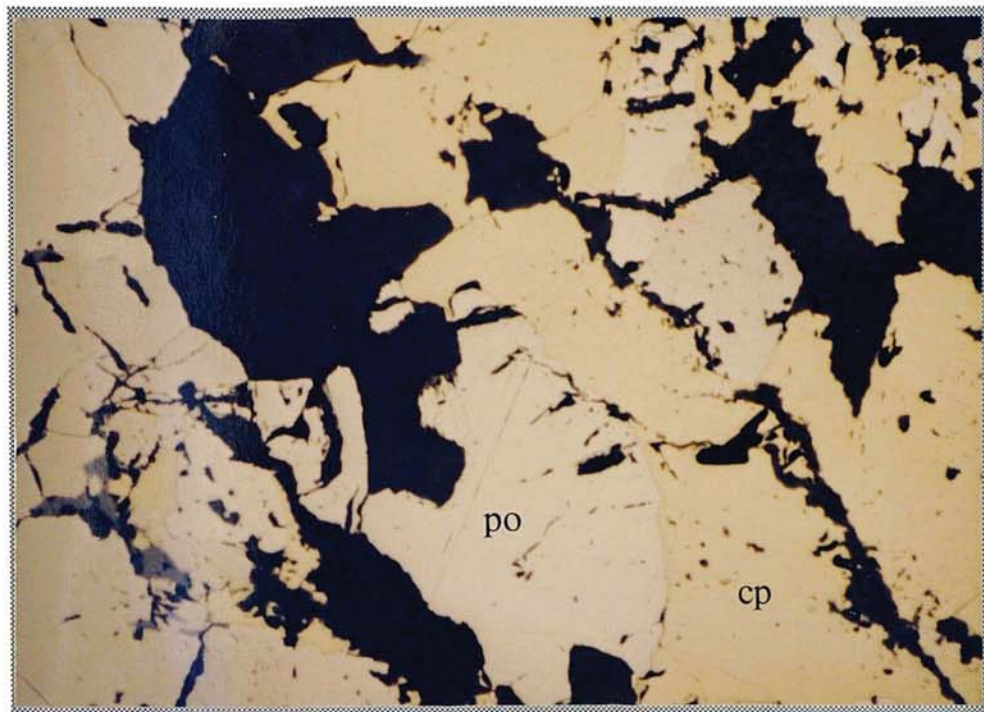


Plate 4.10. Porous zoned pyrite (py) replacing pyrrhotine (po) (field of view 1125 μ m, air, PPL, sample number: JN 41).

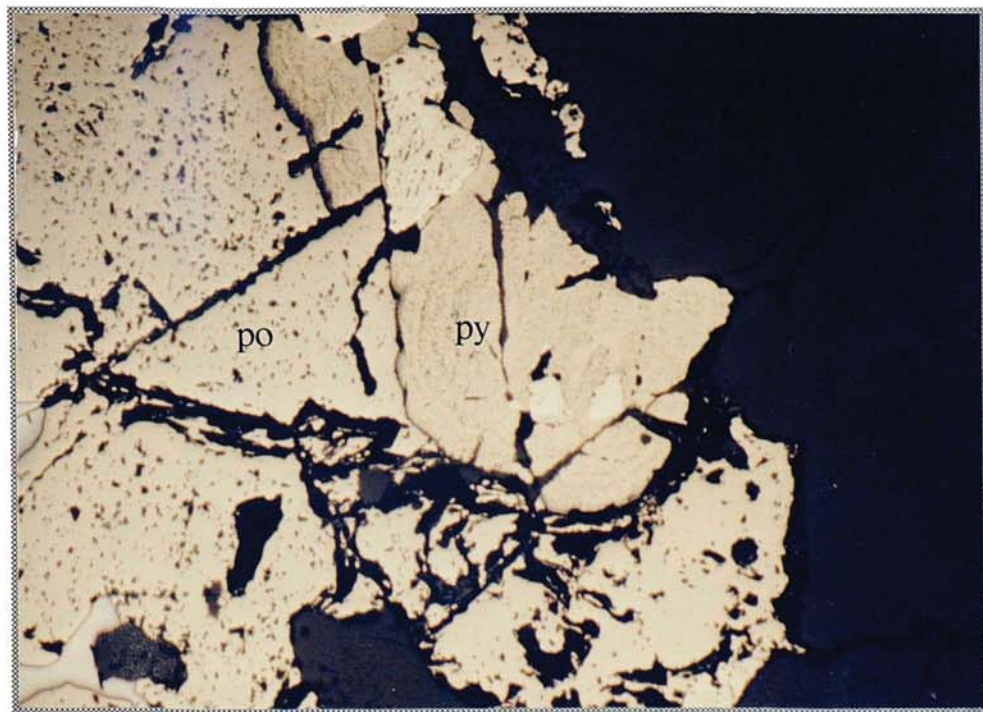


Plate 4.11. Triple point grain boundaries in tellurbismuth (field of view 560 μ m, oil, X-polars, sample number: JN 5).

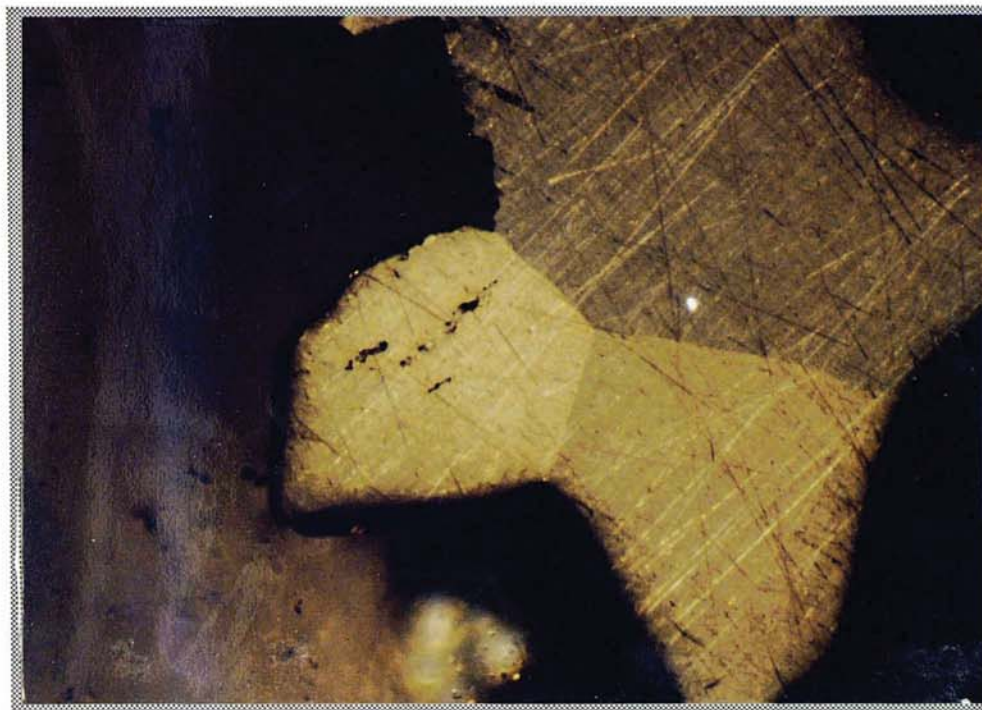


Plate 4.12. Careous grain boundaries within tellurbismuth. Note the formation of galena (gn) and altaite (at) along grain boundaries (field of view 560 μ m, oil, X-polars, sample number: JN 2).

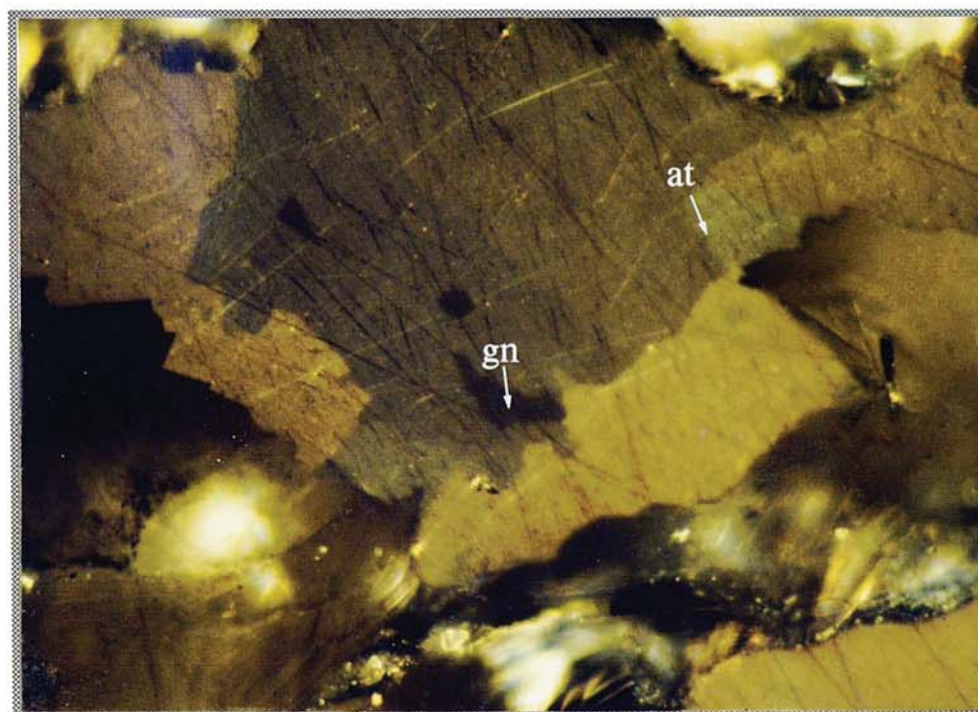


Plate 4.13. Small galena (gn) inclusions forming along cleavage in tellurbismuth (tb) (field of view 560 μ m, oil, PPL, sample number: JN 2).

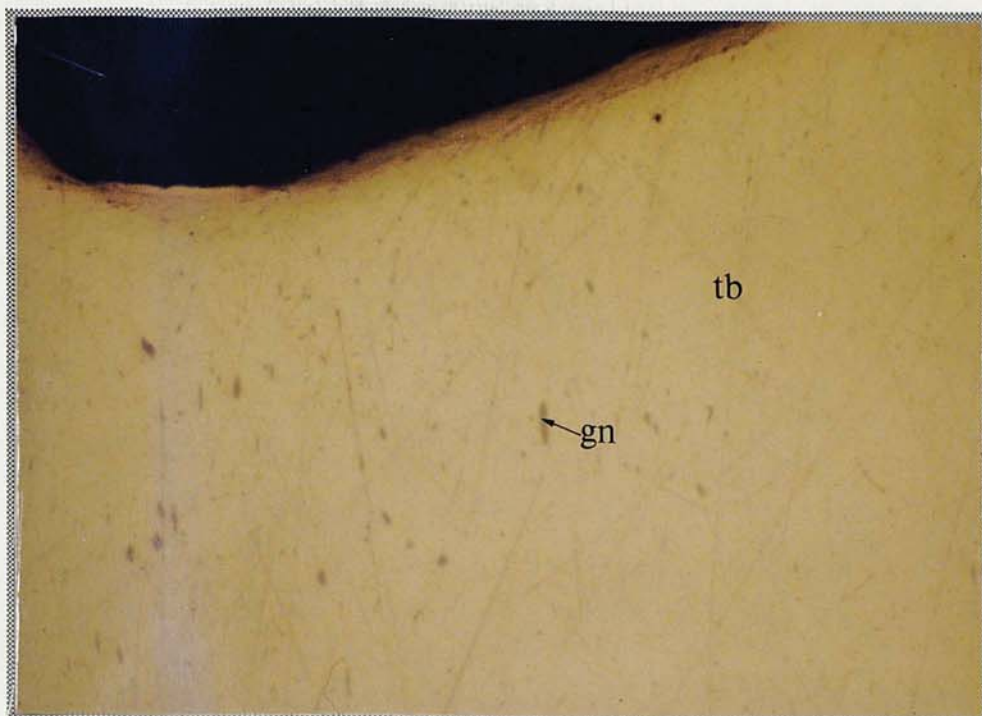


Plate 4.14. Myrmekitic intergrowth of galena (gn) and tellurbismuth (tb). The green grey phase intergrown with galena in the centre of the field of view is tetradyomite (td) (field of view 560 μ m, oil, PPL, sample number: JN 4).

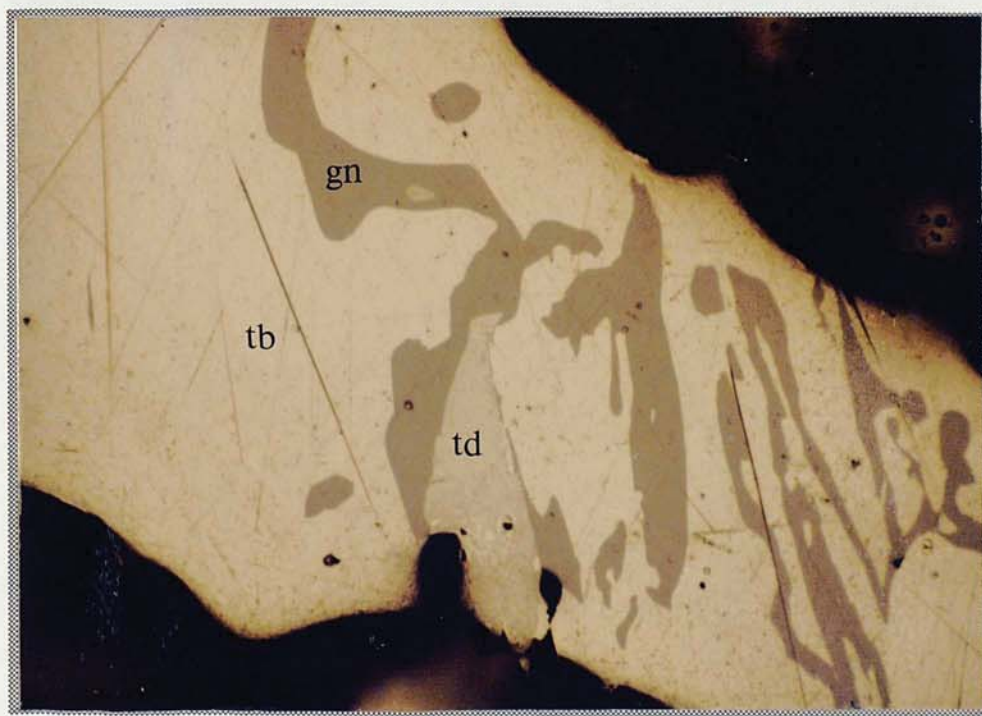


Plate 4.15. Galena (gn) rim on tetradymite (td). Note the triangular pits in galena (field of view 560 μ m, oil, PPL, sample number: JN 4).

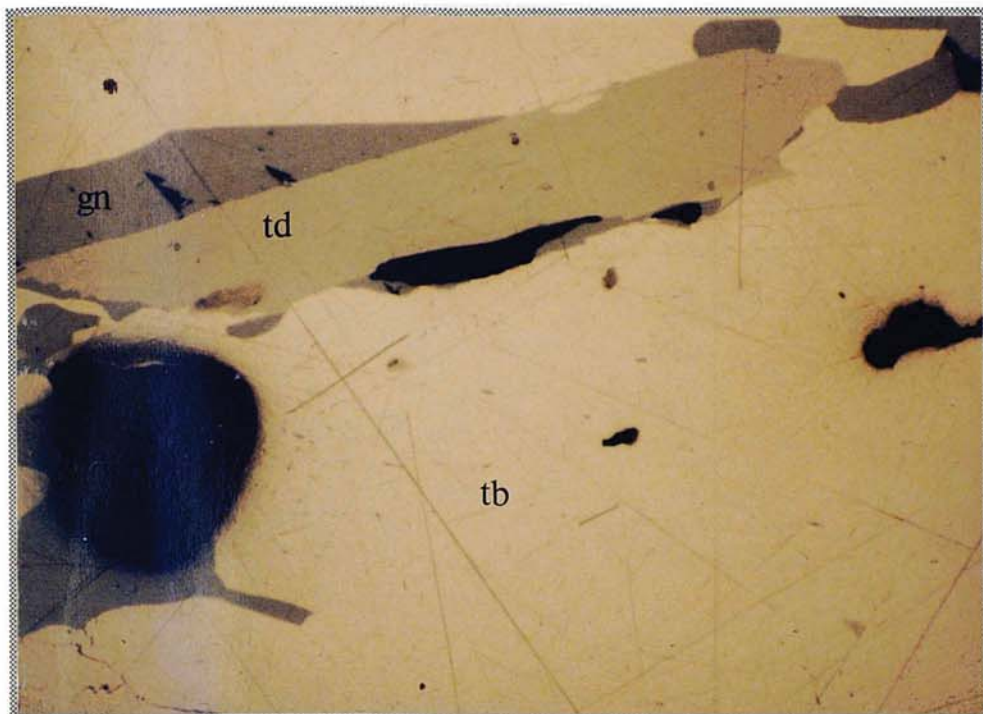


Plate 4.16. Careous boundary between tellurbismuth (tb) and tetradymite (td) (field of view 560 μ m, oil, PPL, sample number: JN 4).

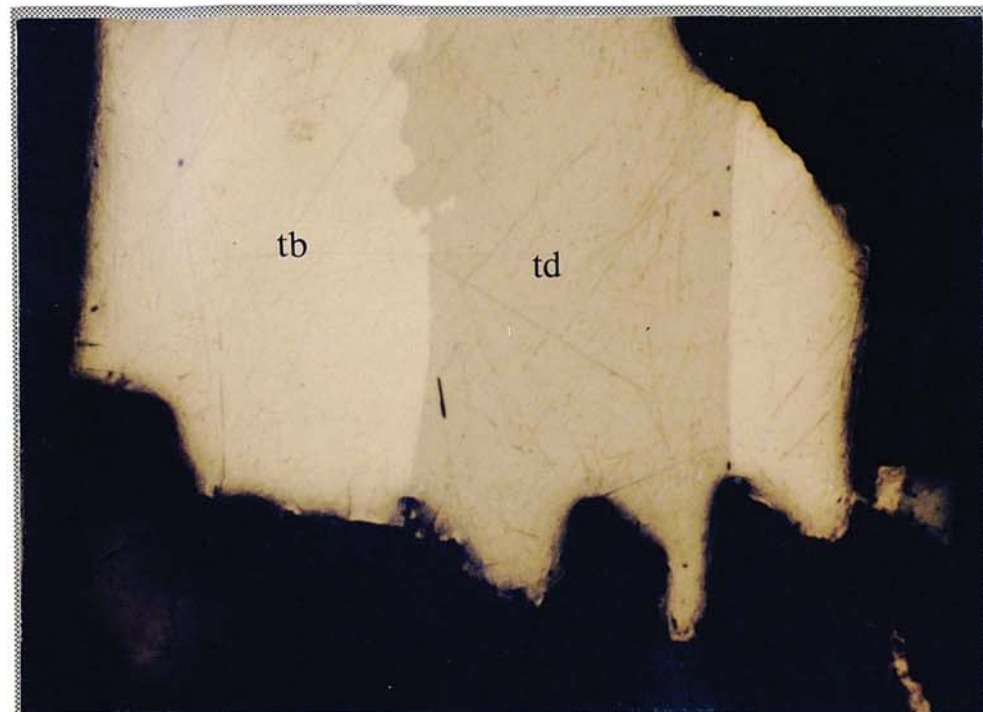


Plate 4.17. Fingerprint (fg) intergrowth at the margin between tetradyomite (td) and quartz (black). The fingerprint intergrowth appears as mottled light blue grey area on the margin of the tetradyomite grain (field of view 560 μ m, oil, PPL, sample number: JN 1).

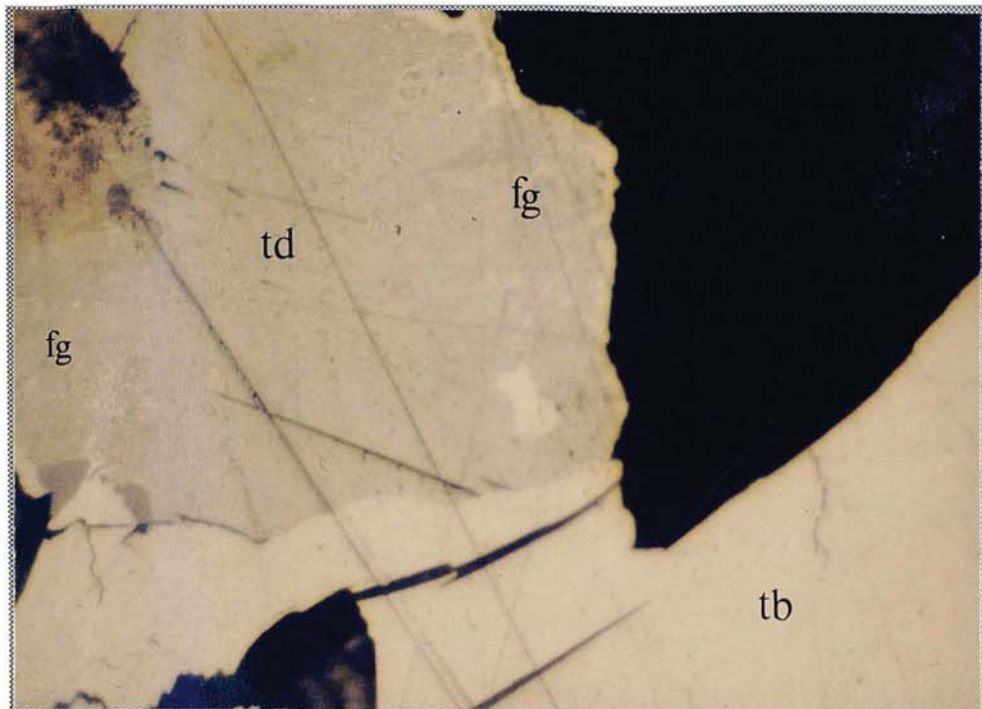


Plate 4.18. Discrete galena grains (gn) in tellurobismuth (tb). Note that the grains of galena tend to occur at the contact between quartz (black) and tellurobismuth, and aligned with the cleavage of tellurbismuth (field of view 560 μ m, oil, PPL, sample number: JN 5).

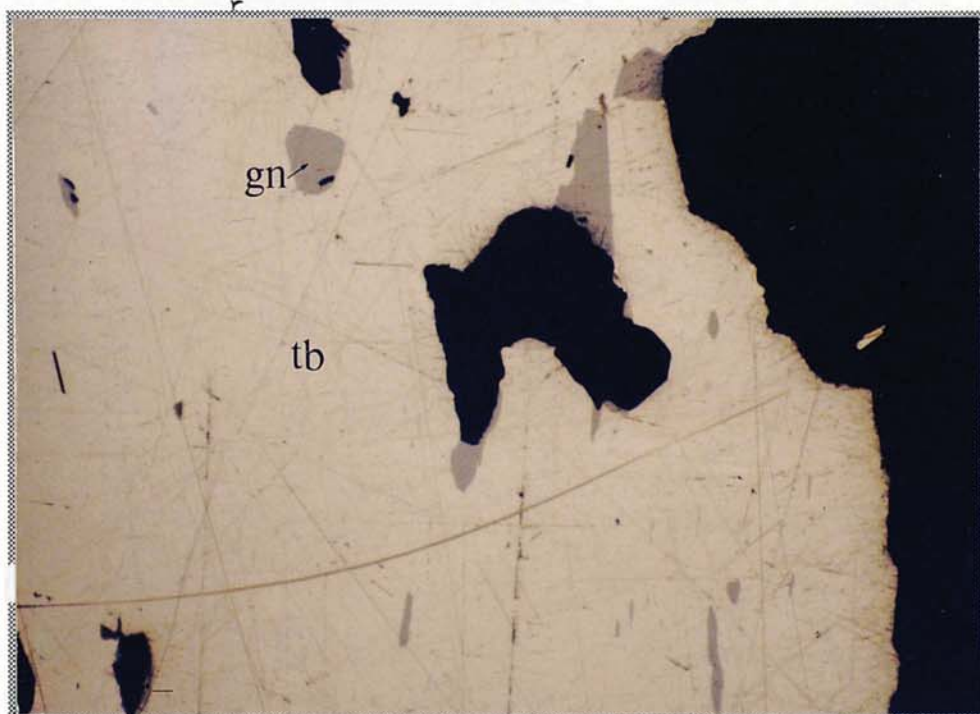


Plate 4.19. Galena (gn) replacing tellurbismuth (tb) along cleavage (field of view 560 μ m, oil, PPL, sample number: JN 16).

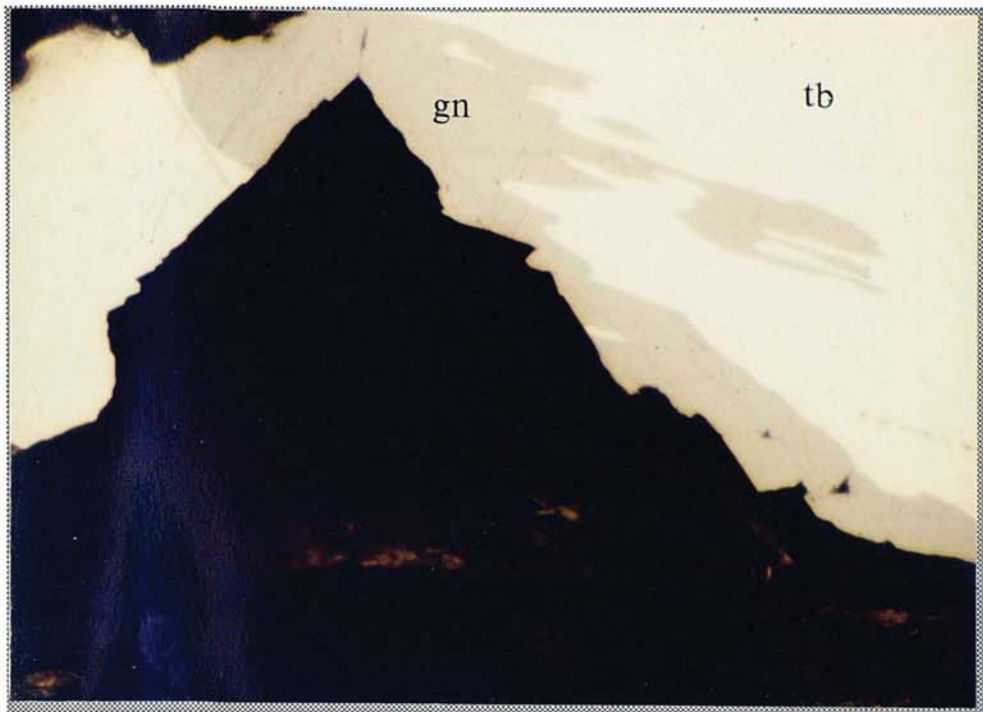


Plate 4.20. Small isolated grain of altaite (at) in tellurbismuth. Note the two small gains of gold (Au) in the centre of the field of view (field of view 225 μ m, oil, PPL, sample number: JN 4).

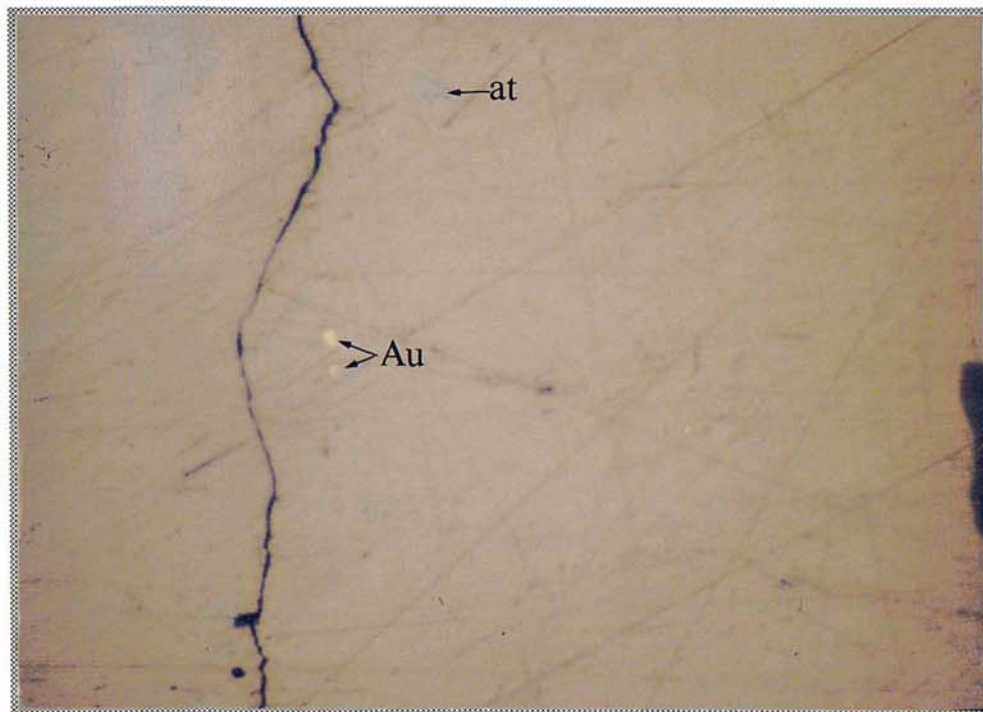


Plate 4.21. Altaite (at) grain with small inclusion of native gold in tellurbismuth. also present is a small grain of hessite (Hs) and galena (Gn). Note the similarity in reflectance and colour between hessite and galena (field of view 225 μ m, oil, PPL, sample number: JN 4).

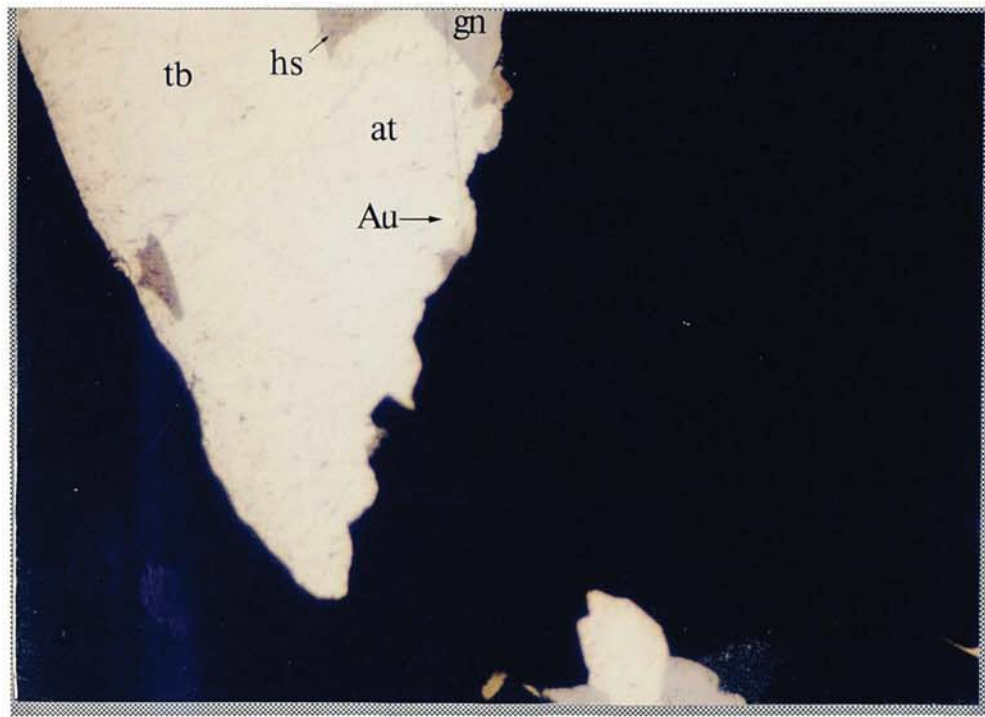


Plate 4.22. Galena (gn) and altaite (At) replacing tellurbismuth along cleavage. Also note the occurrence of hessite (hs) associated with galena (field of view 225 μ m, oil, PPL, sample number: JN 4).

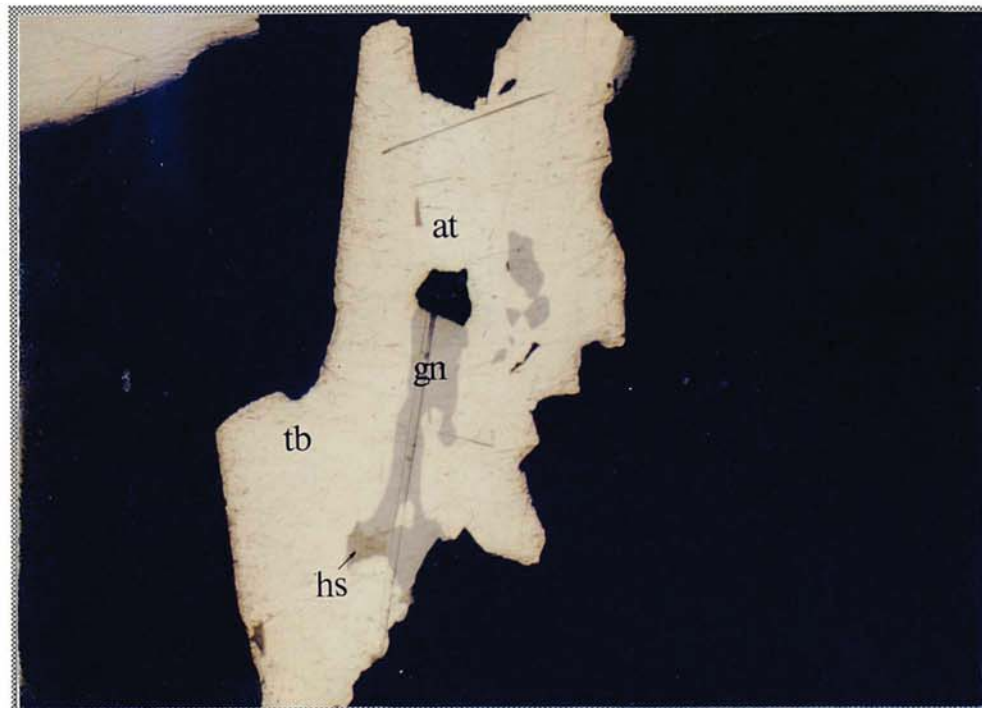


Plate 4.23a. Galena (Gn) and hessite (Hs) in tellurbismuth. Note the slightly lower reflectivity and brown tint of hessite (field of view 225 μ m, oil, PPL, sample number: JN 1).

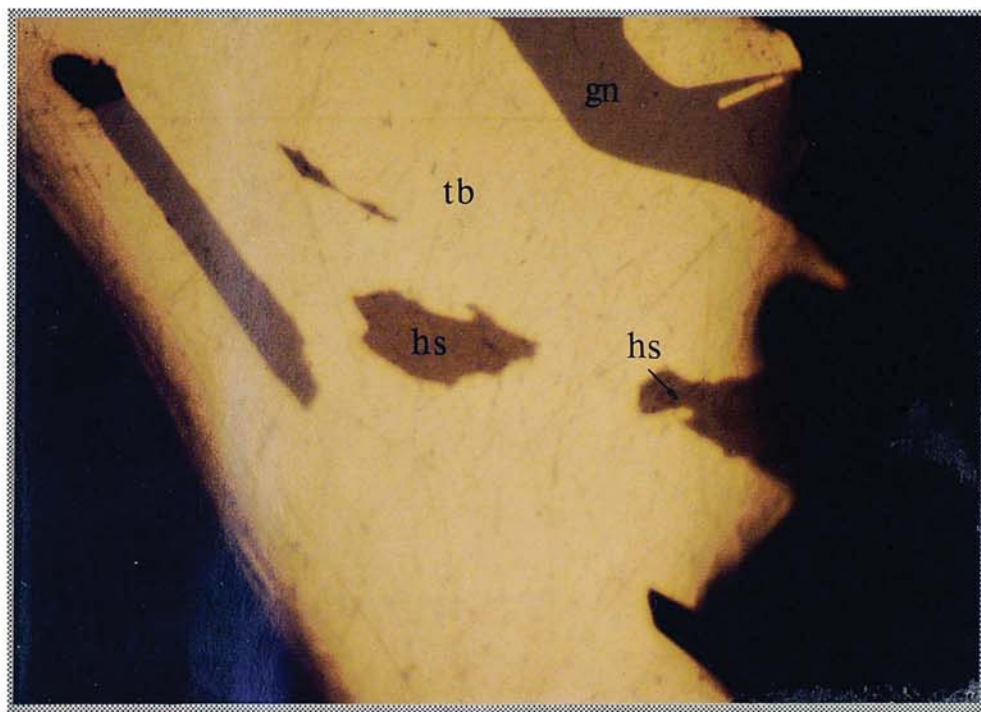


Plate 4.23b. Crossed polars view of figure 4.23a with the hessite (hs) exhibiting blue-red anisotropy colours (field of view 225 μ m, oil, X-polars).



Plate 4.24. Line of small hessite (hs) inclusions forming along a dissolution surface on tellurbismuth (The boundary between the two tellurbismuth ains is shown by slight reflectance differences). Also present are galena (gn) in contact with native gold (Au) and altaite (at) in contact with hessite (hs) (field of view 225 μ m, oil, PPL, sample number: JN 4).

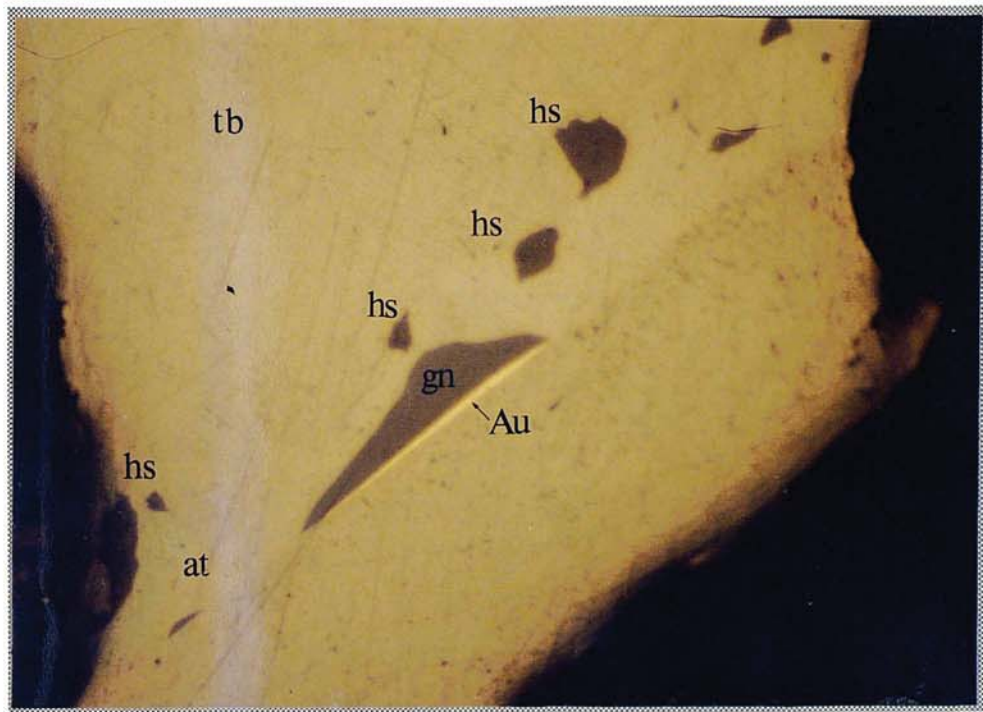


Plate 4.25. Small isolated grain of native gold (Au) in tellurbismuth, occurring with galena (gn) and an unidentified pale brown phase (arrow) (field of view 225 μ m, oil, PPL).

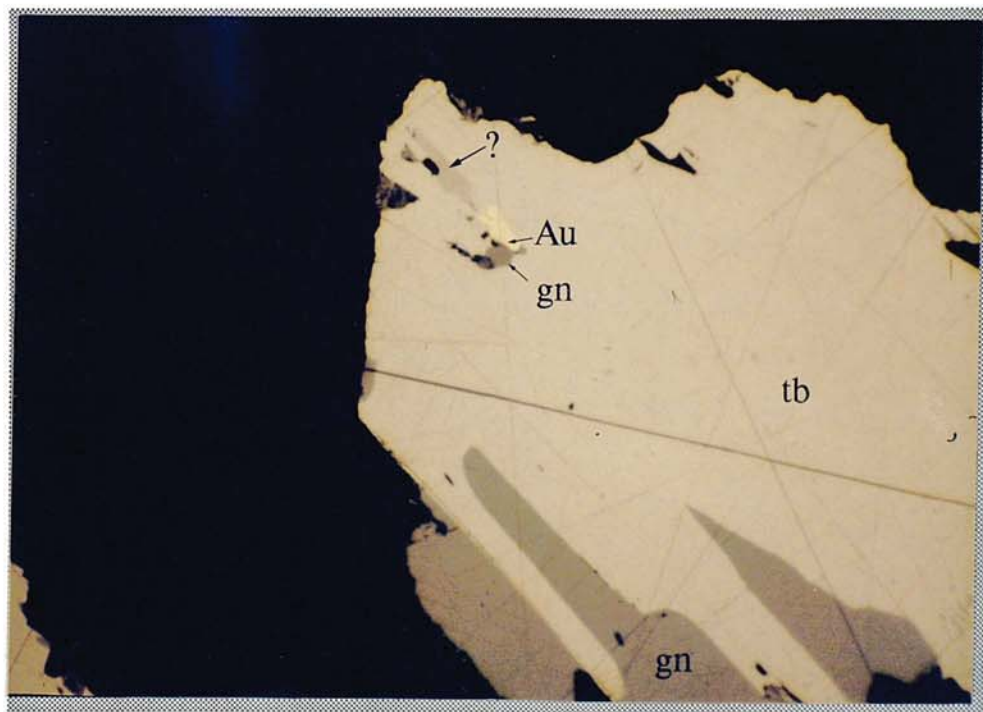


Plate 4.26. Galena (gn) replacing pyrrhotine (po) along grain boundaries. Also note the association of carbonate (ca) with the sulphides (field of view 1125 μ m, air, PPL, sample number: JN 41).

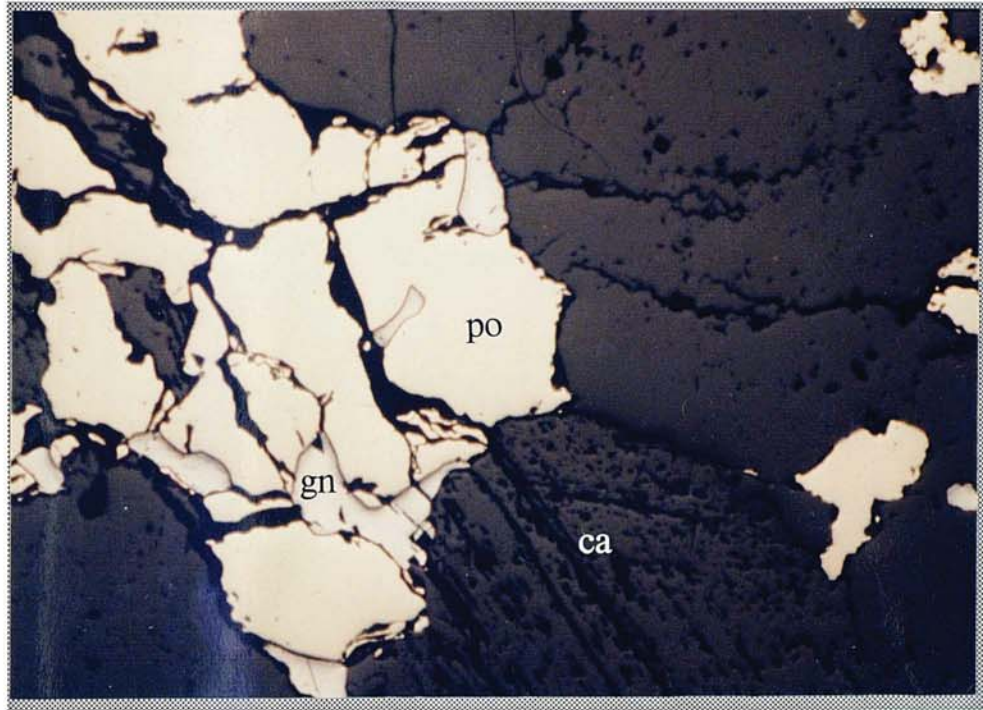


Plate 4.27. Cluster of ragged tetradyomite (Td) and wehrlite laths (Wr) in galena (The phase exhibiting high polishing relief is cobaltite). Also the wehrlite laths are tarnished in places; this is native bismuth (nb) (field of view 560 μ m, oil, PPL, sample number: JN 12).

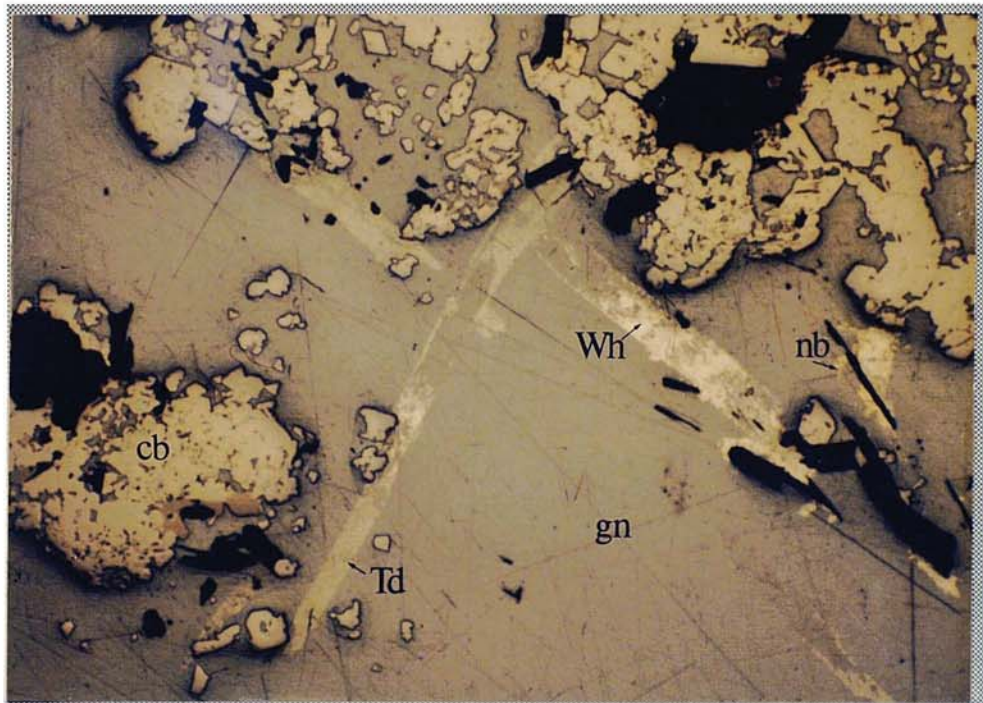


Plate 4.28. Skeletal wehrlite (wh (a)) replacing galena along cleavage, also present are clusters of anhedral grains of wehrlite (wh (b)), native bismuth (nb), bismuthinite (bs) and pyrrhotite (po) (field of view 560 μ m, oil, PPL, sample number: JN 3a).

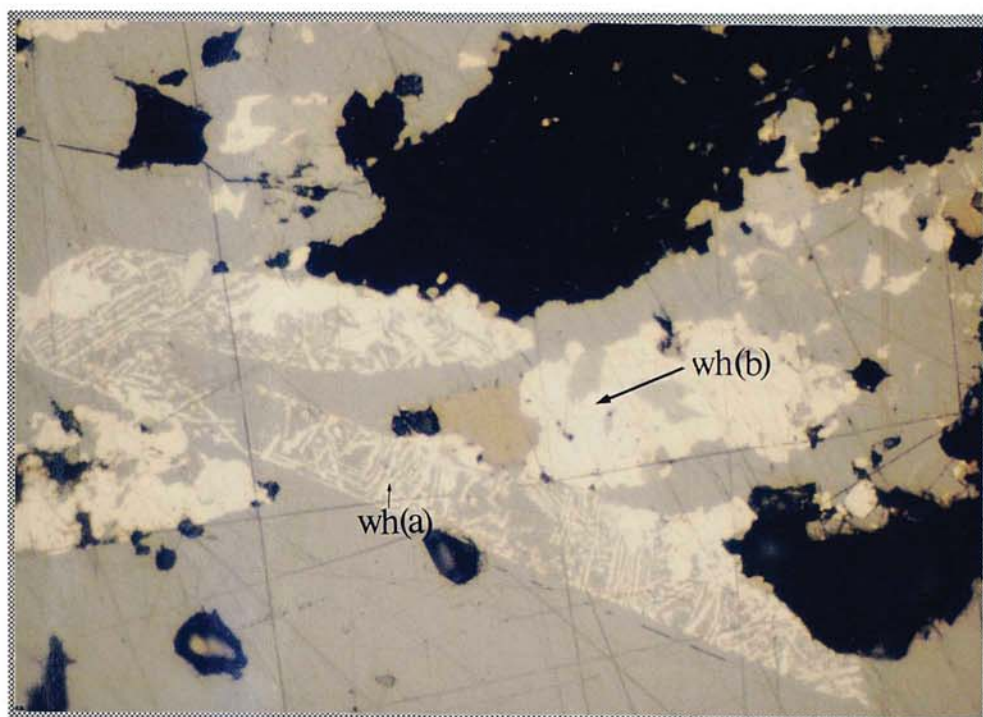


Plate 4.29. Skeletal wehrlite (wh) replacing galena along cleavage. The inclusions exhibiting high polishing relief are cobaltite (cb) (field of view 560 μ m, oil, PPL, sample number: JN 3a).

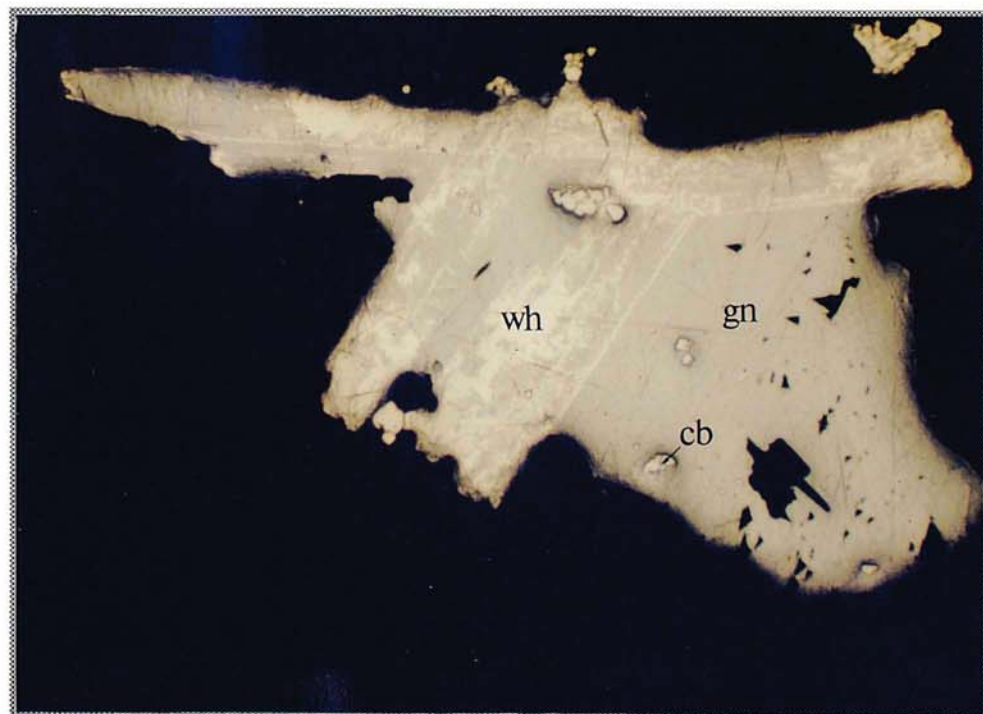


Plate 4.30. Small hessite (hs) grain in galena associated with cleavage. The harder brown phase is pyrrhotine (po) (field of view 225 μ m, oil, PPL, sample number: JN 38).

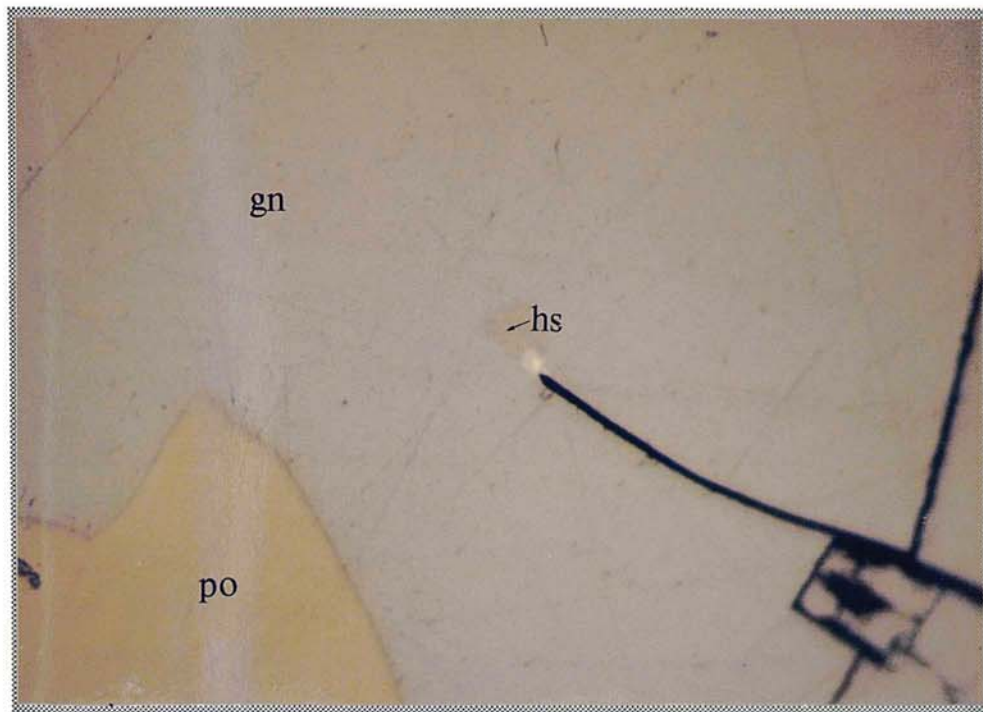


Plate 4.31. Inclusions of native gold (Au) and ?hedleyite (hd) in galena field of view 225 μ m, oil, PPL, sample number: K3).

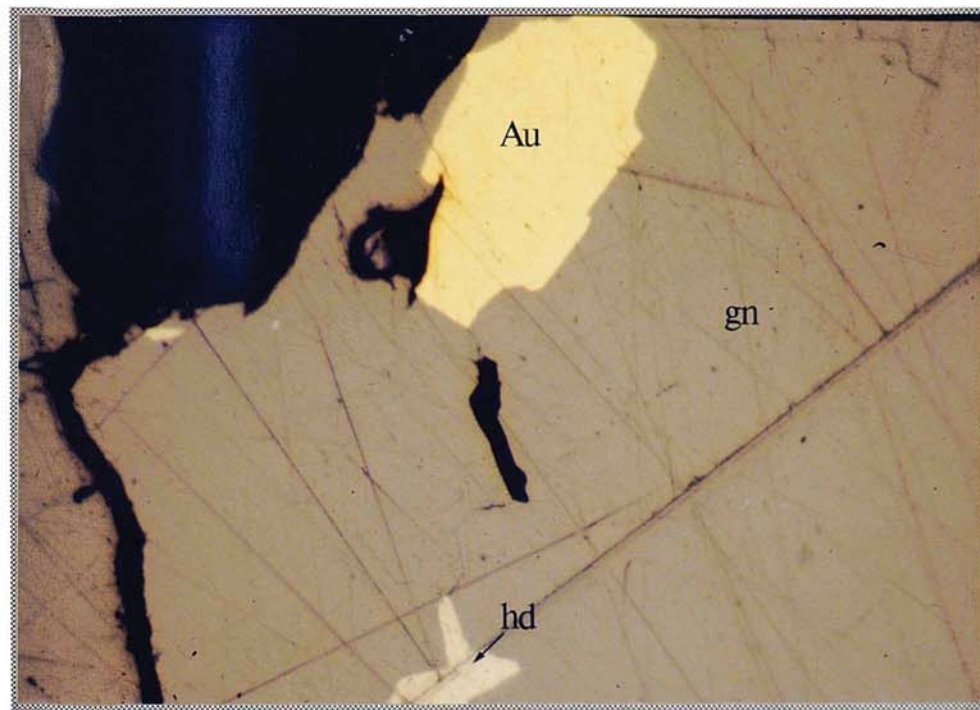


Plate 4.32. Native bismuth (nb) forming along cleavage in galena (steel-grey). Also present are aggregates of bismuthinite (Bs) (field of view 560 μ m, oil, PPL, sample number: JN 12).

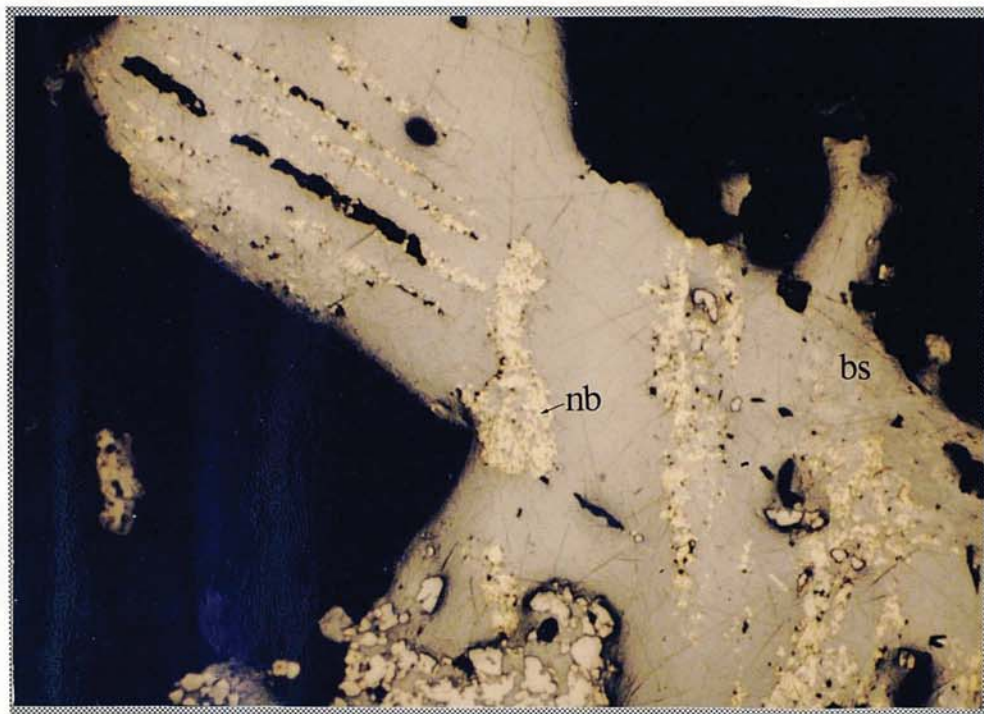


Plate 4.33. Bismuthinite (bs) (lighter grey patches in galena) and native bismuth forming along cleavage, note that the native bismuth is mutually intergrown with the bismuthinite and that there are no reaction rims of bismuthinite on native bismuth (field of view 560 μ m, oil, PPL, sample number: JN 12).

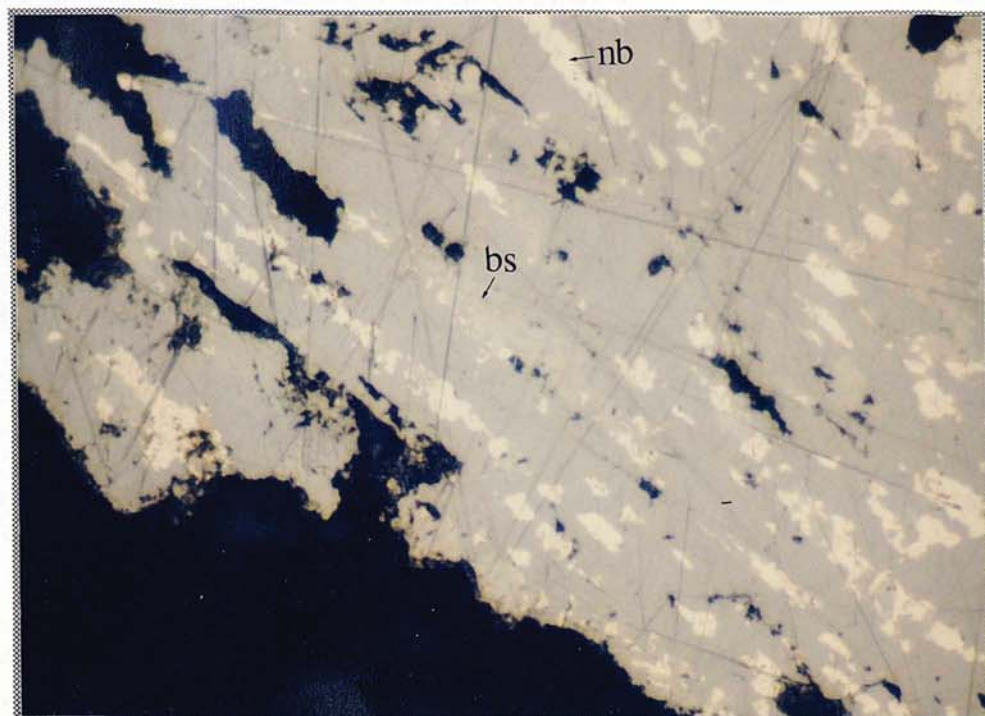


Plate 4.34. Veinlets of native gold (Au) in quartz (field of view 560 μ m, oil, PPL, sample number: K2).

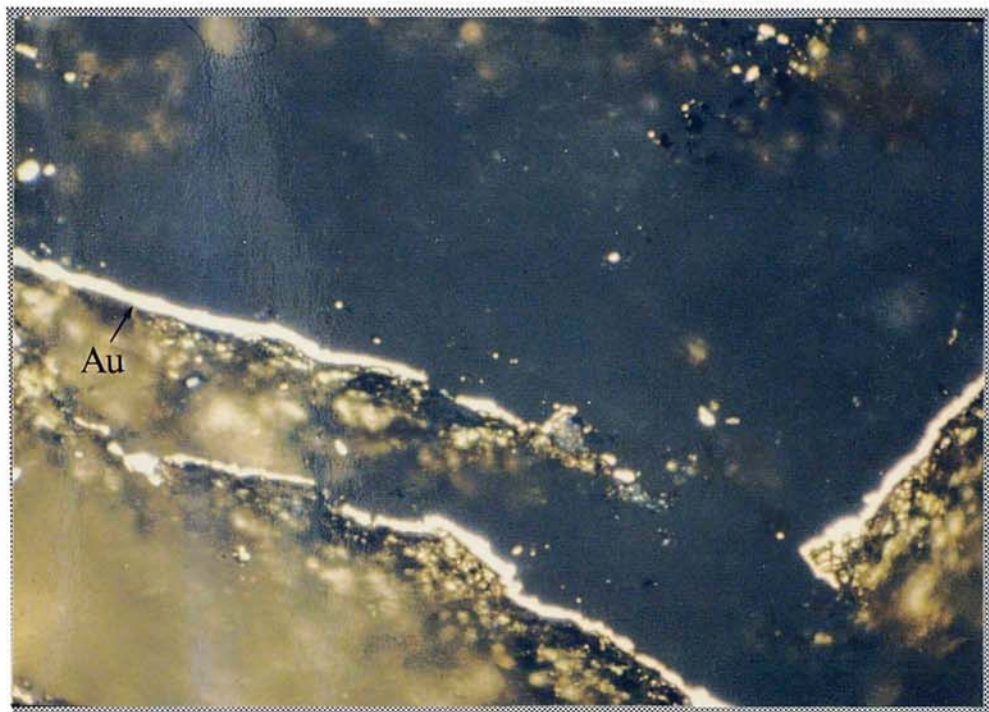


Plate 4.35. Gold (Au) cementing and replacing pyrite (py), note the incipient development of a myrmekitic texture at the lower right hand side of the pyrite grain.(field of view 560 μ m, oil, PPL, sample number: K2).

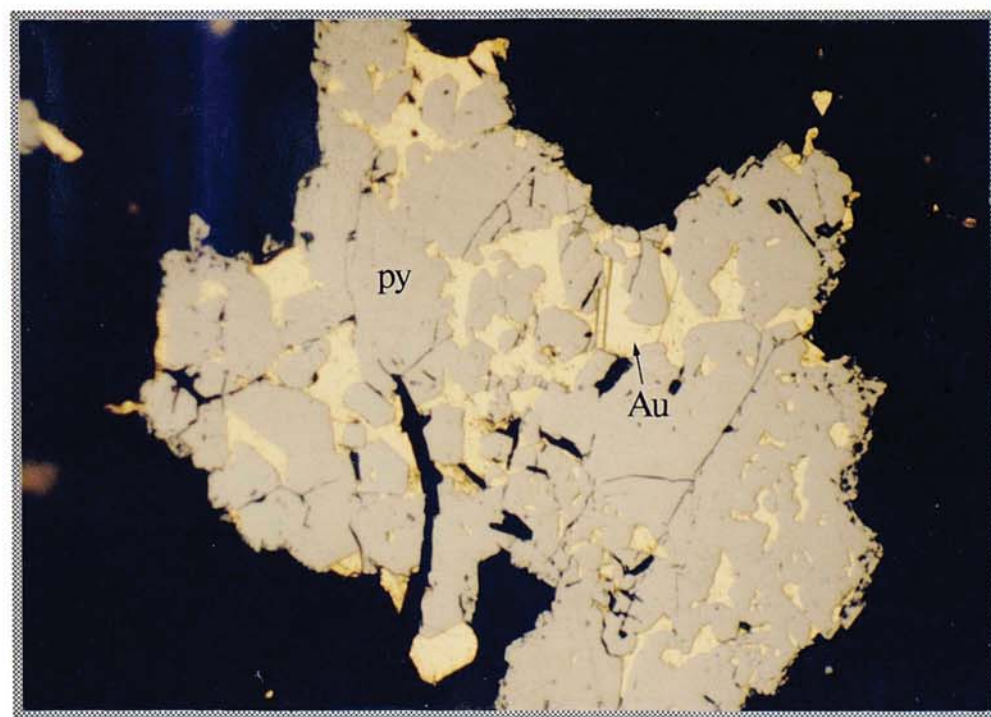


Plate 4.36. Veinlet of native gold in galena. The brown coloured phase being replaced by galena is pyrrhotine (po) (field of view 560 μ m, oil, PPL, sample number: K3).

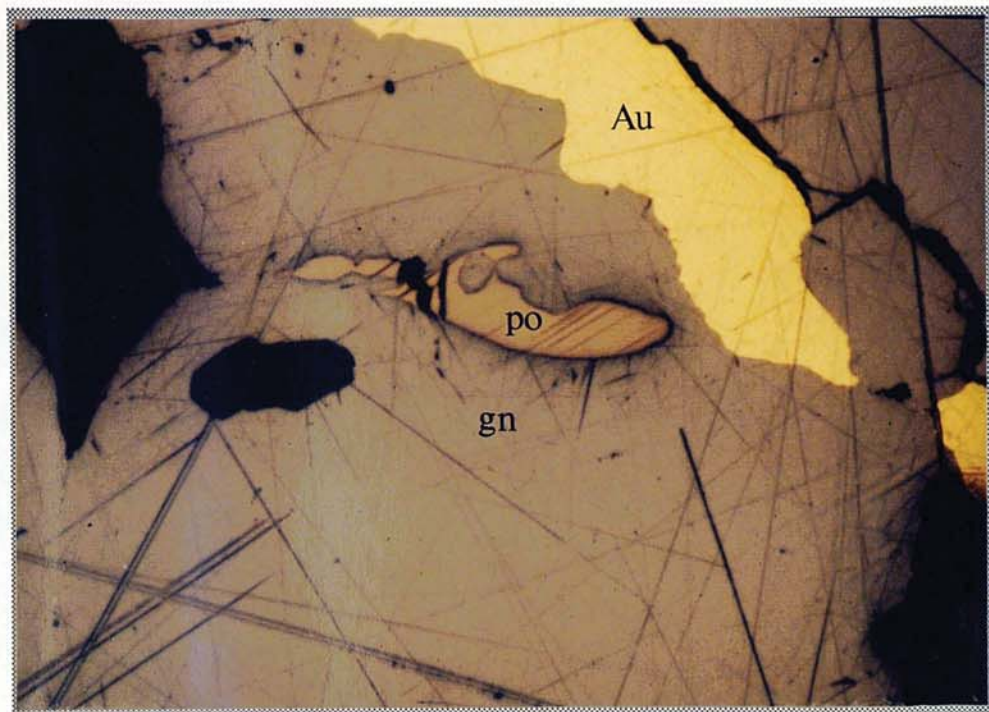


Plate 4.37. Stiboiluzonite (sb) inclusions in galena (field of view 225 μ m, oil, PPL, sample number: K2).

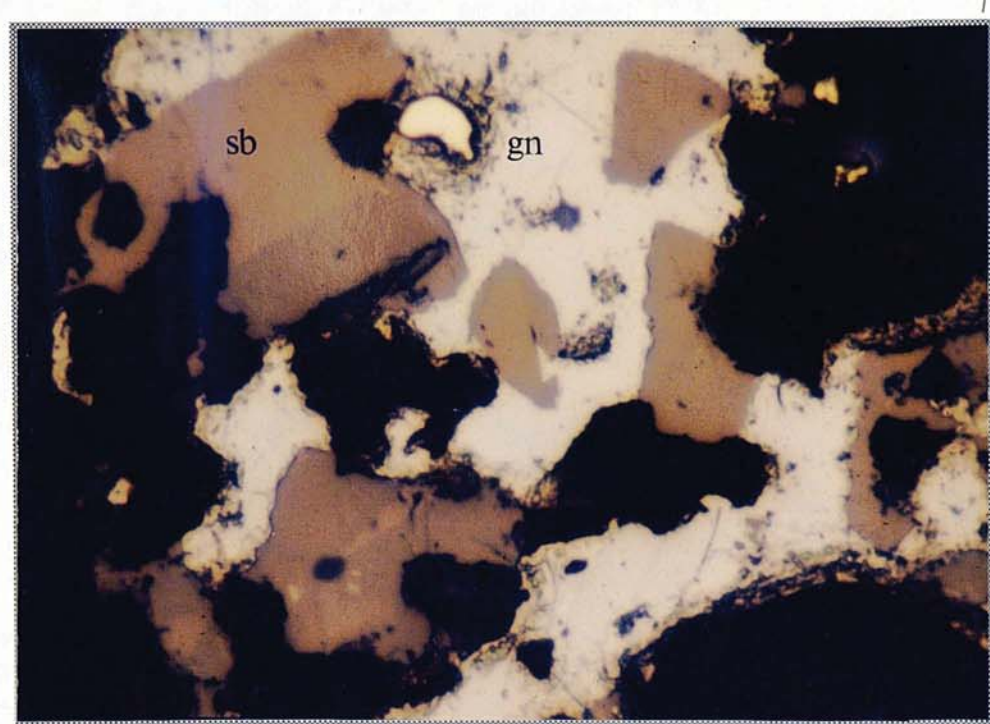


Plate 4.38. Tetrahedrite in a vug in quartz. The small inclusions in the tetrahedrite are arsenopyrite (as) (field of view 225 μ m, oil, PPL, sample number: K2).



Plate 4.39. Pyrrhotine (Po) altering to pyrite (py) and marcasite (mc). The steel grey phase replacing the pyrrhotine is galena (gn) (field of view 560 μ m, oil, PPL, sample number: JN 35).

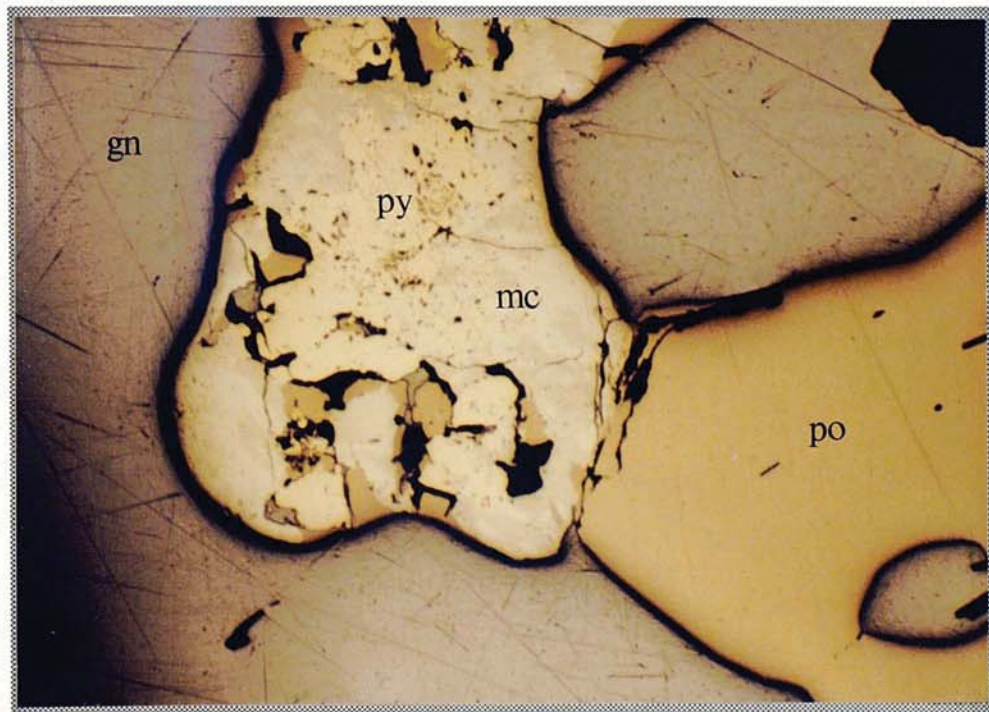


Plate 4.40. Covellite (cv) replacing galena (gn) in quartz (black) (field of view 560 μ m, oil, PPL, sample number: K2).

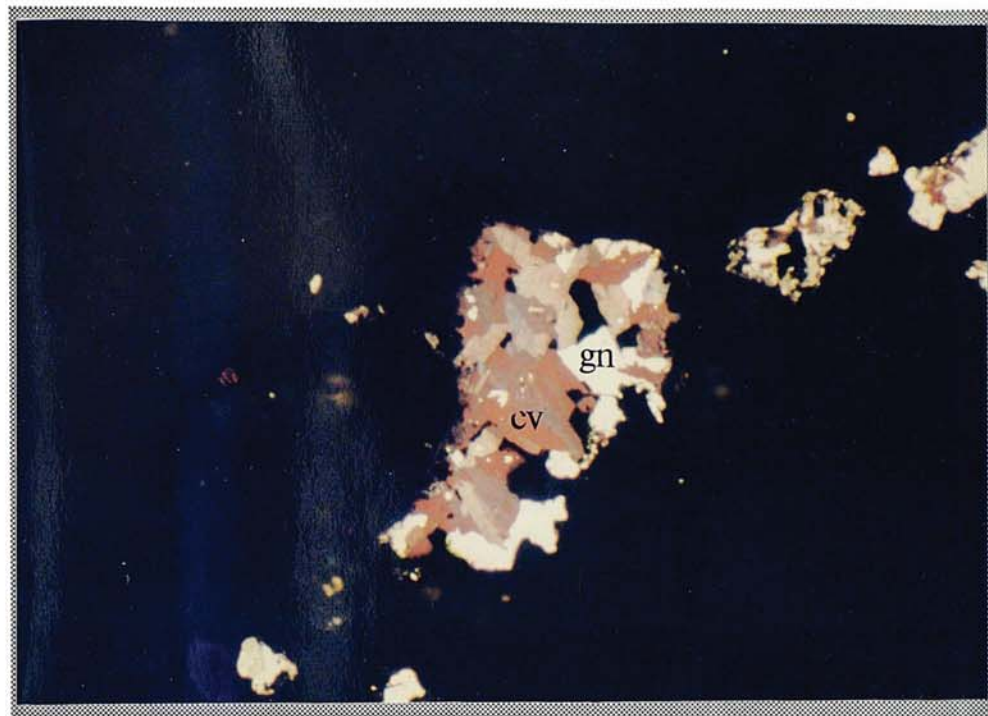


Plate 4.41 Arsenopyrite (as) altering to limonite (lm). Note the isolated grain of native gold (Au) (field of view 560 μ m, oil, PPL, sample number: K2).

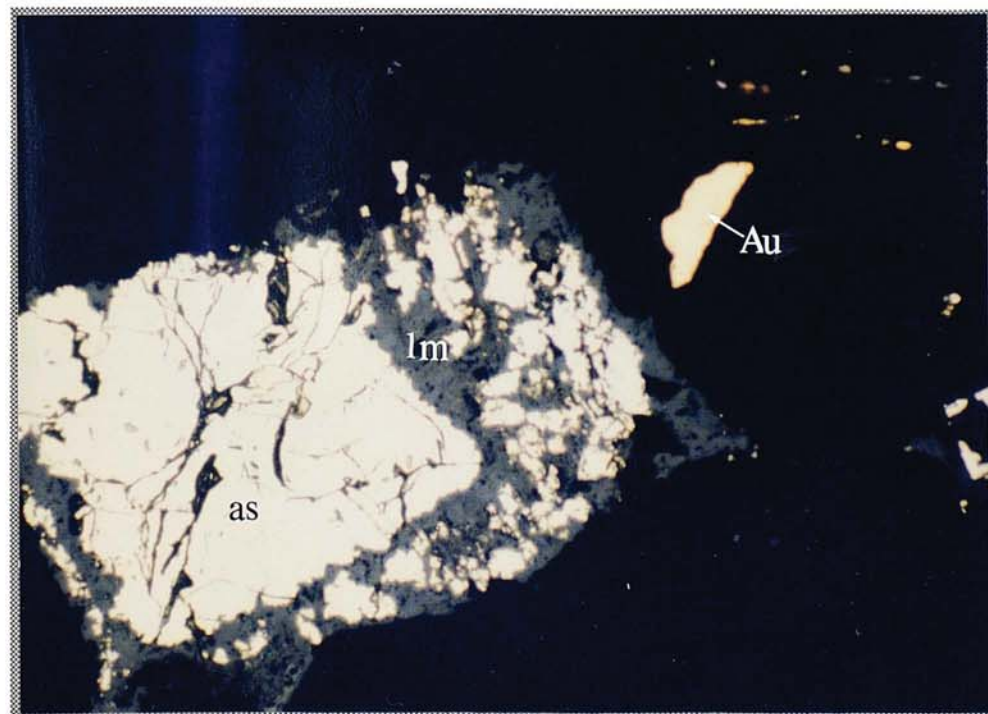


Table 4.3 Analytical details of electron probe micro-analyses.

Analytical data for Tellurbismuth, Tetradymite, Galena, Hessite, Altaite and Gold.

Element	Radiation	Std.	Detection limit (ppm)	Counting time (s)	Analysing Crystal	Error for galena (ppm)	Error for Tellurbismuth (ppm)	Error for Tetradymite (ppm)
Pb	M α	PbS	200	60	PET	880	900	300
Bi	M α	AgBiS ₂	200	60	PET	500	4510	4580
S	K α	Galena	200	60	PET	900	260	640
Te	L α	Pure metal	100	60	PET	350	2700	2330
Sb	L α	CdS	100	60	PET	350	430	450
Cd	L β	Pure metal	200	60	PET	310	660	680
Ag	L α	AgBiS ₂	100	60	PET	300	540	500
Ag	L α	Pure metal	100	60	PET	•	•	•
Au	L α	Pure metal	200	60	LIF	600	550	400

Analytical data for wehrlite, hedleyite, native bismuth and bismuthinite.

Element	Radiation	Std.	Detection limit (ppm)	Counting time (s)	Analysing Crystal	Error for Wehrlite (ppm)	Error for Hedleyite (ppm)	Error for Native bismuth (ppm)
Pb	M α	PbS	200	60	PET	880	900	300
Bi	M α	AgBiS ₂	200	60	PET	500	4510	4580
S	K α	Galena	200	60	PET	900	260	640
Te	L α	Pure metal	100	60	PET	350	2700	2330
Sb	L α	CdS	100	60	PET	350	430	450
Cd	L β	Pure metal	200	60	PET	310	660	680
Ag	L α	AgBiS ₂	100	60	PET	300	540	500
Au	L α	Pure metal	200	60	LIF	600	550	400

Table 4.3 Continued.

Analytical data for Tetrahedrite, Bournonite, Boulangerite and Stibioluzonite.

Element	Radiation	Std.	Detection limit (ppm)	Counting time (s)	Analysing Crystal	Error for Tetrahedrite (ppm)	Error for Bournonite (ppm)	Error for Stibioluzonite (ppm)
Cu	K α	Pure metal	200	60	LIF	800	850	900
Ag	L α	Pure metal	100	60	PET	250	250	250
Fe	K α	FeS ₂	200	60	LIF	800	400	NA
Zn	K α	ZnS	200	60	LIF	800	400	NA
Pb	M α	PbS	200	60	PET	800	400	NA
Sn	L α	Pure metal	200	60	PET	400	300	100
As	L α	Pure metal	300	60	RAP	1000	1000	500
Sb	L α	Pure metal	200	60	PET	800	800	800

Figure 4.4. Line concentration profile across a cobaltite grain showing the variations in major element chemistry.

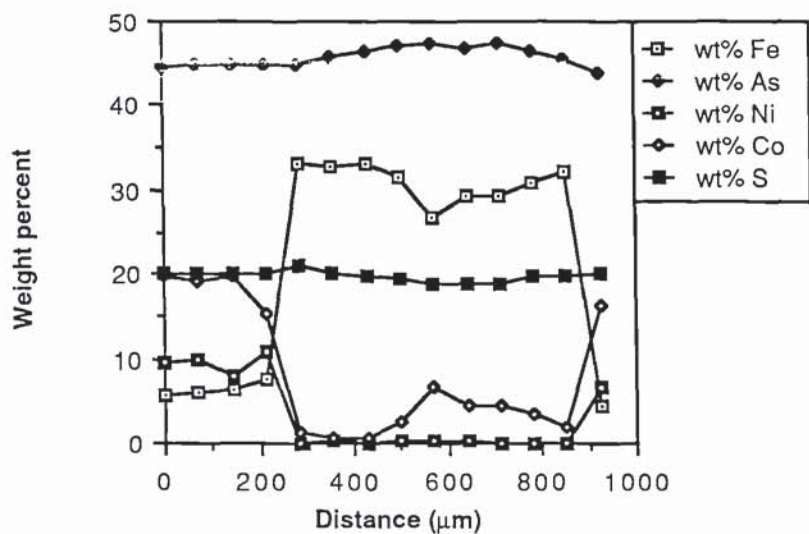


Figure 4.5. Line concentration profile across a cobaltite grain showing the variations in minor element chemistry.

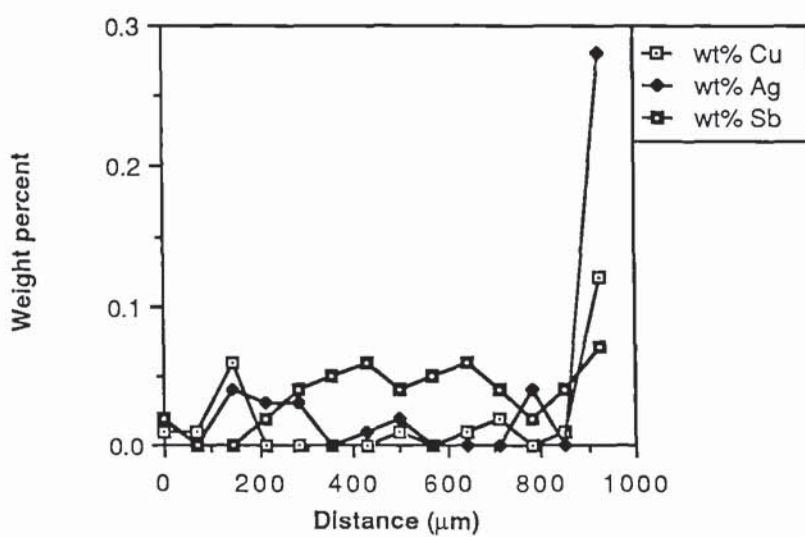


Table 4.5. Summary statistics of the major and minor element chemistry of tellurbismuth.

Statistics	Lead	Bismuth	Sulphur	Tellurium	Antimony	Cadmium	Silver	Total
Minimum	0	43.8	0	41.75	.47	.21	0	94.52
Maximum	6.53	54.47	.12	47.31	.89	.51	.79	99.55
Mean	.31	49.73	.01	46.49	.75	.36	.1	97.76
Median	0	50.01	0	46.58	.76	.36	0	97.83
Std. deviation	.88	1.28	.02	.72	.06	.07	.19	.82
Std. error	.09	.13	0	.07	.01	.01	.02	.08
Kurtosis	25.92	5.46	16.65	19.24	-2.27	-.4	2.79	2.99
Skewness	4.59	-.18	3.59	-3.63	-.74	-.02	1.98	-1.02
Minimum	0	33.87	0	55.01	.64	.3	0	100
Maximum	5.09	43.83	.6	60.31	1.18	.74	1.18	100
Mean	.24	38.73	.04	59.3	1	.52	.16	100
Median	0	38.79	0	59.38	1.01	.52	0	100
Std. deviation	.69	1	.09	.64	.08	.1	.28	•
Std. error	.07	.1	.01	.06	.01	.01	.03	•
Kurtosis	25.45	11.37	17.02	19.86	2.27	-.41	2.7	•
Skewness	4.55	-.12	3.65	-3.41	-.77	-.02	2	•

Figure 4.6a. Histogram of the distribution of lead in tellurbismuth.

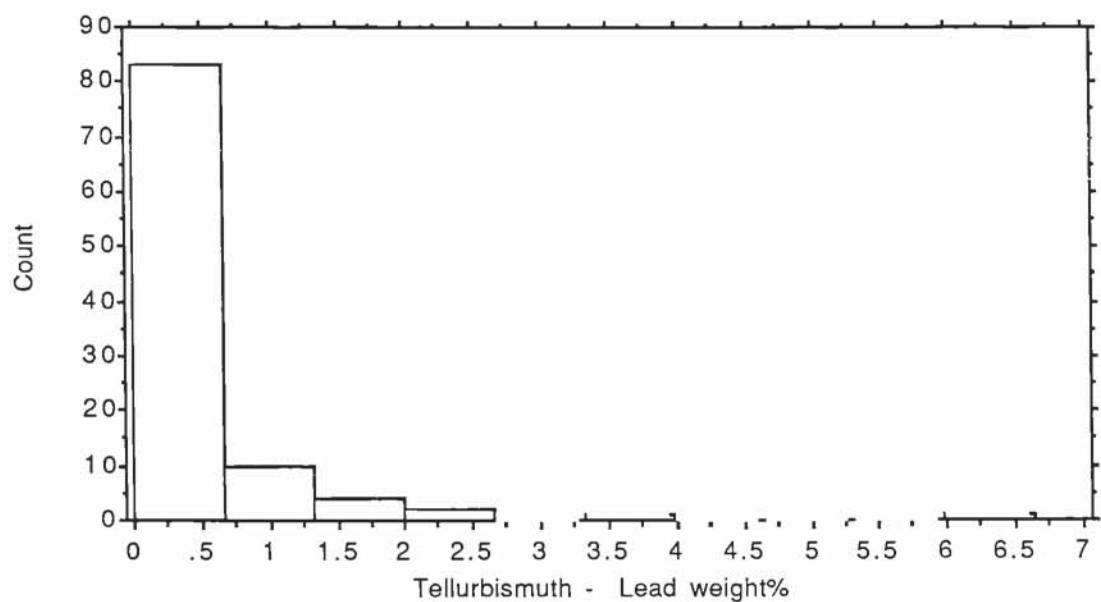


Figure 4.6b. Histogram of the distribution of bismuth in tellurbismuth.

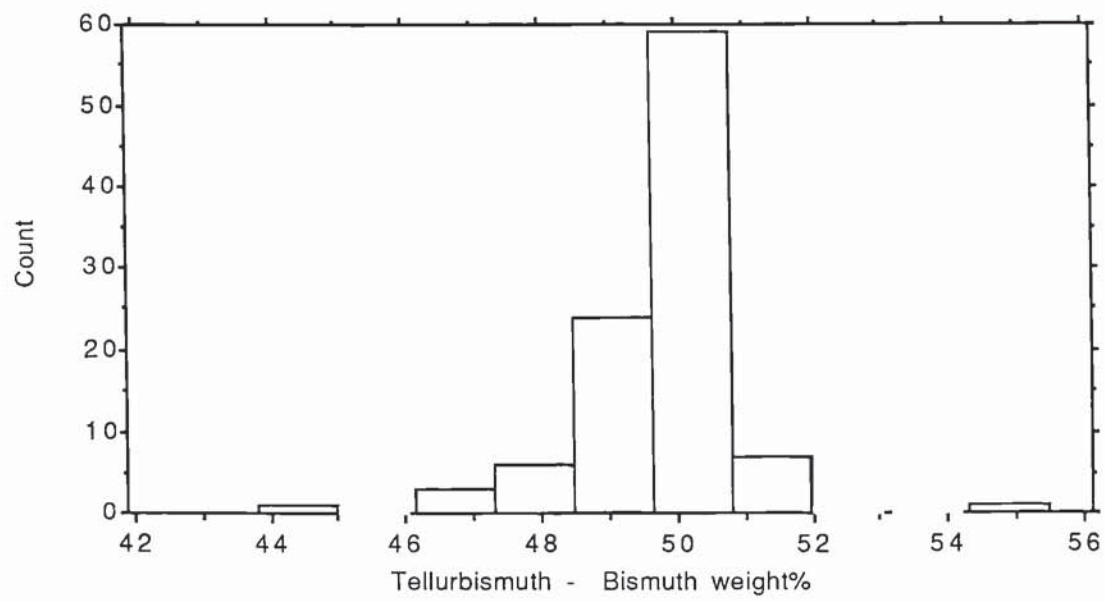


Figure 4.6c. Histogram of the distribution of sulphur in tellurbismuth.

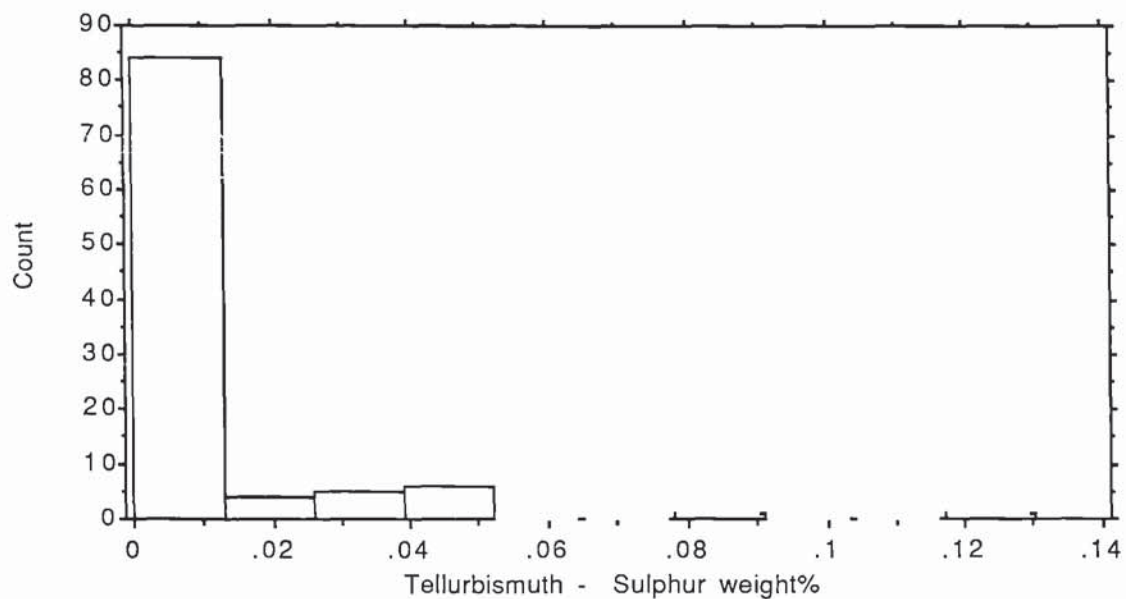


Figure 4.6d. Histogram of the distribution of tellurium in tellurbismuth.

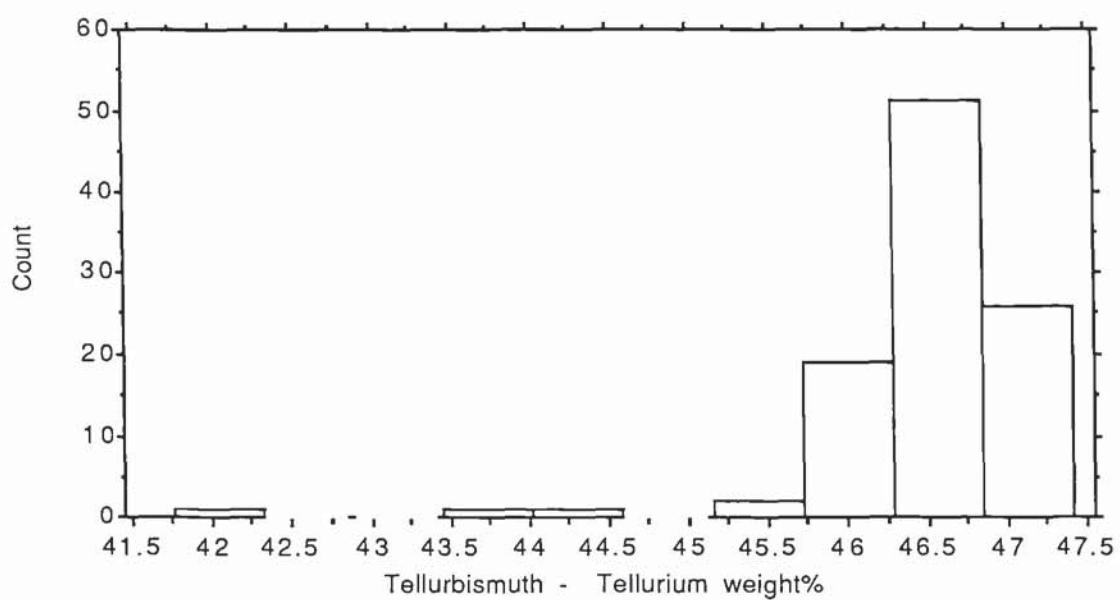


Figure 4.6e. Histogram of the distribution of antimony in tellurbismuth.

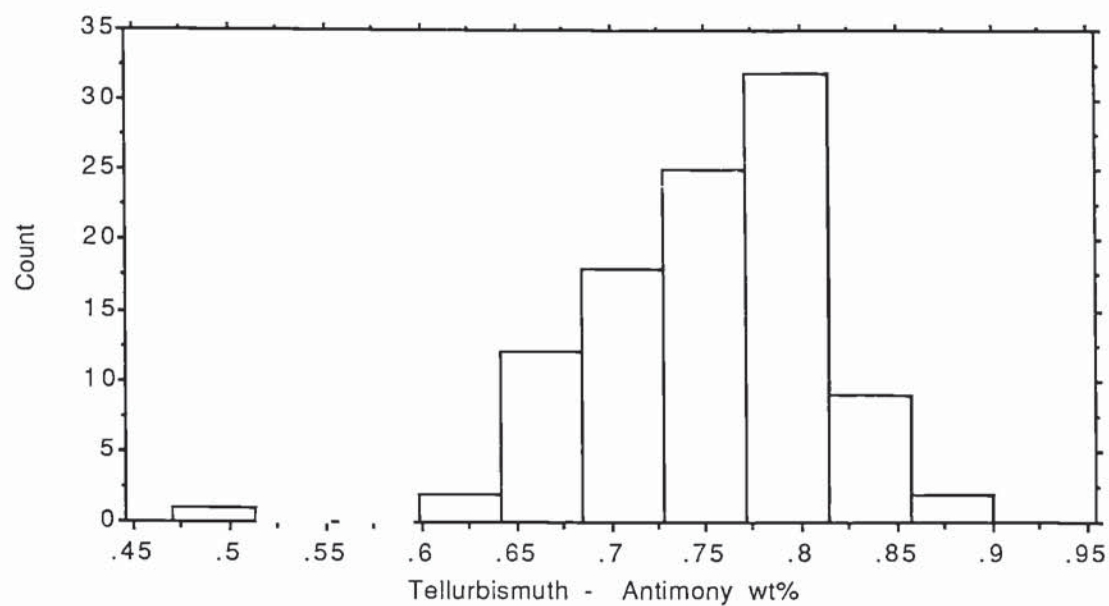


Figure 4.6f. Histogram of the distribution of cadmium in tellurbismuth.

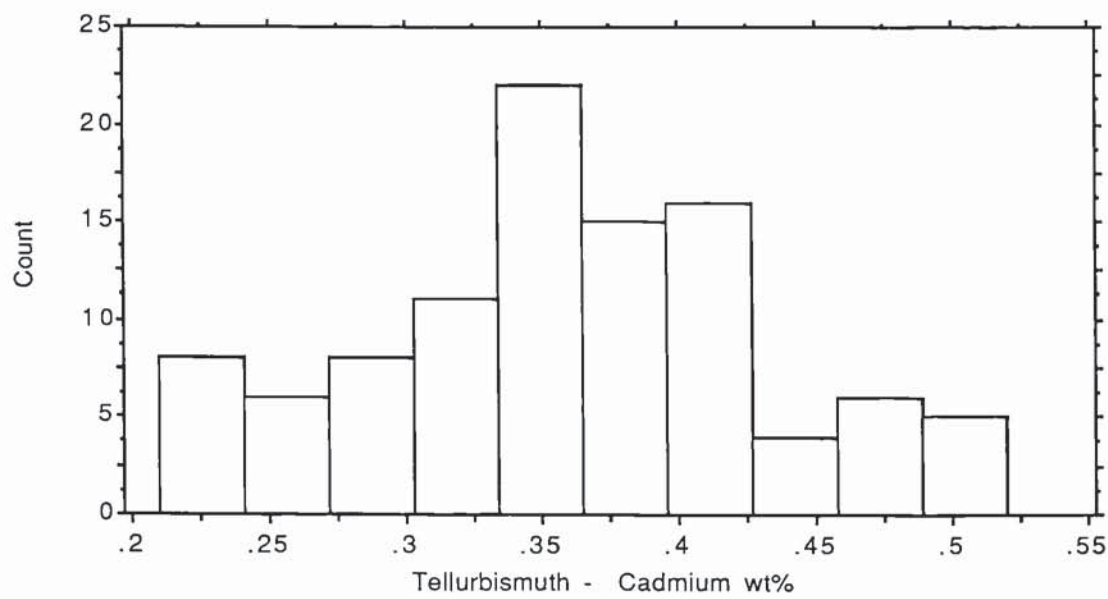


Figure 4.6g. Histogram of the distribution of silver in tellurbismuth.

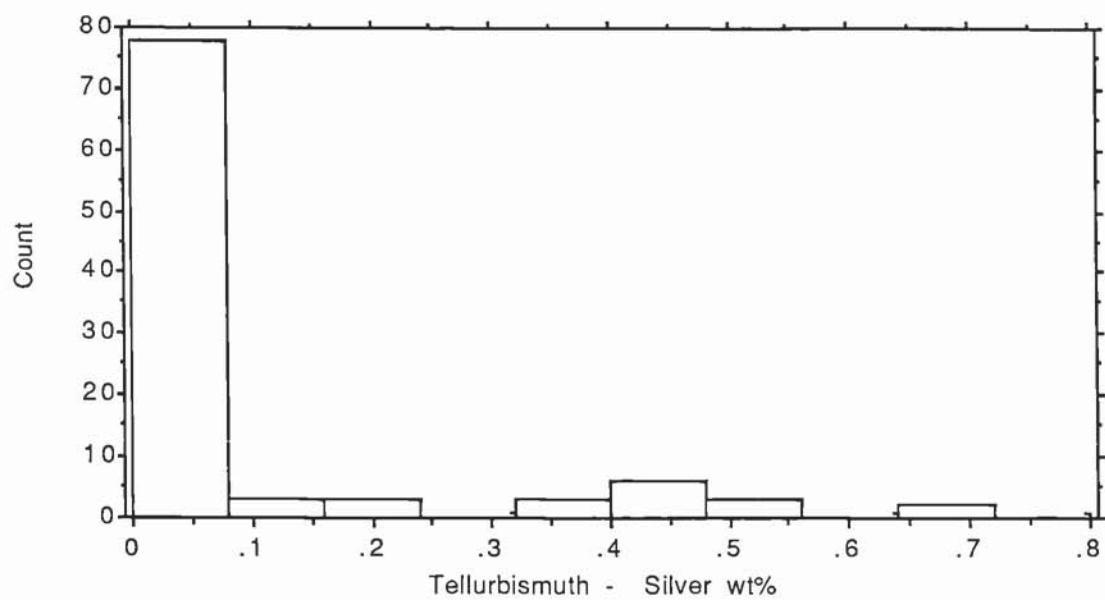


Table 4.6. Correlation matrix for the major and minor elements in tellurbismuth.

	Lead	Bismuth	Sulphur	Tellurium	Antimony	Cadmium	Silver
Lead	1
Bismuth	-.779	1
Sulphur	.127	-.191	1
Tellurium	-.225	-.074	-.095	1	.	.	.
Antimony	.058	-.177	.138	.434	1	.	.
Cadmium	-.038	.05	.021	.087	-.197	1	.
Silver	.86	-.746	.071	-.255	-.051	-.041	1

Table 4.7. Summary statistics of the major and minor element chemical data for Tetradymite.

Statistics	Lead	Bismuth	Sulphur	Tellurium	Antimony	Cadmium	Silver	Total
Minimum	.58	48.95	3.69	29.87	0	.03	0	.
Maximum	10.93	56.17	5.56	35.16	.88	.57	.12	95.55
Mean	7.56	51.97	5.18	32.18	.75	.32	.02	100.72
Median	7.94	51.93	5.21	32.1	.75	.31	0	98.03
Std. deviation	1.63	1.06	.24	.77	.08	.09	.03	97.98
Std. error	.13	.09	.02	.06	.01	.01	0	.89
Kurtosis	3.89	2.71	8.45	3.46	56.23	1.05	2.45	.07
Skewness	-1.77	.7	-2	.87	-6.01	.26	1.64	.45
Minimum	.4	30.05	17.34	33.96	0	.03	0	100
Maximum	7.96	38.7	24.03	49.14	1.03	.72	.12	100
Mean	5.13	35.1	22.79	35.69	.87	.4	.02	100
Median	5.41	34.97	23	35.45	.87	.39	0	100
Std. deviation	1.1	.9	.88	1.2	.09	.12	.03	.
Std. error	.09	.07	.07	.1	.01	.01	0	.
Kurtosis	4.06	7.86	9.53	15.28	50.74	1.26	2.45	.
Skewness	-1.74	.18	-2.37	2.99	-5.41	.28	1.64	.

Figure 4.7. X-Y plot showing the variation of the molar ratios of Bi, Te, S, Sb and Cd in tetradymite, showing a large variation in the concentrations of the major elements Bi, Te and S.

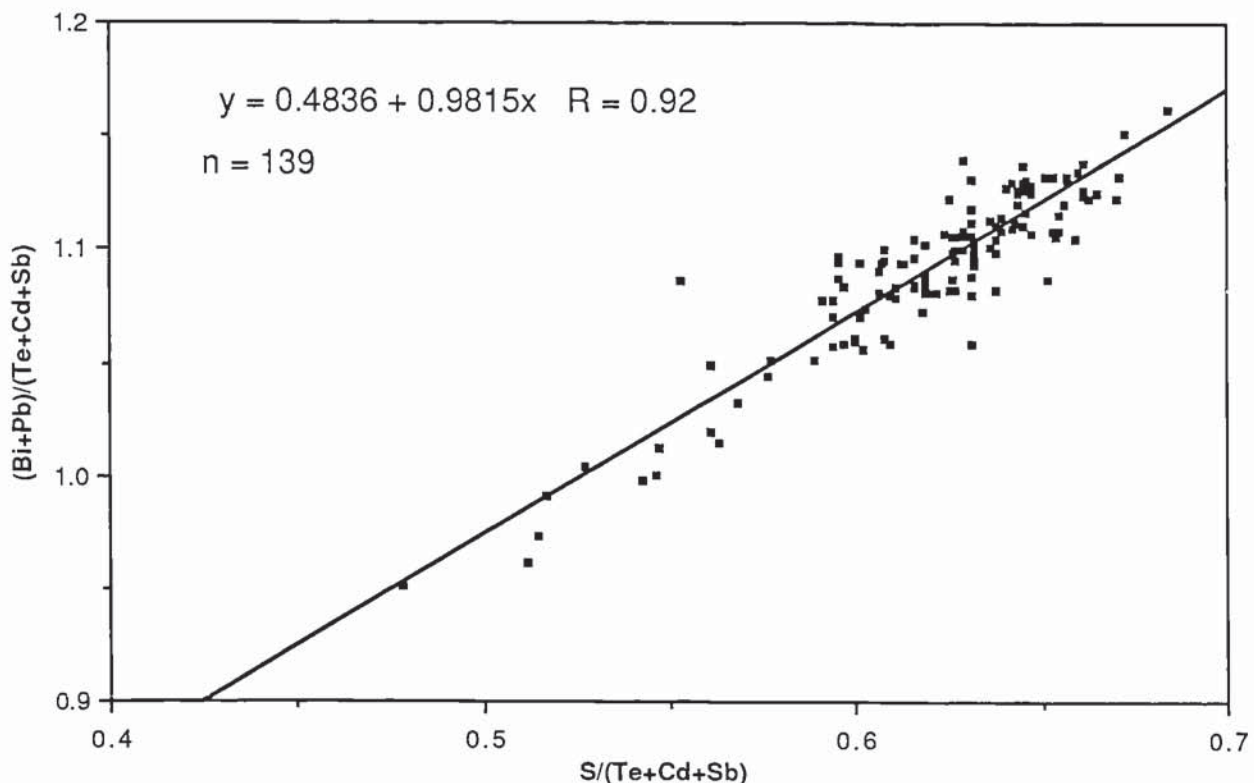


Figure 4.8. X-Y plots of the molar ratios $(\text{Bi}+\text{Pb})/(\text{Te}+\text{Cd}+\text{Sb})$ and $\text{S}/(\text{Te}+\text{Cd}+\text{Sb})$ versus Total wt%, showing that the molar ratio is not correlated with the total weight percent of an analysis, indicating that the correlation illustrated in fig. 4.7 is real and not an artifact of the analyses.

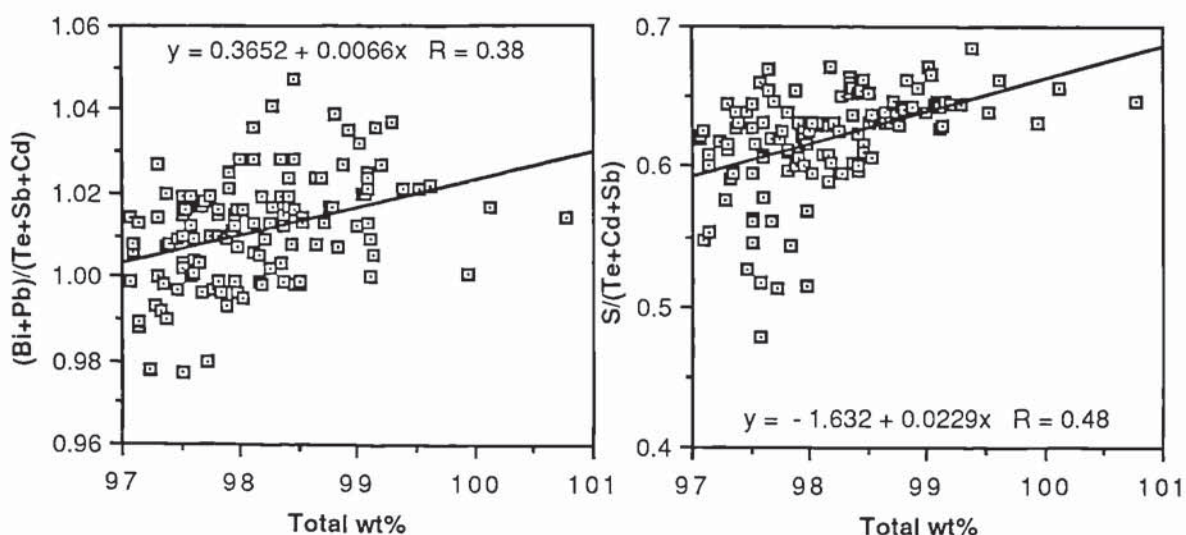


Table 4.8. Correlation matrix for the major and minor elements in tetradyomite.

	Lead	Bismuth	Sulphur	Tellurium	Antimony	Cadmium	Silver
Lead	1	.	-
Bismuth	-.731	1
Sulphur	.636	-.317	1
Tellurium	-.821	.809	-.489	1	.	.	.
Antimony	-.136	.081	-.037	.143	1	.	.
Cadmium	-.095	-.113	-.085	-.033	-.023	1	.
Silver	-.155	.163	-.215	.142	.128	.001	1

Figure 4.9a. Histogram showing the distribution of lead in tetradymite.

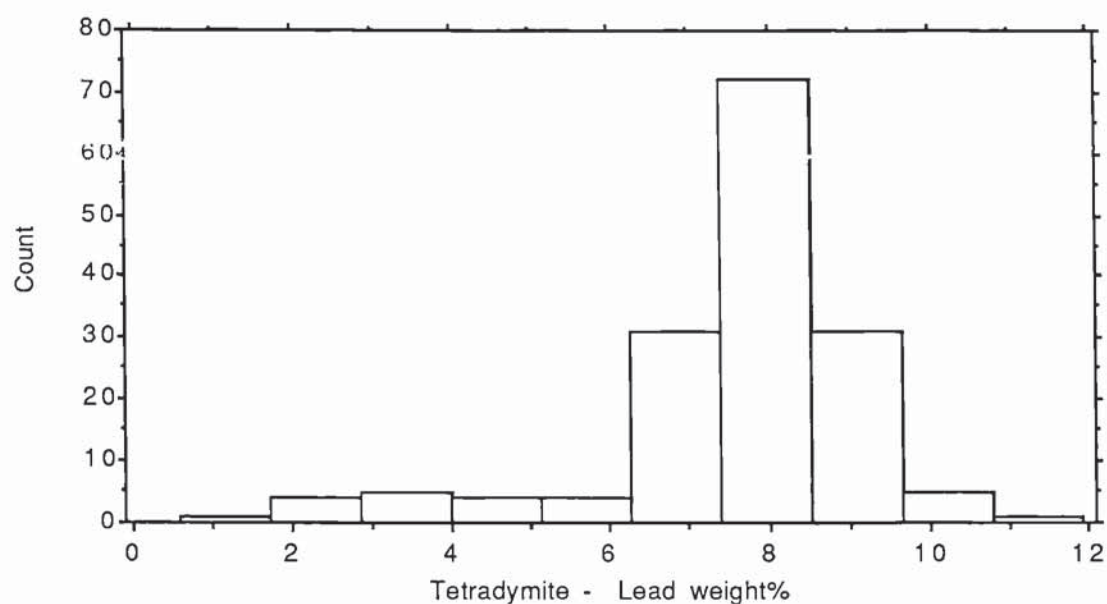


Figure 4.9b. Histogram showing the distribution of bismuth in tetradymite.

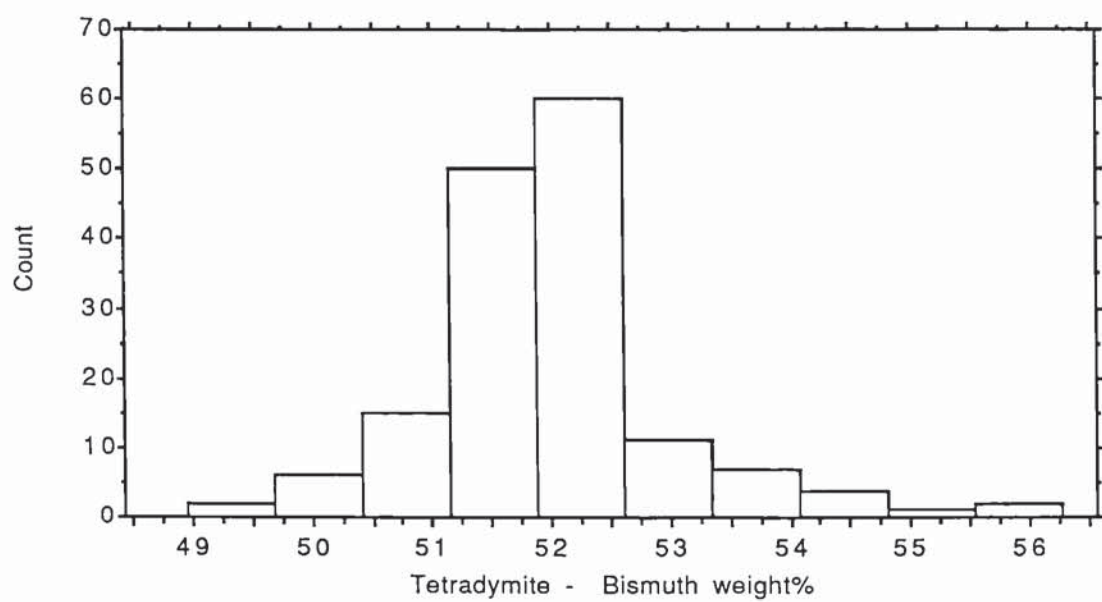


Figure 4.9c. Histogram showing the distribution of sulphur in tetradyomite.

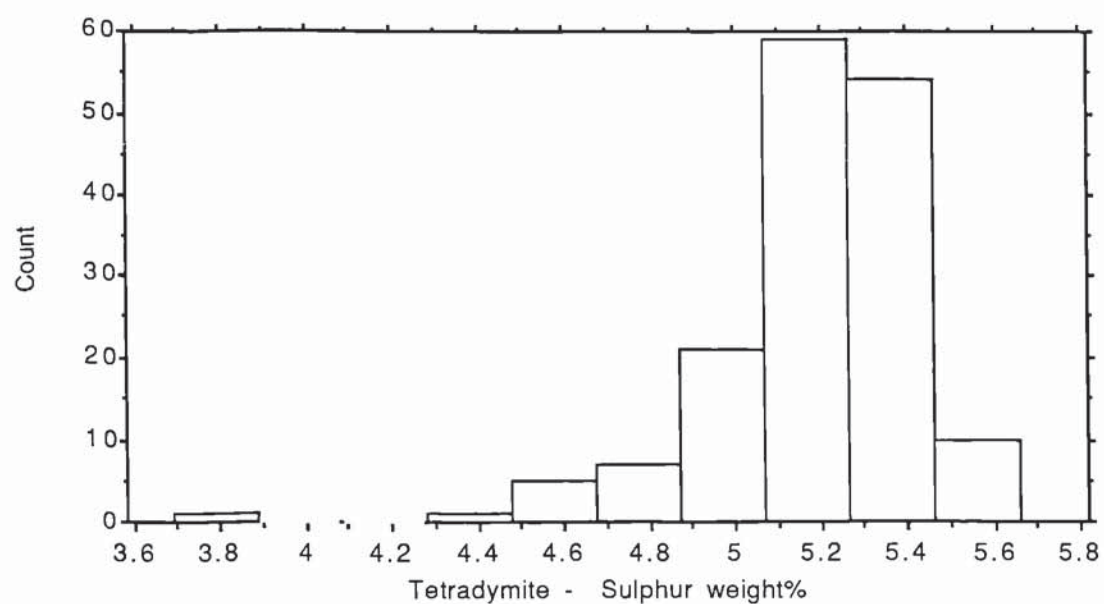


Figure 4.9d. Histogram showing the distribution of tellurium in tetradyomite.

Figure 4.9e. Histogram showing the distribution of antimony in tetradyomite.

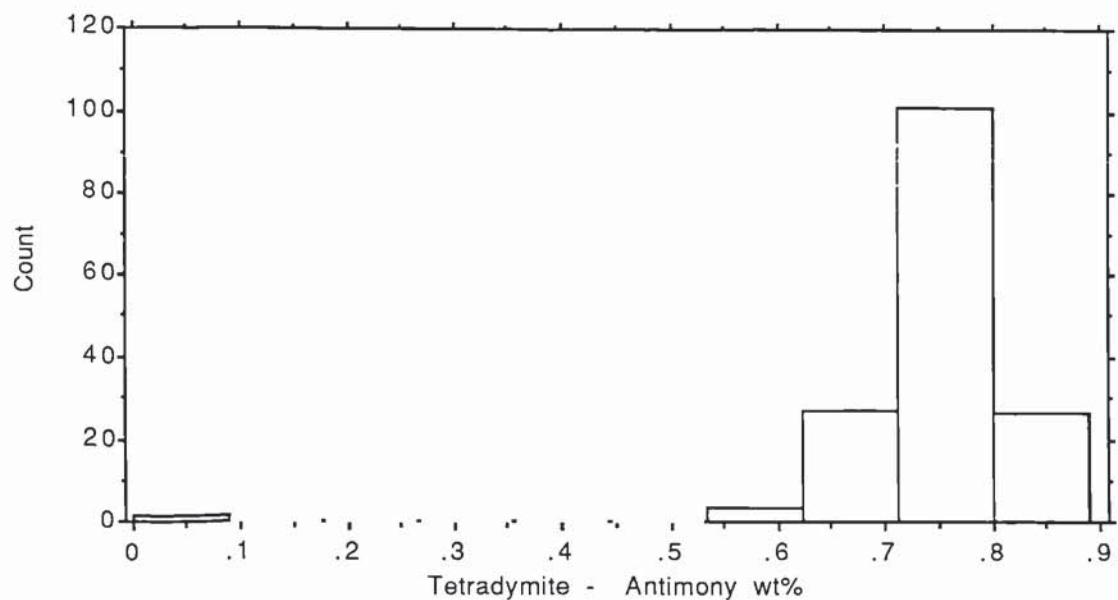


Figure 4.9f. Histogram showing the distribution of cadmium in tetradyomite.

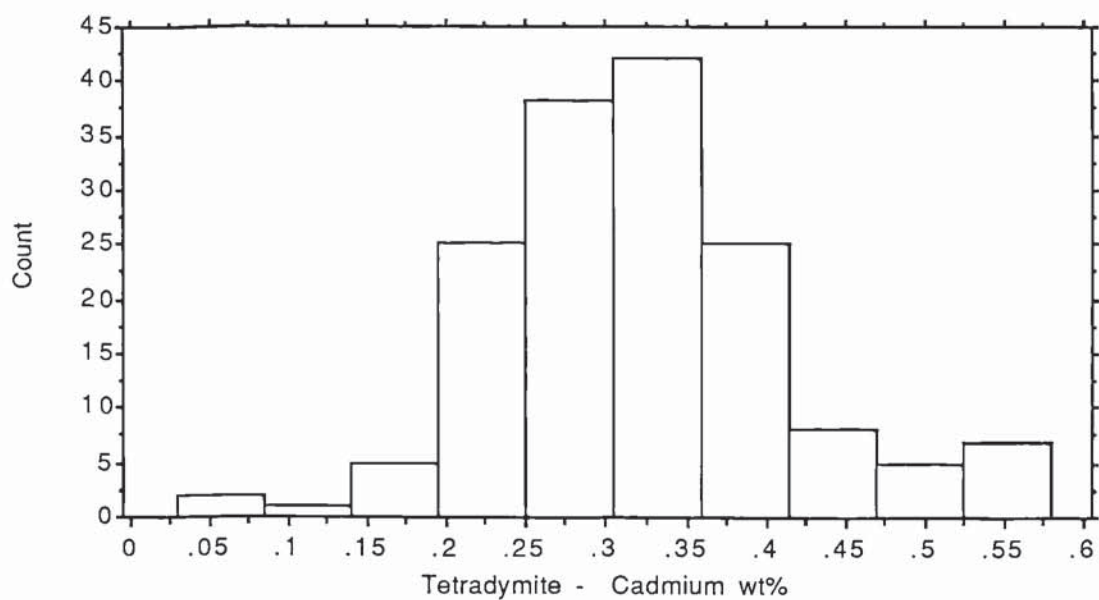


Figure 4.9g. Histogram showing the distribution of silver in tetradyomite.

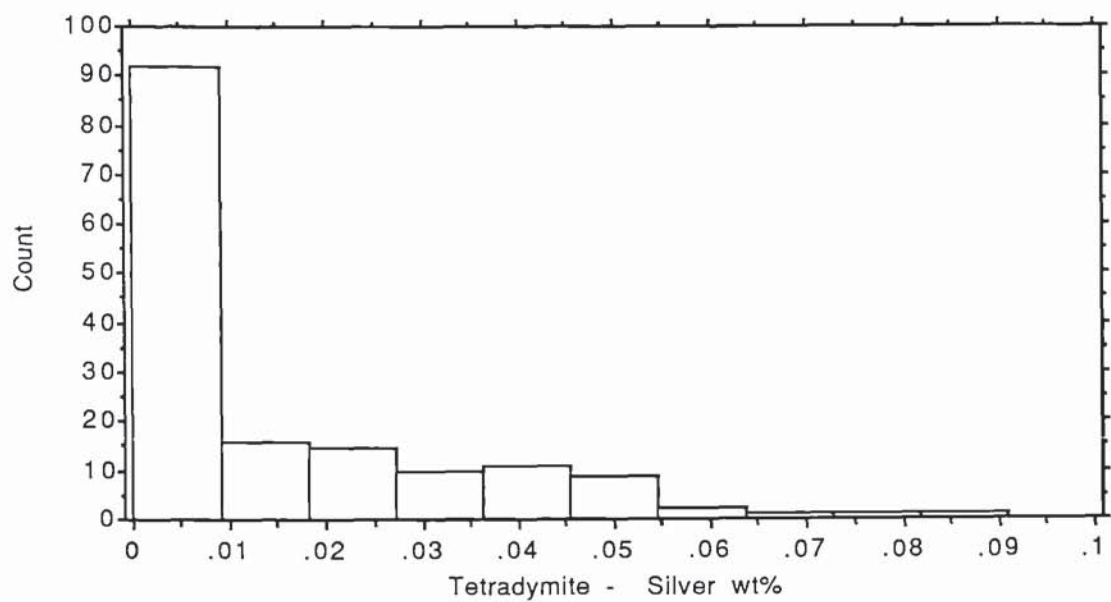


Table 4.9. Summary statistics of the major and minor element data for galena from the tellurbismuth-dominated telluride assemblage.

Statistics	Lead	Bismuth	Sulphur	Tellurium	Antimony	Cadmium	Silver	Total
Minimum	84.43	.53	13.17	0	0	0	0	99.43
Maximum	86.08	4.04	13.74	.51	.11	.24	.19	102.46
Mean	85.44	.95	13.41	.16	.06	.05	0	100.13
Median	85.54	.85	13.4	0	.06	.05	0	100.39
Std. deviation	.43	.55	.16	.2	.04	.07	.05	.55
Std. error	.07	.09	.03	.03	.01	.01	.01	.09
Kurtosis	.26	26.13	-.83	-1.54	-.93	-.53	2.45	7.79
Skewness	-.95	5.12	.36	.47	-.52	.63	1.94	2.31
Minimum	45.72	.3	46.89	0	0	0	0	100
Maximum	49.81	7.19	50.83	.48	.11	.26	.21	100
Mean	49.13	.73	49.81	.15	.06	0	.03	100
Median	49.26	.49	49.85	0	.06	.08	0	100
Std. deviation	.73	1.17	.63	.18	.04	.05	.06	•
Std. error	.12	.2	.11	.03	.01	.08	.01	•
Kurtosis	12	25.6	11.44	-1.53	-.91	-.5	2.45	•
Skewness	-3.08	5.13	-2.72	.47	-.49	.67	1.95	•

Figure 4.10a. Line concentration profile across a tetradyomite-galena-tellurbismuth intergrowth, showing the variation in antimony concentration between tellurbismuth, teradymite and galena.

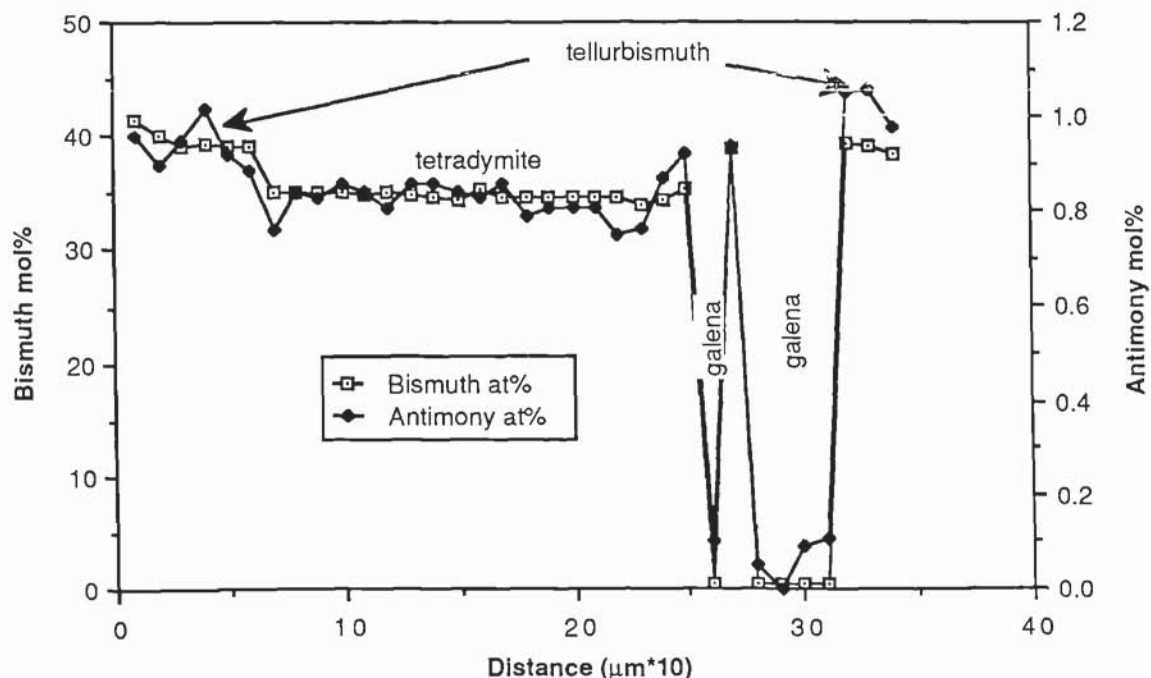


Figure 4.10b. Line concentration profile across a galena-tellurbismuth intergrowth, showing the variation in antimony concentration between the tellurbismuth and galena.

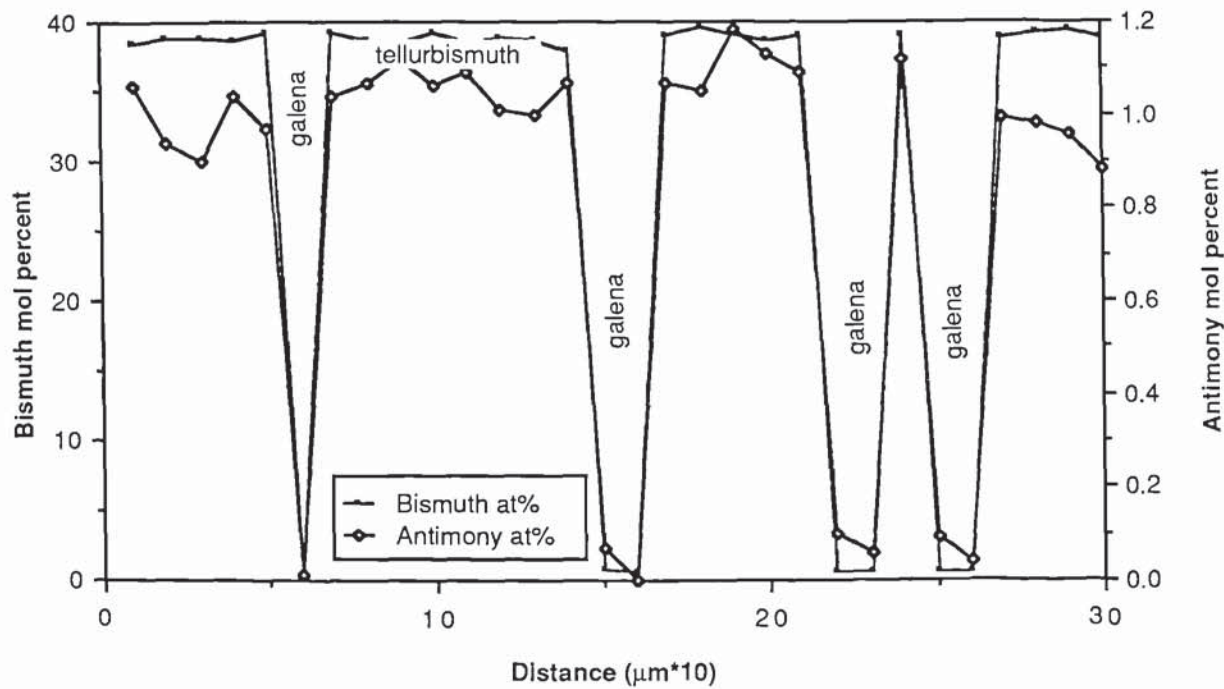


Figure 4.11. Histogram of the distribution of tellurium in galena from the tellurbismuth-dominated assemblage.

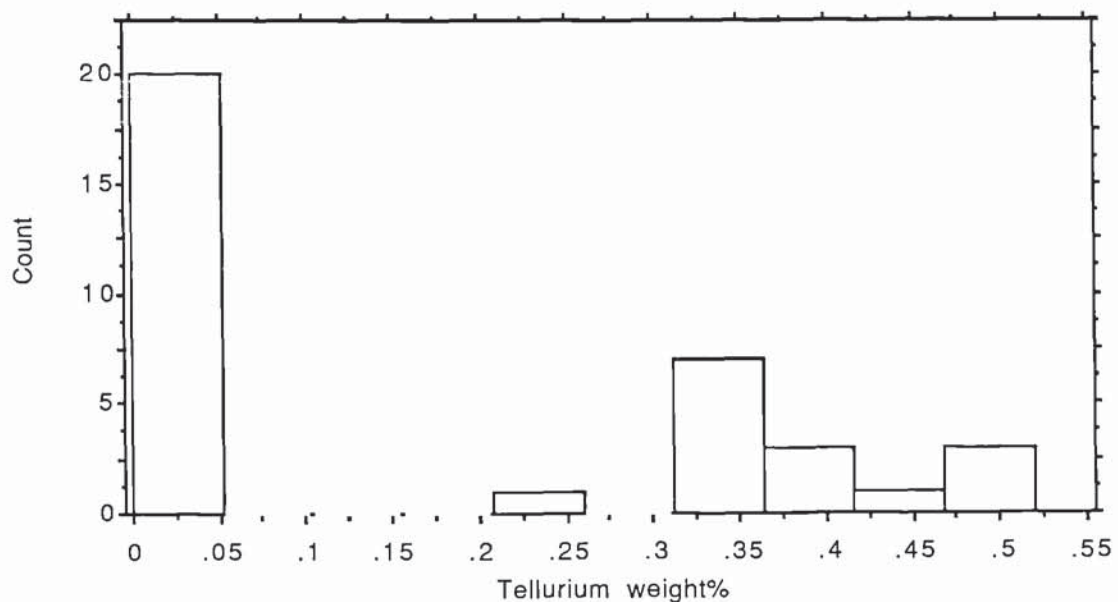


Figure 4.12. Histogram of the distribution of bismuth in galena from the tellurbismuth-dominated assemblage.

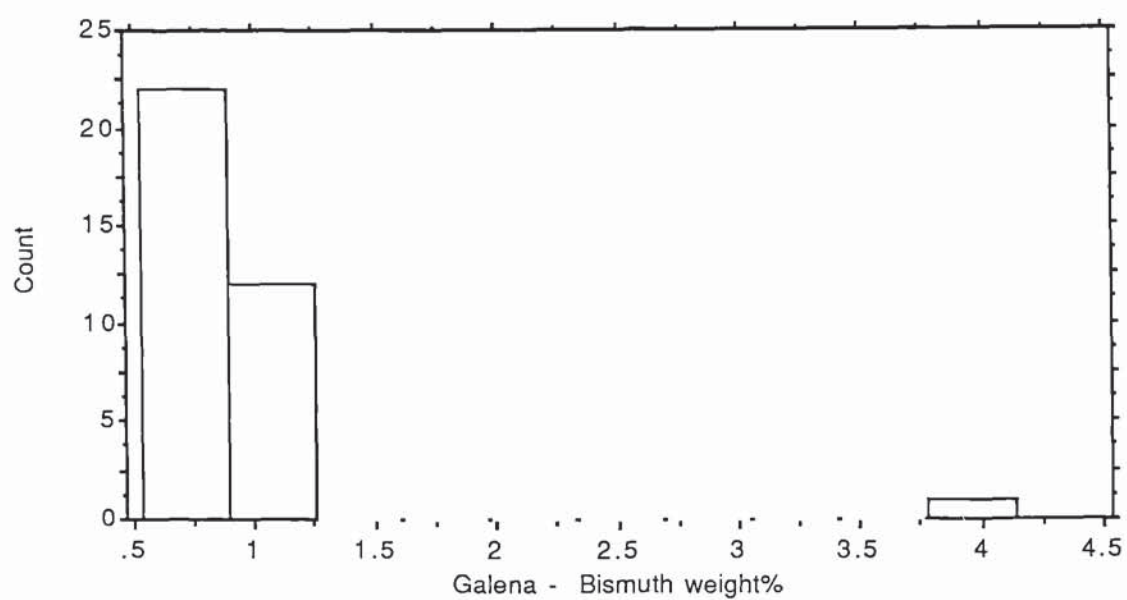


Table 4.10. Correlation matrix for major and minor element chemistry in galena from the tellurbismuth-dominated telluride assemblage.

	Lead	Bismuth	Sulphur	Tellurium	Antimony	Cadmium	Silver
Lead	1
Bismuth	-.457	1
Sulphur	-.169	-.038	1
Tellurium	-.391	.227	.072	1	.	.	.
Antimony	-.007	-.307	.337	.081	1	.	.
Cadmium	-.108	.038	-.272	.1	-.053	1	.
Silver	-.118	.304	-.282	-.111	-.308	-.317	1

Table 4.11. Summary statistics of the major and minor element chemical data for the fingerprint intergrowths.

Statistics	Lead	Bismuth	Sulphur	Tellurium	Antimony	Cadmium	Silver	Total
Minimum	13.78	36.03	2.53	22.19	.24	.05	0	96.47
Maximum	33.48	48.73	5.85	29.73	.6	.42	.1	99.32
Mean	25.79	40.69	4.3	26.89	.39	.32	.21	97.7
Median	26.05	40.73	4.42	26.56	.37	.31	0	97.67
Std. deviation	5.58	3.62	.8	2.14	.1	.09	.03	.87
Std. error	1.44	.93	.21	.55	.03	.01	.01	.23
Kurtosis	-.41	-1.01	.34	72.38	-.39	1.05	2.46	-.48
Skewness	-.59	.69	-2	7.26	.57	.26	1.67	.41
Statistics for weight%								
Minimum	9.74	25.42	12.69	25.92	.29	.07	0	100
Maximum	23.8	35.64	25.87	36.72	.7	.6	.13	100
Mean	18.72	24.32	20.12	31.03	.48	.3	.03	100
Median	18.81	29.15	20.64	31.36	.45	.3	0	100
Std. deviation	3.97	2.88	3.24	2.95	.12	.14	.04	•
Std. error	1.02	.74	.84	.76	.03	.04	.01	•
Kurtosis	-.18	-.06	.24	-.64	-.71	-.09	1.81	•
Skewness	-.73	.73	-.33	-.02	.31	.29	1.54	•
Statistics for mol%								

Figure 4.13. Box plots showing the statistical variation of antimony between tellurbismuth, tetradyomite, galena and the fingerprint intergrowths.

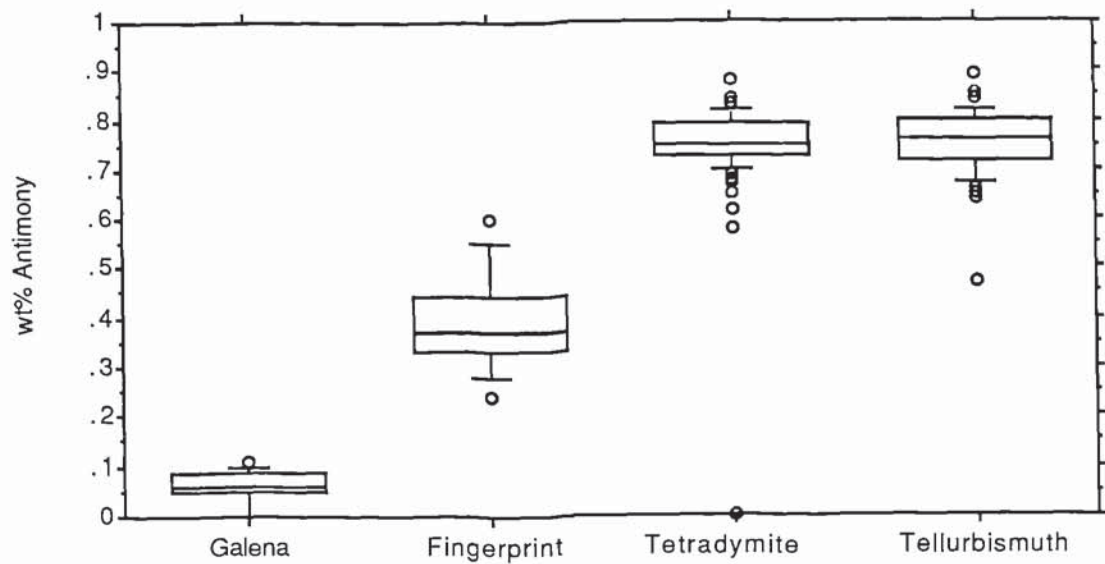


Figure 4.14. Box plots showing the statistical variation of cadmium between tellurbismuth, tetradyomite, galena and the fingerprint intergrowths.

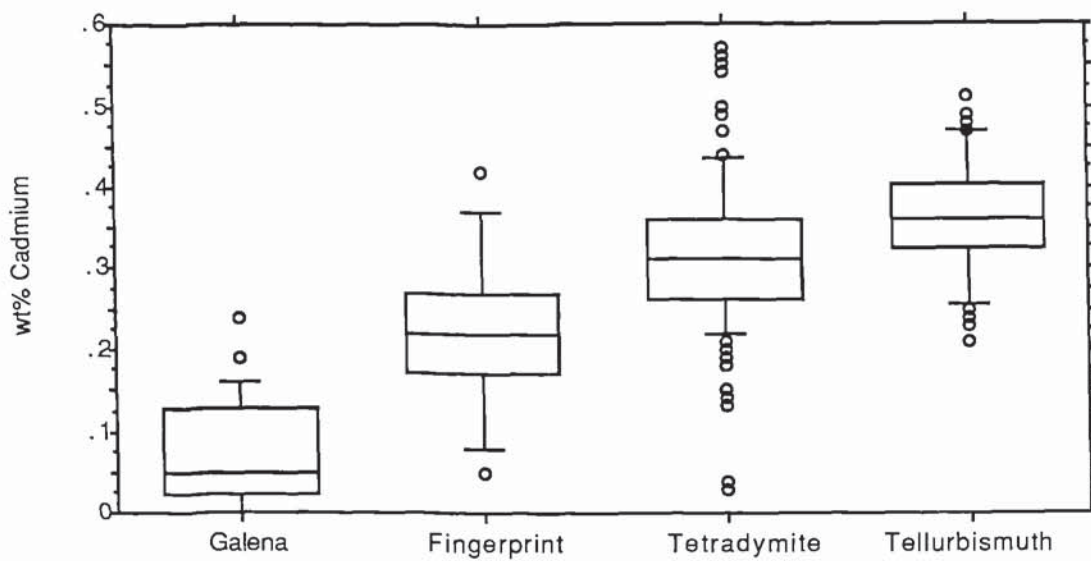


Figure 4.15. Box plots showing the statistical variation of silver between tellurbismuth, tetradymite, galena and the fingerprint intergrowths.

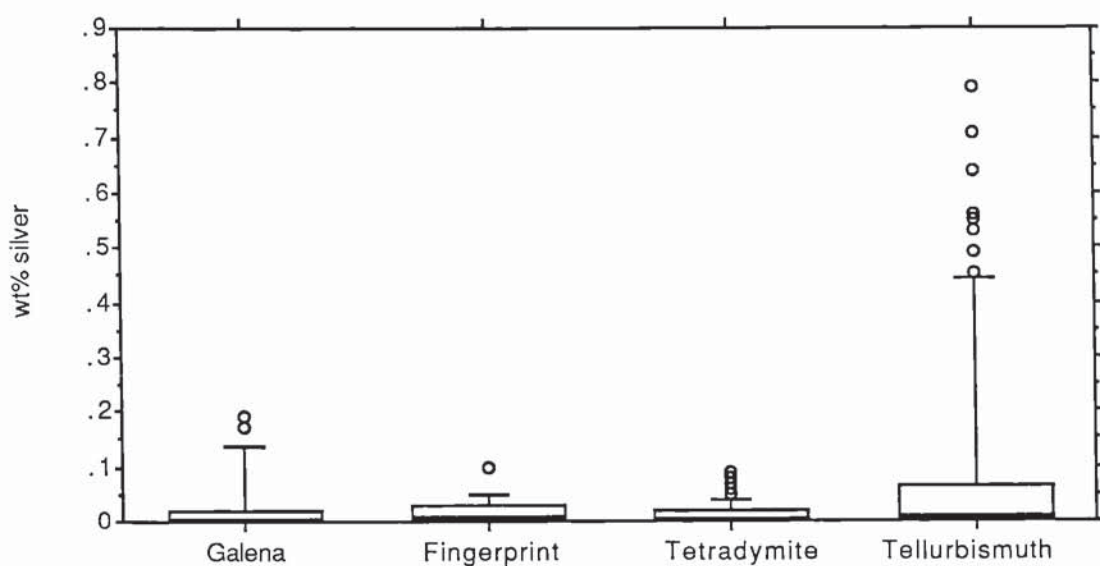


Table 4.12 Summary statistics of the major and minor element chemical data for galena from the sulphide-dominated telluride assemblage.

Statistics	Lead	Bismuth	Sulphur	Tellurium	Antimony	Cadmium	Silver	Total
Minimum	81.72	.09	12.25	0	.03	0	0	98.18
Maximum	87.39	3.3	13.69	.54	.7	.3	1.28	102.08
Mean	85.37	1.14	12.92	.08	.09	.08	.16	99.82
Median	85.71	.8	12.88	0	.08	.07	0	99.77
Std. deviation	1.16	.78	.25	.16	.06	.05	.32	.75
Std. error	.1	.07	.02	.01	.01	.01	.03	.07
Kurtosis	.69	.91	.94	.63	92.98	3.92	1.97	-.11
Skewness	-.98	1.6	.73	1.58	9.06	1.43	1.8	.34
Minimum	47.21	.05	47.66	0	.03	0	0	100
Maximum	51.37	1.89	50.87	.51	.7	.32	1.42	100
Mean	50.03	.66	48.9	.08	.08	.09	.17	100
Median	50.46	.47	48.88	0	.08	.08	0	100
Std. deviation	1.04	.42	.46	.15	.06	.06	.35	•
Std. error	.09	.04	.04	.01	.01	.01	.03	•
Kurtosis	.25	.93	1.79	1.79	92.82	3.94	2.01	•
Skewness	-1.28	1.58	.61	.61	9.05	1.42	1.8	•

Figure 4.16. Histograms comparing the distribution of tellurium in galena between the two telluride assemblages.

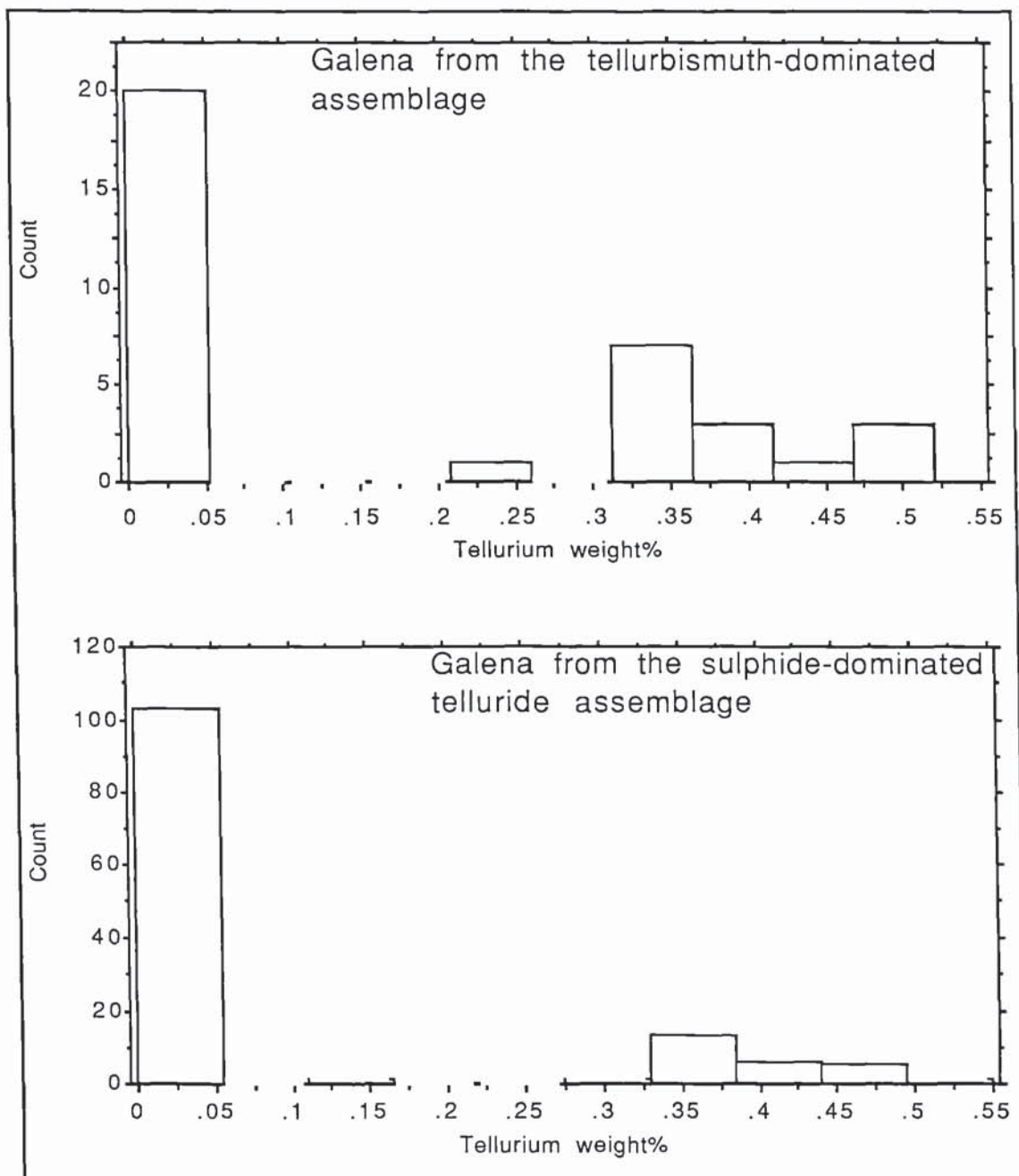


Figure 4.17. Histograms comparing the distribution of silver in galena between the two telluride assemblages.

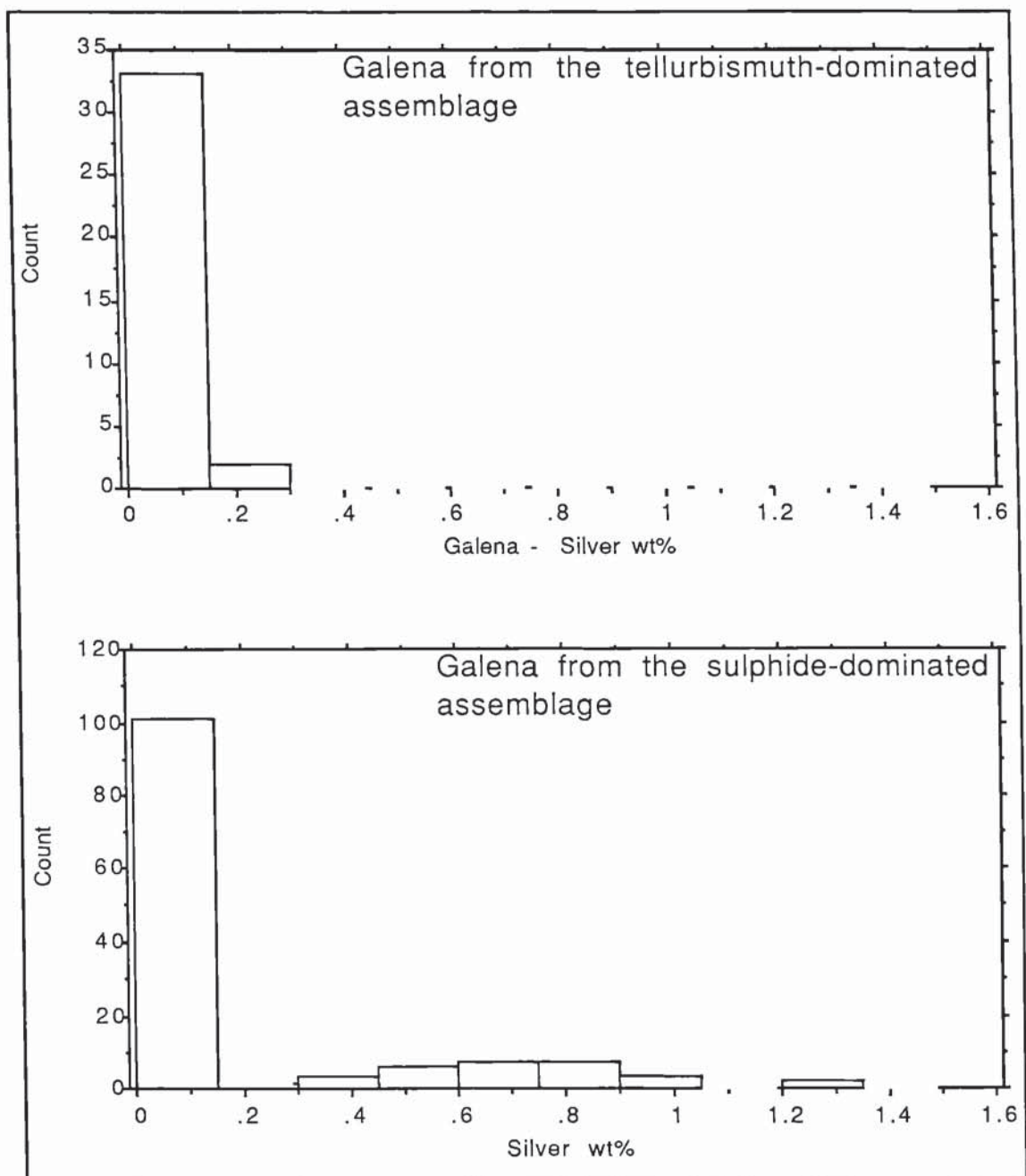


Figure 4.18. Histograms comparing the distribution of bismuth in galena between the two telluride assemblages.

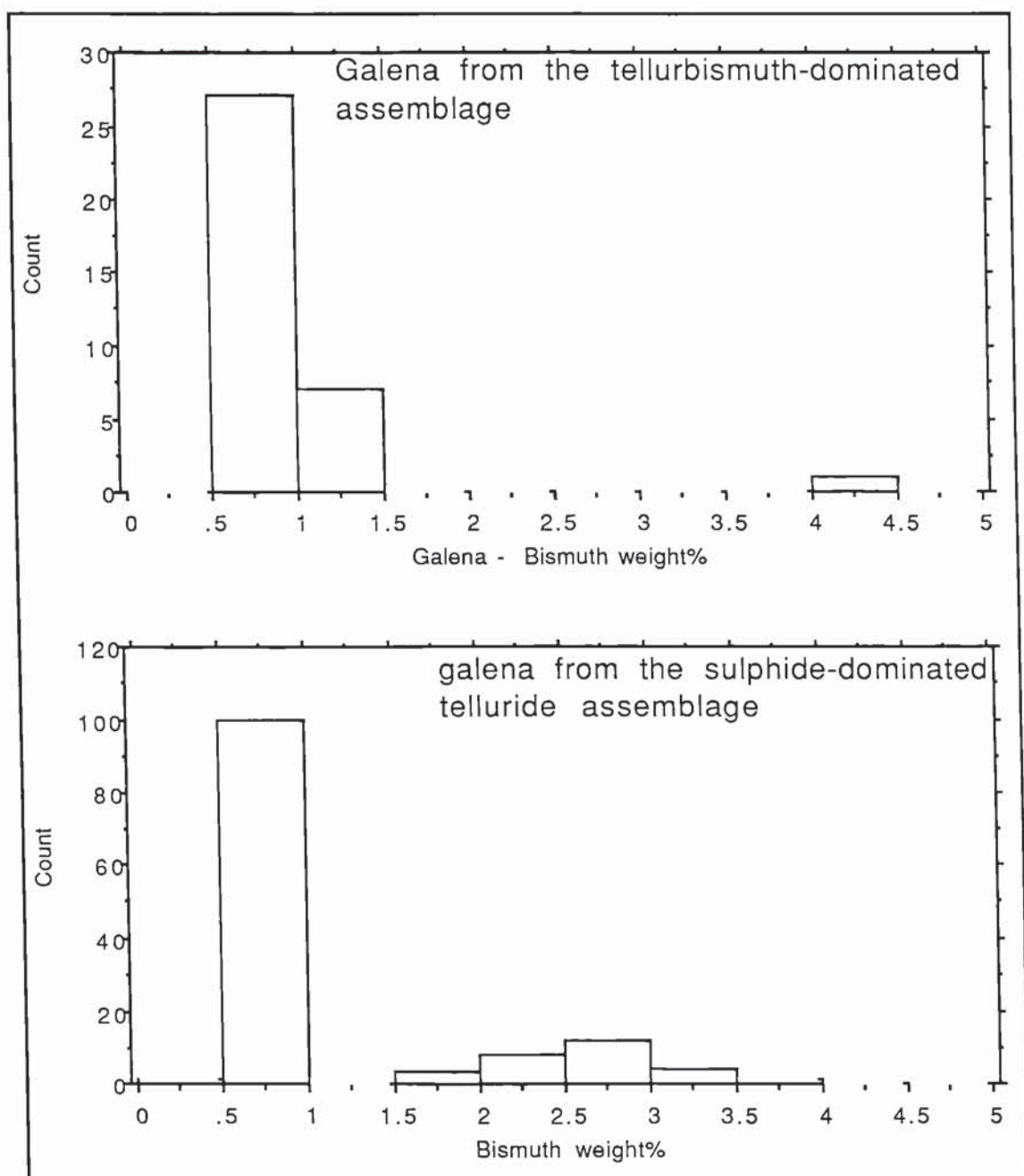


Figure 4.19. Histograms comparing the distribution of cadmium in galena between the two telluride assemblages.

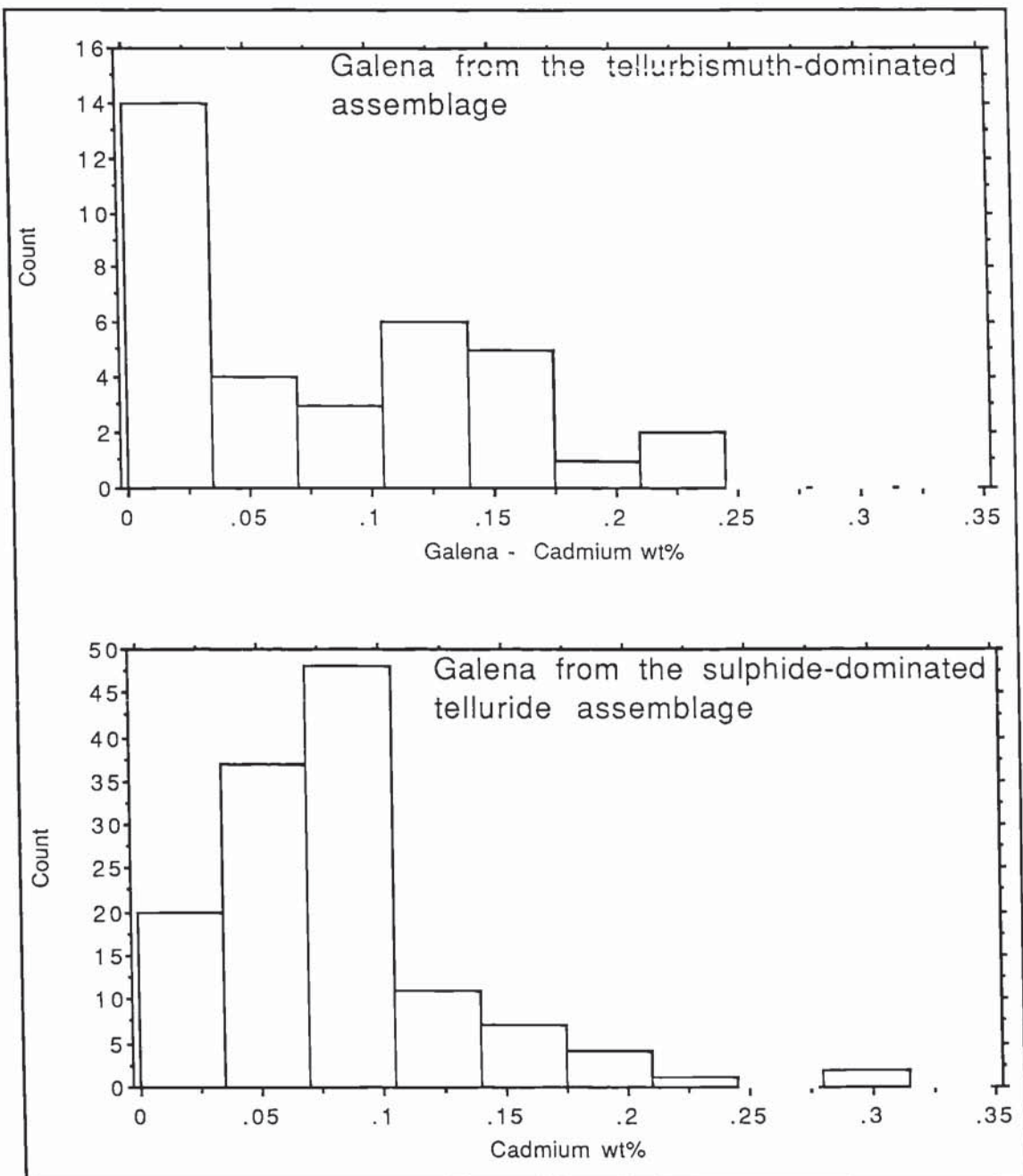


Table 4.13. Correlation matrix for the major and minor elements in galena from the sulphide-dominated telluride assemblage.

	Lead	Bismuth	Sulphur	Tellurium	Antimony	Cadmium	Silver
Lead	1
Bismuth	-.345	1
Sulphur	-.595	-.454	1
Tellurium	.027	-.087	-.009	1	.	.	.
Antimony	.099	-.047	-.085	-.022	1	.	.
Cadmium	-.011	.105	-.064	-.03	.076	1	.
Silver	-.395	.512	.151	-.032	-.062	.284	1

Table 4.14a. Analyses of the minor tellurides, bismuthinite, and native bismuth from No. 4 Level. The bottom line of each analysis is the atomic percent of each element analysed (tr=trace, nd=not detected).

Pb	Bi	S	Te	Sb	Cd	Ag	Total	SAMPLE DETAILS.
0.50 0.25	79.84 39.32	18.7 60.03	nd nd	.38 .32	nd nd	.08 .08	99.50 100.00	bismuthinite.....Mineral JN 12 (cobaltite and galena).....Sample no.
0.76 0.38	79.76 39.74	18.21 59.13	.09 0.07	.59 0.50	.08 0.07	.1 .1	99.59 100.00	bismuthiniteMineral JN 12 (cobaltite and galena).....Sample no.
0.3 0.15	80.01 39.63	18.50 59.73	nd nd	0.45 0.38	nd nd	.11 .11	99.37 100.00	bismuthinite.....Mineral JN 12 (cobaltite and galena).....Sample no.
0.67 0.34	79.91 39.65	18.36 59.38	.07 .06	0.58 0.49	nd nd	0.09 0.09	99.68 100.00	bismuthinite.....Mineral JN 12 (cobaltite and galena).....Sample no.
0.42 0.33	59.52 47.01	0.06 0.31	39.48 51.06	0.95 1.29	nd nd	nd nd	100.43 100.00	?wehrliteMineral BM Kingsbury Clogau mine (K3)....Sample no.
nd nd	57.47 45.15	nd nd	41.75 53.72	0.47 0.63	0.34 0.50	nd nd	100.03 100.00	?wehrliteMineral JN 12 (cobaltite and galena).....Sample no.
59.58 48.16	0.55 0.44	0.03 0.16	37.97 49.83	.88 1.21	nd nd	0.13 0.20	99.14 100.00	altaite.....Mineral BM Kingsbury Clogau mine (K5)....Sample no.
60.33 48.64	0.13 0.1	nd. nd	38.13 49.91	.79 1.08	nd nd	0.17 0.26	99.55 100.00	altaite.....Mineral JN 4 (Tellurides in quartz).....Sample no.
0.13 0.07	0.31 0.17	0.08 0.29	36.87 33.07	.53 .5	0.41 0.42	61.73 65.49	100.06 100.00	hessite.....Mineral JN 6 (Galena in quartz)Sample no.
.08 .04	0.11 0.06	nd nd	37.23 33.46	.12 .11	0.09 0.09	62.31 66.23	99.94 100.00	hessite.....Mineral JN 4 (Tellurides in quartz).....Sample no.
0.14 0.14	97.72 98.44	0.06 0.39	nd nd	.59 1.02	nd nd	nd nd	98.51 100.00	native bismuth.....Mineral JN 12 (cobaltite and galena).....Sample no.
0.18 0.18	98.63 97.73	0.09 0.58	nd nd	.89 1.51	nd nd	nd nd	99.79 100.00	native bismuth.....Mineral JN 12 (cobaltite and galena).....Sample no.
0.12 0.16	78.08 70.16	tr tr	19.33 28.45	0.51 0.79	nd nd	nd nd	98.22 100	hedleyitemineral BM Kingsbury Clogau Mine (K3)....Sample no.

Table 4.14b. Analyses of the sulphosalts in BM Kingsbury (K2). The bottom line of each analysis is the atomic percent of each element analysed (na=not analysed, nd=not detected).

Cu	Ag	Fe	Zn	Sn	Pb	As	Sb	S	Total	SAMPLE DETAILS.
41.76	nd	na	na	0.14	na	1.03	28.29	28.32	99.54	stibioluzonitemineral
36.76	nd	na	na	0.07	na	0.77	13.00	49.40	100.00	BM Kingsbury Clogau Mine (K2)..Sam. no.
41.38	0.03	na	na	0.14	na	0.94	28.39	28.31	99.19	stibioluzonitemineral
36.56	0.02	na	na	0.07	na	0.70	13.09	49.56	100.00	BM Kingsbury Clogau Mine (K2)..Sam. no.
41.37	nd	na	na	0.14	na	1.07	28.15	28.37	99.1	stibioluzonitemineral
36.53	nd	na	na	0.07	na	0.80	12.97	49.64	100.00	BM Kingsbury Clogau Mine (K2)..Sam. no.
41.53	nd	na	na	0.15	na	0.85	28.3	28.50	99.33	stibioluzonite
36.57	nd	na	na	0.07	na	0.63	13.00	49.73	100.00	BM Kingsbury Clogau Mine (K2)..Sam. no.
41.56	0.46	na	na	0.15	na	0.73	28.69	28.63	100.22	stibioluzonitemineral
36.38	0.24	na	na	0.07	na	0.54	13.11	49.66	100.00	BM Kingsbury Clogau Mine (K2)..Sam. no.
13.96	nd	nd	na	na	42.02	nd	25.72	18.11	99.81	bournonitemineral
18.33	nd	nd	na	na	16.92	nd	17.63	47.12	100.00	BM Kingsbury Clogau Mine (K2)..Sam. no.
13.80	nd	0.02	na	na	41.73	na	25.03	18.18	98.76	bournoniteminera
18.23	nd	0.03	na	na	16.9	nd	17.25	47.59	100.00	BM Kingsbury Clogau Mine (K2)..Sam. no.
13.73	nd	na	na	na	42.16	nd	25.45	18.15	99.49	bournonitemineral
18.09	nd	na	na	na	17.03	nd	17.50	47.38	100.00	BM Kingsbury Clogau Mine (K2)..Sam. no.
13.92	nd	nd	na	na	41.89	nd	25.63	18.07	99.51	bournonitemineral
18.33	nd	nd	na	na	16.91	nd	17.61	47.15	100.00	BM Kingsbury Clogau Mine (K2)..Sam. no.
41.71	0.49	2.50	3.89	na	na	3.73	21.93	25.49	99.74	tetrahedrite.....mineral
36.67	0.25	2.50	3.32	na	na	2.78	10.06	44.41	100.00	BM Kingsbury Clogau Mine (K2)..Sam. no.
40.89	0.70	2.61	3.23	na	na	4.03	21.56	26.23	99.25	tetrahedrite.....mineral
35.85	0.36	2.60	2.75	na	na	3.00	9.86	45.57	100.00	BM Kingsbury Clogau Mine (K2)..Sam. no.
0.25	nd	0.09	0.18	na	55.19	1.08	24.4	18.12	99.31	boulangeritemineral
0.37	nd	0.15	0.26	na	25.26	1.37	19.00	53.59	100.00	BM Kingsbury Clogau Mine (K2)..Sam. no.
0.24	nd	0.07	0.11	na	55.50	0.72	24.23	18.53	99.40	boulangeritemineral
0.36	nd	0.12	0.16	na	25.24	0.91	18.76	54.46	100.00	BM Kingsbury Clogau Mine (K2)..Sam. no.
0.57	0.09	0.10	0.13	na	54.98	0.98	24.7	18.05	99.60	boulangeritemineral
0.85	0.08	0.17	0.19	na	25.09	1.24	19.18	53.22	100.00	BM Kingsbury Clogau Mine (K2)..Sam. no.

Figure 4.20. Histogram of the fineness of gold from No. 4 Level.

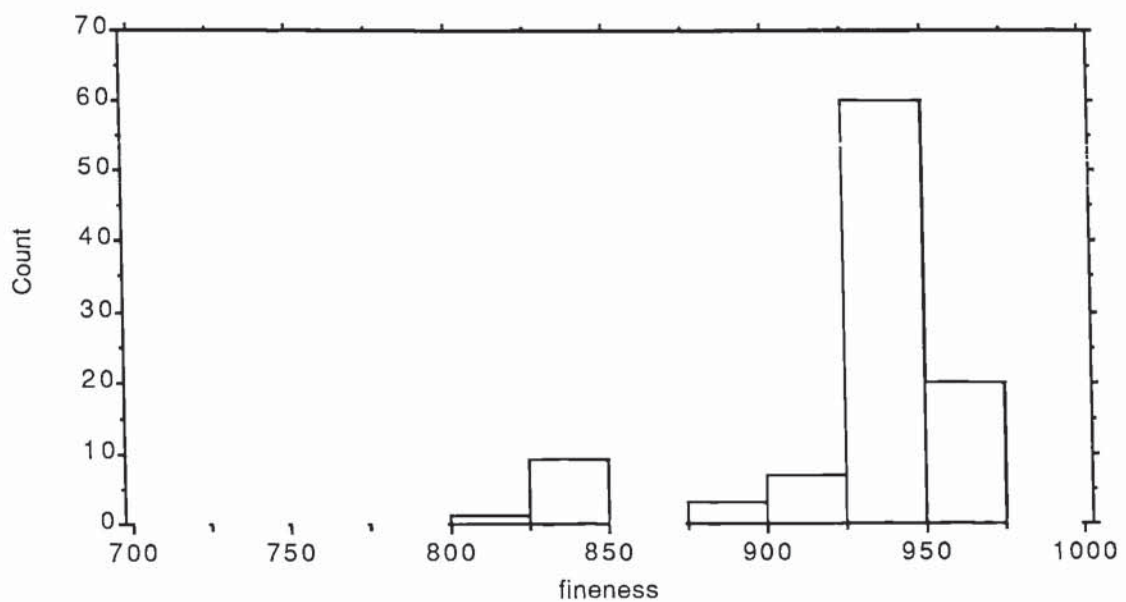


Figure 4.21. Histogram of the fineness of placer gold from the Hirgwm river.

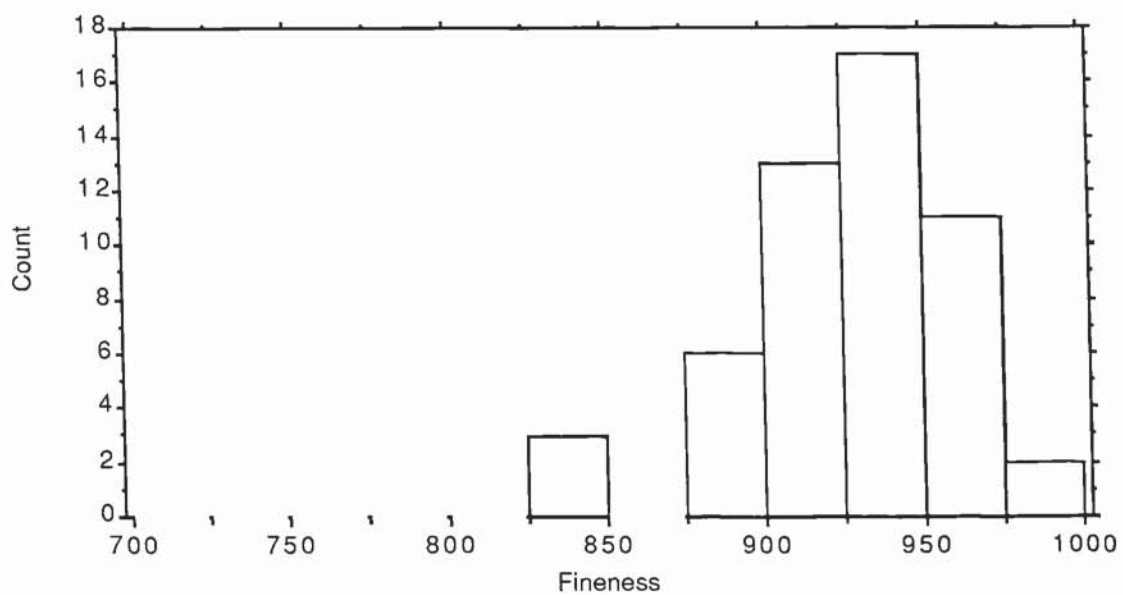


Table 4.15. Fineness of gold in gold-bearing samples loaned from the British Museum (Natural History) and the National Museum of Wales. (BM=British Museum (Natural History), NMW=National Museum of Wales). All samples are from Clogau Mine.

Ag	Au	Cu	Total	Fineness	Sample details
7.04	90.75	nd	97.79	928	BM Kingsbury (K3)
7.14	90.77	nd	97.91	927	BM Kingsbury (K3)
7.10	91.22	0.09	98.41	928	BM Kingsbury (K3)
5.94	93.13	nd	99.07	940	BM Kingsbury (K2)
5.31	95.64	nd	100.95	947	BM Kingsbury (K2)
8.43	91.73	0.07	100.23	916	BM KINGSBURY (K5)
8.76	91.54	nd	100.3	913	BM KINGSBURY (K5)
8.21	91.33	nd	99.54	918	BM KINGSBURY (K5)
5.03	94.06	nd	99.09	949	BM Kingsbury (K2)
15.54	83.8	nd	99.34	844	NMW 70.19G.M5
15.95	84.14	nd	100.09	841	NMW 70.19G.M5
15.73	83.83	nd	99.56	842	NMW 70.19G.M5
16.08	83.51	nd	99.59	839	NMW 70.19G.M5
2.78	98.8	0.07	101.65	973	NMW 77.35G.M18
2.71	98.59	0.07	101.37	973	NMW 70.19G.M221
2.77	98.84	0.09	101.70	973	NMW 70.19G.M221
2.78	98.88	0.11	101.77	973	NMW 70.19G.M221

Table 4.16. Summary statistics of the fineness of native gold from: No. 4 Level Clogau Mine, placer gold from the Hirgwm river, and the gold-bearing samples from the British Museum (Natural History) and the National Museum of Wales. All samples are from Clogau Mine.

Minimum	Maximum	Mean	Median	Std.deviation	Std. error	Kurtosis	Skewness	Data set
823	969	929	939	34	3.5	2.87	-1.96	No.4 Level gold
837	987	927	950	34	4.7	0.56	-0.86	Placer gold
839	973	919	928	49	11.9	-0.89	-0.66	Museum gold

Figures 4.22. Line concentration profile across a tellurbismuth-galena intergrowth showing the variation in major "cation" (Pb and Bi), "anion" (Te and S) and minor element (Sb and Cd) chemistries.

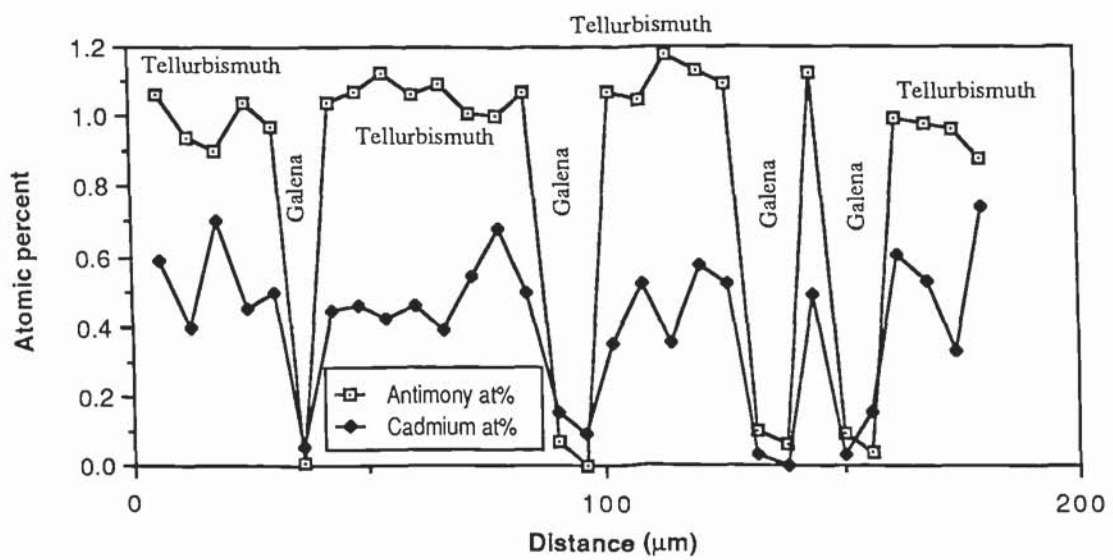
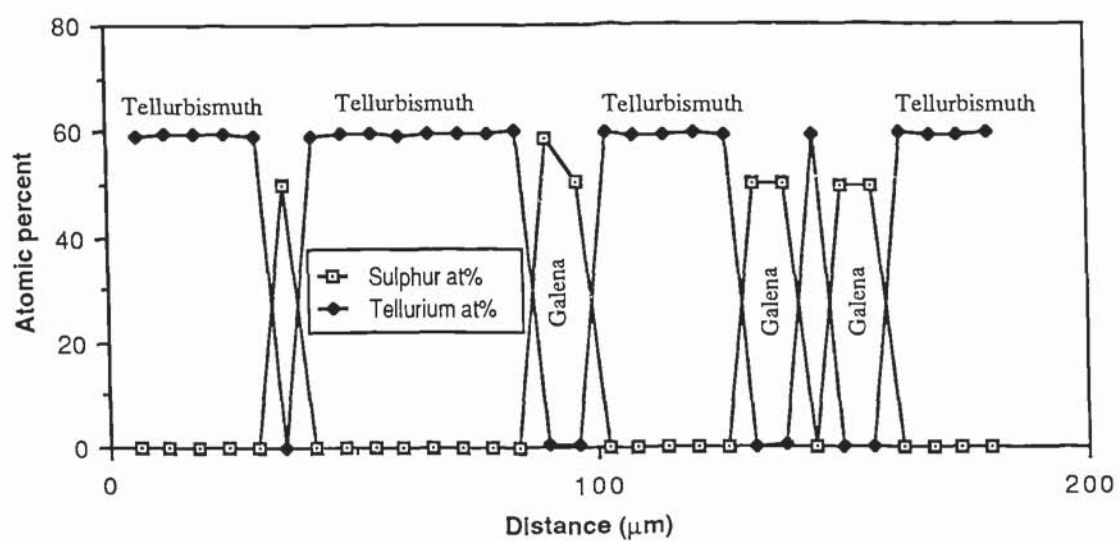
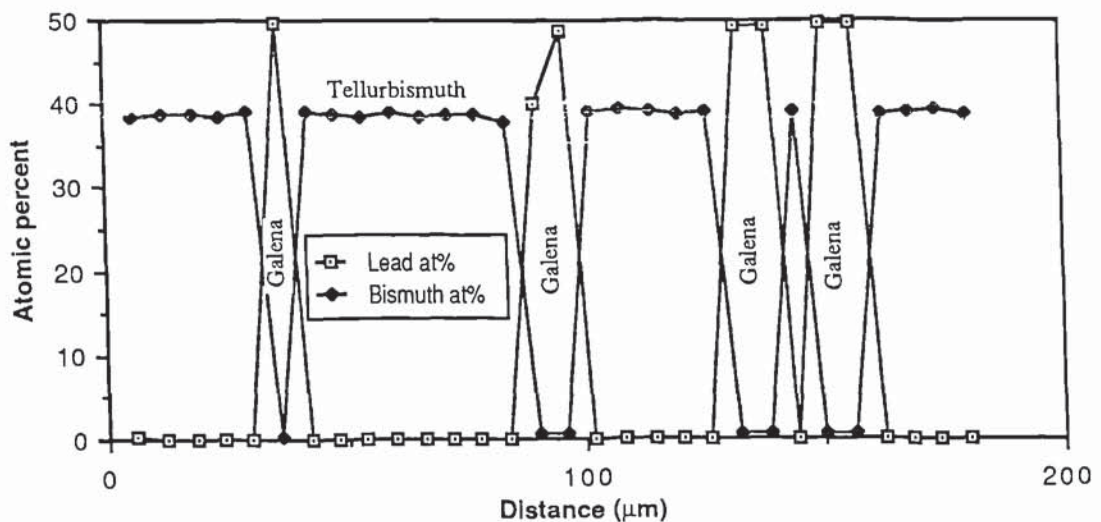


Figure 4.23 Line concentration profile across a tellurbismuth-galena-tetradymite intergrowth showing the variation in major "cation" (Pb and Bi), "anion" (S and Te) and minor element (Sb and Cd) chemistries.

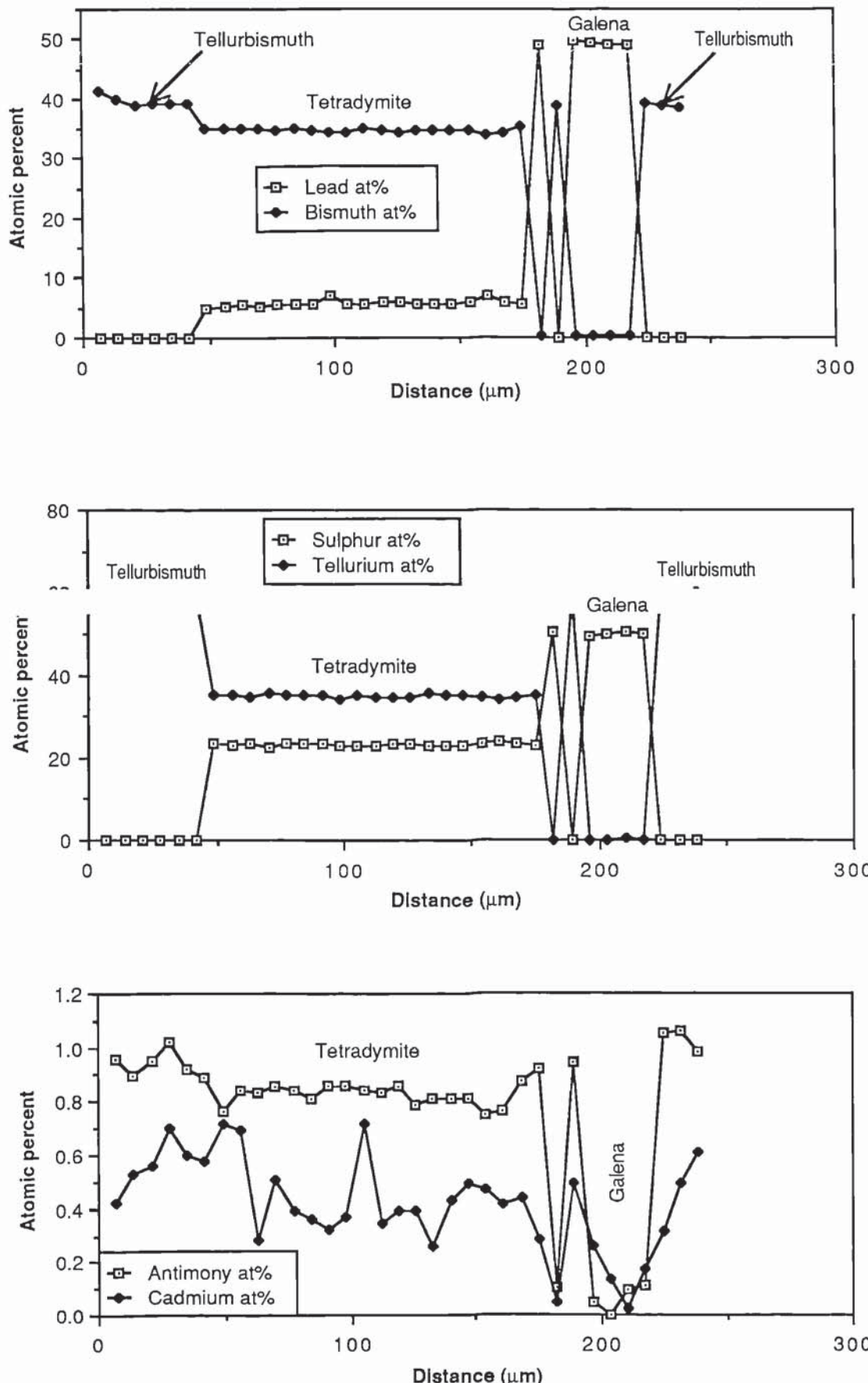
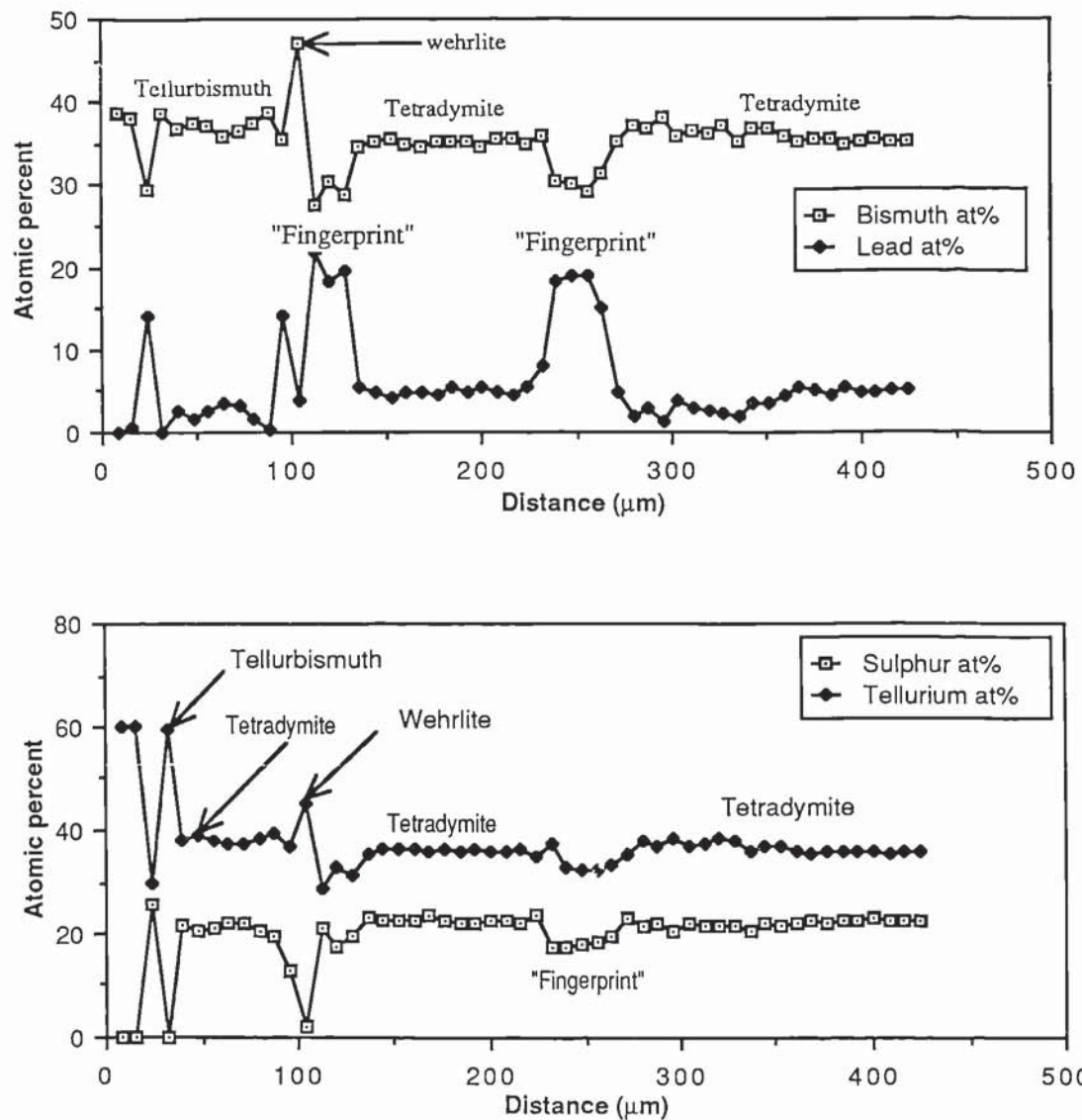


Figure 4.24. Line concentration profiles illustrating the variation in major "cation" (Pb, Bi), "anion" (Te, S) chemistries, across a fingerprint intergrowth associated with tetradyomite and tellurbismuth.



TABLES AND FIGURES FOR
CHAPTER 5:

**CONDITIONS OF ORE FORMATION
AT CLOGAU MINE.**

Table 5.1. Comparison of Gibbs Free energy between data calculated in this thesis and that by Barton and Skinner (1979).

Reaction	Temp(°K)	ΔGT (this thesis)	Δ GT (Barton& Skinner, 1979)	ΔG equation (Barton& Skinner, 1979)
4Ag+Te2=2Ag2Te reaction (5.1)	350	-45318	-45347	-55592+29.27T(25-145°C)
	400	-43964	-43884	
	460	-42718	-42618	-50087+16.10T(145-527°C)
	550	-41183	-41232	
2Pb+S2=2PbS reaction (5.2)	350	-63110	-63116	-77449+40.81T(25-327°C)
	450	-59045	-59085	
	550	-55073	-55003	
	650	-51012	-50762	-78595+48.82T(327-900°C)
2Pb+Te2=2PbS reaction (5.3)	350	-57059	-57025	-70766+39.26T(25-327°C)
	450	-53151	-53099	
	550	-49337	-49173	
	650	-45436	-45124	-72157+41.59T(327-700°C)
Au+Te2=AuTe2 reaction (5.4)	350	-29034	-29020	-42022+37.15T(25-447°C)
	450	-25212	-25305	
	550	-21486	-21590	
	650	-17846	-17875	
4Ag+S2=2Ag2S reaction (5.5)	350	-36524	-37065	-44100+22.10T(25-176°C)
	450	-33995	-34524	-41980+16.53T(176-804°C)
	500	-33028	-33715	
	550	-32177	-32889	
	600	-32512	-32062	
4/3Bi+S2=2/3Bi2S3 reaction (5.6)	350	-48672	-39451	-52121+36.20T(25-271°C)
	450	-44703	-35831	
	550	-40756	-32170	-55600+42.60T(271-900°C)
	650	-36240	-27910	

Table 5.2. Table 5.2 shows the reactions investigated, the data source, the type of data (see text for explanation), the temperature range for which thermochemical data were obtained and the reaction number which refers to the mineral stability fields illustrated in figures 5.4 to 5.7.

System / reaction	data type	data source	temp. range K	reaction number
Bi-Te-S				
$4/3\text{Bi} + \text{Te}_2 = 2/3\text{Bi}_2\text{Te}_3$	2	1	298-700	1
$2\text{Bi}_2\text{Te}_2\text{S} + \text{Te}_2 = 2\text{Bi}_2\text{Te}_3 + \text{S}_2$	3b	1	298-700	2
$\text{Bi}_2\text{S}_3 + \text{Te}_2 = 2/3\text{Bi}_2\text{Te}_3 + \text{S}_2$	2/1	1/2	298-700	-
$\text{Bi}_2\text{S}_3 + \text{Te}_2 = \text{Bi}_2\text{Te}_2\text{S} + \text{Te}_2$	3b	1	298-700	3
$4/3\text{Bi} + \text{S}_2 = 2/3\text{Bi}_2\text{S}_3$	1	4	298-700	4
Fe-S-Te				
$2\text{Fe} + \text{S}_2 = \text{FeS}$	1	2	298-700	8
$\text{FeTe}_2 + \text{S}_2 = \text{FeS}_2 + \text{Te}_2$	2	1	298-700	9
$2\text{FeS} + \text{S}_2 = 2\text{FeS}_2$	1	2	298-700	10
$\text{Fe} + \text{Te}_2 = \text{FeTe}_2$	2	1	298-700	-
Pb-Te-S				
$2\text{Pb} + \text{S}_2 = 2\text{PbS}$	2	1	298-700	-
$2\text{Pb} + \text{Te}_2 = 2\text{PbTe}$	2	1	298-700	-
$2\text{PbS} + \text{Te}_2 = 2\text{PbTe} + \text{S}_2$	2	1	298-700	11
Au-Te				
$\text{Au} + \text{Te}_2 = \text{AuTe}_2$	2	1	298-700	12
Ag-Au-Te-S				
$4\text{Ag} + \text{Te}_2 = 2\text{Ag}_2\text{Te}$	2	1	298-700	5
$4\text{Ag} + \text{S}_2 = 2\text{Ag}_2\text{S}$	1	3	298-700	6
$2\text{Ag}_2\text{S} + \text{Te}_2 = 2\text{Ag}_2\text{Te} + \text{S}_2$	2	1	298-700	7
$4(\text{Au}_x\text{Ag}_y) + y\text{Te}_2 = 2y\text{Ag}_2\text{Te} + 4x\text{Au}$	3c	1/3	298-700	
$4(\text{Au}_x\text{Ag}_y) + y\text{S}_2 = 2y\text{Ag}_2\text{S} + 4x\text{Au}$	3c	1/3	298-700	

References:

1. Mills (1974)
2. Barton and Skinner (1979)
3. Barton and Toulmin (1964)
4. Craig and Barton (1973)

Figure 5.1a Temperature activity grid for the sulphidation of electrum to form silver sulphide. The data used to construct the grid are taken from Barton and Toulmin (1964).

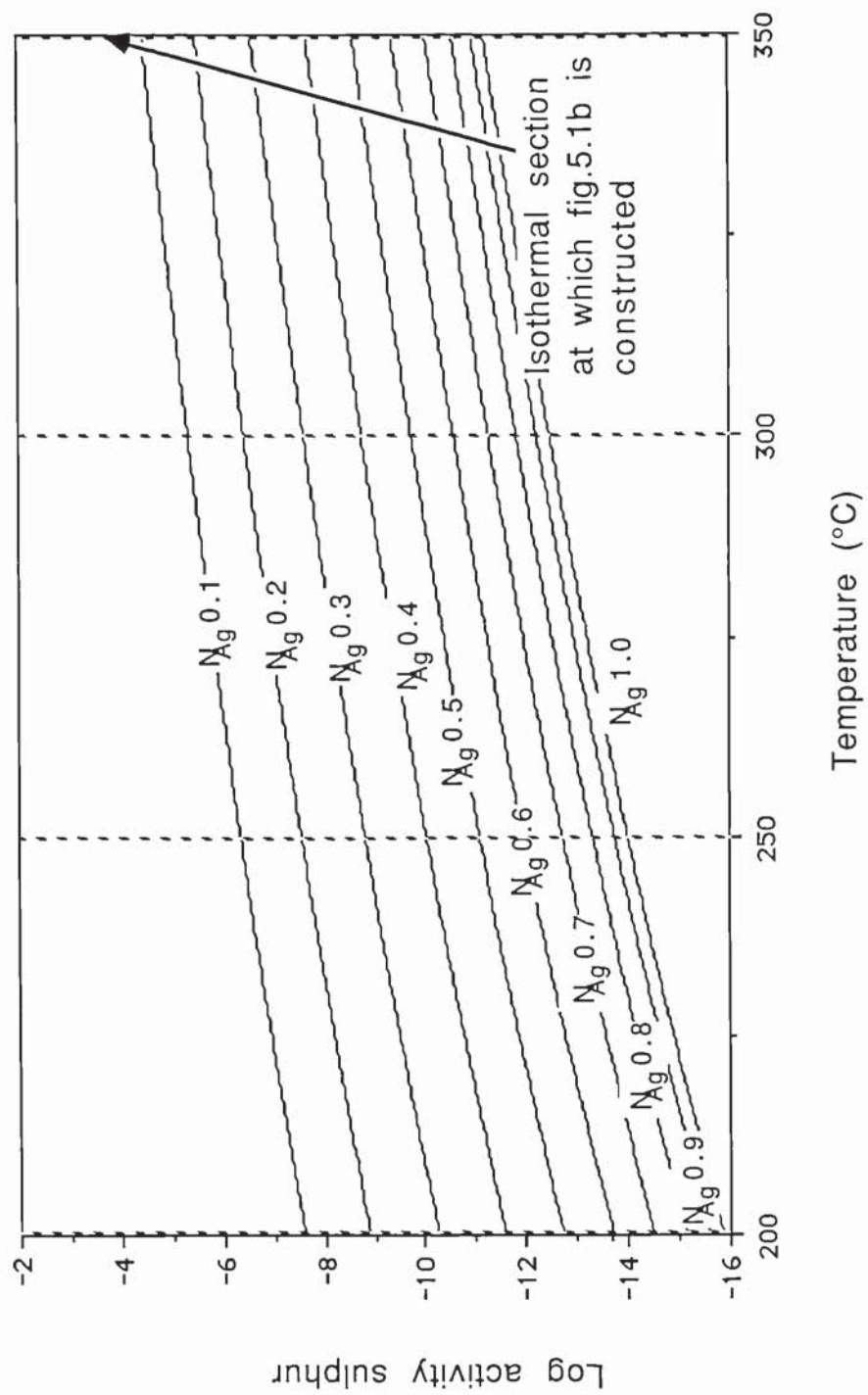


Figure 5.1b. Activity of tellurium-activity sulphur plot showing the method of calculation of tellurium activity in equilibrium with hessite and electrum.

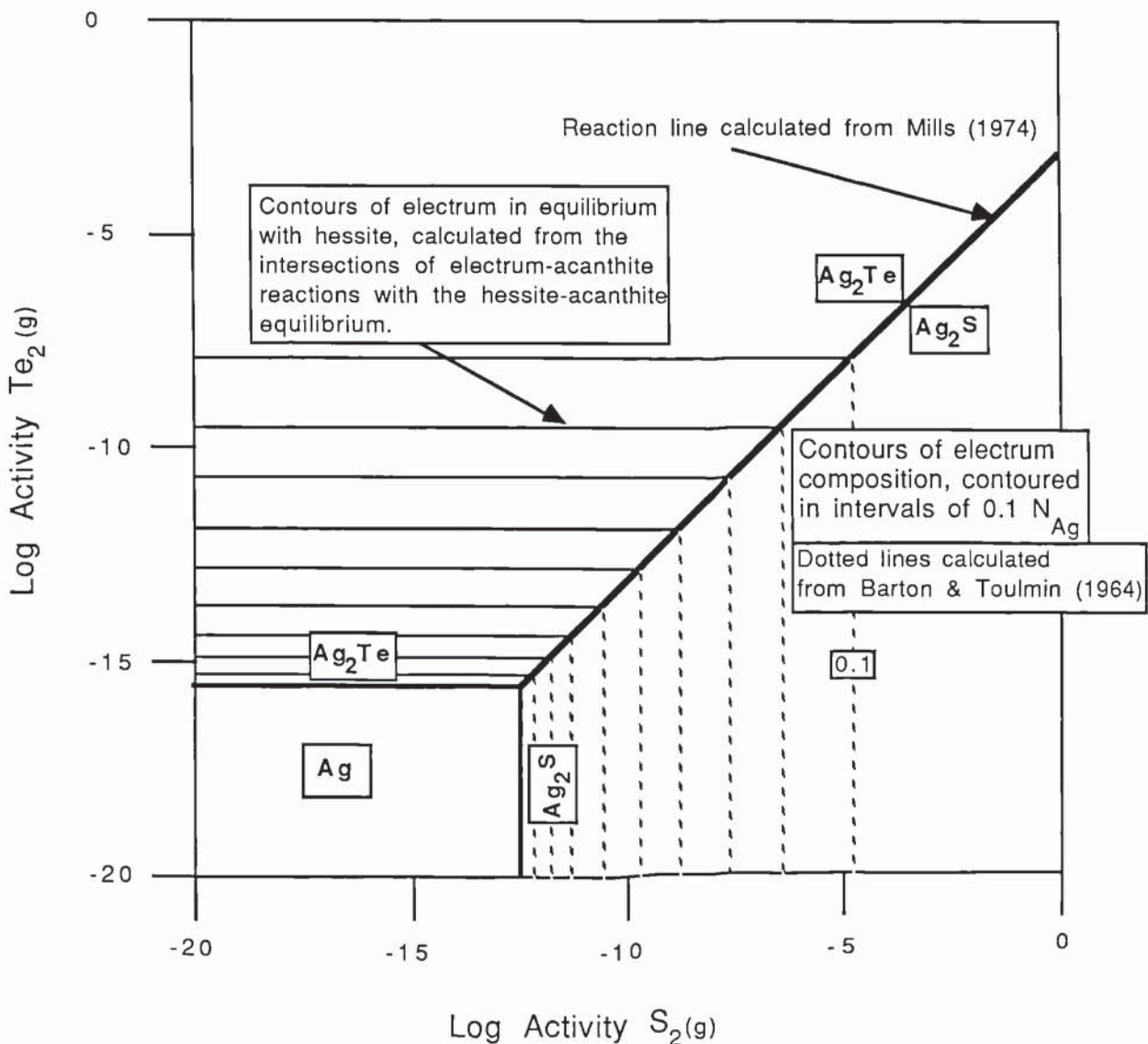


Figure 5.2. Temperature activity grid for the following telluridation reactions: formation of altaite (**At**), frohbergite (FeTe_2) (**Fr**), tellurbismuth (**Tb**), hessite (**Hs**), telluridation of maldonite (Au_2Bi) to form tellurbismuth (**Md to Tb**), and the condensation of tellurium.

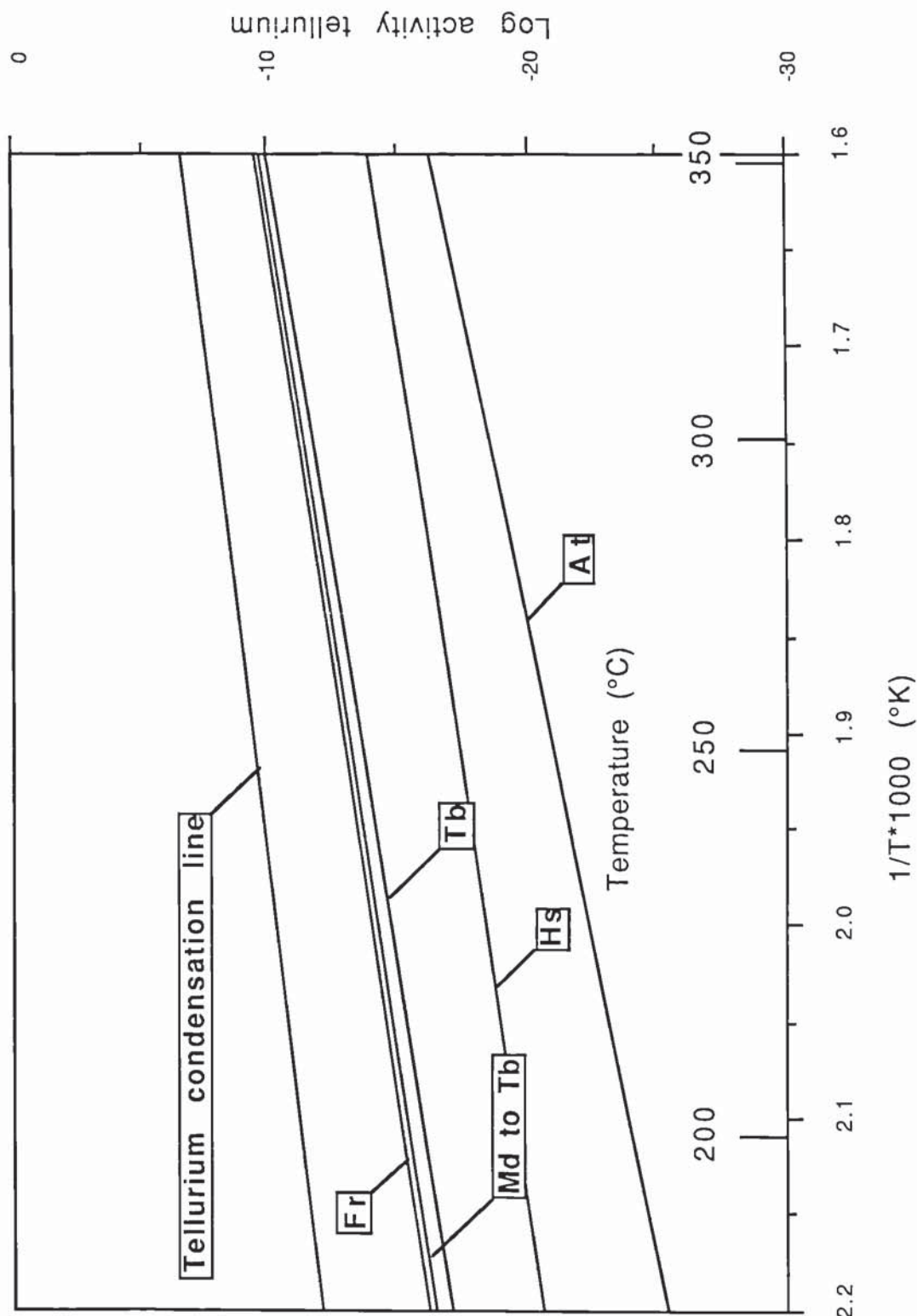


Figure 5.3. Temperature activity grid for the following sulphidation reactions: pyrite=pyrrhotine (Py-Po); bismuth=bismuthinite (Bs); maldonite=bismuthinite+gold (Md); silver=acanthite/argentite (Ac); lead=galena (Gn); iron=pyrrhotine (Po).

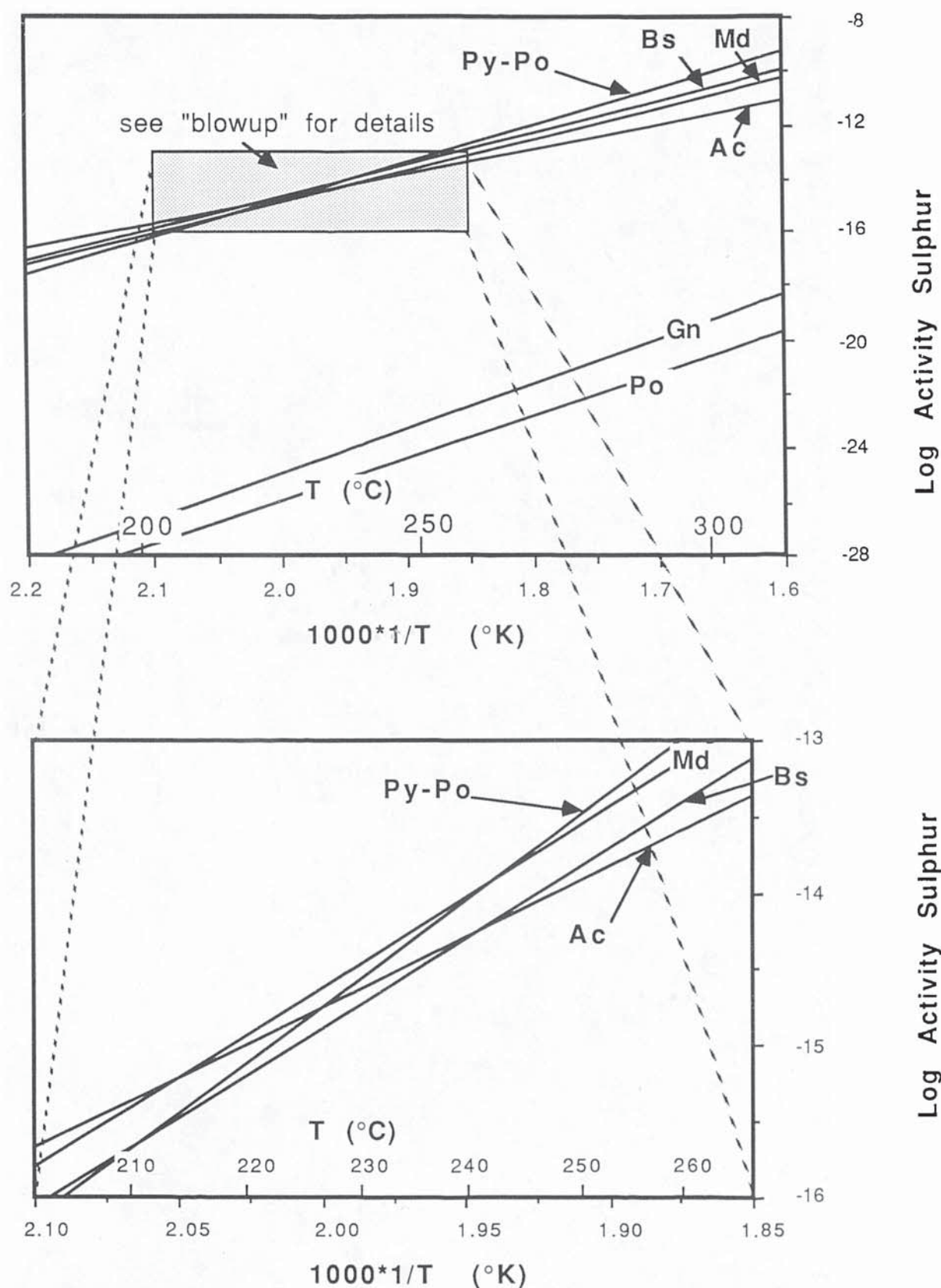
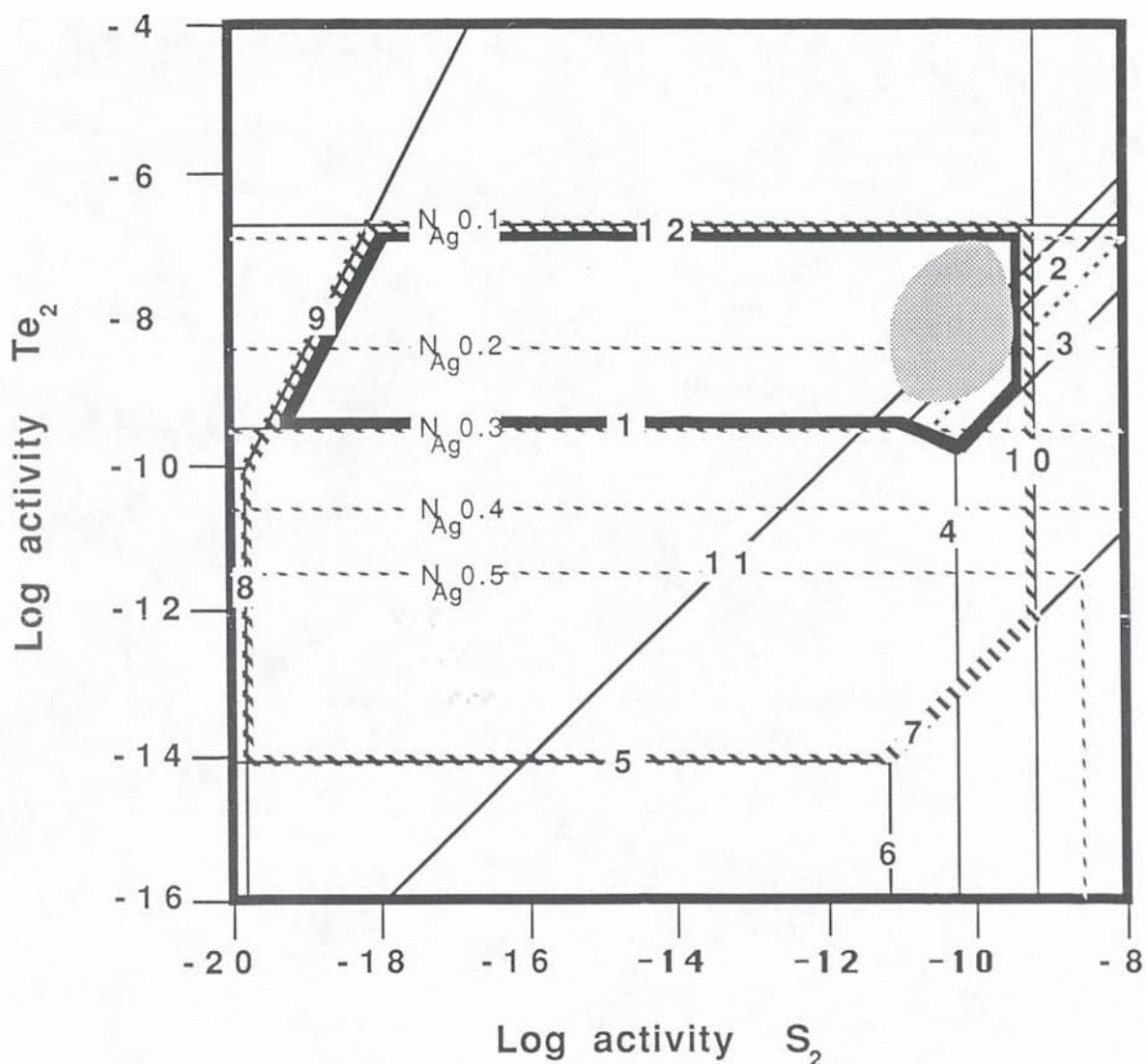


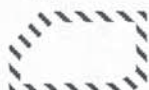
Figure 5.4. Stability fields at 350°C and 1 atmosphere. The numbered lines refer to the reactions listed in table 5.2. The thick hashed polygon shows the range of tellurium and sulphur activity for both assemblages, the heavy black line shows the range of tellurium and sulphur activity associated with the tellurbismuth-dominated telluride assemblage, and the stippled area represents the probable range of tellurium and sulphur activity.



KEY:



Probable limits of ore formation



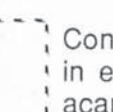
Maximum limits of ore formation



Limits of ore formation for the tellurobismuth assemblage

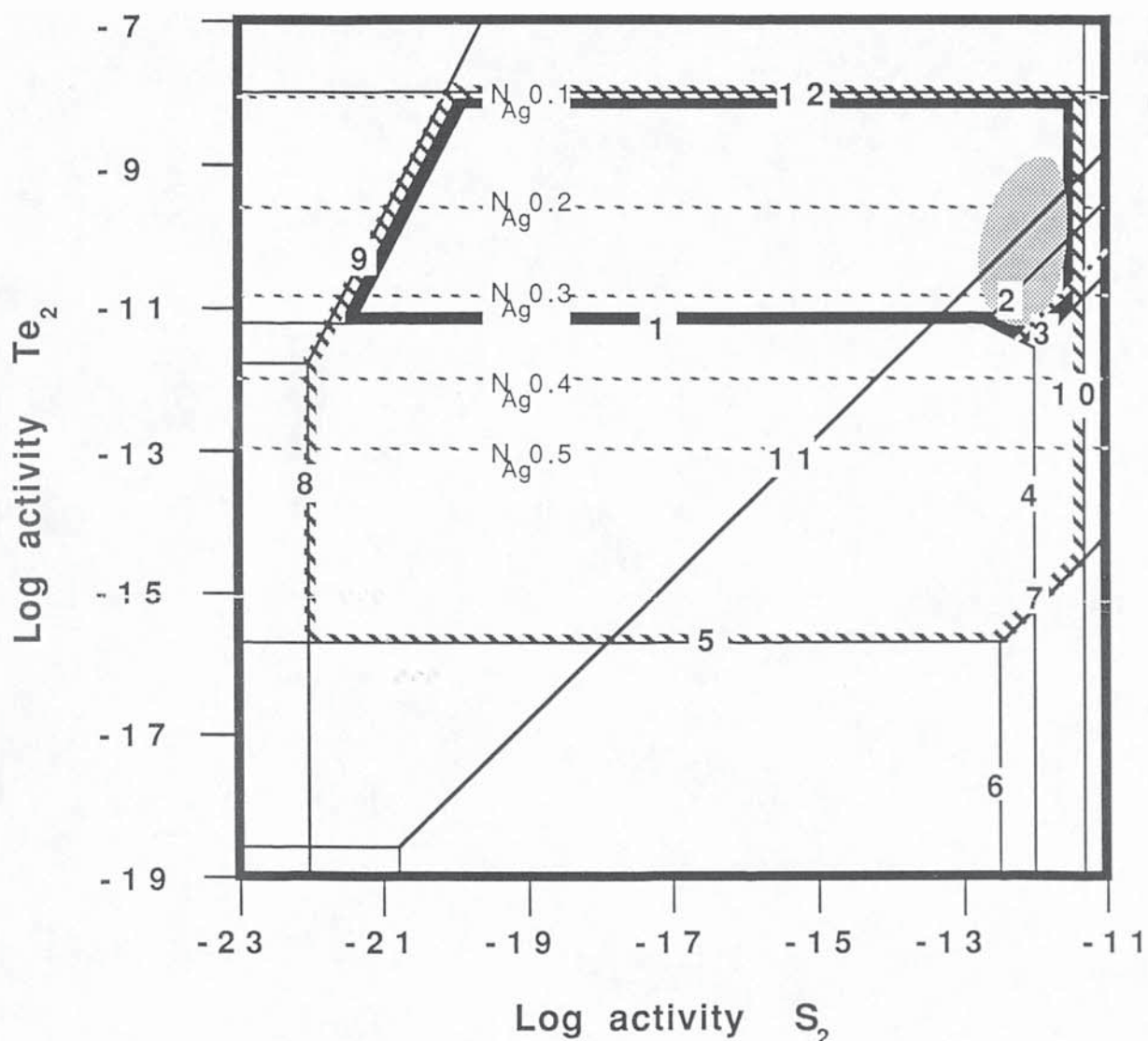


reaction line for the transformation $\text{Bi}_2\text{S}_3 \rightarrow \text{Bi}_2\text{Te}_3$



Contours of electron composition in equilibrium with hessite and acanthite

Figure 5.5. Stability fields at 300°C and 1 atmosphere. The numbered lines refer to the reactions listed in table 5.2. The thick hashed polygon shows the range of tellurium and sulphur activity for both assemblages, the heavy black line shows the range of tellurium and sulphur activity associated with the tellurbismuth-dominated telluride assemblage, and the stippled area represents the probable range of tellurium and sulphur activity.



KEY:



Probable limits of ore formation



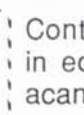
Maximum limits of ore formation



Limits of ore formation for the tellurobismuth assemblage

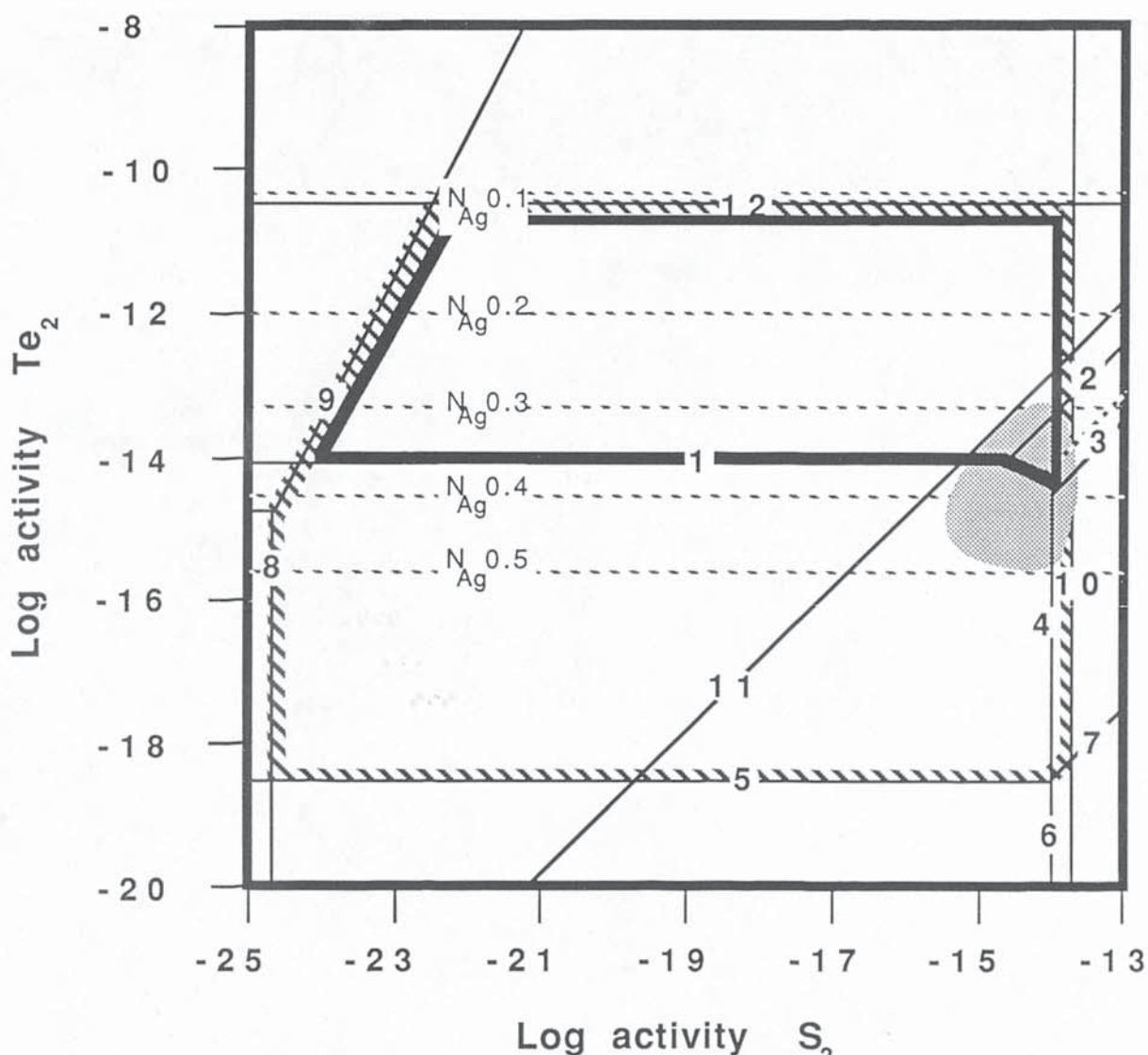


reaction line for the transformation $\text{Bi}_2\text{S}_3 \rightarrow \text{Bi}_2\text{Te}_3$



Contours of electron composition in equilibrium with hessite and acanthite

Figure 5.6. Stability fields at 250°C and 1 atmosphere. The numbered lines refer to the reactions listed in table 5.2. The thick hashed polygon shows the range of tellurium and sulphur activity for both assemblages, the heavy black line shows the range of tellurium and sulphur activity associated with the tellurbismuth-dominated telluride assemblage, and the stippled area represents the probable range of tellurium and sulphur activity.



KEY:



Probable limits of ore formation



Maximum limits of ore formation



Limits of ore formation for the tellurobismuth assemblage

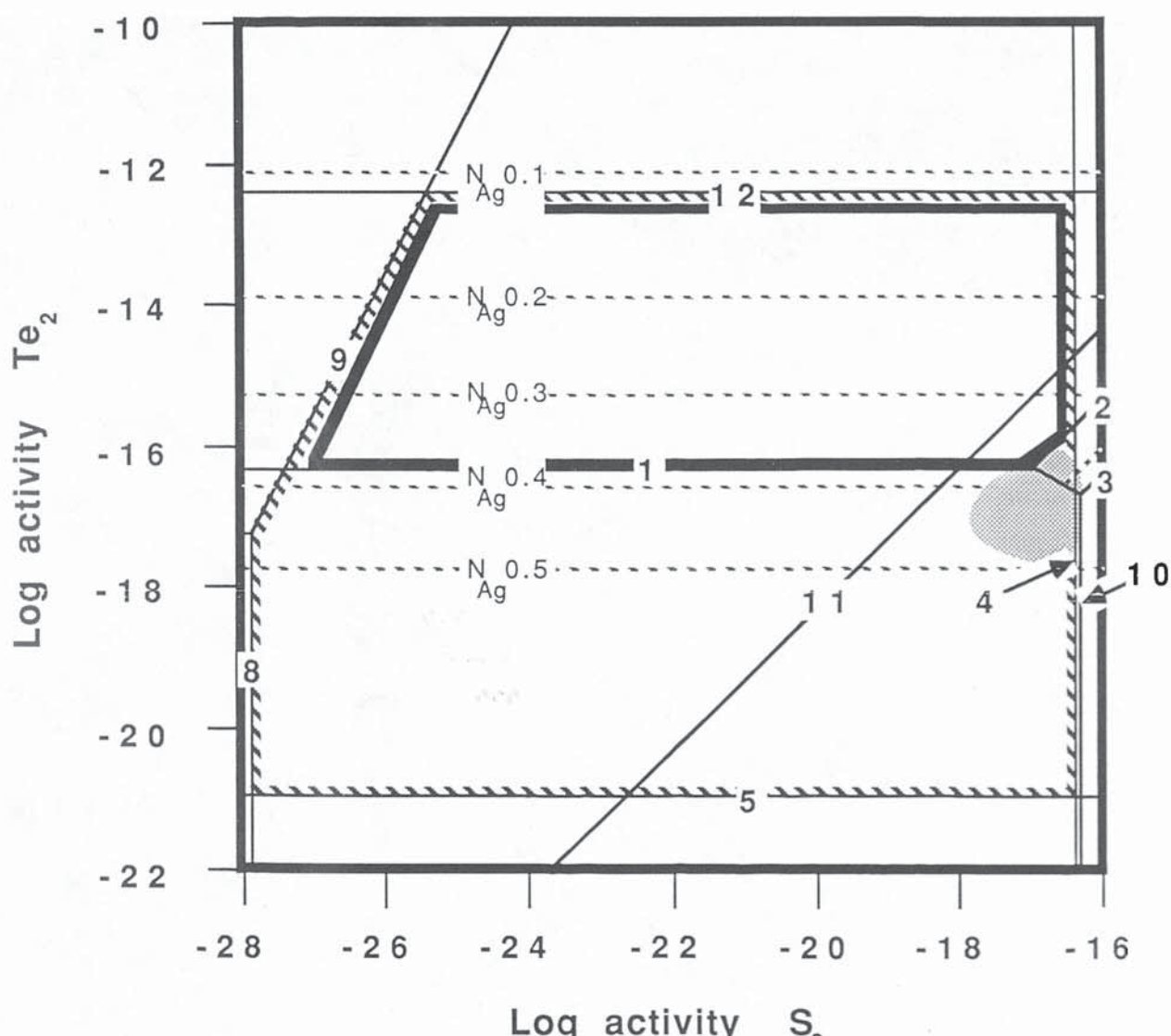


reaction line for the transformation $\text{Bi}_2\text{S}_3 \rightarrow \text{Bi}_2\text{Te}_3$



Contours of electron composition in equilibrium with hessite and acanthite

Figure 5.7. Stability fields at 200°C and 1 atmosphere. The numbered lines refer to the reactions listed in table 5.2. The thick hashed polygon shows the range of tellurium and sulphur activity for both assemblages, the heavy black line shows the range of tellurium and sulphur activity associated with the tellurbismuth-dominated telluride assemblage, and the stippled area represents the probable range of tellurium and sulphur activity.



KEY:



Probable limits of ore formation



Maximum limits of ore formation



Limits of ore formation for the tellurobismuth assemblage



reaction line for the
transformation $\text{Bi}_2\text{S}_3 \rightarrow \text{Bi}_2\text{Te}_3$

Contours of electron composition
in equilibrium with hessite and
acanthite

Figure 5.8. Diagrammatic illustration of the stability ranges of the observed phases at Clogau Mine. Where lines overlap then the phases can co-exist, e.g., gold, hessite, and altaite have overlapping lines so they form a stable assemblage, but the lines for tetradyomite and altaite do not overlap so they cannot form a stable assemblage, the stable assemblage being galena and tetradyomite.

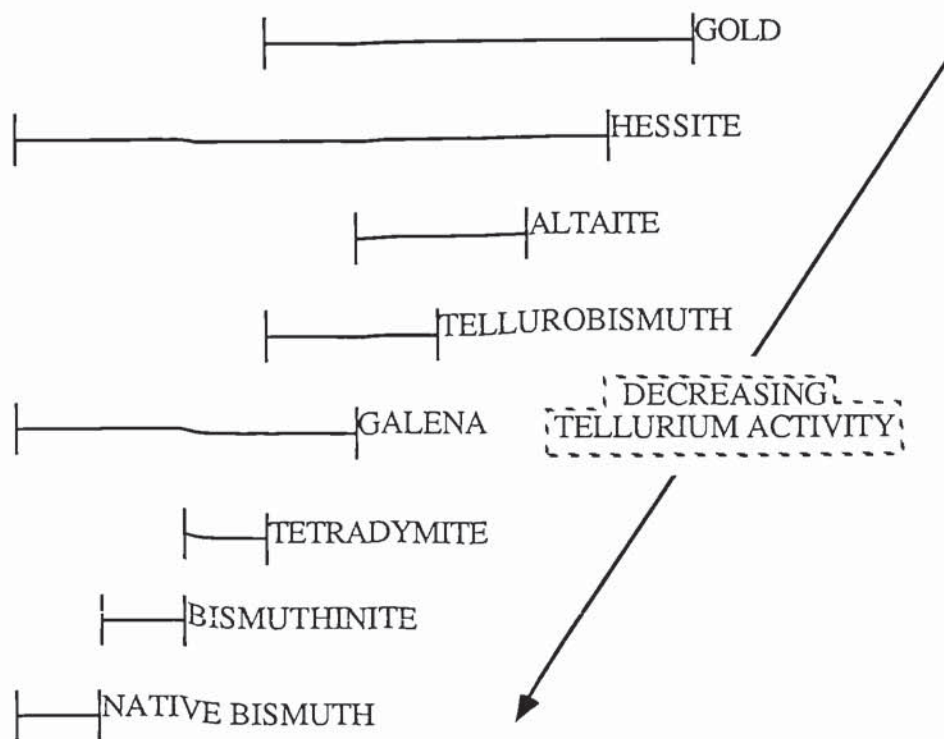


Table 5.3. Comparison of stable and unstable assemblages as defined by the mineral stability diagrams with observed assemblages. Assemblages that have been observed are shown in bold typeface.

STABLE ASSEMBLAGES		UNSTABLE ASSEMBLAGES	
Au-Hs	Au-At	Au-Td	Au-Bs
Au-Tb	Au-Gn-Hs-At	Au-Bi	At-Td
Hs-Tb	Hs-Gn	At-Bs	At-Bi
Hs-Td	Hs-Bs	Tb-Bs	Tb-Bi
Hs-Bi	At-Tb	Td-Bi	Au-Hs-Td
At-Gn	Tb-Gn	Au-Hs-Bs	Au-Hs-Bi
Tb-Td	Gn-Td	Hs-At-Td	Hs-At-Bs
Gn-Bs	Gn-Bi	Hs-At-Bi	At-Tb-Td
Td-Bs	Bs-Bi	At-Tb-Bs	At-Tb-Bi
Au-Hs-At	Au-Hs-Tb	Tb-Gn-Bs	Tb-Gn-Bi
Au-Hs-Gn	Hs-At-Tb	Td-Bs-Bi	
Hs-Alt-Gn	At-Tb-Gn		
Tb-Gn-Td	Gn-Td-Bi		
Au-Hs-At-Tb	Au-Hs-At-Gn		
Hs-At-Gn-Tb			

FIGURES AND PLATES FOR
CHAPTER 7:

**THE GEOLOGY AND
MINERALISATION OF THE
SOUTHERN UPLANDS.**

Figure 7.1. Fault bounded tracts and greywacke formations of the Southern Uplands (after Morris, 1987).



Figure 7.2. Geology of the Leadhills-Wanlockhead mining district (after Mackay, 1959).



Figure 7.3. Distribution of arsenic-antimony mineralisation in the Southern Uplands
(after Gallagher *et al.*, 1983).



Figure 7.4. Geolgy of the area around the Black Stockarton Moor Sub-Volcanic Complex (after Brown *et al.*, 1979b)



Figure 7.5. Geology of the area around the Cu-Fe-As-Mo mineralisation at Caingarroch Bay (after Allen *et al.*, 1981a).



Figure 7.6. Geology of the area around the Fe-Co-Ni mineralisation at Talnotry (after Stanley *et al.*, 1987).



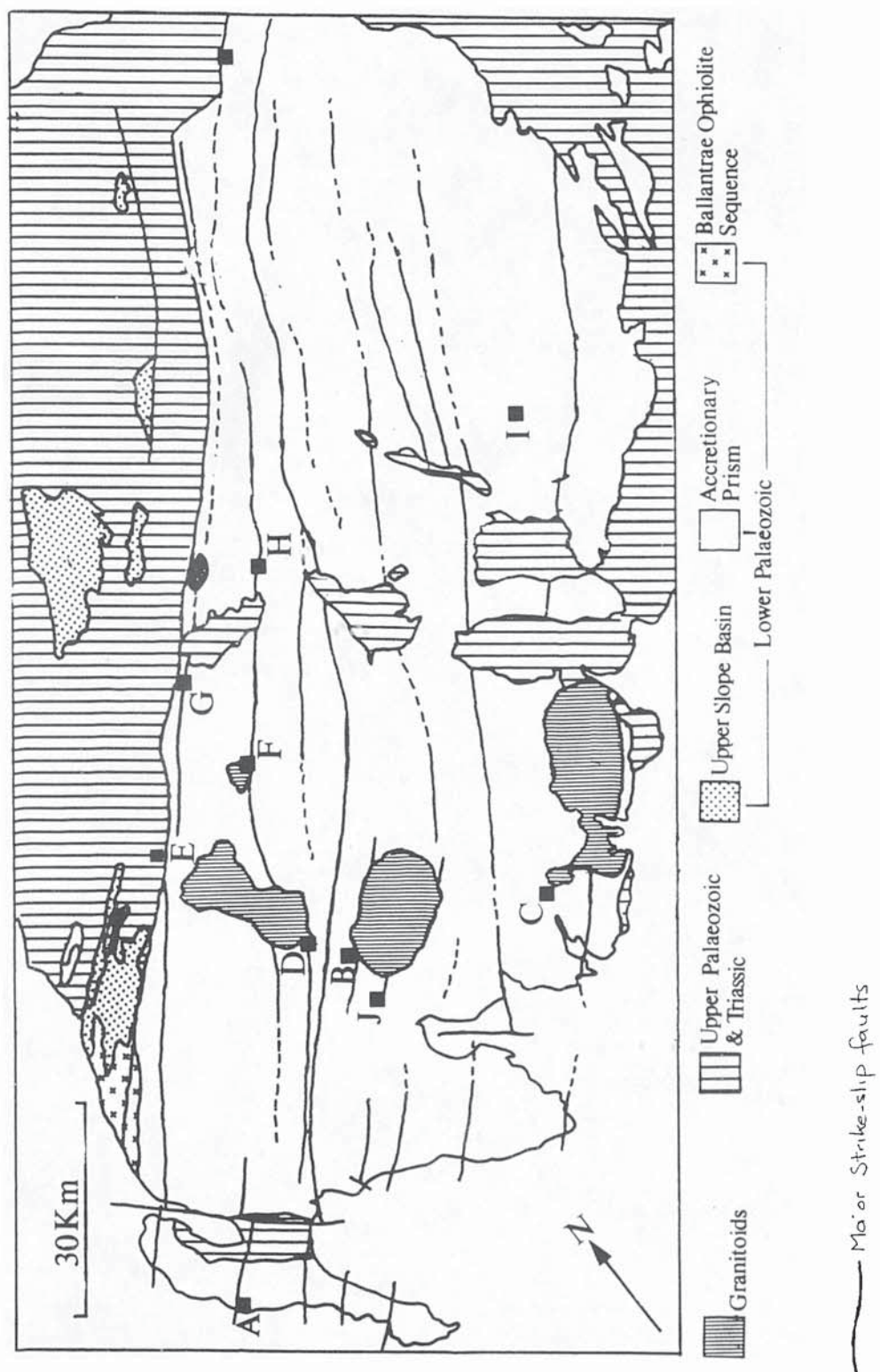
Figure 7.7. Geology of the gold mineralisation at the Fore Burn Igneous Complex
(after Allen *et al.*, 1982).



Figure 7.8. Geology of the gold mineralisation at the margin of the Loch Doon granitoid Complex (after Leake *et al.*, 1981).



Figure 7.9. Relationship between structure intrusives and mineralisation.
 (A=Cairngarroch Bay [porphyry copper style], B=Talnotry [As-Ni], C=Black Stockarton Moor [porphyry copper style], D=Loch Doon [Au-As], E=Foreburn [Au-As-Sb], F=Moorbrook Hill [Au-As], G=The Knipe (Hare Hill) [Sb & Au-As], H=Leadhills [placer gold & Pb-Zn±Ag], I=Glendinning [As-Sb], J=Newton Stewart [Pb-Zn±Ag])

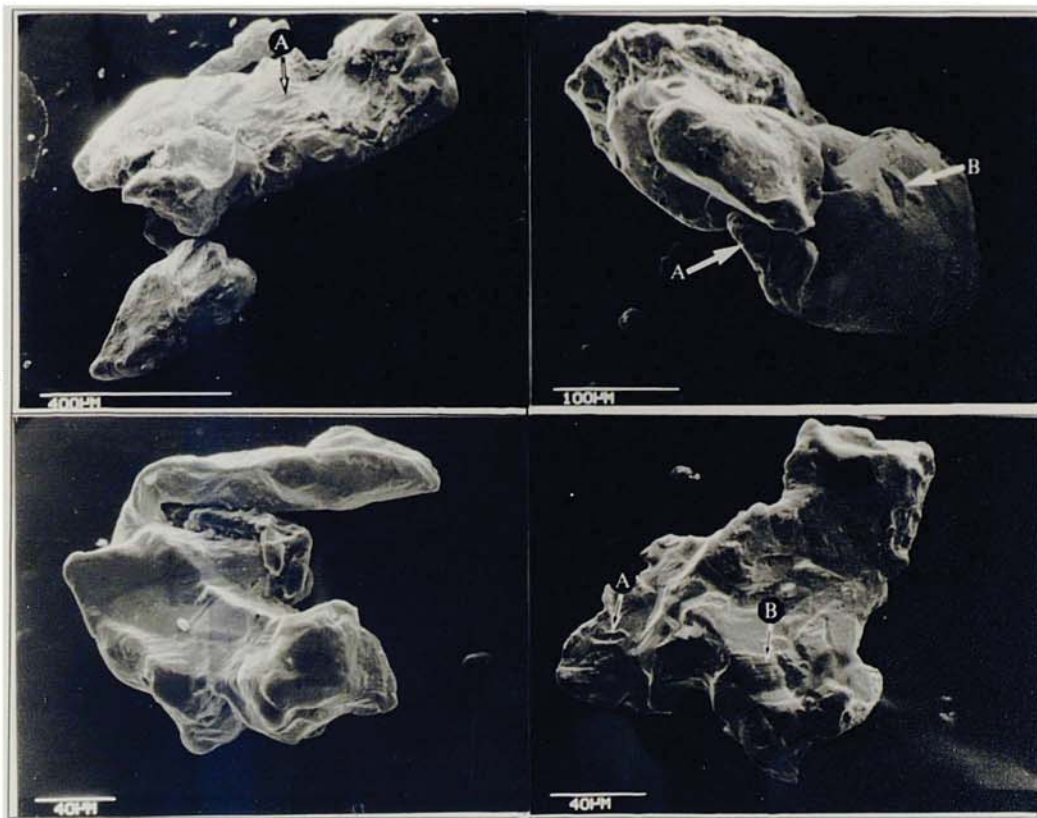


FIGURES, PLATES AND TABLES
FOR CHAPTER 8:

**MORPHOLOGICAL,
PETROLOGICAL AND
COMPOSITIONAL OF THE
SOUTHERN UPLANDS PLACER
GOLD: METHODOLOGY**

Table 8.1.List of morphological characteristics of the Southern Uplands placer gold.

Morphological characteristic 1	Placer gold with with a glazed surface.
Morphological characteristic 2	Placer gold which retains much of its crystalline morphology.
Morphological characteristic 3	Placer gold in which the original morphology has been deformed.
Morphological characteristic 4	Irregularly shaped placer gold grains
Morphological characteristic 5	Placer gold grains which are abraded and subrounded, and show evidence of folding and hammering of edges and vertices.
Morphological characteristic 6	Placer gold grains which exhibit a general elongate shape.
Morphological characteristic 7	Rounded and nugget shaped placer gold grains.
Morphological characteristic 8	Flattened flake shaped placer gold grains.
Morphological characteristic 9	Placer gold grains with a smooth and unabraded surface at high magnification.
Morphological characteristic 10	The inclusion of primary minerals and the presence of inclusion scars.
Morphological characteristic 11	Placer gold grains with an irregular surface at high magnification.
Morphological characteristic 12	Placer gold where mineral grains have been trapped in crevasses and folds.
Morphological characteristic 13	Placer gold with a flaky surface at high magnification.
Morphological characteristic 14	Presence of a smooth, generally worn surface at high magnification.
Morphological characteristic 15	Presence of random scratches at high magnification.
Morphological characteristic 16	Presence of a "dough"-like texture at high magnification.
Morphological characteristic 17.	Presence of a layered texture at high magnification.
Morphological characteristic 18	Presence of a porous/spongy surface at high magnification.



Plates 8.1a to 8.1d are SEM electronmicrographs of placer gold collected from the Hirgwm river, Bonddu, North Wales, 1km downstream form Clogau mine. These grains are used to illustrate the morphological characteristic of a glazed surface.

A	B
C	D

Plate 8.1a.

The surface of the gold grain illustrated in plate 8.1a is smooth and unworn. The lack of abrasion and plastic deformation on the surface give the grain its porcellaneous, glazed appearance. Also primary crystalline features are preserved; e.g., The angular ridges and depressions (arrow A). These irregularities are probably impressions left by the mineral that was originally attached to the gold grain.

Plate 8.1b.

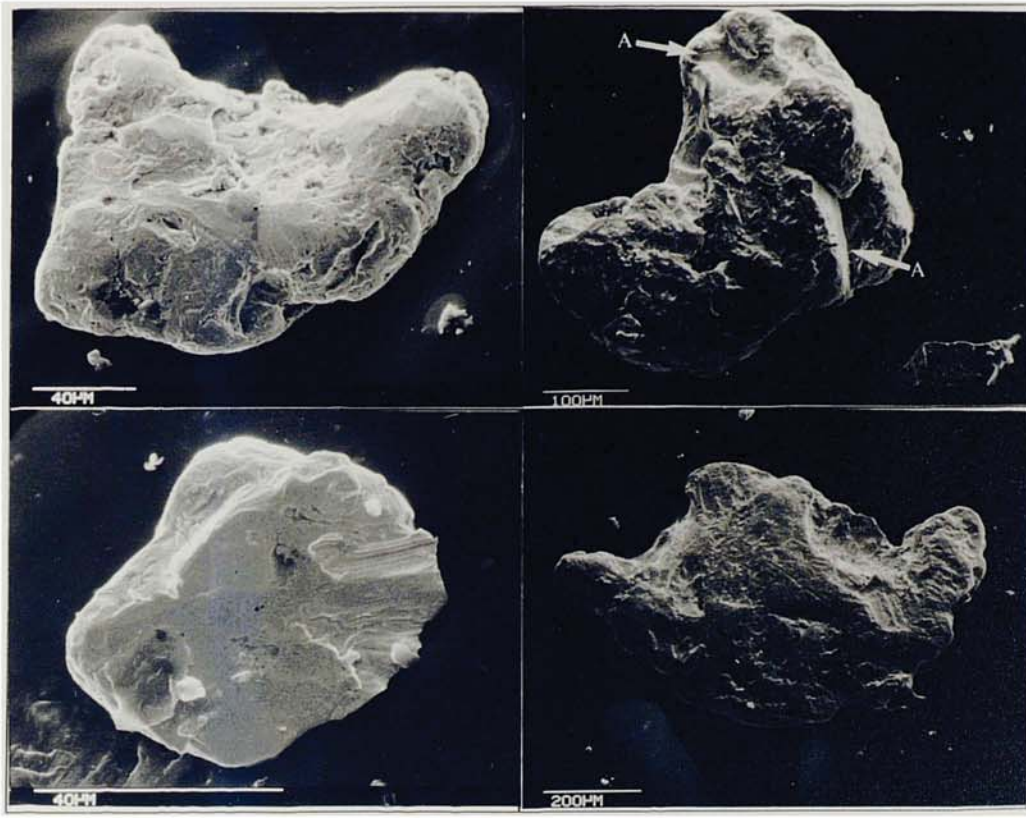
Plate 8.1b shows a grain that is rounded, but the surface is smooth unworn and glazed. However the the original 'crystallinity' of the gold grain has been slightly deformed on the edges of the grain (arrow A), and the surface of the grain has a small impact mark (arrow B). The overall subrounded shape of the grain reflects original growth restrictions and is nothe result of abrasion and deformation.

Plate 8.1c.

Plate 8.1c illustrates a grain where all the original features are preserved, and the surface is glazed and completely unscratched.

Plate 8.1d.

Plate 8.1d illustrates a gold grain that exhibits similar features to the grain in plate 8.1c, but the grain is slightly scratched (arrow A) and has also preserved primary growth structures (arrow B).



Plates 8.1e to 8.1h illustrate placer gold collected from the river Mawddach by T.A. Readwin; BM No. 42545, in 1888 approximately 10km from Gwynfynydd gold mine (Readwin, 1888).

E	F
G	H

Plate 8.1e.

Plate 8.1e illustrates a gold grain where the glazed surface has been removed by abrasion and deformation. The subrounded shape of the grain is probably due to these attrition processes and not a reflection of the original shape of the grain, as is the smooth and worn surface.

Plate 8.1f.

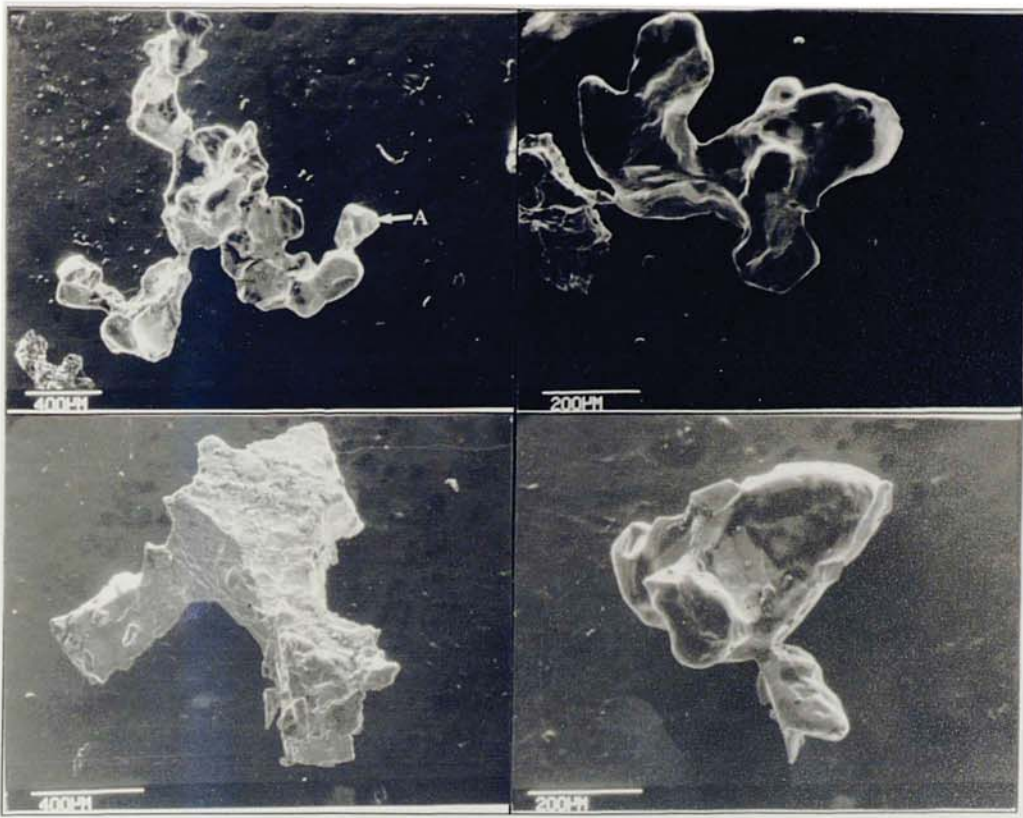
Plate 8.1f shows a grain where the majority of the glazed surface has been removed, but it can still be seen in cavities on the surface of the grain (arrow A).

Plate 8.1g.

Plate 8.1g shows a well rounded grain with a smooth worn surface. Again the smooth unworn (glazed) surface of the grain has been removed.

Plate 8.1h.

Plate 8.1h illustrates a grain with numerous scratches on the surface where extensive abrasion has given the grain a polished surface.



Plates 8.2a to 8.2d illustrate the morphological features of lode gold dissolved from quartz using hydrofluoric acid.

A	B
C	D

Plate 8.2a

Plate 8.2a illustrates a gold grain with a highly irregular shape and some typomorphic crystallographic features (arrow A). Note the surface is smooth, unworn and glazed.

Plate 8.2b

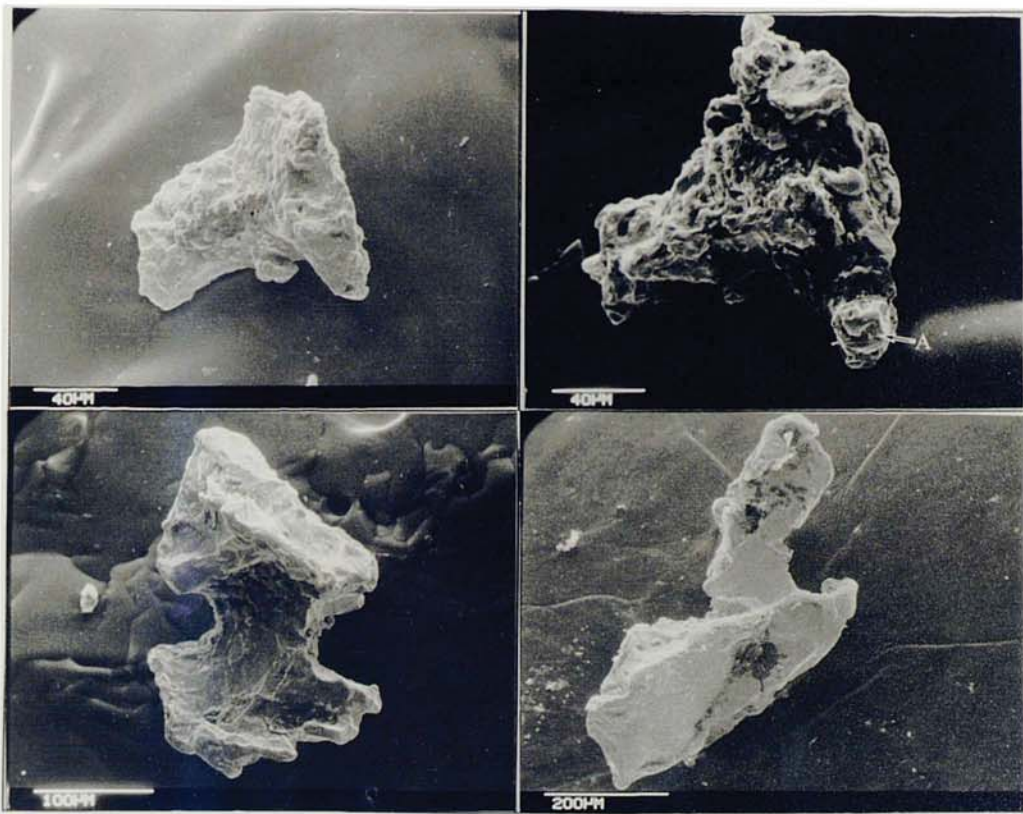
Plate 8.2b shows an amoeboid shaped grain with no obvious typomorphic crystallographic features. Again note that the surface is smooth, unworn and glazed.

Plate 8.2c

Plate 8.2c illustrates a grain where the surface has a glazed appearance but where the surface has an irregular appearance.

Plate 8.2d

Plate 8.2d shows a grain that has a subrounded overall shape, illustrating that the overall shape of a grain is not necessarily indicative of the amount of abrasion and deformation that the grain has undergone.



Plates 8.3a to 8.3d show placer gold grains from the Southern Uplands which illustrate the macro-morphological feature of grains that preserve most of their original crystalline features.

A	B
C	D

Plate 8.3a.

Plate 8.3a illustrates a gold grain that has an angular shape and irregular surface that have undergone little or no abrasion or deformation. This is evidenced by the lack of scratches on the surface of the grain and the lack of plastic deformation at vertices, edges and irregularities on the surface of the grain.

Plate 8.3b.

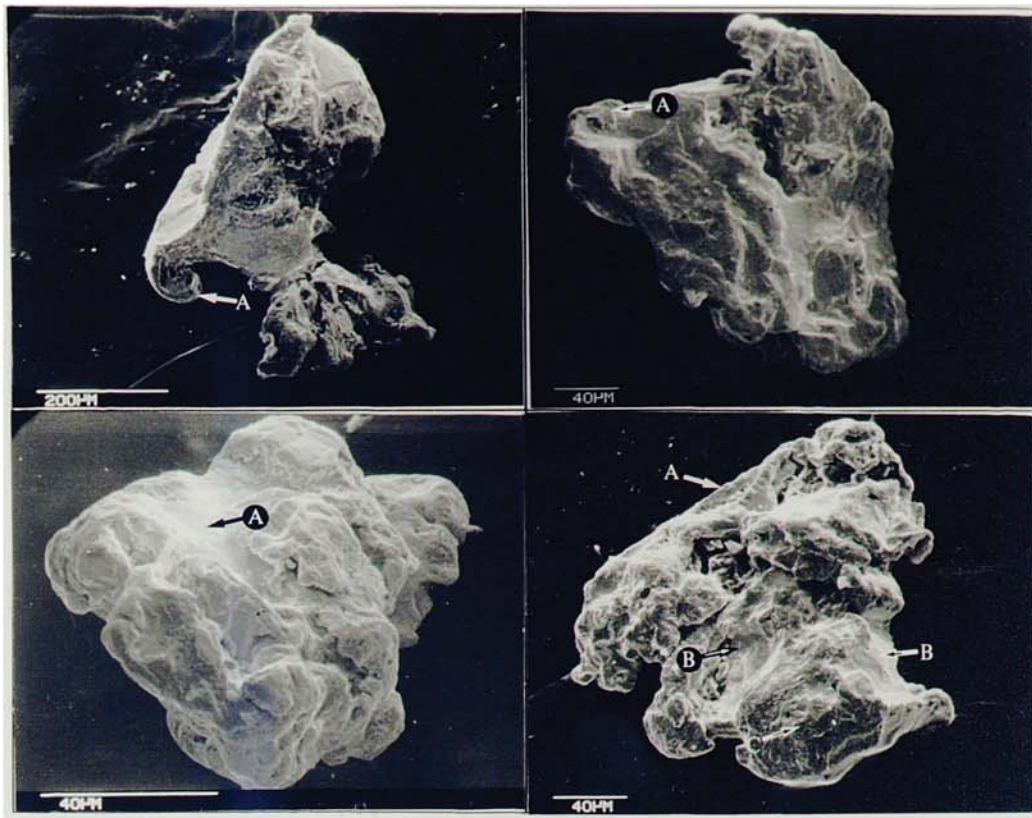
Plate 8.3b shows a gold grain with an overall tetrahedral shape, but a highly irregular surface. In this grain the vertices are slightly deformed (arrow A).

Plate 8.3c.

Plate 8.3c illustrates a gold grain with a relatively smooth and unworn surface, still retaining its glazed surface.

Plate 8.3d.

Plate 8.3d illustrates a gold grain with an angular habit where the surface is smooth and unworn and retaining its glazed surface.



Plates 8.4a to 8.4d show placer gold grains from the Southern Uplands that are used to illustrate the macro morphological features of deformed crystalline texture.

A	B
C	D

Plate 8.4a

Plate 8.4a illustrates an unabraded placer gold grain that still retains its glazed and unabraded surface. However the vertices of the grain are folded and bent (arrow A).

Plate 8.4b.

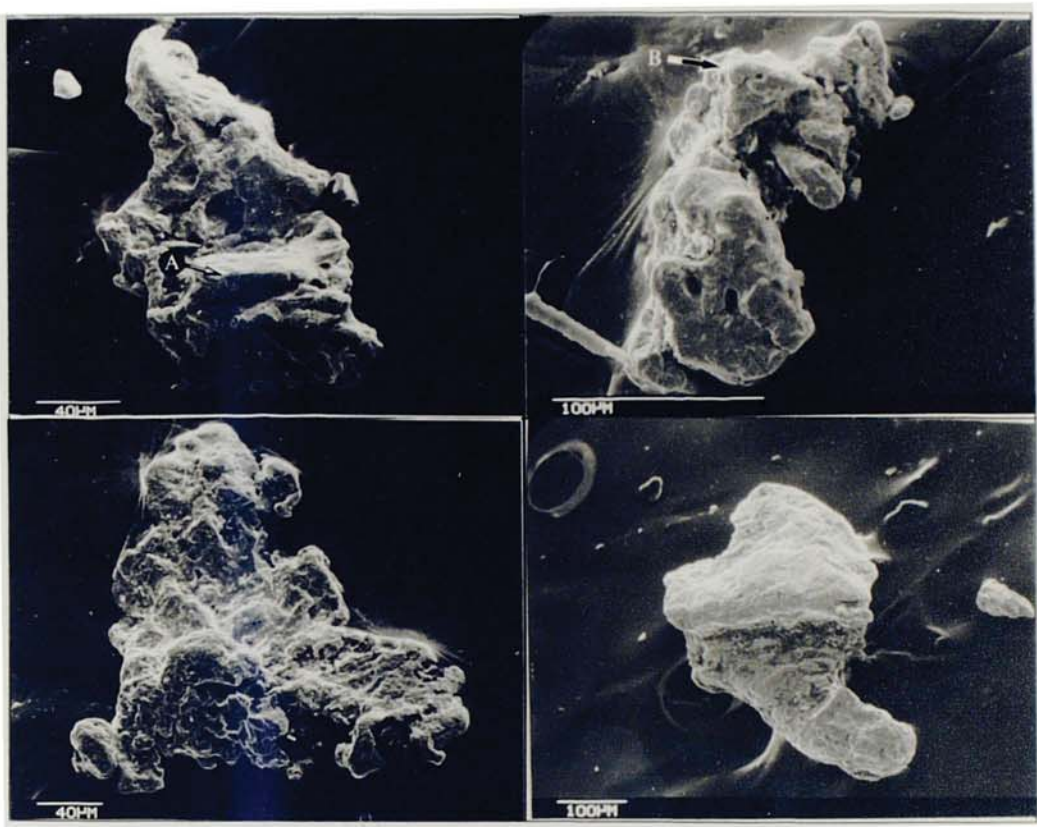
Plate 8.4b illustrates a placer gold grain that has been deformed along its edges (arrow A) and also has abraded and deformed protuberances. Original features such as the glazed and unworn surfaces are restricted to hollows and cavities on the grain surface.

Plate 8.4c.

Plate 8.4c shows a placer gold grain that has undergone deformation and abrasion which has resulted in the destruction of most of the glazed surface. The original glazed surface is restricted to a hollow (arrow A) on the surface of the grain.

Plate 8.4d.

Plate 8.4d illustrates a placer gold grain where only minor facets of the original features of the grain have been preserved. E.g., a straight edge (arrow A), small hollows where the glazed surface remain (arrow B). The processes of attrition have caused the larger protuberances to become rounded and deformed (arrow C).



Plates 8.5a to 8.5d show placer gold grains from the Southern Uplands that are used to illustrate the macro-morphological feature of irregularly shaped gold grains.

A	B
C	D

Plates 8.5a and 8.5b

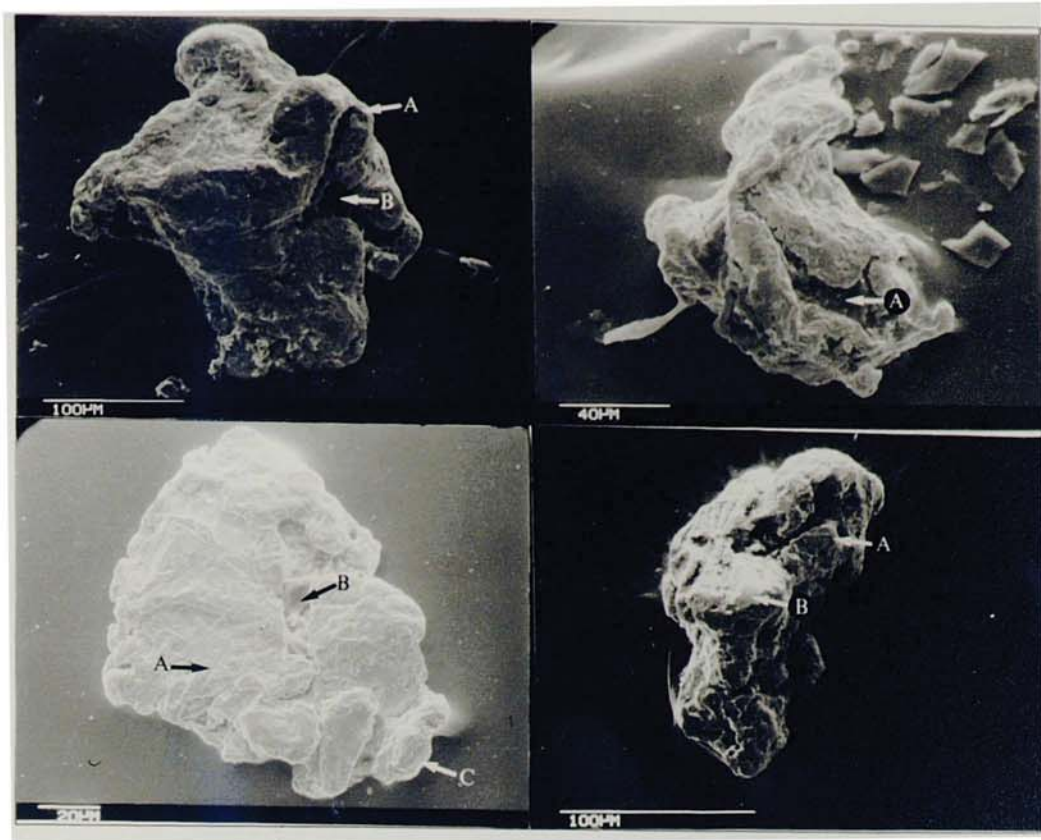
Plates 8.5a and 8.5b illustrate two irregularly shaped placer gold grains that have had their original glazed surface removed by abrasion. However some crystalline forms have been preserved; e.g., cubic features (arrow A) and tetrahedral forms (arrow B).

Plate 8.5c.

Plate 8.5c illustrates a placer gold grain where all the original features have been destroyed; i.e., the smooth unworn glazed surface and original crystalline features are no longer present. However the shape and surface of the grain are irregular.

Plate 8.5d

Plate 8.5d illustrates a placer gold grain with an irregular outline, where the surface of the grain has been worn smooth.



Plates 8.6a to 8.6d show placer gold from the Southern Uplands that illustrates the macro-morphological feature subrounded and elongate grains.

A	B
C	D

Plates 8.6a and 8.6b.

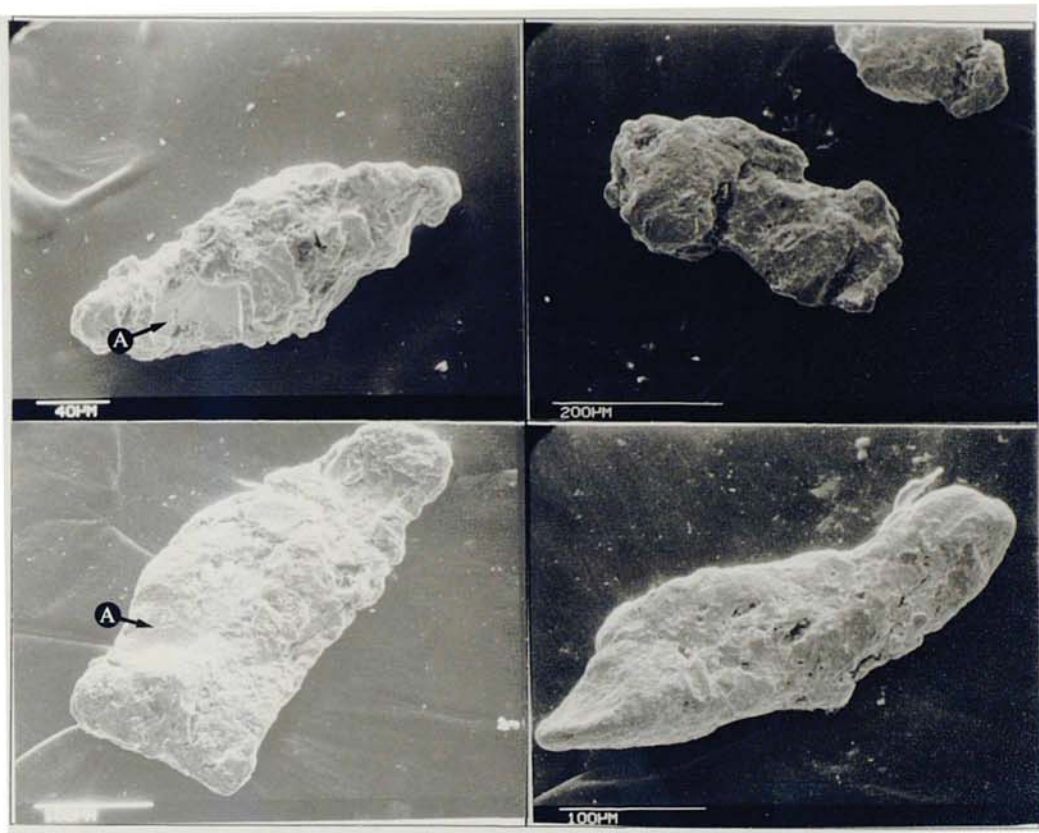
Plates 8.6a and 8.6b illustrate two placer gold grains that are subrounded. Plastic deformation of the two grains has caused folding (arrow A) and within the folds clay minerals have been trapped (arrow B). Abrasion of the grains has totally removed the glazed surface and any original surface irregularities.

Plate 8.6c.

Plate 8.6c illustrates a subrounded grain with a heavily scratched surface (arrow A), where abrasive forces have started to give the surface of the grain a polished appearance, and one of the vertices a layered appearance (arrow C). The small "vein" (arrow B) is in fact a fold in which clay minerals have been trapped.

Plate 8.6d.

Plate 8.6d illustrates a placer gold grain with a subrounded to rounded shape. The grain has been 'rolled' along its longitudinal axis to give the grain an overall elongate shape where thin edges have been folded (arrow A) and larger protuberances hammered (arrow B) to remove major irregularities in the shape of the grain.



Plates 8.7a to 8.7d show placer gold from the Southern Uplands that are used to illustrate the macro-morphological feature of placer gold grains with a generally elongate shape.

A	B
C	D

Plates 8.7a. and 8.7b

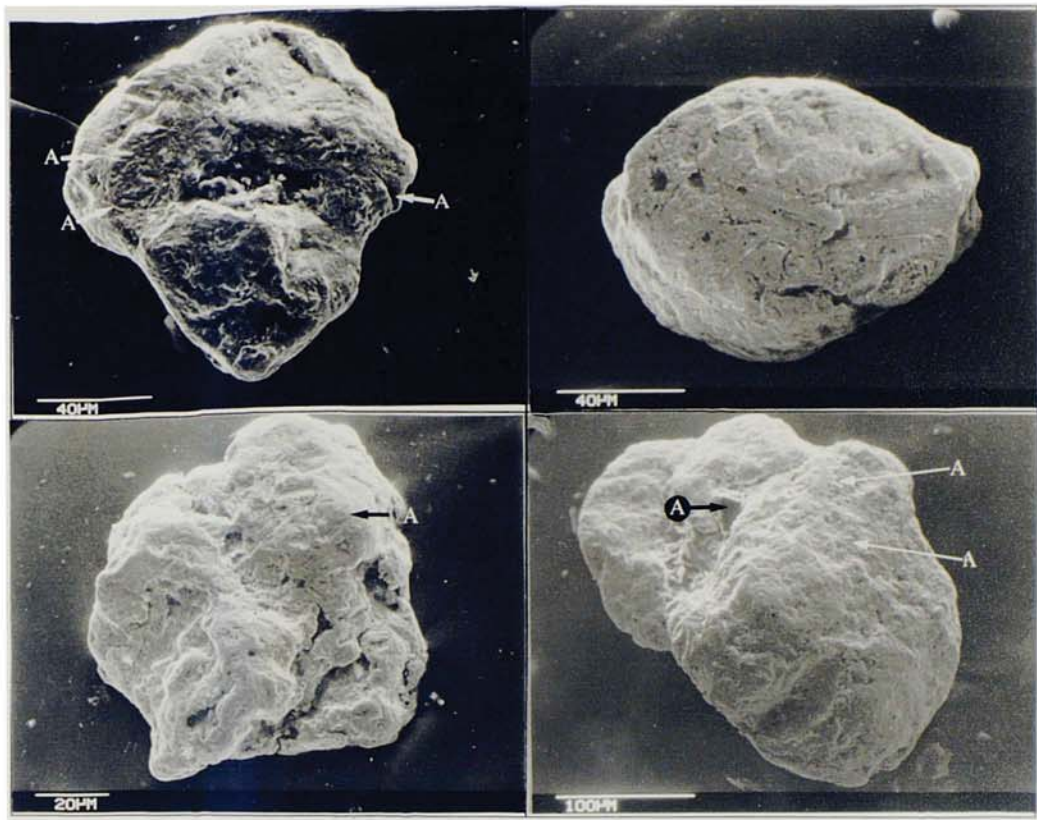
Plate 8.7a and 8.7b illustrate a placer gold grains with a generally elongate shape and slightly irregular surface. The surface is in places unabraded (arrow A).

Plate 8.7c.

Plate 8.7c illustrates an generally elongate shaped placer gold grain. The surface of which is generally smooth and worn and has random scratches (arrow A).

Plate 8.7d.

Plate 8.7d illustrates a placer gold grain with a generally elongate shape where the surface is smooth and worn and is beginning to develop a polish.



Plates 8.8a to 8.8d show placer gold grains from the Southern Uplands which illustrate the macro-morphological feature of placer gold that is nugget shaped.

A	B
C	D

Plate 8.8a.

Plate 8.8a illustrates a placer gold grain that has a rounded nugget shape. The surface of the grain retains none of its original features, it is scratched (arrow A) and has developed a polish through prolonged abrasion.

Plate 8.8b.

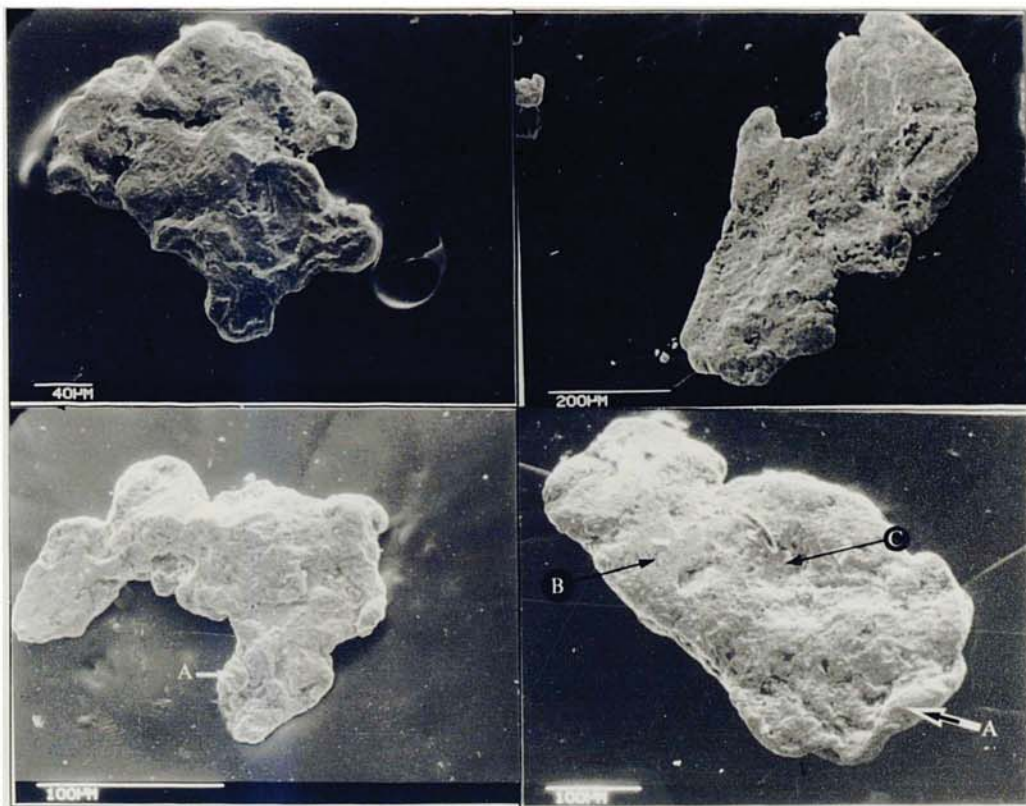
Plate 8.8b illustrates a placer gold grain that is well rounded and has numerous scratches on the surface. Note that the surface is not polished and has a slightly porous nature.

Plate 8.8c.

Plate 8.8c illustrates a rounded nugget shaped grain where the surface is generally smooth and worn, especially on protuberances (arrow A), but the polished and scratched surface exhibited by the grain illustrated in plate 8.8a has not been developed.

Plate 8.8d.

Plate 8.8d illustrates a well rounded placer gold grain with a small included quartz grain (arrow A). The surface of the grain is generally smooth a worn, but contains numerous small pits (arrow B).



Plates 8.9a to 8.9d show placer gold from the Southern Uplands that illustrate placer gold that exhibits the macro-morphological feature of flake shaped grains.

A	B
C	D

Plate 8.9a.

Plate 8.9a illustrates a placer gold grain that hammered and folded and the surface polished smooth by abrasion.

Plate 8.9b.

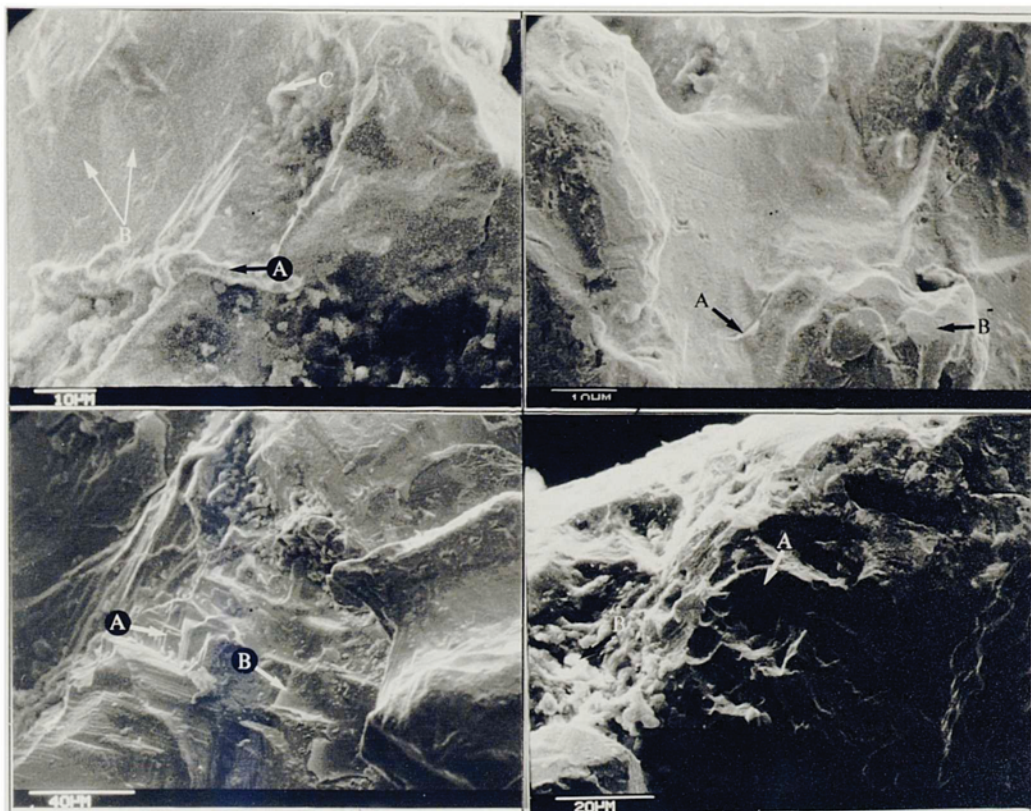
Plate 8.9b illustrates a placer gold grain that does not show any evidence of folding and there are no obvious scratches on the surface.

Plate 8.9c

Plate 8.9c illustrates a placer gold grain that is flake shaped and where protuberances have been folded and flattened (arrow A).

Plate 8.9d.

Plate 8.9d shows a placer gold grain where the edges of the grain have been rolled up (arrow A). The surface of the grain is generally smooth with an overall undulatory appearance. The crests of the undulations have been worn smooth (arrow B), however in the troughs there are a number of small pits (arrow C).



Plates 8.10a to 8.10d show placer gold grains from the Southern Uplands that are used to illustrate the micro-morphological feature of a smooth unworn surface at high magnification.

A	B
C	D

Plate 8.10a.

Plate 8.10a shows a placer gold grain where the original surface features of the grain have been perfectly preserved: the surface shows no sign of attrition and is completely scratch free, and all the fine surface details still present (e.g., the small ridge indicated by arrow A, and the atomic number contrast between compositionally different parts of the grain [dark veins indicated by arrow B]). Also note the formation of authigenic clay minerals (arrow C).

Plate 8.10b.

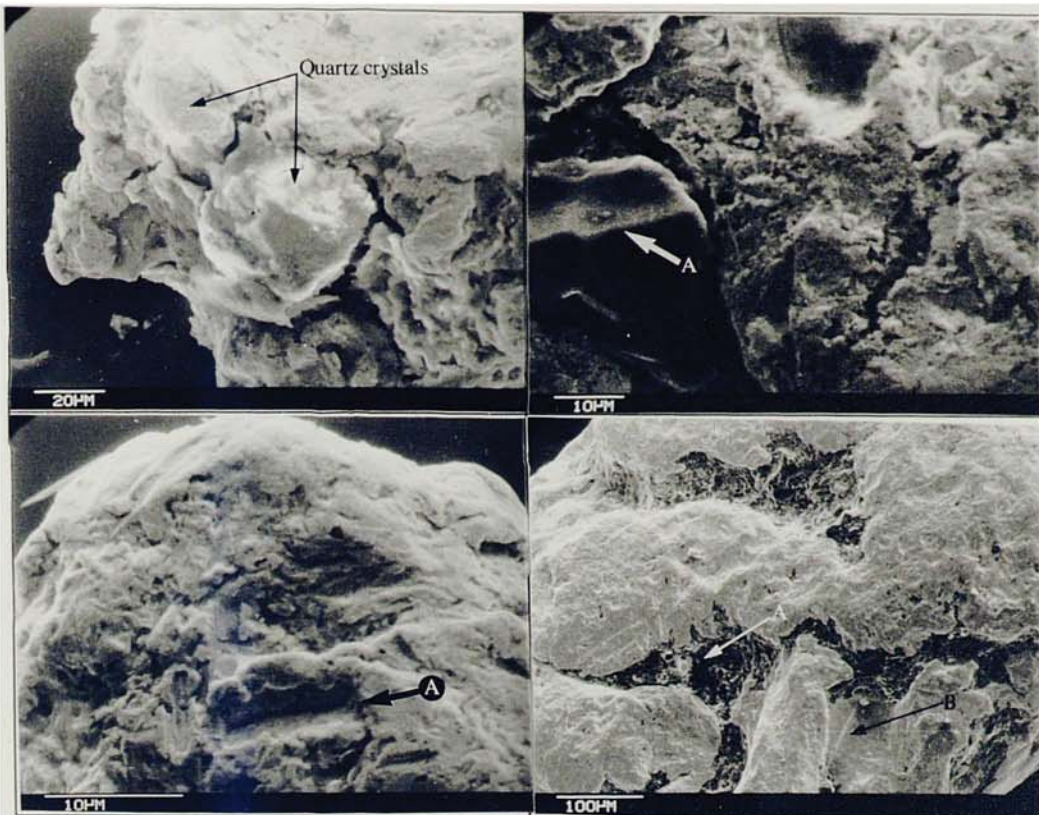
Plate 8.10b illustrates a placer gold grain where the smooth unworn surface is not perfectly preserved: it is scratched (arrow A), and protuberances on the surface show signs of deformation and abrasion (arrow B).

Plate 8.10c.

Plate 8.10c illustrates a grain where original smooth unworn crystal faces have been preserved (arrow A). Also note that in places the surface is coated by clay minerals (arrow B).

Plate 8.10d.

Plate 8.10d shows a placer gold grain where unworn irregularities (arrow A) are preserved. These irregularities have no obvious crystallographic element to them. Also note the trapping of clay minerals within cavities in the irregularities (arrow B).



Plates 8.11a to 8.11d show placer gold from the Southern Uplands that illustrate the micro-morphological feature of original inclusions.

A	B
C	D

Plate 8.11a.

Plate 8.11a shows a placer gold grain where two grains of quartz are present on the surface of the grain.

Plate 8.11b.

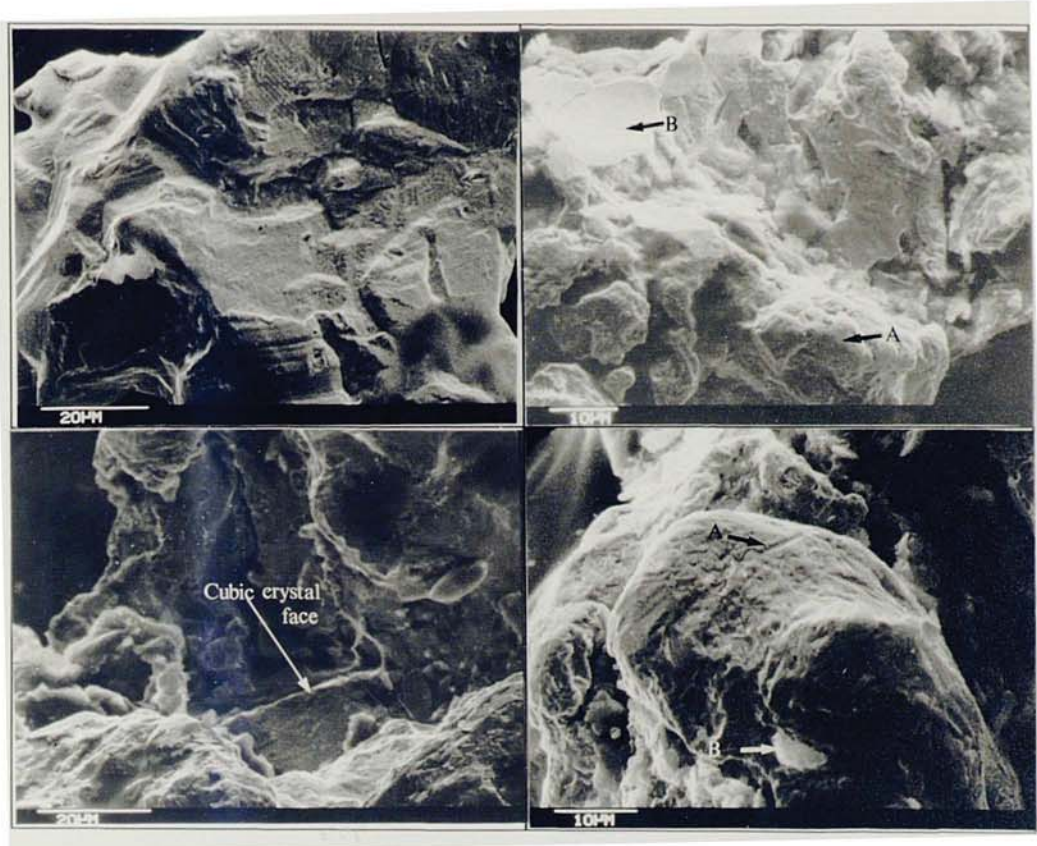
Plate 8.11b illustrates a placer gold grain with an included twinned quartz grain (arrow A).

Plate 8.11c.

Plate 8.11c illustrates a placer gold grain where an included grain that had a cubic or prismatic habit has been removed leaving an inclusion scar.

Plate 8.11d.

Plate 8.11d illustrates a placer gold grain that is intergrown with "vein" quartz (arrow A). Note that the smooth unworn surface is still present in cavities (arrow B) that have been protected from abrasion.



Plates 8.12a to 8.12d show placer gold grains from the Southern Uplands that illustrate the micro-morphological feature of an irregular surface at high magnification.

A	B
C	D

Plate 8.12a.

Plate 8.12a shows a placer gold grain with an irregular surface at high magnification. The surface still retains its glazed appearance and has undergone virtually no abrasion.

Plate 8.12b.

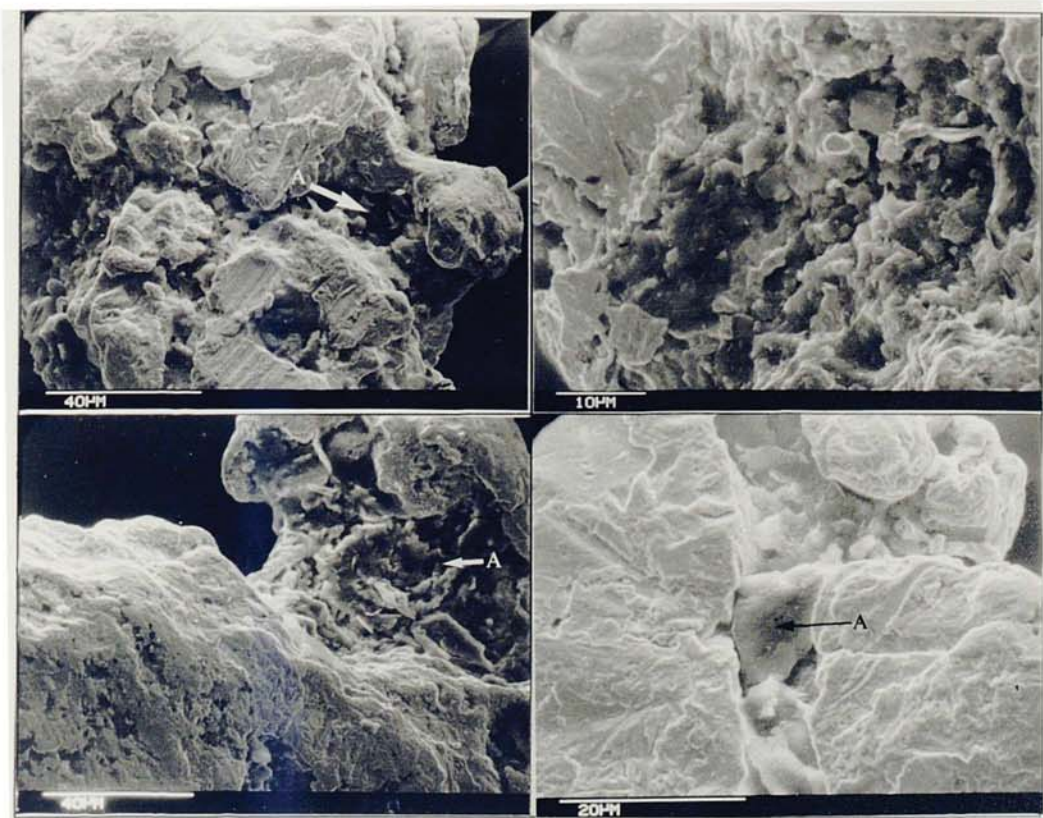
Plate 8.12b illustrates a placer gold grain where surficial irregularities have been rounded and deformed (arrow A). One particular area (arrow A) has been hammered to form a crater on the surface. Also note that clay minerals have been trapped in pockets on the surface of the grain.

Plate 8.12c.

Plate 8.12c shows a grain where irregular protuberances on the surface of the grain have protected crystal faces from abrasion and deformation.

Plate 8.12d.

Plate 8.12d illustrates a placer gold grain where the surface irregularities have been well rounded and scratched (arrow A). Also note the embedded TiO_2 grain (arrow B).



Plates 8.13a to 8.13d illustrate placer gold grains that show the micro-morphological feature of trapped mineral grains.

A	B
C	D

Plate 8.13a.

Plate 8.13a illustrate a placer gold grain with an irregular surface where clay minerals have been trapped in pockets and cavities on the surface of the grain (arrow A).

Plate 8.13b.

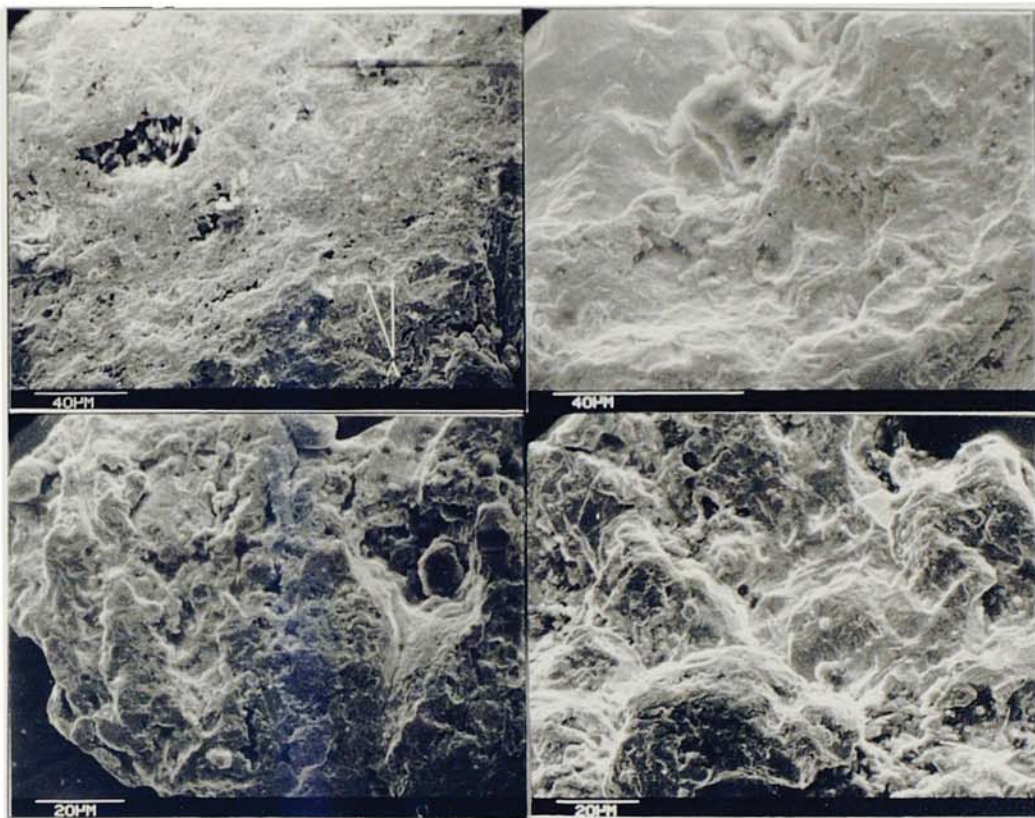
Plate 8.13b illustrates a placer gold grain where the majority of the surface within the field of view is coated with clay minerals.

Plate 8.13c

Plate 8.13c shows a placer gold grain with a smooth and worn surface (arrow A) which is not coated with clay minerals. However clay minerals are trapped within a depression on the surface of the grain (arrow B).

Plate 8.13d.

Plate 8.13d shows a placer gold grain with a surface that has been polished and scratched and clay minerals have been trapped in a crevasse that looks like a vein cutting the grain (arrow A).



Plates 8.14a to 8.14d show placer gold grains from the Southern Uplands that exhibit the micro-morphological feature of a flaky surface at high magnification.

A	B
C	D

Plate 8.14a.

Plate 8.14a illustrates a placer gold grain that exhibits a flaky texture. The flaky appearance of the grain is caused by numerous thin ($1\mu\text{m}$) ridges on the surface the grain (arrow A).

Plate 8.14b.

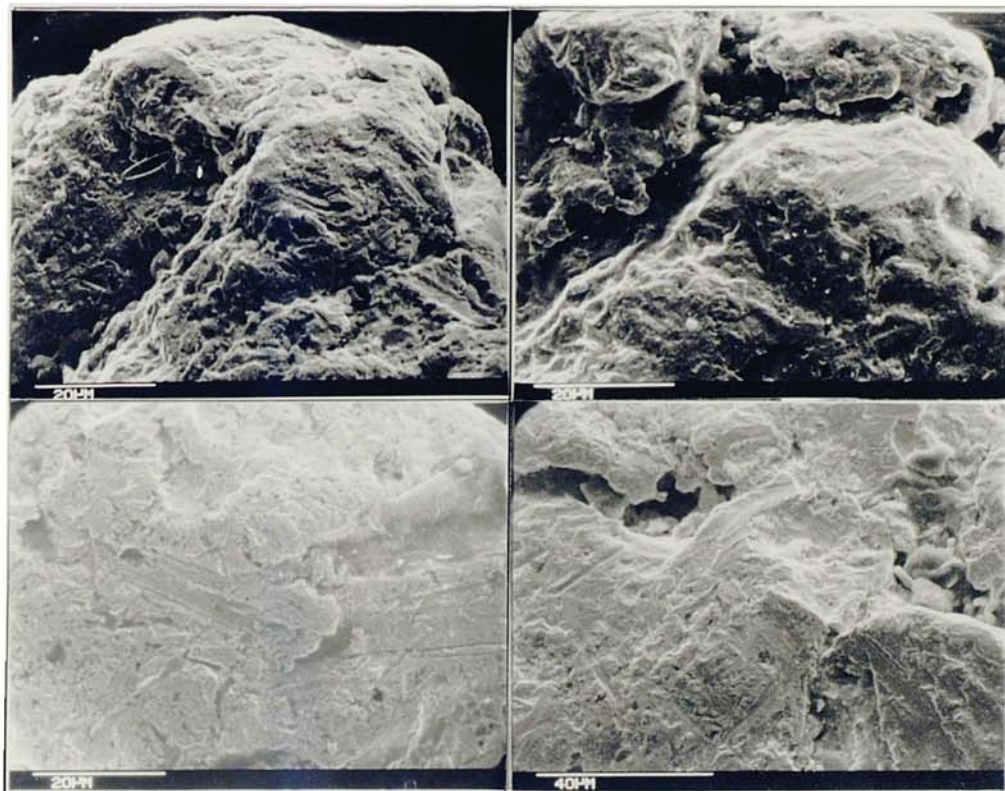
Plate 8.14b illustrates a placer gold grain where the flaky texture is slightly coarser than the grain illustrated in plate 8.14a. In this grain the ridges which give the grain its flaky appearance are more widely spaced.

Plate 8.14c.

Plate 8.14c shows a grain with a very coarse flaky texture, where protuberances have been flattened to the ridges and irregular pattern.

Plate 8.14d.

Plate 8.14d shows a placer gold grain with incipient flaky texture, where rounded protuberances have not been completely flattened to form ridges.



Plates 8.15a to 8.15d illustrate placer gold grains from the Southern Uplands that exhibit the micro-morphological features where the surface is generally smooth and worn at high magnification, and the surface of the grain has random scratches on it.

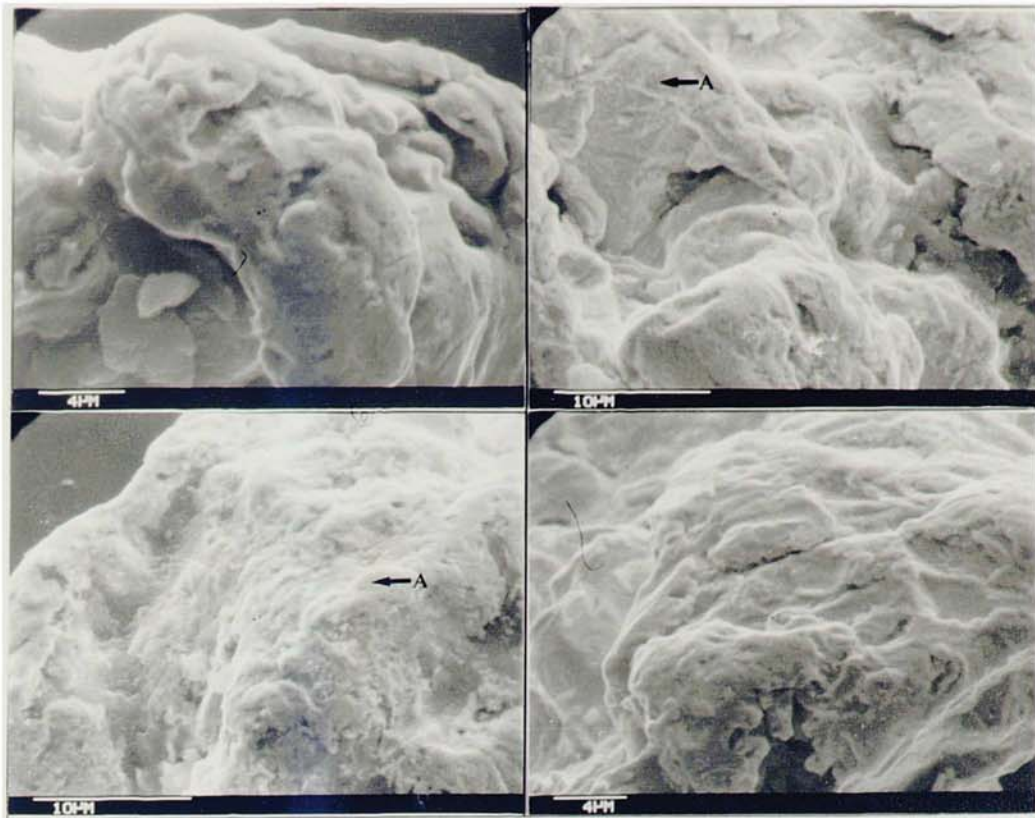
A	B
C	D

Plate 8.15a and plate 8.15b.

The above two plates illustrate placer gold grains where the surface is generally smooth and worn, but random scratches on the surface are rare or absent

Plate 8.15c and plate 8.15d.

The above two plates show placer gold grains where the surface is smooth and polished, and random scratches have been developed on the surface.



Plates 8.16a to 8.16d illustrate placer gold grains from the Southern Uplands that show the micro-morphological feature of the formation of a dough like surface texture at high magnification.

A	B
C	D

Plate 8.16a.

Plate 8.16a illustrates a placer gold grain the surface of which has a similar appearance to that of kneaded bread. This texture is probably the result of plastic deformation of surface irregularities that have not been removed by abrasion (note the absence of abrasive scratches on the surface)

Plate 8.16b.

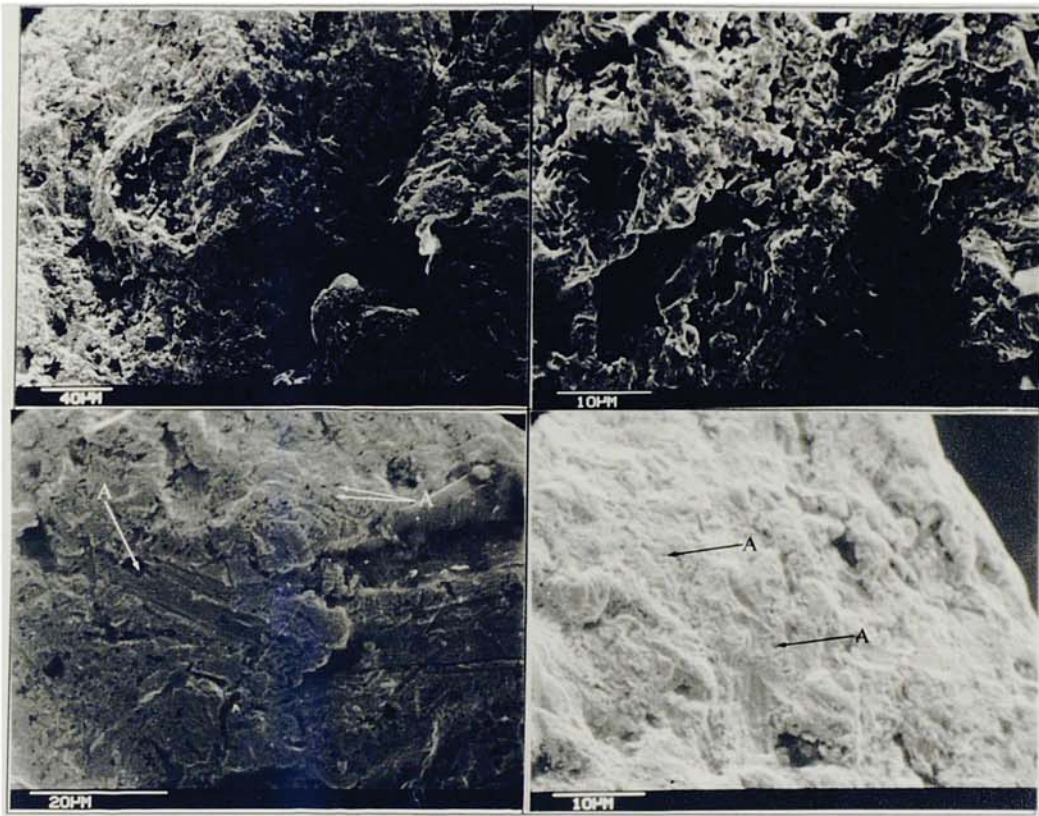
Plate 8.16b shows a placer gold grain the surface of which is generally irregular. However plastic deformation at the vertices of the irregularities is incipient development of the dough texture (arrow A).

Plate 8.16c.

Plate 8.16c illustrates a placer gold grain where the surface is generally smooth and has been deformed and worn. However abrasive scratches are absent from the surface and the small irregularities (arrow A) give the grain a dough like appearance. Also note that in the depressions on the grain the surface has a porous appearance.

Plate 8.16d.

Plate 8.16d shows a placer gold grain with similar surface feature to the grain illustrated in plate 8.16c, but the surface of this grain shows no obvious porosity.



Plates 8.17a to 8.17d illustrate placer gold grains from the Southern Uplands which exhibit the micro-morphological feature of a porous surface at high magnification.

A	B
C	D

Plate 8.17a.

Plate 8.17a illustrates a placer gold grain where the surface appears porous and filamentous, and the surface shows no obvious signs of abrasion and deformation.

Plate 8.17b

Plate 8.17b shows a placer gold with a coarser porous texture than the grain illustrated in plate 8.17a.

Plate 8.17c.

Plate 8.17c shows a placer gold grain where the surface is smooth and worn, but still full of small ($1\mu\text{m}$) pits that give the surface a porous appearance (arrow A).

Plate 8.17d.

Plate 8.17d shows a placer gold grain where the surface is smooth and worn, with numerous small ($<5\mu\text{m}$) surface irregularities (arrow A). These irregularities probably represent relict porous texture (as illustrated in plates 8.17a and 8.17b) that has undergone deformation and abrasion.

Table 8.2. Relationship between macro- and micro-morphologocal characteristics, showing the most commonly associated macro- and micro-morphological characteristics. The numbers in the table refer to the different morphological characteristics (see text and table 8.1 for details), and the asterisks represent the common occurrence of a macro-morphological characteristic with a micro-morphological characteristic.

	9	10	11	12	13	14	15	16	17	18
1	*		*							
2	*		*							
3	*		*					*		
4		*	*	*		*	*	*		
5		*	*	*		*	*	*		
6		*				*	*	*		
7		*			*	*	*	*		*
8					*	*	*		?	*

FIGURES, PLATES AND TABLES
FOR CHAPTER 9:

MORPHOLOGICAL,
PETROLOGICAL AND
MINERALOGICAL DATA FOR THE
SOUTHERN UPLANDS PLACER
GOLD.

Figure 9.1. Map showing the geology and the distribution of placer gold in the Loch Doon-Glenkens area.



Figure 9.2. Map showing the geology and the distribution of placer gold in the Abington-Biggar-Moffat area.



Figure 9.3. Histogram showing the distribution of macro-morphological characteristics of the Loch Doon-Glenkens placer gold.

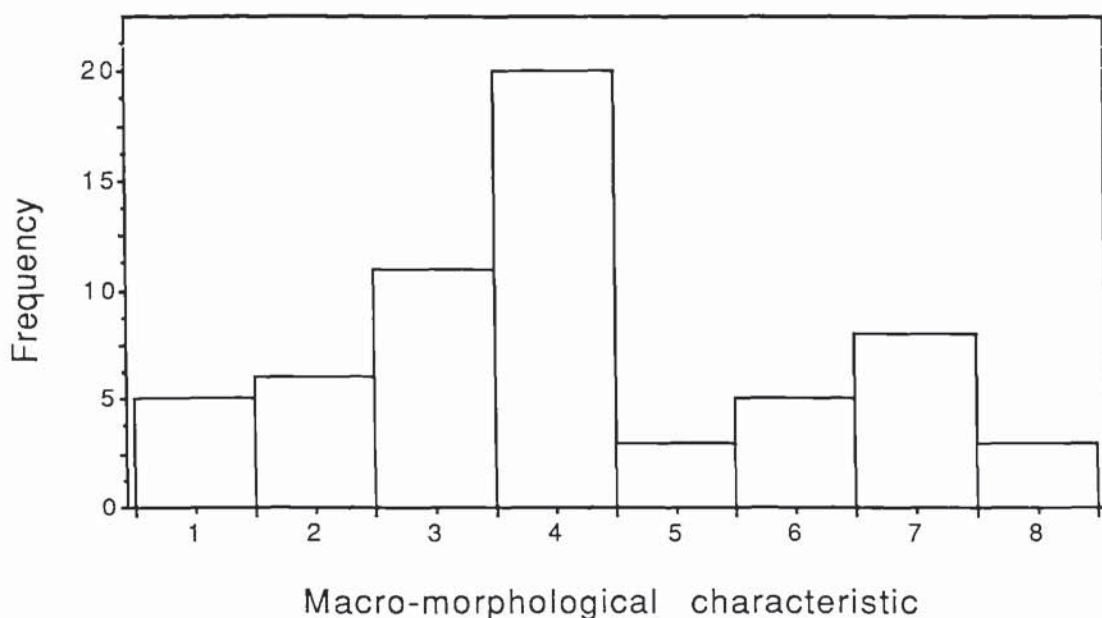


Figure 9.4. Histogram showing the distribution of micro-morphological characteristics of the Loch Doon-Glenkens placer gold.

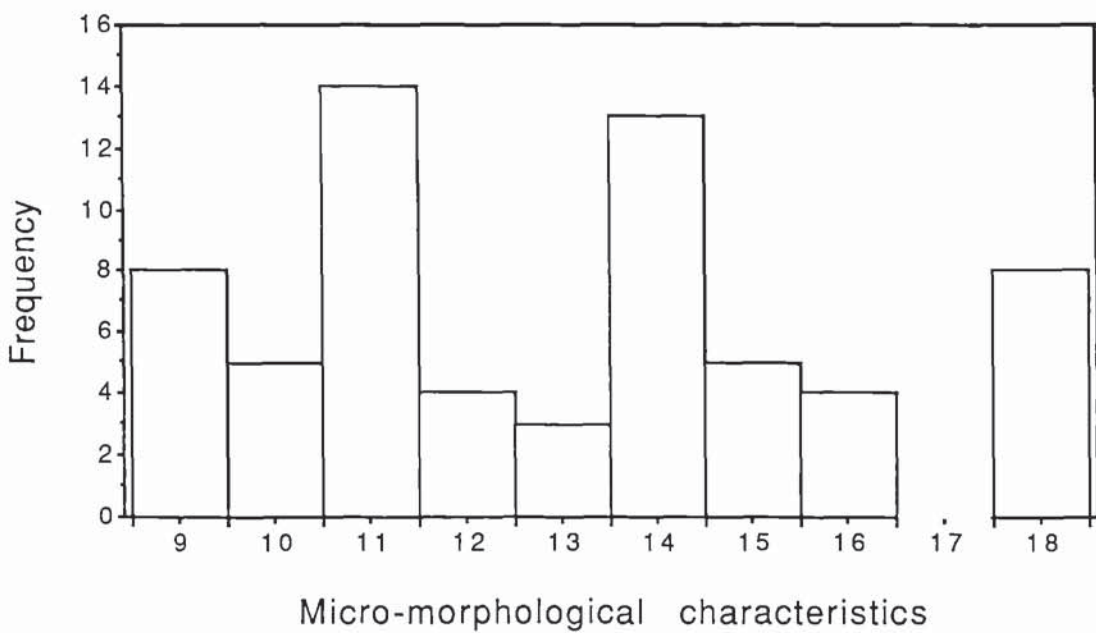


Figure 9.5. Geographical distribution of macro-morphological characteristics for the Loch Doon-Glenkens placer gold. Proximal grains are those which exhibit characteristics 1-4 inclusive, distal represents characteristics 5-8 inclusive and porous refers to grains having characteristic 18.

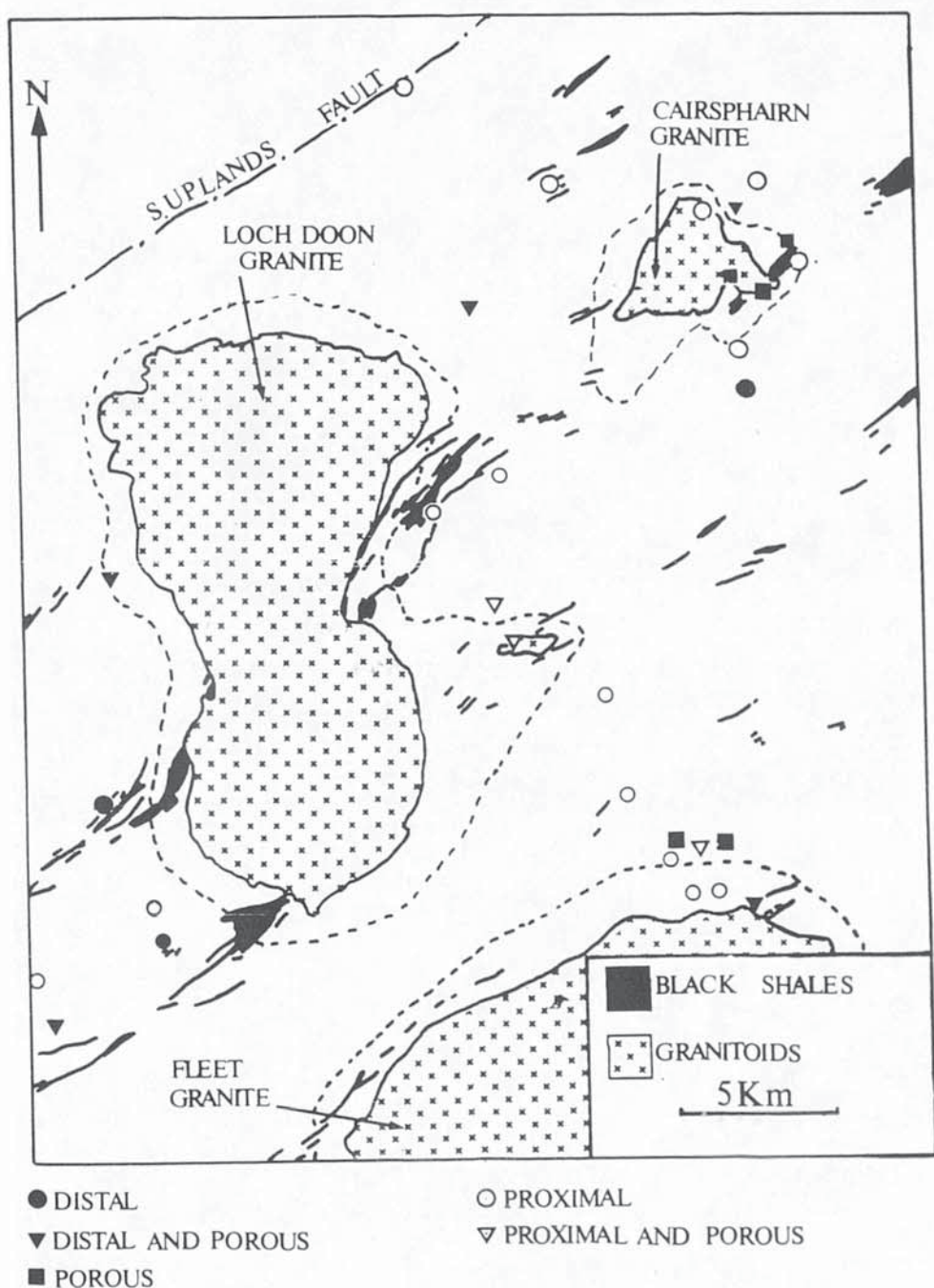


Figure 9.6. Geographical distribution of micro-morphological characteristics for the Loch Doon-Glenkens placer gold. MICRO A grains are those which exhibit characteristics 9 to 13 inclusive, MICRO B represents characteristics 14-18 inclusive and porous refers to grains having characteristic 18.

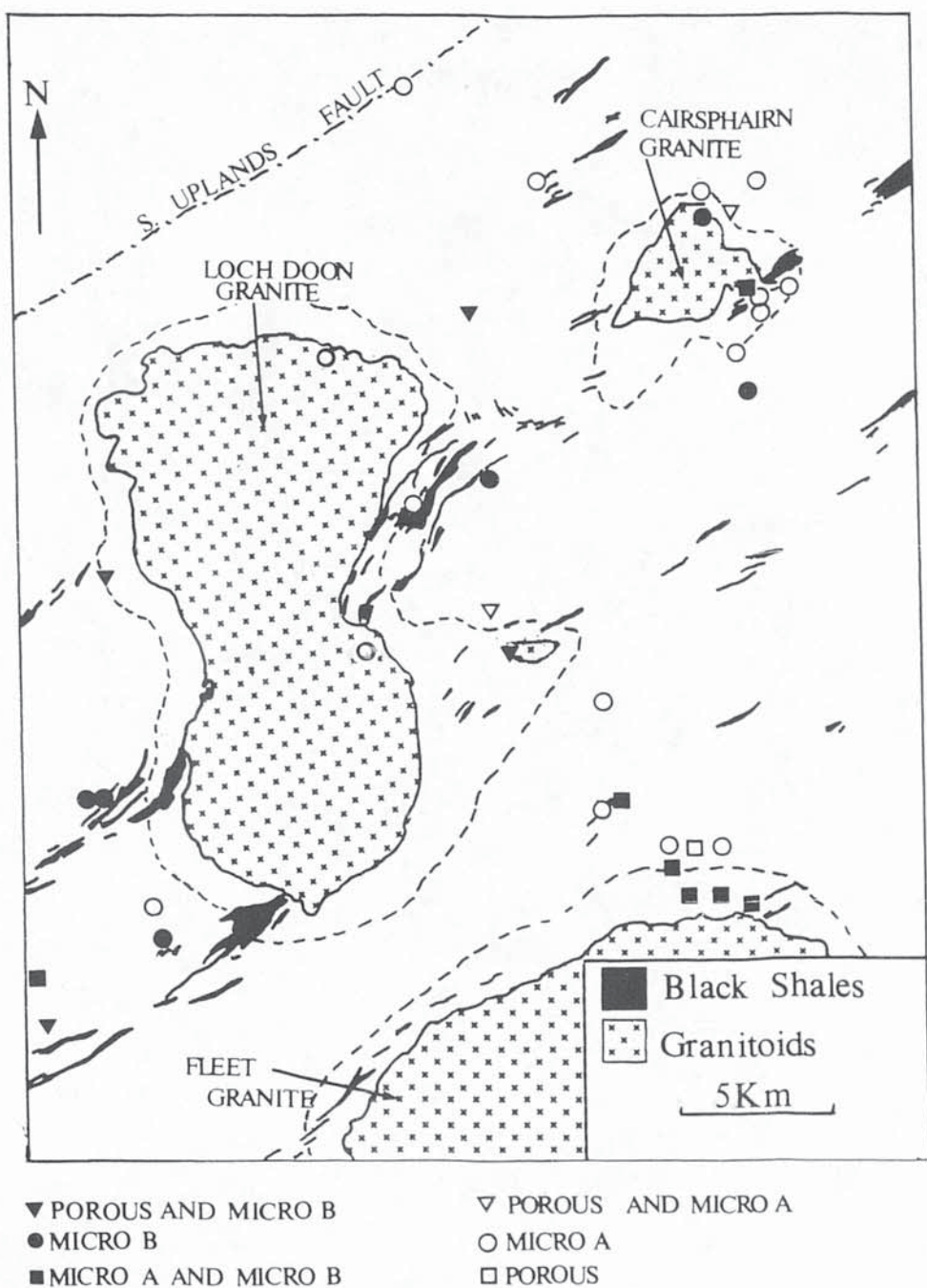
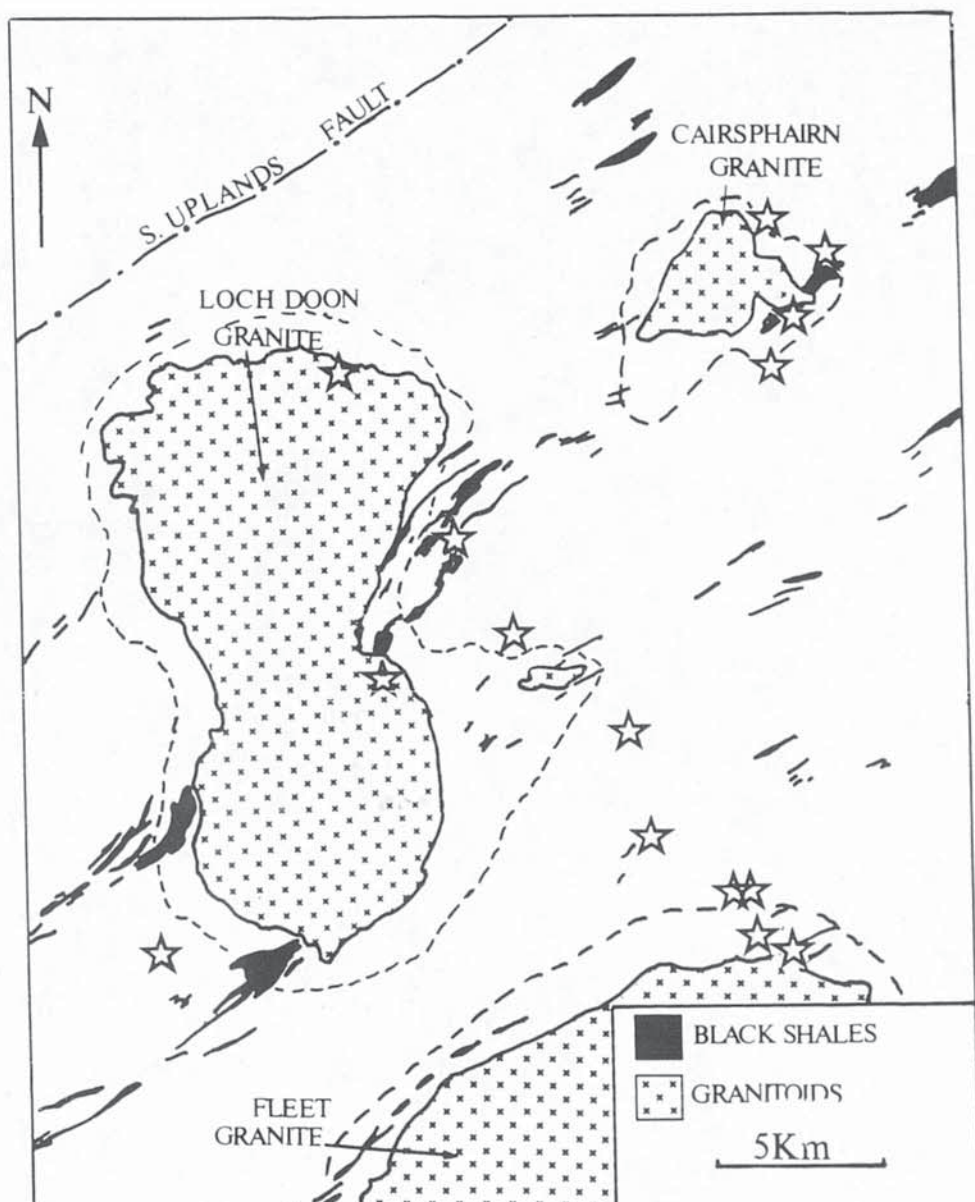


Figure 9.7. Geographical distribution of placer gold preserving original morphological features (characteristics 1-3 inclusive).



★ Morphological Characteristics 1 to 3

Figure 9.8. Histogram showing the surface fineness distribution (from semi-quantitative energy dispersive analysis) of placer gold from the Loch Doon-Glenkens area.

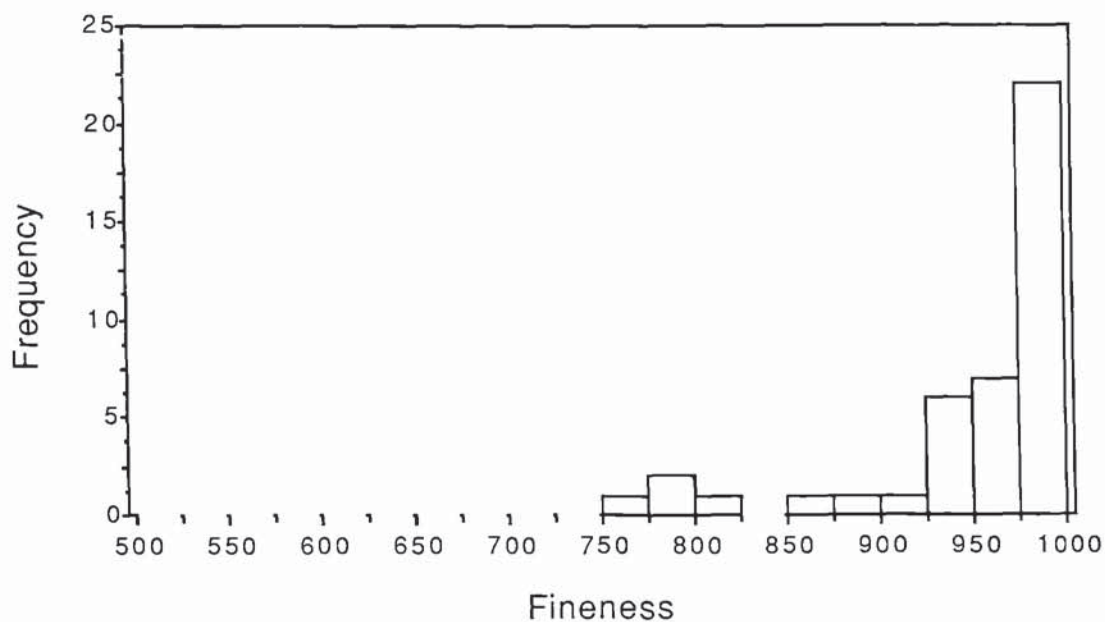


Figure 9.9. Geographical distribution of the surface fineness of placer gold from the Loch Doon-Glenkens area. Showing that the low surface fineness gold clustering around the Loch Doon and Cairsphairn granitoids.

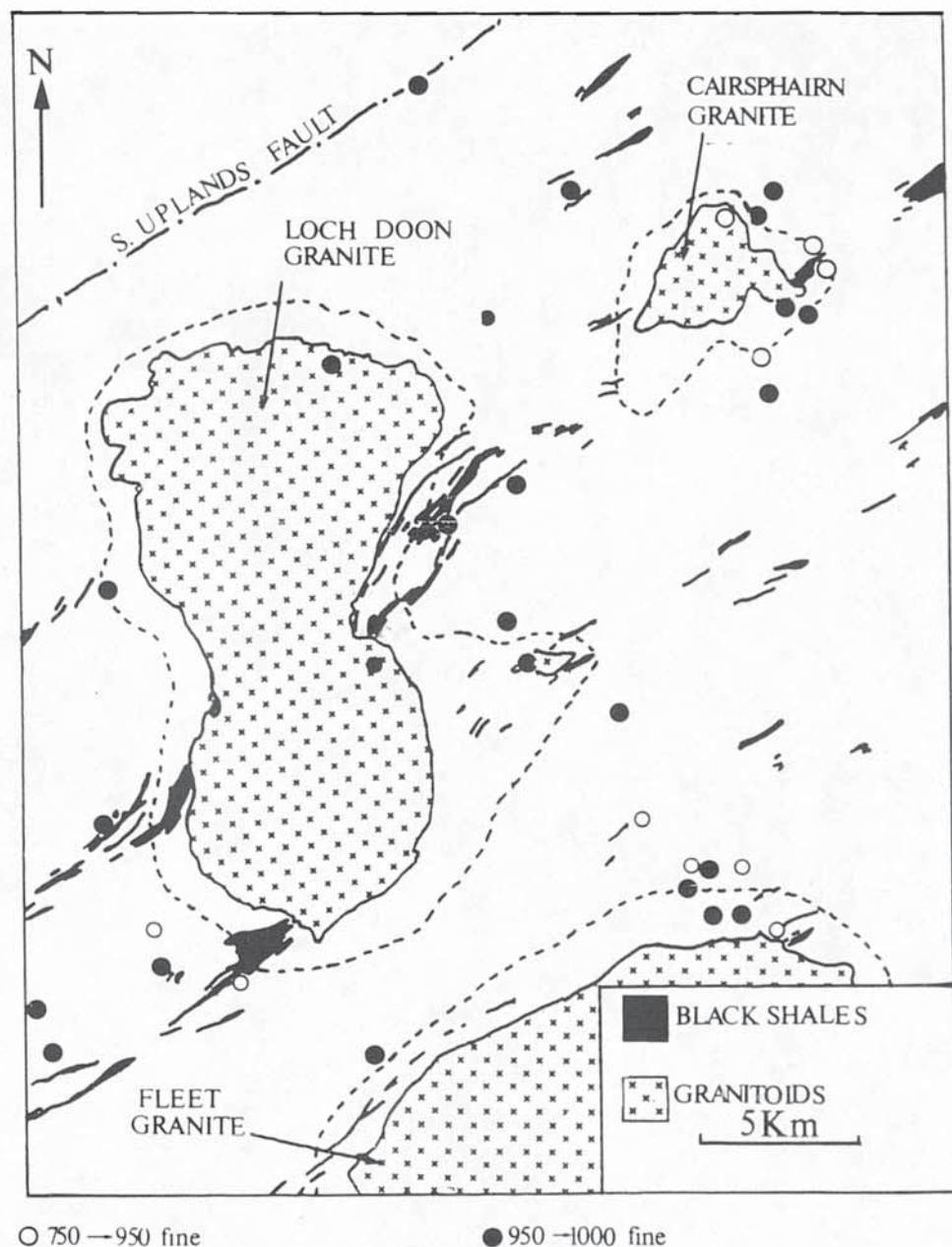


Plate 9.1. Back-scattered electron image and X-ray A-scan of a silver
telluride plater gold grain (sample no. C3). It is shown in the lower plate
in relation with the concentration of silver in the grain.

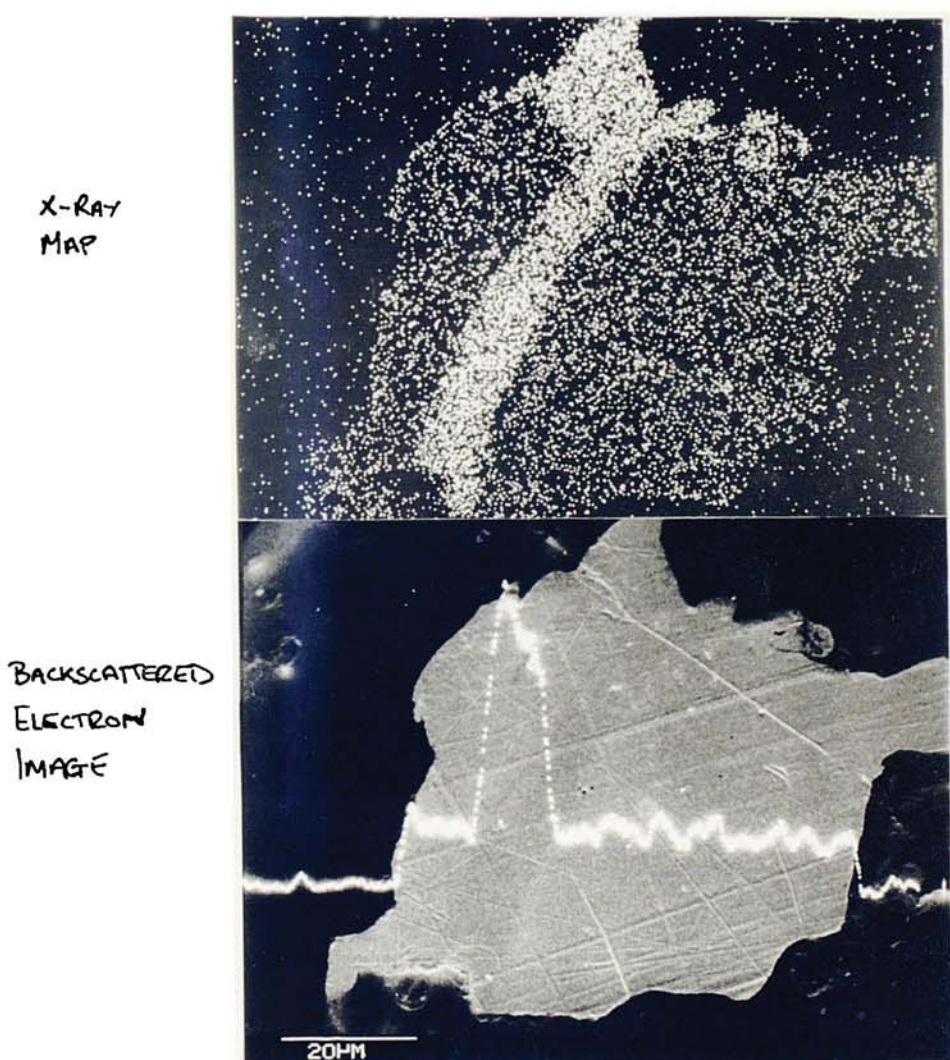


Plate 9.2. Photomicrograph of a thin incomplete gold enrichment rim on a placer gold grain (A). Also note the very thin white veinlet (B) cutting across the grain; this is a silver-rich heterogeneity. (PPL, field of view 225 μ m).

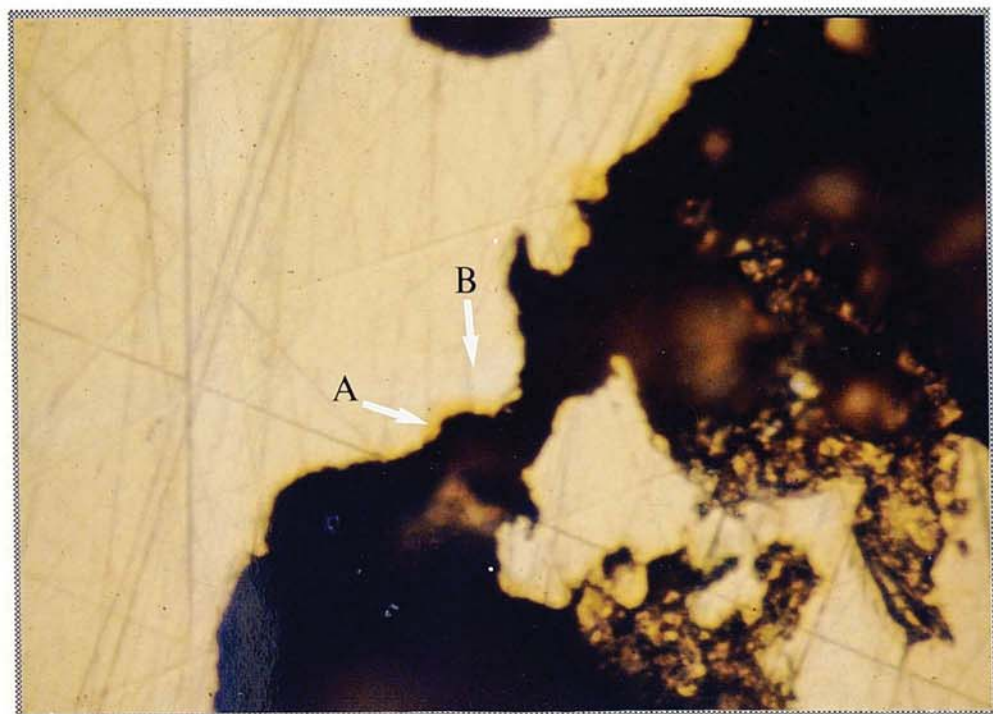


Plate 9.3. Backscattered electron image and X-ray ($\text{Bi}_{\text{M}\alpha}$) map of a native bismuth inclusion in a placer gold grain (sample no. C303).

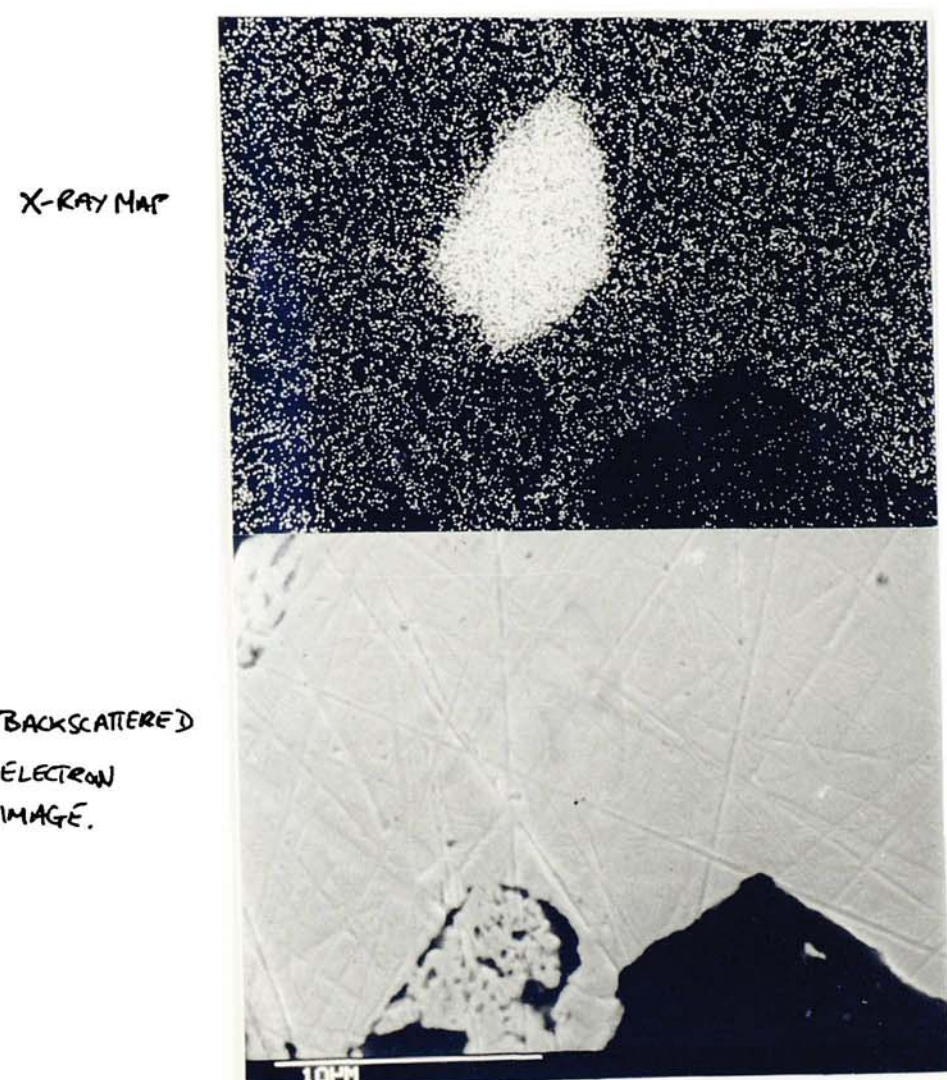


Table 1. Summary statistics of the fineness of the Loch Doon-Glenkens placer gold.

Minimum	511	Std. deviation	100
Maximum	992	Std. Error	18
Mean	886	Kurtosis	4.3
Median	906	Skewness	-1.9

Figure 9.10. Histogram showing the core fineness distribution (from EPMA analysis) of placer gold from the Loch Doon-Glenkens area.

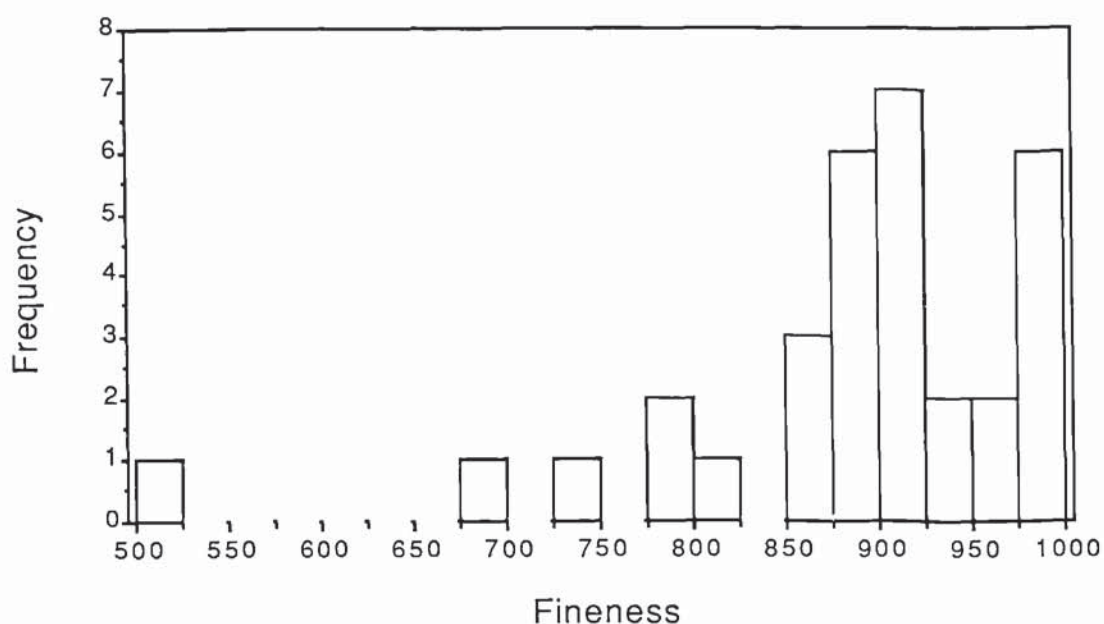


Figure 9.11. Geographical distribution of the core fineness of placer gold from the Loch Doon-Glenkens area. (Note that gold grains with a fineness <800 cluster around the Fleet and Cairspairn granitoids).

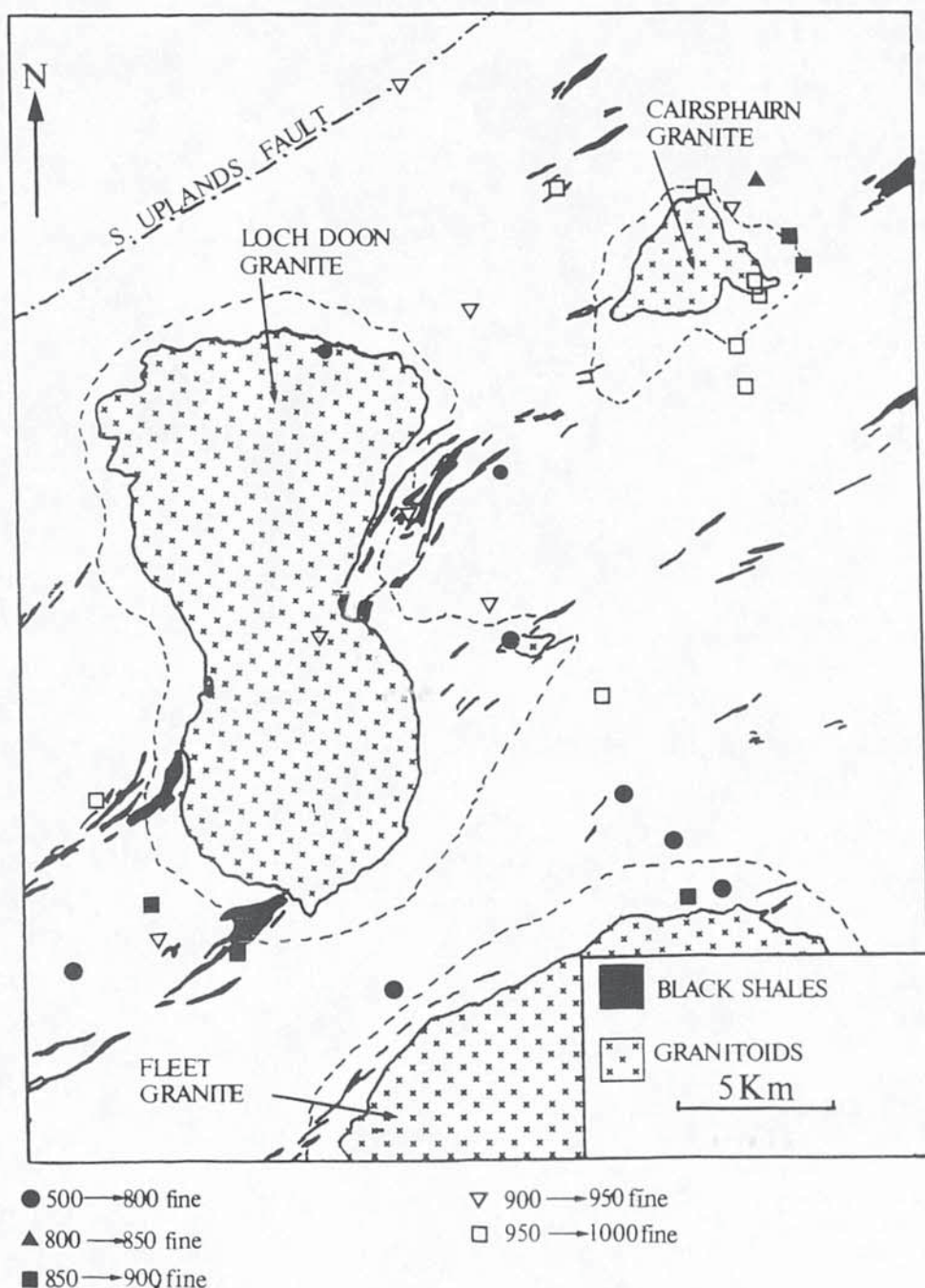


Figure 9.12a. Line concentration profile showing the variation in silver content in placer gold from pan concentrate C18.

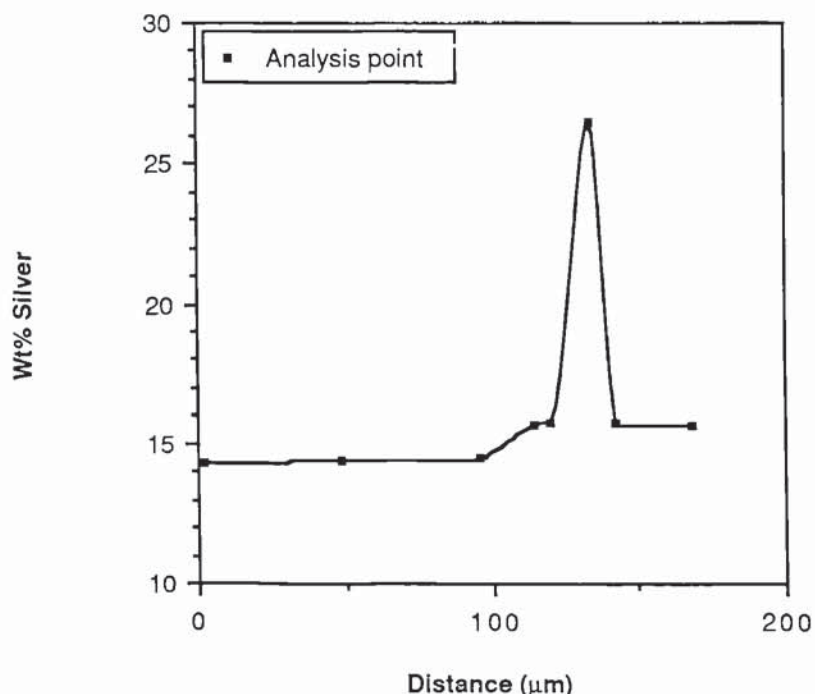


Figure 9.12b. Line concentration profile showing the variation in silver content in placer gold from pan concentrate C22.

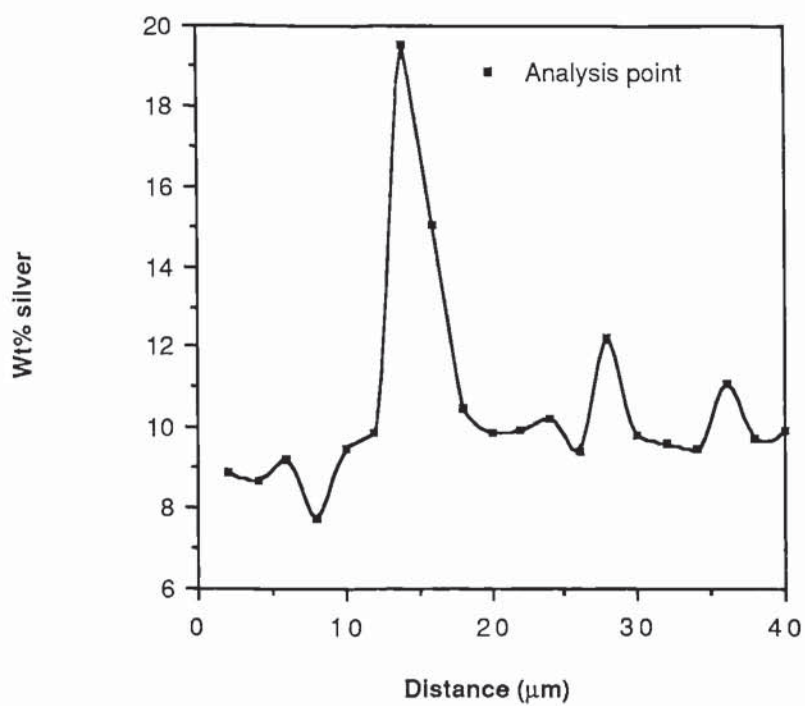


Figure 9.12c. Line concentration profile showing the variation in silver content in placer gold from pan concentrate C22.

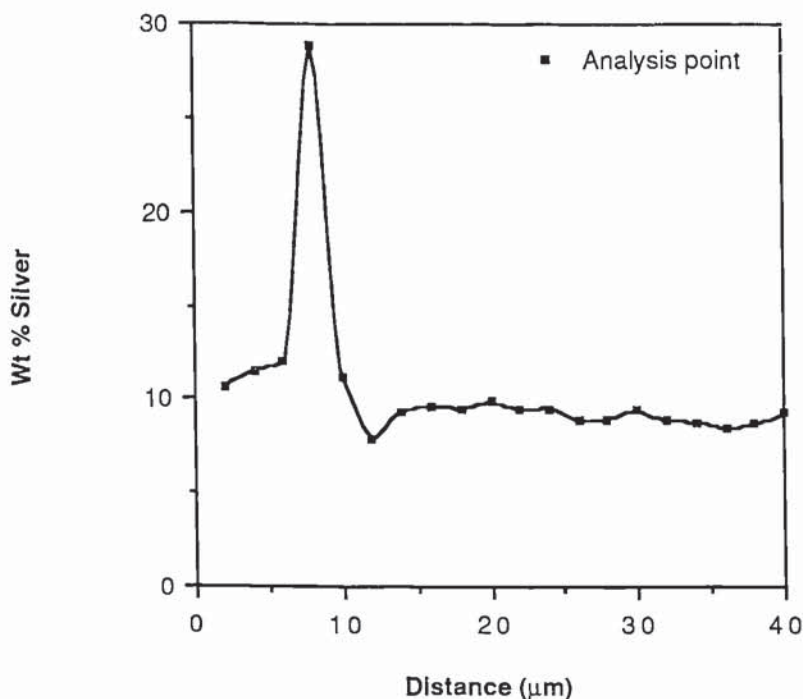


Figure 9.12d. Line concentration profile showing the variation in silver content in placer gold from pan concentrate C35.

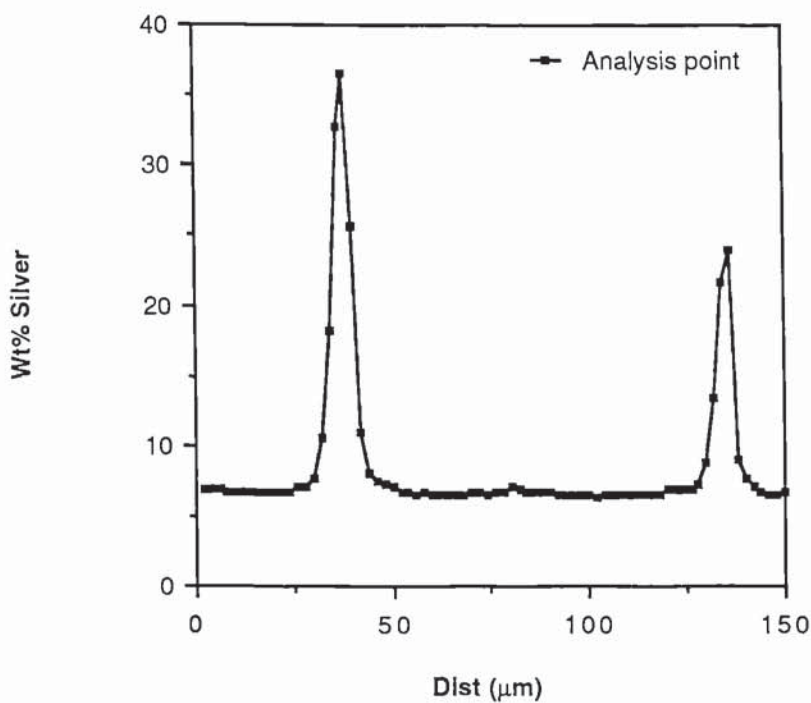


Figure 9.12e. Line concentration profile showing the variation in silver content in placer gold from pan concentrate C37.

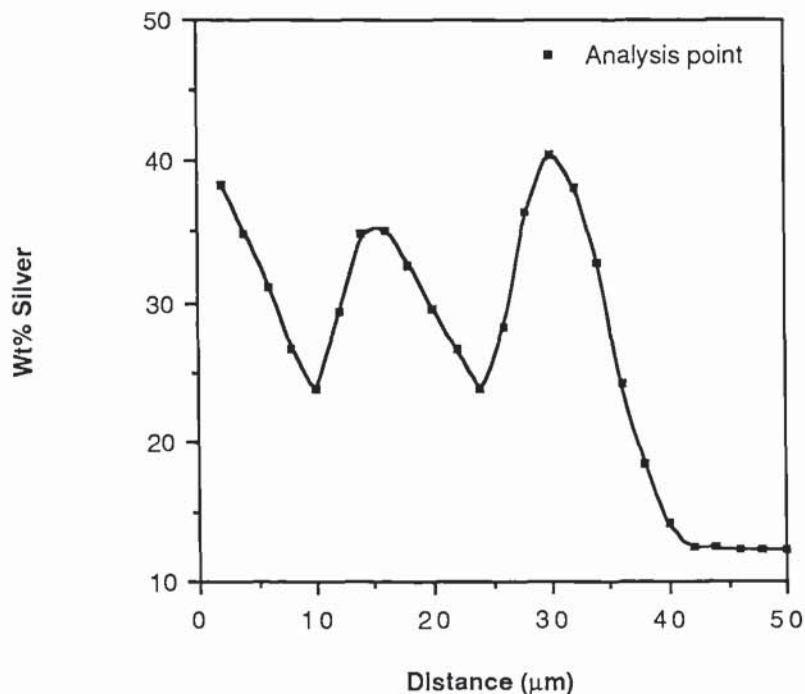


Figure 9.13. Annealing history limits for the heterogeneous placer gold from the Loch Doon-Glenkens area.

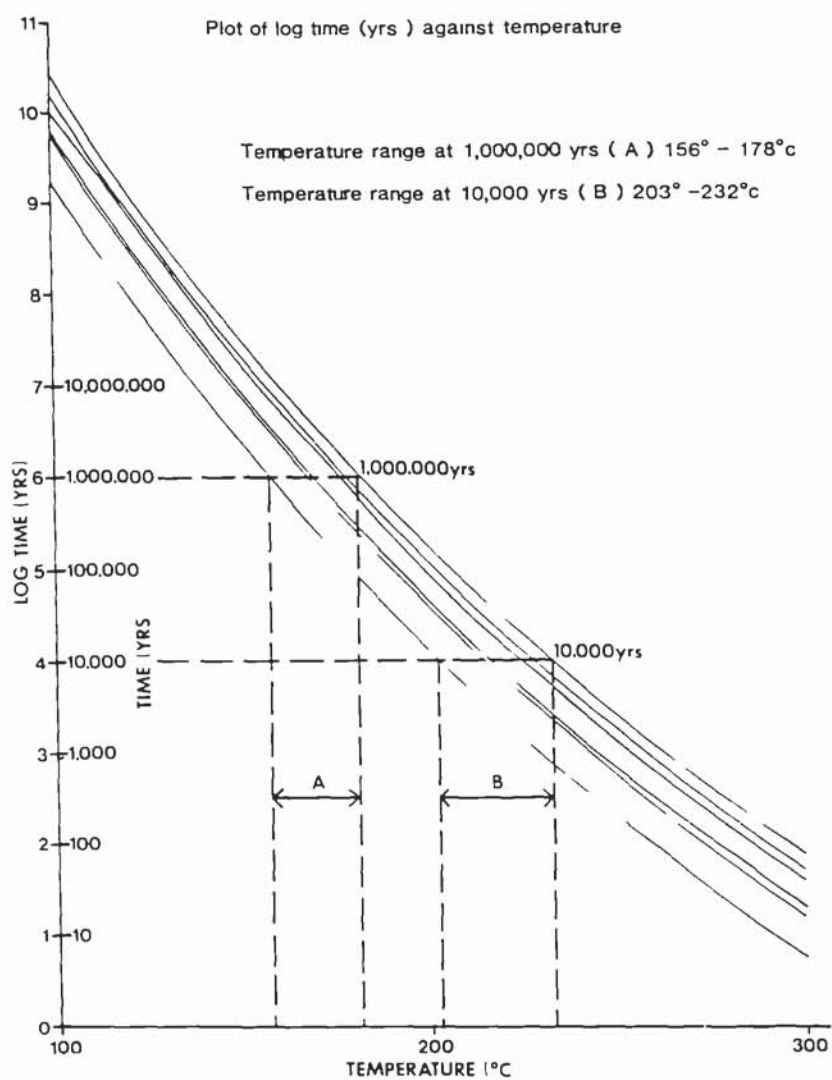


Figure 9.14. histogram of the distribution of macro-morphological characteristics of the Abington-Biggar-Moffat placer gold showing two maxima at characteristics 4 and 7.

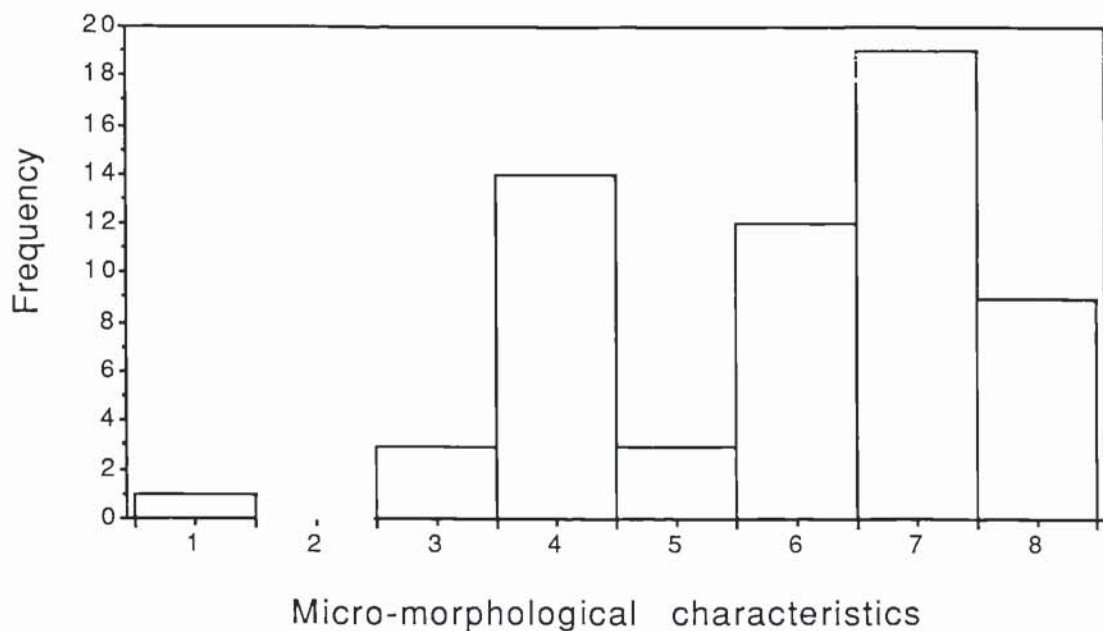


Figure 9.15. histogram of the distribution of micro-morphological characteristics of the Abington-Biggar-Moffat placer gold.

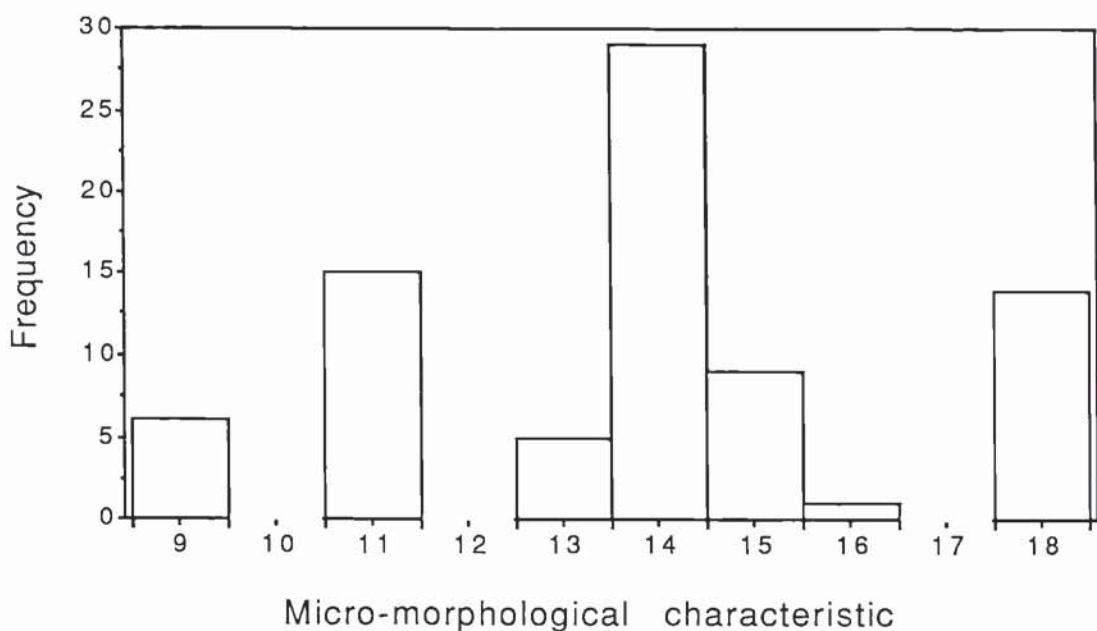


Figure 9.16. Geographical distribution of macro-morphological characteristics for the Abington-Biggar-Moffat placer gold. Proximal grains are those which exhibit characteristics 1-4 inclusive, distal represents characteristics 5-8 inclusive and porous refers to grains having characteristic 18.

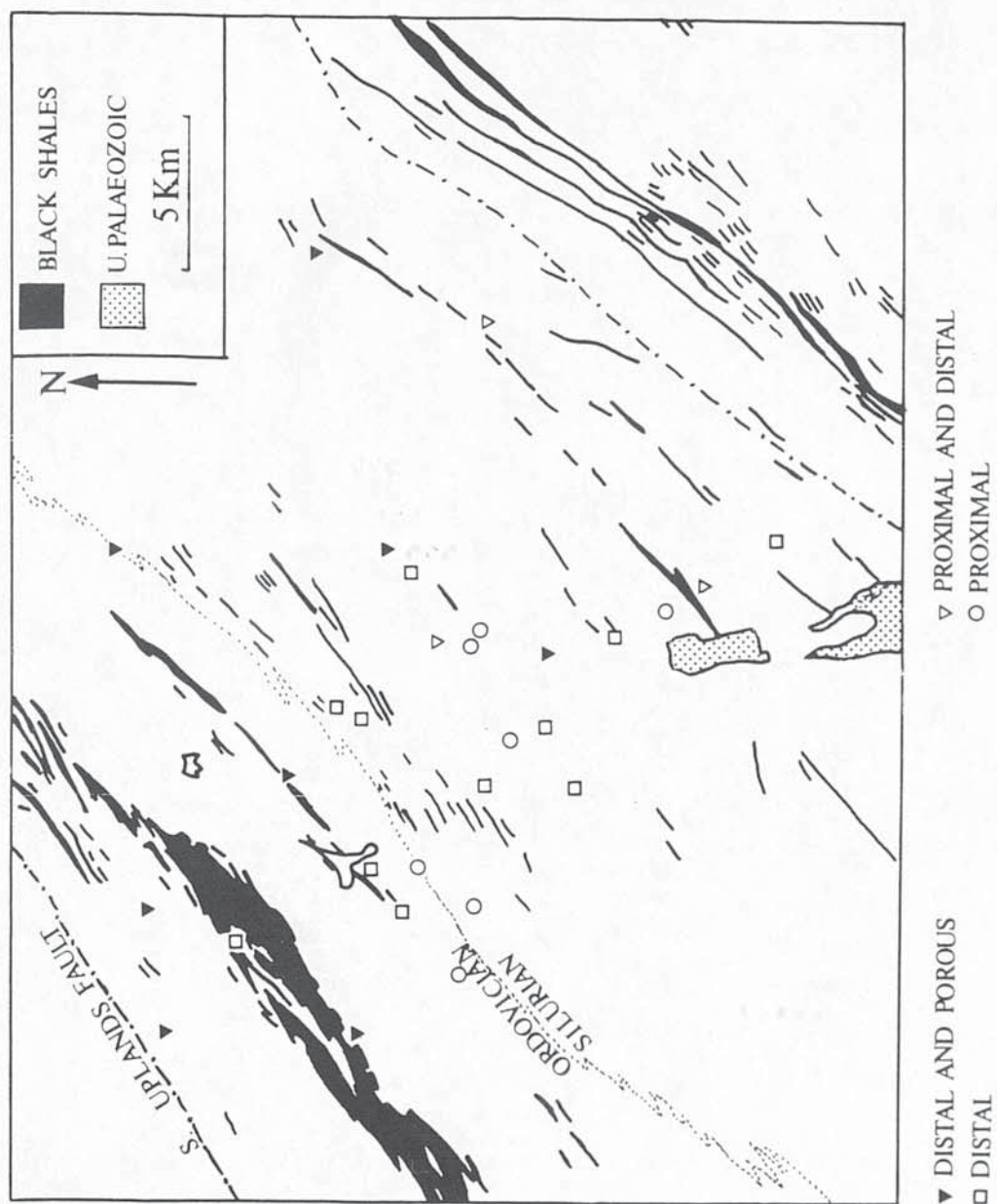


Figure 9.17. Geographical distribution of micro-morphological characteristics for the Abington-Biggar-Moffat placer gold. MICRO A grains are those which exhibit characteristics 9 to 13 inclusive, MICRO B represents characteristics 14-17 inclusive and porous refers to grains having characteristic 18.

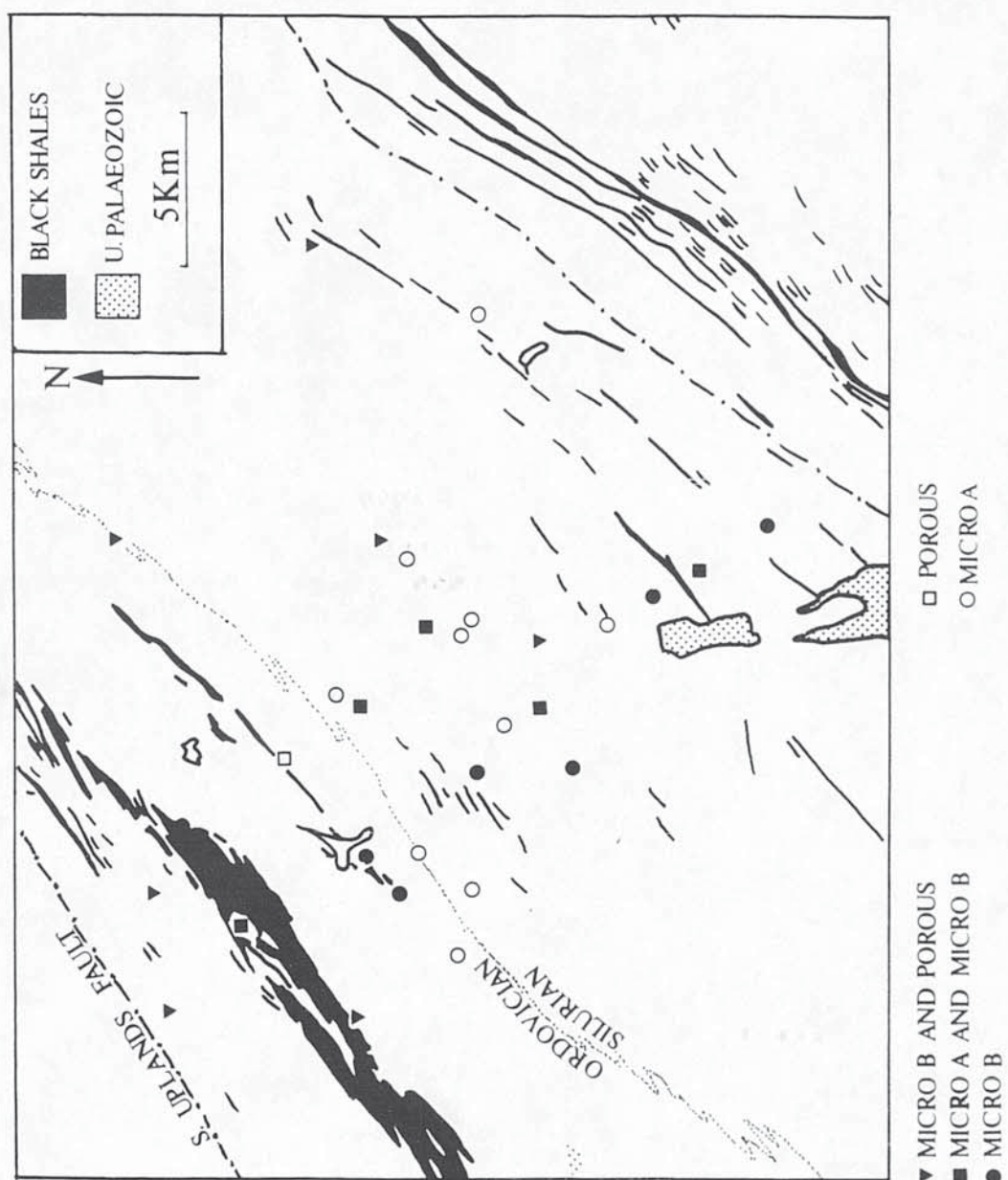


Figure 9.18. Histogram of the distribution of the surface fineness of the Abington-Biggar-Moffat placer gold.

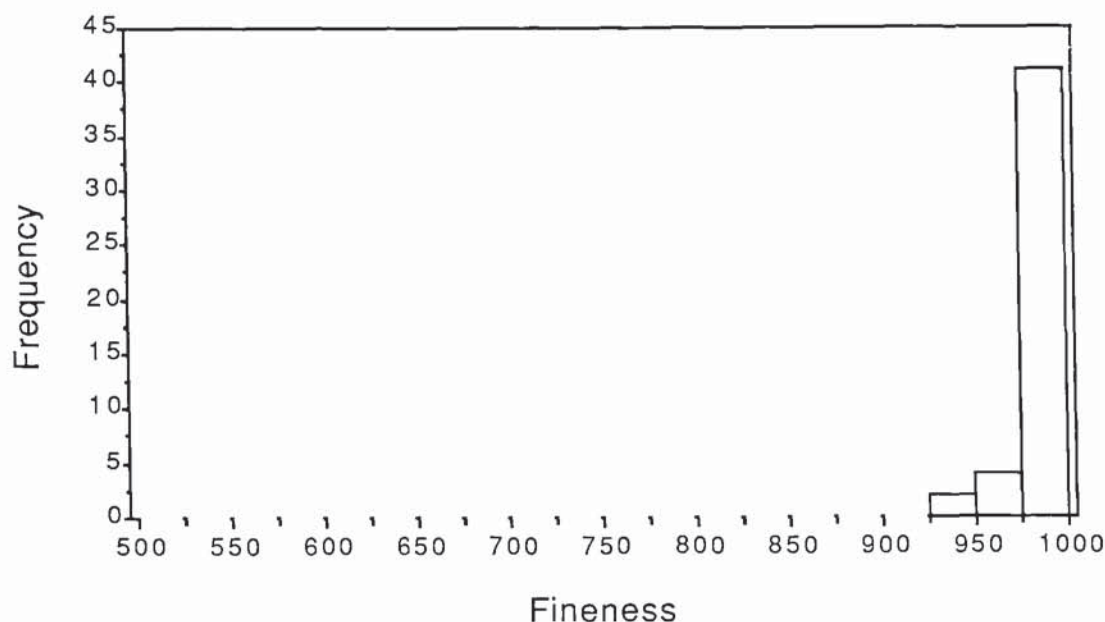


Table 9.2 Summary statistics of the core fineness of the Abington-Biggar-Moffat placer gold.

Minimum	854	Std. deviation	41
Maximum	1000	Std. Error	6
Mean	952	Kurtosis	-.4
Median	954	Skewness	-.6

Figure 9.19. Histogram of the distribution of the core fineness of the Abington-Biggar-Moffat placer gold.

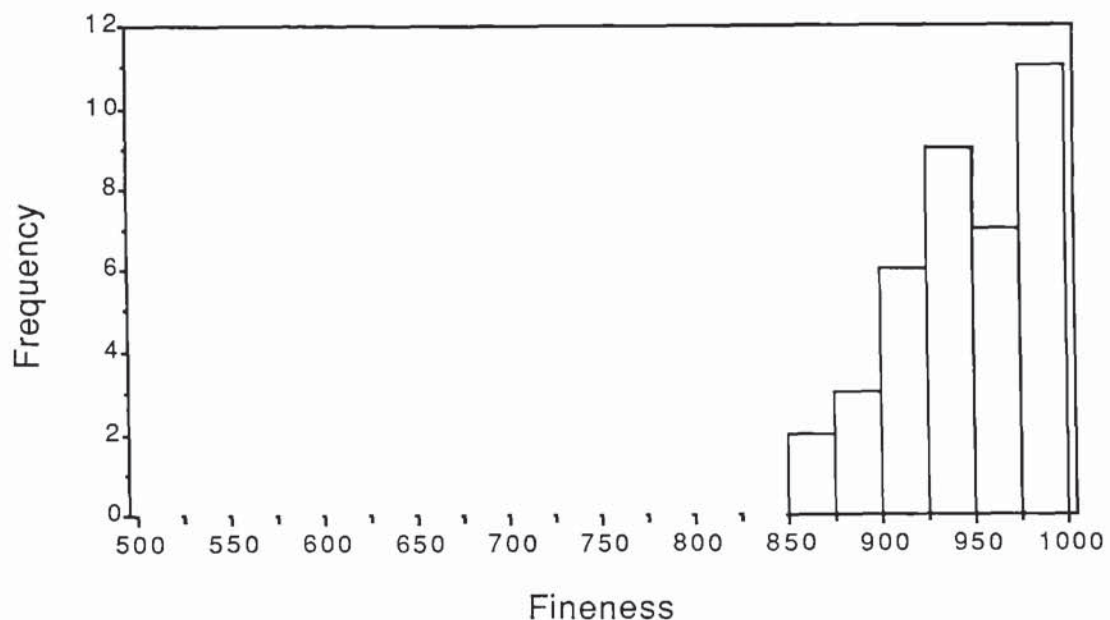


Figure 9.20. Geographical distribution of the core fineness of the placer gold from the Abington-Biggar-Moffat area.

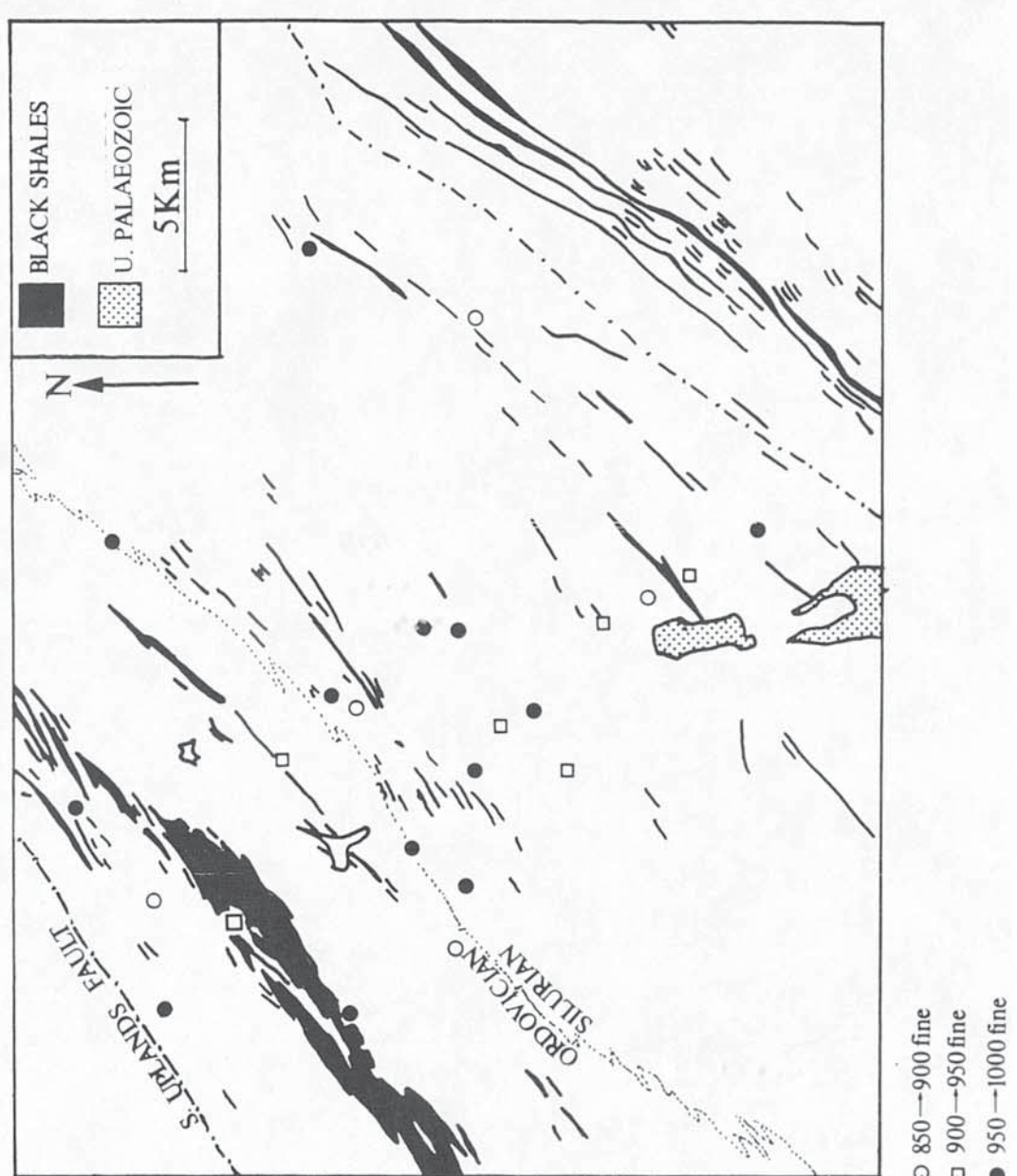


Figure 9.21. Histogram showing the frequency distribution of the macro-morphological characteristics of placer gold from the Loch Doon-Glenkens and the Abington-Biggar-Moffat areas.

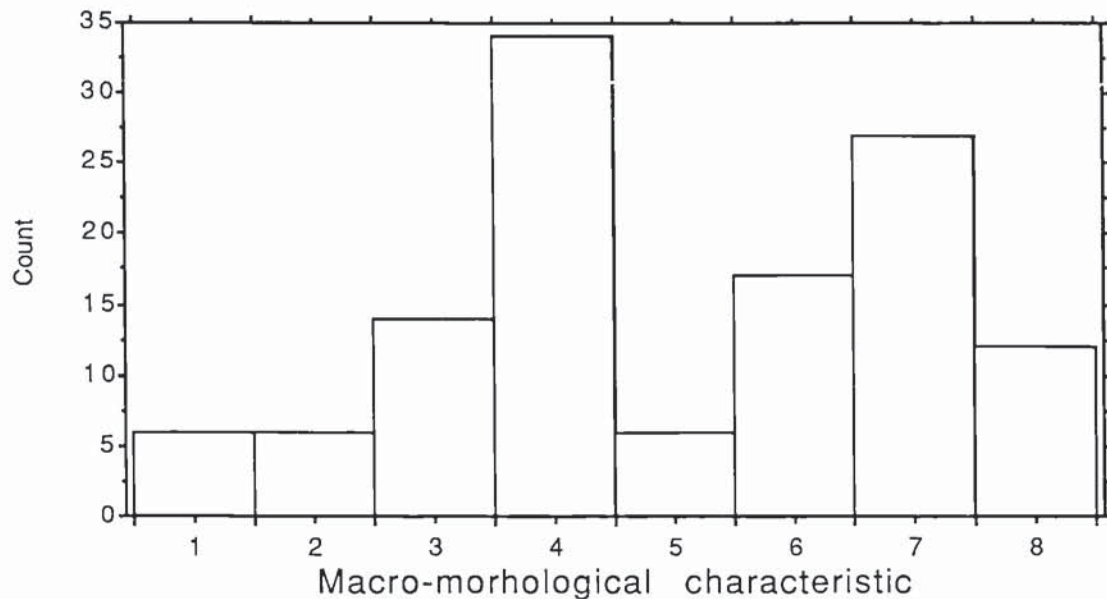


Figure 9.22. Histogram of the morphological characteristics of placer gold with fineness <950.

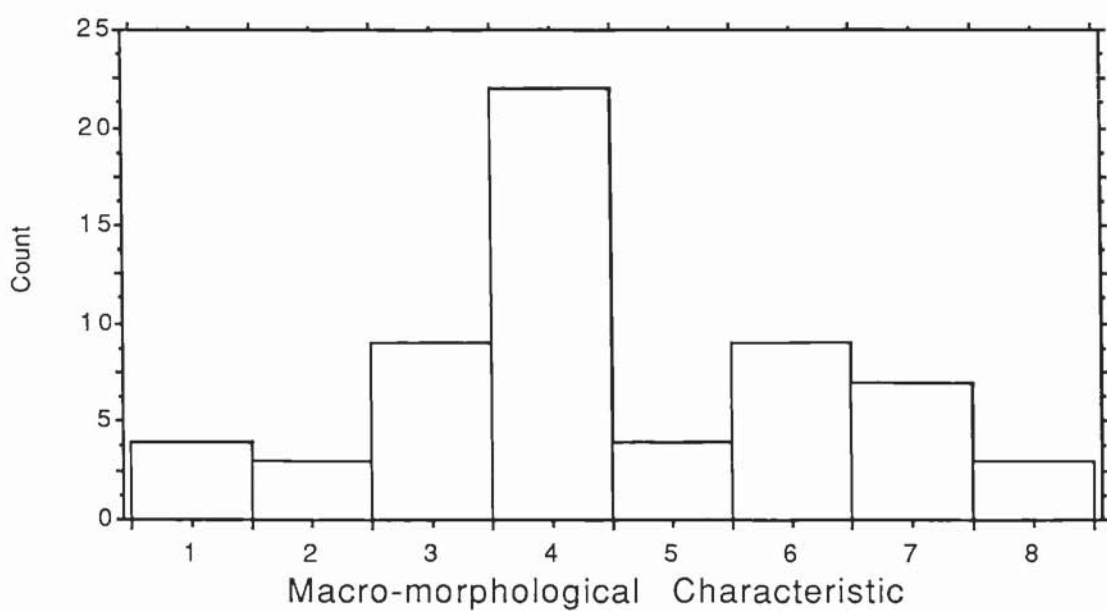
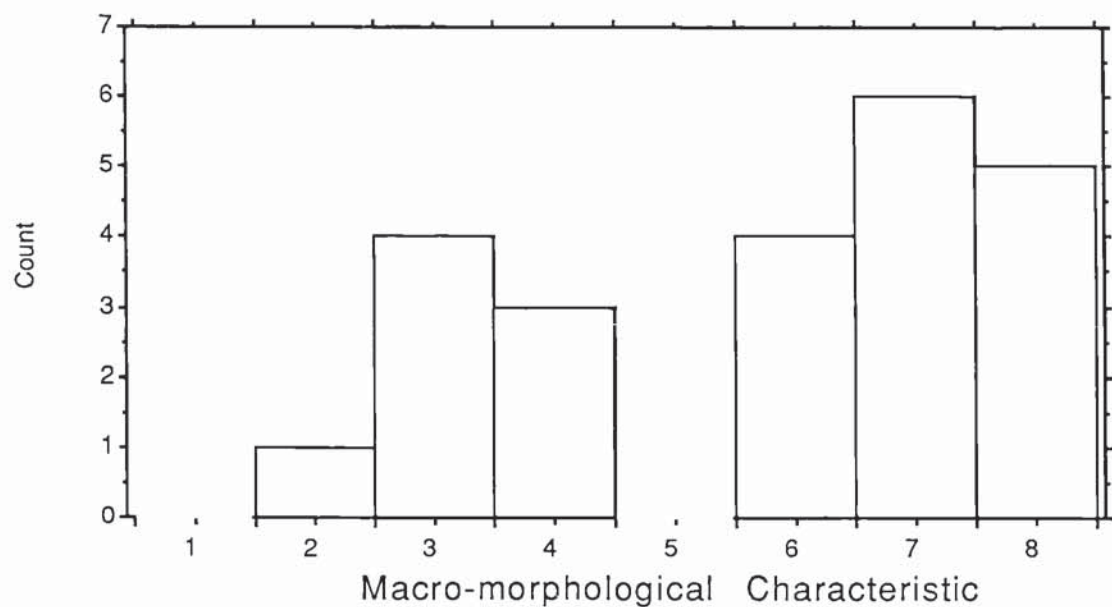


Figure 9.23. Histogram of the morphological characteristics of placer gold with fineness >950.



APPENDIX 1a.

**CALCULATION OF
THERMOCHEMICAL DATA.**

Derivation of Gibbs Free energy at any temperature in terms of heat capacities, standard enthalpies and standard entropies.

The Gibbs Free energy of a substance can be calculated at any temperature if the following are available:

- (1) Heat capacity data at the required temperature.
- (2) Entropy data at 298°.
- (3) Enthalpy data at 298° K.
- (4) Enthalpy and entropy of transformation data, if any phase changes occur at temperatures below those that are under consideration.

The general equation for the Gibbs Free energy of a substance is as follows:

$$G_T = H_{298} + \int_{298}^T C_p dT - TS_{298} - \int_{298}^T C_p/T dT \quad (5)$$

subtracting H_{298} and dividing by T

$$(G_T - H_{298})/T = 1/T \left\{ \int_{298}^T C_p dT - \int_{298}^T C_p/T dT \right\} - S_{298} \quad (6)$$

The left hand side of equation (6) is known as the G-function or free energy function, and provides a useful means of tabulating thermochemical data.

Equation (6) is only valid between 298° K and T° K if no phase transitions occur within that temperature range. If a phase transition occurs in that temperature range, then the enthalpy (ΔH^{trans}) and the entropy (ΔS^{trans}) of that transition must be taken into account. Thus, if the Gibbs Free energy of a substance is required at T_2 ° K and a phase transition occurs at T_1 ° K then the G-function is as follows:

$$\begin{aligned}
 (G_{T_2} - H_{298})/T_2 &= 1/T \left\{ \int_{298}^{T_1} C_p dT - \int_{298}^{T_1} C_p/T dT \right\} + \\
 &\quad 1/T \left\{ \int_{T_1}^{T_2} C_p dT - \int_{T_1}^{T_2} C_p/T dT \right\} - \\
 &\quad (S_{298} + S_{trans}) + \Delta H_{trans}/T_2 \quad (7a)
 \end{aligned}$$

substituting $(G_{T_1} - H_{298})/T_1$ in equation (7a) the G-function at temperature T_2° K is:

$$\begin{aligned}
 (G_{T_2} - H_{298})/T_2 &= (G_{T_1} - H_{298})/T_1 + 1/T \left\{ \int_{T_1}^{T_2} C_p dT - \right. \\
 &\quad \left. \int_{T_1}^{T_2} C_p/T dT \right\} - (S_{298} + S^{trans}) + \\
 &\quad \Delta H^{trans}/T_2 \quad (7b)
 \end{aligned}$$

By using equations (6) and (7b), if the appropriate data are available, it is possible to calculate the free energy function of a number of substances over a wide temperature range. The Gibbs Free energy of a substance is related to the free energy function in the following manner:

$$G_T = H_{298} + T[G_T - H_{298}/T] \quad (8)$$

Therefore, once the free energy function of a substance has been calculated, it is a simple matter to calculate its Gibbs Free energy if the enthalpy of that substance at 298 K is known, and for a particular reaction the Gibbs Free energy of that reaction is simply the sum of the Gibbs Free energies of the components involved in that reaction:

$$\Delta G_T = \sum G_T(\text{products}) - \sum G_T(\text{reactants}) \quad (9)$$

The best means of illustrating the above method is by using worked examples.

Worked example No. 1 (with no phase changes).

reaction:



Data for Fe(s)

$$\Delta H_{f298} = 0$$

$$C_p = 3.04 + 7.58 \times 10^{-3}T + 0.60 \times 10^5 T^{-2}$$

$$S_{298} = 6.52 \text{ cal K}^{-1}\text{mol}^{-1}$$

Calculation of the Free energy function for Fe(s).

Integrating the Cp functions for Fe(s) gives:

$$\int C_p dT = 3.04T + 3.79 \times 10^{-3}T^2 - 0.60 \times 10^5 T^{-1} + k_1$$

$$\int C_p/T dT = 3.04 \ln T + 7.58 \times 10^{-3}T - 0.30 \times 10^5 T^{-2} + k_2$$

Incorporating the above two intergrals into equation (6)

$$(G_T - H_{298})/T = \frac{1}{T} \left[3.04T + 3.79 \times 10^{-3}T^2 - 0.60 \times 10^5 T^{-1} \right] - \left[3.04 \ln T + 7.58 \times 10^{-3}T - 0.30 \times 10^5 T^{-2} \right] - S_{298}$$

for T= 400K

$$\begin{aligned} (G_T - H_{298})/T &= \left\{ \frac{1}{400} \left[[3.04(400) + 3.79 \times 10^{-3}(400)^2 - 0.60 \times 10^5 (400)^{-1}] \right. \right. \\ &\quad \left. \left. - [3.04(298) + 3.97 \times 10^{-3}(298)^2 - 0.60 \times 10^5 (298)^{-1}] \right] \right\} - \\ &\quad \left\{ \left[[3.04 \ln(400) + 7.58 \times 10^{-3}(400) - 0.30 \times 10^5 (400)^{-2}] \right. \right. \\ &\quad \left. \left. - [3.04 \ln(298) + 7.58 \times 10^{-3}(298) - 0.30 \times 10^5 (298)^{-2}] \right] \right\} \\ &\quad - (6.52) \end{aligned}$$

$$\text{Therefore: } (G_T - H_{298})/T = -6.71 \text{ cal K}^{-1}\text{mol}^{-1}$$

$$\text{And: } G_T = -2684 \text{ cal K}^{-1}\text{mol}^{-1}$$

Similarly, using the following data for FeS₂(s) and S₂(g)

Data for S₂(g):

$$\Delta H_{f298} = 30.75 \text{ Kcal mol}^{-1}$$

$$S_{298} = 54.50 \text{ cal K}^{-1}\text{mol}^{-1}$$

$$C_p = 8.72 + 0.16 \times 10^{-3}T - 0.90 \times 10^5$$

The above data, on calculation, give the following value of G_{T(S2)} at 400K

$$G_T = 8834 \text{ cal K}^{-1}\text{mol}^{-1}$$

Data for FeS₂(s):

$$\Delta H_{298} = -41.0 \text{ Kcal mol}^{-1}$$

$$S_{298} = 12.65 \text{ cal K}^{-1}\text{mol}^{-1}$$

$$C_p = 17.88 + 1.32 \times 10^{-3}T - 3.05 \times 10^5 T^{-2}$$

The above data, on calculation, give the following value of G_{T(FeS2)} at 400 K;

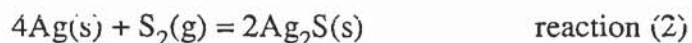
$$G_{T(FeS2)} = -46304 \text{ cal K}^{-1}\text{mol}^{-1}$$

Thus using equation (9)

$$\begin{aligned}\Delta G_{450(\text{reaction})} &= [(-46304)] - [(8834) + (-2684)] \\ &= -52454 \text{ cal K}^{-1}\text{mol}^{-1}.\end{aligned}$$

Worked example No.2 (with one phase change).

reaction:



reaction (2)

In the above reaction, a solid state transition takes place at 452 K, this phase transition must be taken into account when calculating thermochemical data above 452 K.

Thus to calculate the Gibbs Free energy of reaction at 500 K the method for obtaining the free energy function for Ag(s) and $\text{S}_2\text{(g)}$ is exactly the same as given in the first worked example; However, to compute the free energy function for $\text{Ag}_2\text{S(s)}$, equation (7b) must be used.

Data for Ag(s) :

$$\Delta H_{298} = 0$$

$$S_{298} = 10.20 \text{ cal K}^{-1}\text{mol}^{-1}$$

$$C_p = 5.09 + 2.04 \times 10^{-3}T + 0.36 \times 10^5 T^{-2}$$

Using the above data, and the data in the first worked example coupled with the prescribed method in that example, the Gibbs Free energies of Ag(s) and $\text{S}_2\text{(g)}$ are as follows:

$$G_{T\text{Ag(s)}} = -5405 \text{ cal K}^{-1}\text{mol}^{-1}$$

$$G_{T\text{S}_2\text{(g)}} = 3045 \text{ cal K}^{-1}\text{mol}^{-1}$$

Data for $\text{Ag}_2\text{S(s)}$:

$$\Delta H_{f298} = -7.55 \text{ Kcal mol}^{-1}$$

$$\Delta H^{\text{trans}} = 0.95 \text{ Kcal mol}^{-1}$$

$$S_{298} = 34.3 \text{ cal K}^{-1}\text{mol}^{-1}$$

$$\Delta S^{\text{trans}} = 2.11 \text{ cal K}^{-1}\text{mol}^{-1}$$

$$C_p = 10.13 + 26.40 \times 10^{-3}T$$

(298-452 K)

$$C_p' = 21.64$$

(452-850 K)

Using equation (7b)

$$(G_{500} - H_{298})/T = \left[(G_{452} - H_{298})/T \right] + \left[\frac{1}{500} \int_{452}^{500} Cp' dT - \int_{452}^{500} \frac{Cp'}{T} dT \right] - \Delta S^{\text{trans}} + \Delta H^{\text{trans}}/500 \quad (10)$$

Using equation (6) the $(G_{452} - H_{298})/T$ term on the right hand side of equation (10) evaluates at **-36.36 cal K⁻¹mol⁻¹**. Therefore: $(G_{500} - H_{298})/T$ is given by the following equation:

$$(G_{500} - H_{298})/T = -36.36 + \left[\frac{1}{500} \int_{452}^{500} Cp' dT - \int_{452}^{500} \frac{Cp'}{T} dT \right] - \Delta S^{\text{trans}} + \Delta H^{\text{trans}}/500 \quad (11)$$

Using the above data, Equation (11) computes in the following manner:

$$\begin{aligned} (G_{500} - H_{298})/T &= -36.36 + [1/T[21.64T] - [21.64\ln T]] - (2.11) + \\ &\quad (950)/(500) \\ &= -36.57 + \left\{ \left[\frac{1}{(500)}[21.64(500) - 21.64(452)] \right] \right. \\ &\quad \left. - [21.64\ln(500) - 21.64\ln(452)] \right\} \\ &= -36.67 \text{ cal K}^{-1}\text{mol}^{-1} \end{aligned}$$

And:

$$G_{500(\text{Ag}_2\text{S})} = -25885 \text{ cal K}^{-1}\text{mol}^{-1}$$

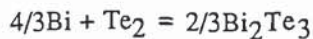
Using equation (9) the Gibbs energy of reaction is:

$$\begin{aligned} \Delta G_T &= 2(-25885) - [4(-5405) + (3405)] \\ &= -33195 \text{ cal K}^{-1}\text{mol}^{-1} \end{aligned}$$

APPENDIX 1b.

THERMOCHEMICAL DATA.

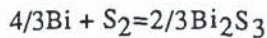
Reaction



(1)

Temp	GT Bi	GT Te ₂	GT Bi ₂ Te ₃	Σ GT reactants	Σ GT products	$\Delta G_{reaction}$	Log a_{Te_2}
298	-4040.9	19892.7	-37395.2	14506.2	-24930.2	-39436.4	-28.92
300	-4068.6	19768.9	-37520.2	14346.2	-25013.5	-39359.7	-23.57
310	-4205.1	19148.2	-38151.1	13542.9	-25434.1	-38977.0	-27.48
320	-4344.1	18524.7	-38791.7	12734.0	-25861.1	-38595.2	-26.36
330	-4485.0	17898.5	-39441.6	11919.9	-26294.4	-38214.3	-25.31
340	-4627.9	17269.5	-40100.7	11100.6	-26733.8	-37834.4	-24.32
350	-4772.6	16638.1	-40768.7	10276.2	-27179.1	-37455.3	-23.39
360	-4919.1	16004.1	-41445.4	9446.9	-27630.2	-37077.2	-22.51
370	-5067.4	15367.6	-42130.5	8612.8	-28087.0	-36699.8	-21.68
380	-5217.5	14728.8	-42824.0	7773.9	-28549.4	-36323.2	-20.89
390	-5369.3	14087.7	-43525.6	6930.4	-29017.1	-35947.5	-20.14
400	-5522.8	13444.3	-44235.1	6082.4	-29490.1	-35572.5	-19.44
410	-5677.9	12798.6	-44952.4	5229.9	-29968.3	-35198.2	-18.76
420	-5834.7	12150.8	-45677.3	4373.1	-30451.6	-34824.7	-18.12
430	-5993.1	11500.9	-46409.7	3512.1	-30939.8	-34451.9	-17.51
440	-6153.1	10848.9	-47149.4	2646.8	-31433.0	-34079.8	-16.93
450	-6314.7	10194.9	-47896.3	1777.4	-31930.9	-33708.3	-16.37
460	-6477.7	9538.9	-48650.3	904.0	-32433.5	-33337.6	-15.84
470	-6642.3	8880.9	-49411.2	26.6	-32940.8	-32967.4	-15.33
480	-6808.4	8221.0	-50178.8	-854.6	-33452.6	-32597.9	-14.84
490	-6976.0	7559.2	-50953.2	-1739.8	-33968.8	-32229.1	-14.37
500	-7145.0	6895.6	-51734.2	-2628.7	-34489.5	-31860.8	-13.93
510	-7315.5	6230.2	-52521.7	-3521.3	-35014.5	-31493.1	-13.50
520	-7487.4	5563.0	-53315.5	-4417.7	-35543.7	-31126.0	-13.08
530	-7660.6	4894.0	-54115.6	-5317.6	-36077.1	-30759.5	-12.68
540	-7835.3	4223.4	-54921.9	-6221.1	-36614.7	-30393.5	-12.30
550	-8039.3	3551.0	-55734.4	-7165.4	-37156.3	-29990.9	-11.92
560	-8266.1	2877.0	-56552.8	-8141.7	-37701.9	-29560.1	-11.54
570	-8494.1	2201.4	-57377.1	-9121.3	-38251.4	-29130.2	-11.17
580	-8273.2	1524.1	-58207.3	-9504.1	-38804.9	-29300.8	-11.04
590	-8953.4	845.3	-59043.3	-11089.6	-39362.2	-28272.6	-10.47
600	-9184.8	164.9	-59885.0	-12078.4	-39923.3	-27845.0	-10.14
610	-9417.2	-517.0	-60732.3	-13070.1	-40488.2	-27418.1	-9.82
620	-9650.7	-1200.5	-61585.1	-14064.8	-41056.8	-26992.0	-9.51
630	-9885.2	-1885.4	-62443.4	-15062.4	-41629.0	-26566.6	-9.22
640	-10120.8	-2571.8	-63307.2	-16062.8	-42204.8	-26142.0	-8.93
650	-10357.3	-3259.7	-64176.3	-17066.0	-42784.2	-25718.2	-8.65
660	-10594.9	-3948.9	-65050.7	-18071.9	-43367.1	-25295.2	-8.38
670	-10833.5	-4639.6	-65930.3	-19080.6	-43953.6	-24872.9	-8.11
680	-11073.0	-5331.7	-66815.1	-20092.0	-44543.4	-24451.4	-7.86
690	-11313.5	-6025.1	-67705.0	-21106.0	-45136.7	-24030.7	-7.61
700	-11554.5	-6720.0	-68599.9	-22122.2	-45733.3	-23611.2	-7.37
710	-11797.3	-7416.1	-69499.9	-23141.9	-46333.3	-23191.4	-7.14
720	-12040.5	-8113.6	-70404.9	-24163.6	-46936.6	-22773.0	-6.91
730	-12284.7	-8812.4	-71314.7	-25187.9	-47543.1	-22355.2	-6.69
740	-12529.8	-9512.4	-72229.4	-26214.7	-48152.9	-21938.3	-6.48
750	-12775.7	-10213.8	-73148.9	-27243.8	-48765.9	-21522.1	-6.27
760	-13022.5	-10916.4	-74073.1	-28275.5	-49382.1	-21106.7	-6.07
770	-13270.2	-11620.2	-75002.1	-29309.4	-50001.4	-20692.0	-5.87
780	-13518.7	-12325.3	-75935.8	-30345.8	-50623.9	-20278.1	-5.68
790	-13768.1	-13031.6	-76874.0	-31384.5	-51249.4	-19864.9	-5.50
800	-14018.2	-13739.1	-77816.9	-32425.5	-51877.9	-19452.5	-5.31

Reaction



(2)

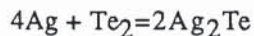
Temp	GT Bi	GT S ₂	GT Bi ₂ S ₃	Σ GT reactants	Σ GT products	ΔG reaction	$\log \alpha_{\text{S}_2}$
298	-4040.9	14509.0	-47572.2	9121.2	-31715.0	-40836.1	-28.9
300	-4068.0	14400.0	-47668.2	8975.9	-31779.0	-40754.9	-28.7
310	-4205.1	13853.1	-48154.0	8246.4	-32102.8	-40349.2	-27.4
320	-4344.1	13303.8	-48649.3	7511.7	-32433.0	-39944.7	-26.3
330	-4485.0	12752.0	-49153.8	6772.0	-32769.4	-39541.3	-25.2
340	-4627.9	12197.8	-49667.3	6027.3	-33111.7	-39139.0	-24.2
350	-4772.6	11641.3	-50189.4	5277.8	-33459.8	-38737.6	-23.2
360	-4919.1	11082.4	-50720.1	4523.6	-33813.6	-38337.1	-22.3
370	-5067.4	10521.3	-51259.0	3764.7	-34172.8	-37937.6	-21.4
380	-5217.5	9958.0	-51806.0	3001.3	-34537.5	-37538.8	-20.6
390	-5369.3	9392.6	-52360.8	2233.5	-34907.4	-37140.8	-19.8
400	-5522.8	8825.0	-52923.3	1461.3	-35282.4	-36743.7	-19.1
410	-5677.9	8255.4	-53493.3	684.8	-35662.4	-36347.2	-18.4
420	-5834.7	7683.8	-54070.7	-95.8	-36047.3	-35951.5	-17.7
430	-5993.1	7110.2	-54655.2	-880.6	-36437.0	-35556.4	-17.1
440	-6153.1	6534.7	-55246.8	-1669.4	-36831.4	-35161.9	-16.5
450	-6314.7	5957.3	-55845.2	-2462.2	-37230.3	-34768.1	-15.9
460	-6477.7	5378.1	-56450.4	-3258.9	-37633.8	-34374.8	-15.3
470	-6642.3	4797.0	-57062.2	-4059.5	-38041.6	-33982.2	-14.8
480	-6808.4	4214.1	-57680.4	-4863.8	-38453.8	-33590.0	-14.3
490	-6976.0	3629.5	-58305.1	-5671.8	-38870.2	-33198.4	-13.8
500	-7145.0	3043.2	-58935.9	-6483.5	-39290.8	-32807.3	-13.3
510	-7315.5	2455.1	-59572.9	-7298.8	-39715.5	-32416.7	-12.9
520	-7487.4	1165.5	-60216.0	-8817.7	-40144.2	-31326.5	-12.2
530	-7660.6	1274.2	-60865.0	-8940.0	-40576.8	-31636.8	-12.1
540	-7835.3	681.2	-61519.8	-9765.8	-41013.4	-31247.5	-11.7
550	-8039.3	86.8	-62180.3	-10632.3	-41453.7	-30821.4	-11.2
560	-8266.1	-509.3	-62846.4	-11530.8	-41897.8	-30367.0	-10.8
570	-8494.1	-1106.8	-63518.1	-12432.3	-42345.6	-29913.3	-10.5
580	-8273.2	-1705.9	-64195.3	-12736.8	-42797.1	-30060.3	-10.3
590	-8953.4	-2306.4	-64877.8	-14244.3	-43252.1	-29007.8	-9.8
600	-9184.8	-2908.4	-65565.7	-15154.7	-43710.7	-28555.9	-9.4
610	-9417.2	-3511.8	-66258.7	-16068.0	-44172.7	-28104.7	-9.1
620	-9650.7	-4116.6	-66957.0	-16984.1	-44638.2	-27654.1	-8.8
630	-9885.2	-4722.8	-67660.2	-17903.0	-45107.1	-27204.0	-8.4
640	-10120.8	-5330.3	-68368.5	-18824.7	-45579.2	-26754.6	-8.1
650	-10357.3	-5939.2	-69081.8	-19749.0	-46054.7	-26305.7	-7.8
660	-10594.9	-6549.5	-69799.9	-20676.0	-46533.5	-25857.5	-7.6
670	-10833.5	-7161.0	-70522.8	-21605.6	-47015.4	-25409.8	-7.3
680	-11073.0	-7773.8	-71250.4	-22537.8	-47500.5	-24962.7	-7.0
690	-11313.5	-8387.9	-71982.8	-23472.5	-47988.8	-24516.2	-6.8
700	-11554.5	-9003.2	-72719.8	-24409.3	-48480.1	-24070.8	-6.5
710	-11797.3	-9619.8	-73461.3	-25349.5	-48974.4	-23624.9	-6.3
720	-12040.5	-10237.6	-74207.3	-26291.7	-49471.8	-23180.2	-6.0
730	-12284.7	-10856.6	-74958.0	-27236.2	-49972.2	-22736.0	-5.8
740	-12529.8	-11476.8	-75712.8	-28183.2	-50475.4	-22292.3	-5.6
750	-12775.7	-12098.1	-76472.1	-29132.5	-50981.6	-21849.2	-5.4
760	-13022.5	-12720.7	-77235.7	-30084.0	-51490.7	-21406.7	-5.2
770	-13270.2	-13344.3	-78003.5	-31037.9	-52002.6	-20964.7	-5.0
780	-13518.7	-13969.1	-78775.6	-31994.1	-52517.3	-20523.2	-4.8
790	-13768.1	-14595.0	-79551.8	-32952.4	-53034.8	-20082.4	-4.6
800	-14018.2	-15222.0	-80332.2	-33913.0	-53555.1	-19642.1	-4.4

Reaction



Temp	GTAg	GT S ₂	GT Ag ₂ S	Σ GT reactants	Σ GT products	ΔG reaction	log α_{S_2}
298	-3038.6	14510.0	-17770.4	2351.6	-35541.8	-37892.4	-26.8
300	-3059.0	14401.0	-17839.1	2160.8	-35679.2	-37839.0	-26.6
310	-3162.4	13854.1	-18186.3	1206.3	-36373.7	-37572.0	-25.5
320	-3267.8	13304.8	-18539.5	229.4	-37079.9	-37308.4	-24.5
330	-3375.1	12753.0	-18898.3	-751.5	-37797.7	-37045.2	-23.5
340	-3484.2	12198.8	-19262.8	-1742.2	-38526.6	-36783.4	-22.6
350	-3595.2	11642.3	-19632.7	-2742.5	-39266.5	-36523.0	-21.8
360	-3707.8	11083.4	-20008.0	-3752.0	-40017.0	-36264.0	-21.0
370	-3822.2	10522.3	-20388.5	-4770.5	-40777.9	-36006.4	-20.3
380	-3938.2	9959.0	-20774.0	-5797.9	-41549.0	-35750.1	-19.6
390	-4055.8	9393.6	-21164.5	-6833.8	-42330.0	-35495.2	-18.9
400	-4175.0	8826.0	-21559.9	-7878.1	-43120.8	-35241.6	-18.3
410	-4295.8	8256.4	-21960.0	-8930.7	-43921.1	-34989.4	-17.6
420	-4418.0	7684.8	-22365.0	-9991.1	-44730.9	-34738.8	-17.1
430	-4541.7	7111.2	-22774.3	-11059.5	-45549.5	-34489.0	-16.5
440	-4666.8	6535.7	-23188.2	-12135.5	-46377.3	-34240.8	-16.0
450	-4793.3	5958.3	-23606.5	-13219.0	-47213.9	-33993.9	-15.5
460	-4921.2	5379.1	-24050.9	-14309.9	-48102.8	-33791.9	-15.1
470	-5050.5	4798.0	-24501.0	-15407.9	-49003.0	-33594.1	-14.6
480	-5181.1	4215.1	-24956.9	-16513.1	-49914.7	-33400.6	-14.2
490	-5312.9	3630.5	-25418.4	-17625.2	-50837.7	-33211.6	-13.8
500	-5446.1	3044.2	-25885.6	-18744.1	-51772.1	-33027.1	-13.4
510	-5580.4	2456.1	-26358.4	-19869.7	-52717.8	-32847.2	-13.1
520	-5706.2	1166.5	-26836.9	-21662.2	-53674.8	-32011.6	-12.4
530	-5852.9	1275.2	-27321.1	-22140.5	-54643.1	-32501.7	-12.4
540	-5990.9	682.2	-27810.9	-23285.4	-55622.7	-32336.3	-12.1
550	-6130.1	87.8	-28306.3	-24436.6	-56613.6	-32176.0	-11.8
560	-6270.4	-508.3	-28807.4	-25594.0	-57615.7	-32020.7	-11.5
570	-6411.9	-1105.8	-29314.1	-26757.5	-58629.1	-31870.7	-11.2
580	-6554.5	-1704.9	-29826.4	-27926.9	-59653.7	-31725.9	-11.0
590	-6698.2	-2305.4	-30344.3	-29102.2	-60689.6	-31586.4	-10.7
600	-6843.0	-2907.4	-30867.8	-30283.2	-61736.6	-31452.4	-10.5
610	-6988.8	-3510.8	-31397.0	-31470.0	-62794.9	-31324.0	-10.2
620	-7135.7	-4115.6	-31931.7	-32662.4	-63864.4	-31201.0	-10.0
630	-7283.6	-4721.8	-32482.1	-33860.3	-64965.1	-31103.8	-9.8
640	-7432.6	-5329.3	-33034.4	-35063.7	-66069.9	-31005.2	-9.6
650	-7582.6	-5938.2	-33590.2	-36272.5	-67181.4	-30907.9	-9.4
660	-7733.5	-6548.5	-34149.3	-37486.6	-68299.6	-30812.0	-9.2
670	-7885.5	-7160.0	-34711.7	-38706.0	-69424.3	-30717.3	-9.0
680	-8038.4	-7772.8	-35286.3	-39930.6	-70573.5	-30641.9	-8.8
690	-8192.4	-8386.9	-35846.0	-41160.3	-71693.0	-30531.7	-8.7
700	-8347.2	-9002.2	-36417.9	-42395.1	-72836.8	-30440.8	-8.5
710	-8503.0	-9618.8	-36992.9	-43634.8	-73986.8	-30351.0	-8.3
720	-8659.7	-10236.6	-37570.9	-44879.5	-75142.8	-30262.3	-8.2
730	-8817.4	-10855.6	-38151.9	-46129.1	-76304.9	-30174.8	-8.0
740	-8975.9	-11475.8	-38735.9	-47383.6	-77472.9	-30088.3	-7.9
750	-9135.4	-12097.1	-39322.8	-48642.8	-78646.7	-30002.9	-7.7
760	-9295.8	-12719.7	-39912.6	-49906.7	-79826.2	-29918.5	-7.6
770	-9457.0	-13343.3	-40505.2	-51175.2	-81011.5	-29835.2	-7.5
780	-9619.1	-13968.1	-41100.7	-52448.5	-82202.3	-29752.8	-7.3
790	-9782.1	-14594.0	-41698.9	-53726.3	-83398.7	-29671.5	-7.2
800	-9945.9	-15221.0	-42299.4	-55008.6	-84599.8	-29590.3	-7.1

Reaction



(4)

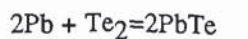
Temp	ΔG reaction	Ln aTe2
298	-46869.54	-34.37
300	-46811.00	-34.10
310	-46518.30	-32.79
320	-46225.60	-31.57
330	-45932.90	-30.42
340	-45640.20	-29.33
350	-45347.50	-28.31
360	-45054.80	-27.35
370	-44762.10	-26.44
380	-44469.40	-25.57
390	-44176.70	-24.75
400	-43884.00	-23.98
410	-43591.30	-23.23
418	-43357.14	-22.67
418	-43357.20	-22.67
420	-43325.00	-22.54
430	-43164.00	-21.94
440	-43003.00	-21.36
450	-42842.00	-20.81
460	-42681.00	-20.28
470	-42520.00	-19.77
480	-42359.00	-19.28
490	-42198.00	-18.82
500	-42037.00	-18.37
510	-41876.00	-17.94
520	-41715.00	-17.53
530	-41554.00	-17.13
540	-41393.00	-16.75
550	-41232.00	-16.38
560	-41071.00	-16.03
570	-40910.00	-15.68
580	-40749.00	-15.35
590	-40588.00	-15.03
600	-40427.00	-14.72
610	-40266.00	-14.43
620	-40105.00	-14.14
630	-39944.00	-13.86
640	-39783.00	-13.58
650	-39622.00	-13.32
660	-39461.00	-13.07
670	-39300.00	-12.82
680	-39139.00	-12.58
690	-38978.00	-12.34
700	-38817.00	-12.12
710	-38656.00	-11.90
720	-38495.00	-11.68
730	-38334.00	-11.48
740	-38173.00	-11.27
750	-38012.00	-11.08
760	-37851.00	-10.88
770	-37690.00	-10.70
780	-37529.00	-10.51
790	-37368.00	-10.34
800	-37207.00	-10.16

Reaction



Temp	GT Pb	GT S ₂	GT PbS	Σ GT reactants	Σ GT products	ΔG reaction	log α_{S_2}
298	-4616.0	14509.0	-29996.4	5277.0	-59992.8	-65269.8	-47.9
300	-4647.0	14400.0	-30040.1	5105.9	-60080.2	-65186.0	-47.5
310	-4663.3	13853.1	-30260.8	4246.6	-60521.6	-64768.2	-45.7
320	-4961.4	13303.8	-30485.4	3381.0	-60970.8	-64351.8	-44.0
330	-5121.3	12752.0	-30713.7	2509.3	-61427.3	-63936.7	-42.3
340	-5283.0	12197.8	-30945.5	1631.7	-61891.1	-63522.8	-40.8
350	-5446.5	11641.3	-31180.9	748.3	-62361.9	-63110.2	-39.4
360	-5611.6	11082.4	-31419.7	-140.7	-62839.5	-62698.8	-38.1
370	-5778.2	10521.3	-31661.9	-1035.2	-63323.7	-62288.5	-36.8
380	-5946.5	9958.0	-31907.2	-1935.1	-63814.4	-61879.4	-35.6
390	-6116.4	9392.6	-32155.8	-2840.2	-64311.5	-61471.3	-34.5
400	-6287.7	8825.0	-32407.3	-3750.4	-64814.7	-61064.3	-33.4
410	-6460.5	8255.4	-32662.0	-4665.5	-65323.9	-60658.4	-32.3
420	-6634.7	7683.8	-32919.5	-5585.6	-65839.1	-60253.5	-31.4
430	-6810.3	7110.2	-33180.0	-6510.4	-66360.0	-59849.5	-30.4
440	-6987.3	6534.7	-33443.2	-7439.9	-66886.5	-59446.6	-29.5
450	-7165.7	5957.3	-33709.3	-8374.0	-67418.5	-59044.5	-28.7
460	-7345.3	5378.1	-33978.0	-9312.5	-67956.0	-58643.5	-27.9
470	-7526.2	4797.0	-34249.4	-10255.5	-68498.7	-58243.3	-27.1
480	-7708.4	4214.1	-34523.3	-11202.7	-69046.7	-57844.0	-26.3
490	-7891.8	3629.5	-34799.8	-12154.1	-69599.7	-57445.6	-25.6
500	-8076.4	3043.2	-35078.9	-13109.7	-70157.7	-57048.1	-24.9
510	-8262.2	2455.1	-35360.3	-14069.3	-70720.7	-56651.4	-24.3
520	-8449.2	1165.5	-35644.2	-15732.9	-71288.4	-55555.5	-23.4
530	-8637.3	1274.2	-35930.5	-16000.4	-71860.9	-55860.5	-23.0
540	-8826.5	681.2	-36219.0	-16971.8	-72438.1	-55466.3	-22.4
550	-9016.8	86.8	-36509.9	-17946.9	-73019.8	-55072.9	-21.9
560	-9208.2	-509.3	-36803.0	-18925.8	-73606.0	-54680.3	-21.3
570	-9400.7	-1106.8	-37098.3	-19908.2	-74196.7	-54288.5	-20.8
580	-9594.2	-1705.9	-37395.9	-20894.3	-74791.7	-53897.4	-20.3
590	-9788.8	-2306.4	-37695.5	-21883.9	-75391.0	-53507.1	-19.8
600	-9984.3	-2908.4	-37997.3	-22877.0	-75994.6	-53117.6	-19.4
610	-10187.7	-3511.8	-38301.1	-23887.2	-76602.3	-52715.1	-18.9
620	-10404.3	-4116.6	-38607.0	-24925.1	-77214.1	-52288.9	-18.4
630	-10622.1	-4722.8	-38915.0	-25967.0	-77829.9	-51862.9	-18.0
640	-10841.1	-5330.3	-39224.9	-27012.6	-78449.8	-51437.2	-17.6
650	-11061.4	-5939.2	-39536.8	-28061.9	-79073.5	-51011.6	-17.1
660	-11282.8	-6549.5	-39850.6	-29115.0	-79701.2	-50586.2	-16.8
670	-11505.3	-7161.0	-40166.3	-30171.6	-80332.6	-50161.0	-16.4
680	-11729.0	-7773.8	-40483.9	-31231.8	-80967.9	-49736.1	-16.0
690	-11953.8	-8387.9	-40803.4	-32295.6	-81606.8	-49311.3	-15.6
700	-12179.8	-9003.2	-41124.8	-33362.8	-82249.5	-48886.7	-15.3
710	-12406.8	-9619.8	-41447.9	-34433.4	-82895.8	-48462.4	-14.9
720	-12634.9	-10237.6	-41772.8	-35507.3	-83545.6	-48038.3	-14.6
730	-12864.0	-10856.6	-42099.5	-36584.7	-84199.0	-47614.4	-14.2
740	-13094.2	-11476.8	-42428.0	-37665.3	-84855.9	-47190.7	-13.9
750	-13325.5	-12098.1	-42758.2	-38749.1	-85516.3	-46767.2	-13.6
760	-13557.7	-12720.7	-43090.1	-39836.1	-86180.1	-46344.0	-13.3
770	-13791.0	-13344.3	-43432.6	-40926.2	-86865.3	-45939.0	-13.0
780	-14025.2	-13969.1	-43758.9	-42019.5	-87517.8	-45498.2	-12.8
790	-14260.4	-14595.0	-44095.8	-43115.9	-88191.6	-45075.7	-12.5
800	-14496.6	-15222.0	-44434.3	-44215.2	-88868.7	-44653.4	-12.2

Reaction



(6)

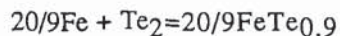
Temp	GT Pb	GT Te ₂	GT PbTe	Σ GT reactants	Σ GT products	ΔG reaction	Log α_{Te_2}
298	-4616.0	19892.7	-24237.4	10660.7	-48474.8	-59135.5	-43.4
300	-4647.0	19768.9	-24290.1	10474.9	-48580.2	-59055.0	-43.0
310	-4803.3	19148.2	-24555.2	9541.7	-49111.8	-59553.4	-41.4
320	-4961.4	18524.7	-24825.6	8601.9	-49651.2	-58253.1	-39.8
330	-5121.3	17898.5	-25099.1	7655.8	-50198.2	-57854.0	-38.3
340	-5283.0	17269.5	-25376.3	6703.5	-50752.6	-57456.1	-36.9
350	-5446.5	16638.1	-25657.1	5745.1	-51314.1	-57059.3	-35.6
360	-5611.6	16004.1	-25941.3	4781.0	-51882.7	-56663.7	-34.4
370	-5778.2	15367.6	-26229.0	3811.2	-52458.0	-56269.2	-33.2
380	-5946.5	14728.8	-26520.0	2835.8	-53040.0	-55875.8	-32.1
390	-6116.4	14087.7	-26814.2	1855.0	-53628.5	-55483.4	-31.1
400	-6287.7	13444.3	-27111.6	868.9	-54223.3	-55092.2	-30.1
410	-6460.5	12798.6	-27412.1	-122.3	-54824.2	-54701.9	-29.2
420	-6634.7	12150.8	-27715.6	-1118.6	-55431.2	-54312.7	-28.3
430	-6810.3	11500.9	-28022.1	-2119.8	-56044.2	-53924.4	-27.4
440	-6987.3	10848.9	-28331.4	-3125.8	-56662.9	-53537.1	-26.6
450	-7165.7	10194.9	-28643.6	-4136.4	-57287.2	-53150.8	-25.8
460	-7345.3	9538.9	-28958.6	-5151.7	-57917.1	-52765.4	-25.1
470	-7526.2	8880.9	-29276.2	-6171.6	-58552.5	-52380.9	-24.4
480	-7708.4	8221.0	-29596.6	-7195.8	-59193.2	-51997.4	-23.7
490	-7891.8	7559.2	-29919.6	-8224.4	-59839.1	-51614.7	-23.0
500	-8076.4	6895.6	-30245.1	-9257.2	-60490.2	-51233.0	-22.4
510	-8262.2	6230.2	-30573.2	-10294.3	-61146.3	-50852.1	-21.8
520	-8449.2	5563.0	-30903.7	-11335.4	-61807.4	-50472.0	-21.2
530	-8637.3	4894.0	-31236.7	-12380.5	-62473.4	-50092.9	-20.7
540	-8826.5	4223.4	-31572.1	-13429.6	-63144.2	-49714.5	-20.1
550	-9016.8	3551.0	-31909.8	-14482.6	-63819.6	-49337.0	-19.6
560	-9208.2	2877.0	-32249.9	-15539.5	-64499.8	-48960.3	-19.1
570	-9400.7	2201.4	-32592.2	-16600.0	-65184.4	-48584.4	-18.6
580	-9594.2	1524.1	-32936.8	-17664.3	-65873.6	-48209.3	-18.2
590	-9788.8	845.3	-33283.6	-18732.2	-66567.2	-47835.0	-17.7
600	-9984.3	164.9	-33632.6	-19803.8	-67265.2	-47461.4	-17.3
610	-10187.7	-517.0	-33983.7	-20892.4	-67967.5	-47075.1	-16.9
620	-10404.3	-1200.5	-34337.0	-22009.0	-68674.0	-46664.9	-16.4
630	-10622.1	-1885.4	-34692.3	-23129.6	-69384.7	-46255.1	-16.1
640	-10841.1	-2571.8	-35049.7	-24254.1	-70099.5	-45845.4	-15.7
650	-11061.4	-3259.7	-35409.2	-25382.3	-70818.3	-45436.0	-15.3
660	-11282.8	-3948.9	-35770.6	-26514.4	-71541.2	-45026.8	-14.9
670	-11505.3	-4639.6	-36134.0	-27650.2	-72268.0	-44617.8	-14.6
680	-11729.0	-5331.7	-36499.4	-28789.7	-72998.8	-44209.0	-14.2
690	-11953.8	-6025.1	-36866.7	-29932.8	-73733.4	-43800.6	-13.9
700	-12179.8	-6720.0	-37235.9	-31079.5	-74471.8	-43392.3	-13.6
710	-12406.8	-7416.1	-37607.0	-32229.7	-75213.9	-42984.2	-13.2
720	-12634.9	-8113.6	-37979.9	-33383.3	-75959.8	-42576.5	-12.9
730	-12864.0	-8812.4	-38354.7	-34540.4	-76709.3	-42168.9	-12.6
740	-13094.2	-9512.4	-38731.3	-35700.9	-77462.5	-41761.6	-12.3
750	-13325.5	-10213.8	-39109.6	-36864.7	-78219.3	-41354.6	-12.1
760	-13557.7	-10916.4	-39489.8	-38031.8	-78979.6	-40947.8	-11.8
770	-13791.0	-11620.2	-39871.7	-39202.2	-79743.4	-40541.2	-11.5
780	-14025.2	-12325.3	-40255.3	-40375.7	-80510.7	-40134.9	-11.2
790	-14260.4	-13031.6	-40640.7	-41552.5	-81281.4	-39728.9	-11.0
800	-14496.6	-13739.1	-41027.8	-42732.3	-82055.5	-39323.2	-10.7

Reaction



Temp	GT Au	GT Te ₂	GT AuTe ₂	Σ GT reactants	Σ GT products	ΔG reaction	Log a_{Te_2}
298	-3373.4	19892.7	-14543.3	16519.4	-14543.3	-31062.6	-22.8
300	-3396.0	19768.9	-14611.1	16372.9	-14611.1	-30984.0	-22.6
310	-3510.6	19148.2	-14954.1	15637.6	-14954.1	-30551.7	-21.6
320	-3627.2	18524.7	-15303.0	14897.5	-15303.0	-30200.5	-20.6
330	-3745.6	17898.5	-15657.6	14152.8	-15657.6	-29810.4	-19.7
340	-3865.9	17269.5	-16017.9	13403.6	-16017.9	-29421.5	-18.9
350	-3988.0	16638.1	-16383.6	12650.1	-16383.6	-29033.7	-18.1
360	-4111.8	16004.1	-16754.7	11892.3	-16754.7	-28647.0	-17.4
370	-4237.3	15367.6	-17131.0	11130.4	-17131.0	-28261.3	-16.7
380	-4364.5	14728.8	-17512.3	10364.4	-17512.3	-27876.7	-16.0
390	-4493.2	14087.7	-17898.7	9594.5	-17898.7	-27493.1	-15.4
400	-4623.6	13444.3	-18289.9	8820.7	-18289.9	-27110.5	-14.8
410	-4755.5	12798.6	-18685.8	8043.2	-18685.8	-26729.0	-14.2
420	-4888.9	12150.8	-19086.4	7262.0	-19086.4	-26348.4	-13.7
430	-5023.7	11500.9	-19491.6	6477.2	-19491.6	-25968.8	-13.2
440	-5160.0	10848.9	-19901.2	5688.9	-19901.2	-25590.1	-12.7
450	-5297.8	10194.9	-20315.3	4897.1	-20315.3	-25212.4	-12.2
460	-5436.9	9538.9	-20733.7	4102.0	-20733.7	-24835.7	-11.8
470	-5577.3	8880.9	-21156.3	3303.6	-21156.3	-24459.8	-11.4
480	-5719.1	8221.0	-21583.1	2501.9	-21583.1	-24084.9	-11.0
490	-5862.2	7559.2	-22013.9	1697.0	-22013.9	-23711.0	-10.6
500	-6006.5	6895.6	-22448.8	889.1	-22448.8	-23337.9	-10.2
510	-6152.2	6230.2	-22887.7	78.0	-22887.7	-22965.7	-9.8
520	-6299.0	5563.0	-23330.5	-736.0	-23330.5	-22594.4	-9.5
530	-6447.1	4894.0	-23777.1	-1553.1	-23777.1	-22224.0	-9.2
540	-6596.4	4223.4	-24227.5	-2373.0	-24227.5	-21854.5	-8.8
550	-6746.8	3551.0	-24681.6	-3195.8	-24681.6	-21485.9	-8.5
560	-6898.4	2877.0	-25139.5	-4021.3	-25139.5	-21118.1	-8.2
570	-7051.1	2201.4	-25600.9	-4849.7	-25600.9	-20751.2	-8.0
580	-7204.9	1524.1	-26066.0	-5680.8	-26066.0	-20385.2	-7.7
590	-7359.9	845.3	-26534.5	-6514.6	-26534.5	-20020.0	-7.4
600	-7515.9	164.9	-27006.6	-7351.0	-27006.6	-19655.6	-7.2
610	-7673.0	-517.0	-27482.1	-8190.0	-27482.1	-19292.1	-6.9
620	-7831.1	-1200.5	-27961.0	-9031.6	-27961.0	-18929.4	-6.7
630	-7990.3	-1885.4	-28443.3	-9875.7	-28443.3	-18567.6	-6.4
640	-8150.5	-2571.8	-28928.3	-10722.3	-28928.3	-18206.0	-6.2
650	-8311.7	-3259.7	-29417.8	-11571.3	-29417.8	-17846.4	-6.0
660	-8473.9	-3948.9	-29909.9	-12422.8	-29909.9	-17487.1	-5.8
670	-8637.1	-4639.6	-30405.2	-13276.7	-30405.2	-17128.5	-5.6
680	-8801.2	-5331.7	-30903.7	-14132.9	-30903.7	-16770.8	-5.4
690	-8966.3	-6025.1	-31405.4	-14991.5	-31405.4	-16413.9	-5.2
700	-9132.4	-6720.0	-31910.1	-15852.3	-31910.1	-16057.8	-5.0

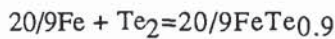
Reaction



(8)

Temp	GT Fe	GT Te ₂	GT FeTe _{0.9}	Σ GT reactants	Σ GT products	ΔG reaction	Log a_{Te_2}
298	-1943.0	19892.7	-11253.7	15575.0	-25005.8	-40580.8	-29.8
300	-1956.0	19768.9	-11292.1	15422.2	-25091.0	-40513.2	-29.5
310	-2022.6	19148.2	-11486.2	14653.5	-25522.4	-40175.9	-28.3
320	-2091.2	18524.7	-11684.2	13877.7	-25962.4	-39840.1	-27.2
330	-2161.6	17898.5	-11886.0	13095.0	-26410.8	-39505.7	-26.2
340	-2233.8	17269.5	-12091.5	12305.5	-26867.3	-39172.7	-25.2
350	-2307.9	16638.1	-12300.5	11509.4	-27331.7	-38841.1	-24.2
360	-2383.8	16004.1	-12513.0	10706.6	-27803.9	-38510.6	-23.4
370	-2461.3	15367.6	-12728.9	9898.0	-28283.7	-38181.7	-22.6
380	-2540.6	14728.8	-12948.2	9083.1	-28770.8	-37853.9	-21.8
390	-2621.6	14087.7	-13170.7	8261.9	-29265.2	-37527.2	-21.0
400	-2704.1	13444.3	-13396.4	7435.2	-29766.7	-37201.9	-20.3
410	-2788.3	12798.6	-13625.1	6602.5	-30275.1	-36877.5	-19.7
420	-2874.1	12150.8	-13857.0	5764.1	-30790.2	-36554.3	-19.0
430	-2961.4	11500.9	-14091.8	4920.0	-31312.0	-36232.0	-18.4
440	-3050.3	10848.9	-14329.5	4070.6	-31840.2	-35910.8	-17.8
450	-3140.7	10194.9	-14570.1	3215.6	-32374.8	-35590.5	-17.3
460	-3232.6	9538.9	-14813.5	2355.4	-32915.7	-35271.1	-16.8
470	-3325.9	8880.9	-15059.7	1489.9	-33462.7	-34952.6	-16.2
480	-3420.8	8221.0	-15308.6	619.3	-34015.6	-34634.9	-15.8
490	-3517.1	7559.2	-15560.1	-256.5	-34574.4	-34318.0	-15.3
500	-3614.8	6895.6	-15814.2	-1137.2	-35139.1	-34001.9	-14.9
510	-3713.9	6230.2	-16070.8	-2022.9	-35709.3	-33686.4	-14.4
520	-3814.4	5563.0	-16330.0	-2913.5	-36285.2	-33371.7	-14.0
530	-3916.3	4894.0	-16591.6	-3808.9	-36866.5	-33057.6	-13.6
540	-4019.6	4223.4	-16855.6	-4709.1	-37453.2	-32744.1	-13.2
550	-4124.2	3551.0	-17122.1	-5614.0	-38045.2	-32431.3	-12.9
560	-4230.2	2877.0	-17390.8	-6523.5	-38642.4	-32118.9	-12.5
570	-4337.6	2201.4	-17661.9	-7437.6	-39244.7	-31807.1	-12.2
580	-4446.2	1524.1	-17935.2	-8356.4	-39852.1	-31495.8	-11.9
590	-4556.2	845.3	-18210.8	-9279.5	-40464.4	-31184.9	-11.6
600	-4667.4	164.9	-18488.6	-10207.2	-41081.6	-30874.4	-11.2
610	-4780.0	-517.0	-18768.5	-11139.2	-41703.6	-30564.3	-10.9
620	-4893.8	-1200.5	-19050.5	-12075.6	-42330.3	-30254.7	-10.7
630	-5008.9	-1885.4	-19334.7	-13016.4	-42961.7	-29945.3	-10.4
640	-5125.3	-2571.8	-19620.9	-13961.4	-43597.7	-29636.3	-10.1
650	-5242.9	-3259.7	-19909.2	-14910.6	-44238.2	-29327.6	-9.9
660	-5361.8	-3948.9	-20199.5	-15864.1	-44883.2	-29019.1	-9.6
670	-5481.9	-4639.6	-20491.7	-16821.7	-45532.6	-28710.9	-9.4
680	-5603.3	-5331.7	-20785.9	-17783.5	-46186.3	-28402.8	-9.1
690	-5725.9	-6025.1	-21082.1	-18749.3	-46844.4	-28095.0	-8.9
700	-5849.7	-6720.0	-21380.1	-19719.2	-47506.6	-27787.4	-8.7
710	-5974.7	-7416.1	-21680.0	-20693.2	-48173.0	-27479.8	-8.5
720	-6100.9	-8113.6	-21981.8	-21671.1	-48843.6	-27172.5	-8.2
730	-6228.3	-8812.4	-22285.4	-22653.0	-49518.2	-26865.2	-8.0
740	-6356.9	-9512.4	-22590.4	-23638.8	-50195.9	-26557.0	-7.8
750	-6486.6	-10213.8	-22898.0	-24628.6	-50879.4	-26250.8	-7.7
760	-6617.6	-10916.4	-23207.0	-25622.2	-51565.9	-25943.7	-7.5
770	-6749.7	-11620.2	-23517.7	-26619.7	-52256.3	-25636.7	-7.3
780	-6883.0	-12325.3	-23830.1	-27620.9	-52950.5	-25329.6	-7.1
790	-7017.5	-13031.6	-24144.2	-28626.0	-53648.5	-25022.5	-6.9
800	-7153.1	-13739.1	-24460.0	-29634.9	-54350.2	-24715.3	-6.8

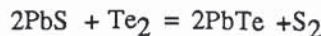
Reaction



(9)

Temp	GT FeTe _{0.9}	GT Te ₂	GT FeTe2	Σ GT reactants	Σ GT products	ΔG reaction	Log α_{Te_2}
298	-11253.7	19892.7	-24434.1	-566.5	-44421.2	-43854.7	-32.2
300	-11292.1	19768.9	-24482.1	-760.1	-44508.5	-43748.4	-31.9
310	-11486.2	19148.2	-24725.6	-1733.8	-44951.2	-43217.4	-30.5
320	-11684.2	18524.7	-24974.8	-2717.3	-45404.3	-42687.0	-29.1
330	-11886.0	17898.5	-25229.7	-3710.3	-45867.5	-42157.2	-27.9
340	-12091.5	17269.5	-25489.9	-4712.8	-46340.7	-41627.9	-26.8
350	-12300.5	16638.1	-25755.5	-5724.2	-46823.5	-41099.3	-25.7
360	-12513.0	16004.1	-26026.3	-6744.6	-47315.8	-40571.2	-24.6
370	-12728.9	15367.6	-26302.1	-7773.5	-47817.3	-40043.8	-23.6
380	-12948.2	14728.8	-26583.0	-8810.9	-48327.8	-39516.9	-22.7
390	-13170.7	14087.7	-26868.6	-9856.6	-48847.2	-38990.6	-21.9
400	-13396.4	13444.3	-27159.1	-10910.3	-49375.2	-38464.9	-21.0
410	-13625.1	12798.6	-27454.2	-11971.9	-49911.7	-37939.8	-20.2
420	-13857.0	12150.8	-27753.8	-13041.2	-50456.4	-37415.3	-19.5
430	-14091.8	11500.9	-28057.9	-14118.0	-51009.3	-36891.3	-18.8
440	-14329.5	10848.9	-28366.5	-15202.2	-51570.2	-36368.0	-18.1
450	-14570.1	10194.9	-28679.3	-16293.6	-52138.9	-35845.2	-17.4
460	-14813.5	9538.9	-28996.3	-17392.2	-52715.3	-35323.1	-16.8
470	-15059.7	8880.9	-29317.5	-18497.7	-53299.2	-34801.5	-16.2
480	-15308.6	8221.0	-29642.7	-19610.0	-53890.5	-34280.5	-15.6
490	-15560.1	7559.2	-29972.0	-20729.0	-54489.1	-33760.1	-15.1
500	-15814.2	6895.6	-30305.2	-21854.5	-55094.8	-33240.3	-14.5
510	-16070.8	6230.2	-30642.2	-22986.5	-55707.6	-32721.0	-14.0
520	-16330.0	5563.0	-30983.1	-24124.9	-56327.2	-32202.3	-13.5
530	-16591.6	4894.0	-31327.7	-25269.5	-56953.7	-31684.2	-13.1
540	-16855.6	4223.4	-31676.0	-26420.2	-57586.9	-31166.8	-12.6
550	-17122.1	3551.0	-32027.9	-27576.9	-58226.7	-30649.8	-12.2
560	-17390.8	2877.0	-32383.4	-28739.5	-58873.0	-30133.5	-11.8
570	-17661.9	2201.4	-32742.4	-29908.0	-59525.7	-29617.7	-11.4
580	-17935.2	1524.1	-33104.9	-31082.2	-60184.7	-29102.5	-11.0
590	-18210.8	845.3	-33470.8	-32261.9	-60849.9	-28587.9	-10.6
600	-18488.6	164.9	-33840.1	-33447.3	-61521.2	-28073.9	-10.2
610	-18768.5	-517.0	-34212.7	-34638.1	-62198.6	-27560.5	-9.9
620	-19050.5	-1200.5	-34588.5	-35834.4	-62881.9	-27047.6	-9.5
630	-19334.7	-1885.4	-34967.7	-37035.9	-63571.2	-26535.3	-9.2
640	-19620.9	-2571.8	-35349.9	-38242.7	-64266.2	-26023.6	-8.9
650	-19909.2	-3259.7	-35735.4	-39454.6	-64967.0	-25512.5	-8.6
660	-20199.5	-3948.9	-36124.0	-40671.6	-65673.4	-25001.9	-8.3
670	-20491.7	-4639.6	-36515.7	-41893.6	-66385.5	-24491.9	-8.0
680	-20785.9	-5331.7	-36910.3	-43120.5	-67103.0	-23982.5	-7.7
690	-21082.1	-6025.1	-37308.0	-44352.3	-67826.0	-23473.7	-7.4
700	-21380.1	-6720.0	-37708.7	-45589.0	-68554.4	-22965.4	-7.2
710	-21680.0	-7416.1	-38112.3	-46830.4	-69288.1	-22457.7	-6.9
720	-21981.8	-8113.6	-38518.8	-48076.5	-70027.1	-21950.6	-6.7
730	-22285.4	-8812.4	-38928.1	-49327.2	-70771.3	-21444.1	-6.4
740	-22590.4	-9512.4	-39340.3	-50581.8	-71520.7	-20938.9	-6.2
750	-22898.0	-10213.8	-39755.3	-51842.4	-72275.1	-20432.8	-6.0
760	-23207.0	-10916.4	-40173.1	-53106.7	-73034.6	-19928.0	-5.7
770	-23517.7	-11620.2	-40593.6	-54375.4	-73799.1	-19423.7	-5.5
780	-23830.1	-12325.3	-41016.8	-55648.5	-74568.5	-18920.0	-5.3
790	-24144.2	-13031.6	-41442.7	-56925.9	-75342.8	-18416.9	-5.1
800	-24460.0	-13739.1	-41871.2	-58207.5	-76121.9	-17914.4	-4.9

Reaction

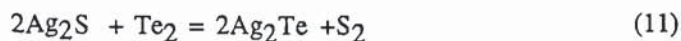


(10)

TempΔG reaction (5)ΔGreaction (6)ΔG reaction (10)log aS₂ Log aTe₂(Log aTe₂=0)(log aS₂=0)

298	-65269.8	-59135.5	-6134.3	-4.498	4.498
300	-65186.0	-59055.0	-6131.0	-4.466	4.466
310	-64768.2	-58653.4	-6114.8	-4.311	4.311
320	-64351.8	-58253.1	-6098.7	-4.165	4.165
330	-63936.7	-57854.0	-6082.7	-4.028	4.028
340	-63522.8	-57456.1	-6066.7	-3.899	3.899
350	-63110.2	-57059.3	-6050.9	-3.778	3.778
360	-62698.8	-56663.7	-6035.1	-3.663	3.663
370	-62288.5	-56269.2	-6019.3	-3.555	3.555
380	-61879.4	-55875.8	-6003.6	-3.453	3.453
390	-61471.3	-55483.4	-5987.9	-3.355	3.355
400	-61064.3	-55092.2	-5972.1	-3.263	3.263
410	-60658.4	-54701.9	-5956.5	-3.175	3.175
420	-60253.5	-54312.7	-5940.8	-3.091	3.091
430	-59849.5	-53924.4	-5925.1	-3.011	3.011
440	-59446.6	-53537.1	-5909.5	-2.935	2.935
450	-59044.5	-53150.8	-5893.7	-2.862	2.862
460	-58643.5	-52765.4	-5878.1	-2.792	2.792
470	-58243.3	-52380.9	-5862.4	-2.726	2.726
480	-57844.0	-51997.4	-5846.6	-2.662	2.662
490	-57445.6	-51614.7	-5830.9	-2.600	2.600
500	-57048.1	-51233.0	-5815.1	-2.542	2.542
510	-56651.4	-50852.1	-5799.3	-2.485	2.485
520	-55555.5	-50472.0	-5083.5	-2.136	2.136
530	-55860.5	-50092.9	-5767.6	-2.378	2.378
540	-55466.3	-49714.5	-5751.8	-2.328	2.328
550	-55072.9	-49337.0	-5735.9	-2.279	2.279
560	-54680.3	-48960.3	-5720.0	-2.232	2.232
570	-54288.5	-48584.4	-5704.1	-2.187	2.187
580	-53897.4	-48209.3	-5688.1	-2.143	2.143
590	-53507.1	-47835.0	-5672.1	-2.101	2.101
600	-53117.6	-47461.4	-5656.2	-2.060	2.060
610	-52715.1	-47075.1	-5640.0	-2.021	2.021
620	-52288.9	-46664.9	-5624.0	-1.982	1.982
630	-51862.9	-46255.1	-5607.8	-1.945	1.945
640	-51437.2	-45845.4	-5591.8	-1.909	1.909
650	-51011.6	-45436.0	-5575.6	-1.875	1.875
660	-50586.2	-45026.8	-5559.4	-1.841	1.841
670	-50161.0	-44617.8	-5543.2	-1.808	1.808
680	-49736.1	-44209.0	-5527.1	-1.776	1.776
690	-49311.3	-43800.6	-5510.7	-1.745	1.745
700	-48886.7	-43392.3	-5494.4	-1.715	1.715
710	-48462.4	-42984.2	-5478.2	-1.686	1.686
720	-48038.3	-42576.5	-5461.8	-1.658	1.658
730	-47614.4	-42168.9	-5445.5	-1.630	1.630
740	-47190.7	-41761.6	-5429.1	-1.603	1.603
750	-46767.2	-41354.6	-5412.6	-1.577	1.577
760	-46344.0	-40947.8	-5396.2	-1.552	1.552
770	-45939.0	-40541.2	-5397.8	-1.532	1.532
780	-45498.2	-40134.9	-5363.3	-1.503	1.503
790	-45075.7	-39728.9	-5346.8	-1.479	1.479
800	-44653.4	-39323.2	-5330.2	-1.456	1.456

Reaction



TempΔG reaction (3)ΔGreaction (4)ΔG reaction (11)log α_{S_2} Log α_{Te_2}
 (Log $\alpha_{\text{Te}_2}=0$) (log $\alpha_{\text{S}_2}=0$)

290	37892.4	-46869.54	8077.14	6.58	-6.58
300	-37839.0	-46811.00	8972.00	6.54	-6.54
310	-37573.0	-46518.30	8945.30	6.31	-6.31
320	-37308.4	-46225.60	8917.20	6.09	-6.09
330	-37045.2	-45932.90	8887.70	5.89	-5.89
340	-36783.4	-45640.20	8856.80	5.69	-5.69
350	-36523.0	-45347.50	8824.50	5.51	-5.51
360	-36264.0	-45054.80	8790.80	5.34	-5.34
370	-36006.4	-44762.10	8755.70	5.17	-5.17
380	-35750.1	-44469.40	8719.30	5.01	-5.01
390	-35495.2	-44176.70	8681.50	4.86	-4.86
400	-35241.6	-43884.00	8642.40	4.72	-4.72
410	-34989.4	-43591.30	8601.90	4.58	-4.58
420	-34738.8	-43325.00	8586.20	4.47	-4.47
430	-34489.0	-43164.00	8675.00	4.41	-4.41
440	-34240.8	-43003.00	8762.20	4.35	-4.35
450	-33993.9	-42842.00	8848.10	4.30	-4.30
460	-33791.9	-42681.00	8889.10	4.22	-4.22
470	-33594.1	-42520.00	8925.90	4.15	-4.15
480	-33400.6	-42359.00	8958.40	4.08	-4.08
490	-33211.6	-42198.00	8986.40	4.01	-4.01
500	-33027.1	-42037.00	9009.90	3.94	-3.94
510	-32847.2	-41876.00	9028.80	3.87	-3.87
520	-32011.6	-41715.00	9703.40	4.08	-4.08
530	-32501.7	-41554.00	9052.30	3.73	-3.73
540	-32336.3	-41393.00	9056.70	3.67	-3.67
550	-32176.0	-41232.00	9056.00	3.60	-3.60
560	-32020.7	-41071.00	9050.30	3.53	-3.53
570	-31870.7	-40910.00	9039.30	3.47	-3.47
580	-31725.9	-40749.00	9023.10	3.40	-3.40
590	-31586.4	-40588.00	9001.60	3.33	-3.33
600	-31452.4	-40427.00	8974.60	3.27	-3.27
610	-31324.0	-40266.00	8942.00	3.20	-3.20
620	-31201.0	-40105.00	8904.00	3.14	-3.14
630	-31103.8	-39944.00	8840.20	3.07	-3.07
640	-31005.2	-39783.00	8777.80	3.00	-3.00
650	-30907.9	-39622.00	8714.10	2.93	-2.93
660	-30812.0	-39461.00	8649.00	2.86	-2.86
670	-30717.3	-39300.00	8582.70	2.80	-2.80
680	-30641.9	-39139.00	8497.10	2.73	-2.73
690	-30531.7	-38978.00	8446.30	2.68	-2.68
700	-30440.8	-38817.00	8376.20	2.61	-2.61
710	-30351.0	-38656.00	8305.00	2.56	-2.56
720	-30262.3	-38495.00	8232.70	2.50	-2.50
730	-30174.8	-38334.00	8159.20	2.44	-2.44
740	-30088.3	-38173.00	8084.70	2.39	-2.39
750	-30002.9	-38012.00	8009.10	2.33	-2.33
760	-29918.5	-37851.00	7932.50	2.28	-2.28
770	-29835.2	-37690.00	7854.80	2.23	-2.23
780	-29752.8	-37529.00	7776.20	2.18	-2.18
790	-29671.5	-37368.00	7696.50	2.13	-2.13
800	-29590.3	-37207.00	7616.70	2.08	-2.08

Reaction



TempΔG reaction (2)ΔGreaction (2)ΔG reaction (12)log aS₂ Log aTe₂
 (Log aTe₂=0)(log aS₂=0)

298	-40836.1	-39436.4	-1399.7	-1.026	1.026
300	-40754.9	-39359.7	-1395.2	-1.016	1.016
310	-40349.2	-38977.0	-1372.2	-0.967	0.967
320	-39944.7	-38595.2	-1349.5	-0.922	0.922
330	-39541.3	-38214.3	-1327.0	-0.879	0.879
340	-39139.0	-37834.4	-1304.6	-0.839	0.839
350	-38737.6	-37455.3	-1282.3	-0.801	0.801
360	-38337.1	-37077.2	-1259.9	-0.765	0.765
370	-37937.6	-36699.8	-1237.8	-0.731	0.731
380	-37538.8	-36323.2	-1215.6	-0.699	0.699
390	-37140.8	-35947.5	-1193.3	-0.669	0.669
400	-36743.7	-35572.5	-1171.2	-0.640	0.640
410	-36347.2	-35198.2	-1149.0	-0.612	0.612
420	-35951.5	-34824.7	-1126.8	-0.586	0.586
430	-35556.4	-34451.9	-1104.5	-0.561	0.561
440	-35161.9	-34079.8	-1082.1	-0.537	0.537
450	-34768.1	-33708.3	-1059.8	-0.515	0.515
460	-34374.8	-33337.6	-1037.2	-0.493	0.493
470	-33982.2	-32967.4	-1014.8	-0.472	0.472
480	-33590.0	-32597.9	-992.1	-0.452	0.452
490	-33198.4	-32229.1	-969.3	-0.432	0.432
500	-32807.3	-31860.8	-946.5	-0.414	0.414
510	-32416.7	-31493.1	-923.6	-0.396	0.396
520	-31326.5	-31126.0	-900.5	-0.084	0.084
530	-31636.8	-30759.5	-877.3	-0.362	0.362
540	-31247.5	-30393.5	-854.0	-0.346	0.346
550	-30821.4	-29990.9	-830.5	-0.330	0.330
560	-30367.0	-29560.1	-806.9	-0.315	0.315
570	-29913.3	-29130.2	-783.1	-0.300	0.300
580	-30060.3	-29300.8	-759.5	-0.286	0.286
590	-29007.8	-28272.6	-735.2	-0.272	0.272
600	-28555.9	-27845.0	-710.9	-0.259	0.259
610	-28104.7	-27418.1	-686.6	-0.246	0.246
620	-27654.1	-26992.0	-662.1	-0.233	0.233
630	-27204.0	-26566.6	-637.4	-0.221	0.221
640	-26754.6	-26142.0	-612.6	-0.209	0.209
650	-26305.7	-25718.2	-587.5	-0.198	0.198
660	-25857.5	-25295.2	-562.3	-0.186	0.186
670	-25409.8	-24872.9	-536.9	-0.175	0.175
680	-24962.7	-24451.4	-511.3	-0.164	0.164
690	-24516.2	-24030.7	-485.5	-0.154	0.154
700	-24070.8	-23611.2	-459.6	-0.143	0.143
710	-23624.9	-23191.4	-433.5	-0.133	0.133
720	-23180.2	-22773.0	-407.2	-0.124	0.124
730	-22736.0	-22355.2	-380.8	-0.114	0.114
740	-22292.3	-21938.3	-354.0	-0.105	0.105
750	-21849.2	-21522.1	-327.1	-0.095	0.095
760	-21406.7	-21106.7	-300.0	-0.086	0.086
770	-20964.7	-20692.0	-272.7	-0.077	0.077
780	-20523.2	-20278.1	-245.1	-0.069	0.069
790	-20082.4	-19864.9	-217.5	-0.060	0.060
800	-19642.1	-19452.5	-189.6	-0.052	0.052

Reaction

$\text{Bi}_2\text{S}_3 + \text{Te}_2 = \text{Bi}_2\text{Te}_2\text{S} + \text{S}_2$								(13)
Temp	ΔGT	ΔGT	ΔGT	ΔGT	ΣGT	ΣGT	ΔGT	$\log \alpha_{\text{S}_2} \log \alpha_{\text{Te}_2}$
	Bi_2S_3	Te_2	$\text{Bi}_2\text{Te}_2\text{S}$	S_2	reactants	products	reaction	$\alpha_{\text{Te}_2=0} \alpha_{\text{S}_2=0}$
298	-47572.2	19892.7	-40091.6	14509.0	-27679.5	-25582.6	2096.8	1.54 -1.54
300	-47668.2	19768.9	-40202.3	14400.0	-27899.3	-25802.4	2096.9	1.53 -1.53
310	-48154.0	19148.2	-40761.5	13853.1	-29005.8	-26908.3	2097.4	1.48 -1.48
320	-48649.3	18524.7	-41330.3	13303.8	-30124.6	-28026.5	2098.1	1.43 -1.43
330	-49153.8	17898.5	-41908.4	12752.0	-31255.3	-29156.4	2099.0	1.39 -1.39
340	-49667.3	17269.5	-42495.6	12197.8	-32397.7	-30297.8	2099.9	1.35 -1.35
350	-50189.4	16638.1	-43091.6	11641.3	-33551.4	-31450.3	2101.0	1.31 -1.31
360	-50720.1	16004.1	-43696.3	11082.4	-34716.0	-32613.9	2102.1	1.28 -1.28
370	-51259.0	15367.6	-44309.3	10521.3	-35891.3	-33788.0	2103.3	1.24 -1.24
380	-51806.0	14728.8	-44930.6	9958.0	-37077.1	-34972.6	2104.5	1.21 -1.21
390	-52360.8	14087.7	-45559.9	9392.6	-38273.1	-36167.4	2105.7	1.18 -1.18
400	-52923.3	13444.3	-46197.1	8825.0	-39479.0	-37372.1	2106.9	1.15 -1.15
410	-53493.3	12798.6	-46842.0	8255.4	-40694.7	-38586.6	2108.1	1.12 -1.12
420	-54070.7	12150.8	-47494.3	7683.8	-41919.8	-39810.5	2109.3	1.10 -1.10
430	-54655.2	11500.9	-48154.1	7110.2	-43154.3	-41043.8	2110.4	1.07 -1.07
440	-55246.8	10848.9	-48821.1	6534.7	-44397.8	-42286.3	2111.5	1.05 -1.05
450	-55845.2	10194.9	-49495.1	5957.3	-45650.3	-43537.8	2112.5	1.03 -1.03
460	-56450.4	9538.9	-50176.1	5378.1	-46911.5	-44798.1	2113.5	1.00 -1.00
470	-57062.2	8880.9	-50863.9	4797.0	-48181.3	-46067.0	2114.3	0.98 -0.98
480	-57680.4	8221.0	-51558.5	4214.1	-49459.4	-47344.4	2115.1	0.96 -0.96
490	-58305.1	7559.2	-52259.6	3629.5	-50745.8	-48630.1	2115.8	0.94 -0.94
500	-58935.9	6895.6	-52967.2	3043.2	-52040.3	-49924.0	2116.3	0.92 -0.92
510	-59572.9	6230.2	-53681.2	2455.1	-53342.8	-51226.0	2116.8	0.91 -0.91
520	-60216.0	5563.0	-54401.4	1165.5	-54653.0	-53235.9	1417.1	0.60 -0.60
530	-60865.0	4894.0	-55127.8	1274.2	-55970.9	-53853.6	2117.3	0.87 -0.87
540	-61519.8	4223.4	-55860.2	681.2	-57296.4	-55179.0	2117.4	0.86 -0.86
550	-62180.3	3551.0	-56598.6	86.8	-58629.2	-56511.9	2117.4	0.84 -0.84
560	-62846.4	2877.0	-57342.9	-509.3	-59969.4	-57852.2	2117.2	0.83 -0.83
570	-63518.1	2201.4	-58093.1	-1106.8	-61316.8	-59199.9	2116.9	0.81 -0.81
580	-64195.3	1524.1	-58848.9	-1705.9	-62671.2	-60554.8	2116.4	0.80 -0.80
590	-64877.8	845.3	-59610.4	-2306.4	-64032.5	-61916.8	2115.8	0.78 -0.78
600	-65565.7	164.9	-60377.4	-2908.4	-65400.8	-63285.8	2115.0	0.77 -0.77
610	-66258.7	-517.0	-61150.0	-3511.8	-66775.8	-64661.7	2114.0	0.76 -0.76
620	-66957.0	-1200.5	-61927.9	-4116.6	-68157.4	-66044.5	2112.9	0.74 -0.74
630	-67660.2	-1885.4	-62711.2	-4722.8	-69545.6	-67434.0	2111.7	0.73 -0.73
640	-68368.5	-2571.8	-63499.8	-5330.3	-70940.3	-68830.1	2110.2	0.72 -0.72
650	-69081.8	-3259.7	-64293.6	-5939.2	-72341.4	-70232.8	2108.6	0.71 -0.71
660	-69799.9	-3948.9	-65092.5	-6549.5	-73748.8	-71642.0	2106.8	0.70 -0.70
670	-70522.8	-4639.6	-65896.5	-7161.0	-75162.4	-73057.5	2104.9	0.69 -0.69
680	-71250.4	-5331.7	-66705.6	-7773.8	-76582.1	-74479.4	2102.7	0.68 -0.68
690	-71982.8	-6025.1	-67519.6	-8387.9	-78007.9	-75907.5	2100.4	0.67 -0.67
700	-72719.8	-6720.0	-68338.6	-9003.2	-79439.7	-77341.8	2097.9	0.65 -0.65
710	-73461.3	-7416.1	-69162.4	-9619.8	-80877.4	-78782.2	2095.2	0.64 -0.64
720	-74207.3	-8113.6	-69991.0	-10237.6	-82320.9	-80228.6	2092.3	0.64 -0.64
730	-74958.0	-8812.4	-70824.4	-10856.6	-83770.3	-81681.0	2089.3	0.63 -0.63
740	-75712.8	-9512.4	-71662.5	-11476.8	-85225.2	-83139.3	2086.0	0.62 -0.62
750	-76472.1	-10213.8	-72505.2	-12098.1	-86685.9	-84603.4	2082.5	0.61 -0.61
760	-77235.7	-10916.4	-73352.6	-12720.7	-88152.1	-86073.2	2078.8	0.60 -0.60
770	-78003.5	-11620.2	-74204.5	-13344.3	-89623.8	-87548.8	2075.0	0.59 -0.59
780	-78775.6	-12325.3	-75060.9	-13969.1	-91100.9	-89030.0	2070.9	0.58 -0.58
790	-79551.8	-13031.6	-75921.8	-14595.0	-92583.5	-90516.8	2066.6	0.57 -0.57
800	-80332.2	-13739.1	-76787.2	-15222.0	-94071.4	-92009.2	2062.2	0.56 -0.56

Reaction



Temp	ΔGT	ΔGT	ΔGT	ΔGT	ΣGT	ΣGT	ΔGT	$\log \frac{\alpha_{\text{S}_2}}{\alpha_{\text{Te}_2}}$	
	Te_2	$\text{Bi}_2\text{Te}_2\text{S}$	S_2	Bi_2Te_3	reactants	products	reaction	$\alpha_{\text{Te}_2=0}$	$\alpha_{\text{S}_2=0}$
298	19892.7	-40091.6	14509.0	-37395.2	-60290.5	-60281.4	9.1	0.01	-0.01
300	19768.9	-40202.3	14400.0	-37520.2	-60635.7	-60640.4	-4.8	0.00	0.00
310	19148.2	-40761.5	13853.1	-38151.1	-62374.8	-62449.1	-74.3	-0.05	0.05
320	18524.7	-41330.3	13303.8	-38791.7	-64135.9	-64279.5	-143.7	-0.10	0.10
330	17898.5	-41908.4	12752.0	-39441.6	-65918.3	-66131.2	-212.9	-0.14	0.14
340	17269.5	-42495.6	12197.8	-40100.7	-67721.6	-68003.6	-282.0	-0.18	0.18
350	16638.1	-43091.6	11641.3	-40768.7	-69545.1	-69896.1	-350.9	-0.22	0.22
360	16004.1	-43696.3	11082.4	-41445.4	-71388.4	-71808.3	-419.9	-0.25	0.25
370	15367.6	-44309.3	10521.3	-42130.5	-73251.0	-73739.8	-488.8	-0.29	0.29
380	14728.8	-44930.6	9958.0	-42824.0	-75132.4	-75690.0	-557.6	-0.32	0.32
390	14087.7	-45559.9	9392.6	-43525.6	-77032.2	-77658.7	-626.5	-0.35	0.35
400	13444.3	-46197.1	8825.0	-44235.1	-78949.9	-79645.2	-695.3	-0.38	0.38
410	12798.6	-46842.0	8255.4	-44952.4	-80885.3	-81649.4	-764.1	-0.41	0.41
420	12150.8	-47494.3	7683.8	-45677.3	-82837.9	-83670.9	-833.0	-0.43	0.43
430	11500.9	-48154.1	7110.2	-46409.7	-84807.2	-85709.2	-902.0	-0.46	0.46
440	10848.9	-48821.1	6534.7	-47149.4	-86793.2	-87764.2	-971.0	-0.48	0.48
450	10194.9	-49495.1	5957.3	-47896.3	-88795.4	-89835.3	-1040.0	-0.51	0.51
460	9538.9	-50176.1	5378.1	-48650.3	-90813.4	-91922.5	-1109.1	-0.53	0.53
470	8880.9	-50863.9	4797.0	-49411.2	-92847.0	-94025.3	-1178.3	-0.55	0.55
480	8221.0	-51558.5	4214.1	-50178.8	-94896.0	-96143.6	-1247.6	-0.57	0.57
490	7559.2	-52259.6	3629.5	-50953.2	-96960.0	-98277.0	-1317.0	-0.59	0.59
500	6895.6	-52967.2	3043.2	-51734.2	-99038.8	-100425.2	-1386.5	-0.61	0.61
510	6230.2	-53681.2	2455.1	-52521.7	-101132.1	-102588.2	-1456.1	-0.62	0.62
520	5563.0	-54401.4	1165.5	-53315.5	-103239.8	-105465.6	-2225.8	-0.94	0.94
530	4894.0	-55127.8	1274.2	-54115.6	-105361.5	-106957.1	-1595.6	-0.66	0.66
540	4223.4	-55860.2	681.2	-54921.9	-107497.1	-109162.7	-1665.6	-0.67	0.67
550	3551.0	-56598.6	86.8	-55734.4	-109646.2	-111382.0	-1735.7	-0.69	0.69
560	2877.0	-57342.9	-509.3	-56552.8	-111808.9	-113614.9	-1806.0	-0.70	0.70
570	2201.4	-58093.1	-1106.8	-57377.1	-113984.8	-115861.1	-1876.3	-0.72	0.72
580	1524.1	-58848.9	-1705.9	-58207.3	-116173.7	-118120.6	-1946.9	-0.73	0.73
590	845.3	-59610.4	-2306.4	-59043.3	-118375.5	-120393.0	-2017.5	-0.75	0.75
600	164.9	-60377.4	-2908.4	-59885.0	-120590.0	-122678.4	-2088.4	-0.76	0.76
610	-517.0	-61150.0	-3511.8	-60732.3	-122816.9	-124976.3	-2159.4	-0.77	0.77
620	-1200.5	-61927.9	-4116.6	-61585.1	-125056.3	-127286.8	-2230.5	-0.79	0.79
630	-1885.4	-62711.2	-4722.8	-62443.4	-127307.8	-129609.7	-2301.9	-0.80	0.80
640	-2571.8	-63499.8	-5330.3	-63307.2	-129571.4	-131944.7	-2373.3	-0.81	0.81
650	-3259.7	-64293.6	-5939.2	-64176.3	-131846.8	-134291.8	-2445.0	-0.82	0.82
660	-3948.9	-65092.5	-6549.5	-65050.7	-134134.0	-136650.8	-2516.8	-0.83	0.83
670	-4639.6	-65896.5	-7161.0	-65930.3	-136432.7	-139021.6	-2588.9	-0.84	0.84
680	-5331.7	-66705.6	-7773.8	-66815.1	-138742.9	-141404.0	-2661.1	-0.86	0.86
690	-6025.1	-67519.6	-8387.9	-67705.0	-141064.4	-143797.9	-2733.4	-0.87	0.87
700	-6720.0	-68338.6	-9003.2	-68599.9	-143397.1	-146203.1	-2806.0	-0.88	0.88
710	-7416.1	-69162.4	-9619.8	-69499.9	-145740.9	-148619.6	-2878.8	-0.89	0.89
720	-8113.6	-69991.0	-10237.6	-70404.9	-148095.6	-151047.3	-2951.7	-0.90	0.90
730	-8812.4	-70824.4	-10856.6	-71314.7	-150461.2	-153486.0	-3024.8	-0.91	0.91
740	-9512.4	-71662.5	-11476.8	-72229.4	-152837.4	-155935.5	-3098.2	-0.91	0.91
750	-10213.8	-72505.2	-12098.1	-73148.9	-155224.2	-158395.9	-3171.7	-0.92	0.92
760	-10916.4	-73352.6	-12720.7	-74073.1	-157621.5	-160866.9	-3245.4	-0.93	0.93
770	-11620.2	-74204.5	-13344.3	-75002.1	-160029.2	-163348.5	-3319.3	-0.94	0.94
780	-12325.3	-75060.9	-13969.1	-75935.8	-162447.2	-165840.6	-3393.5	-0.95	0.95
790	-13031.6	-75921.8	-14595.0	-76874.0	-164875.3	-168343.1	-3467.8	-0.96	0.96
800	-13739.1	-76787.2	-15222.0	-77816.9	-167313.5	-170855.8	-3542.3	-0.97	0.97

APPENDIX 2.

SAMPLE PREPARATION OF THE SOUTHERN UPLANDS PLACER GOLD FOR SEM AND EPMA ANALYSES.

A2.1. Preparation of the Southern Uplands placer gold for SEM analysis.

The placer gold was mounted (using double sided clear sticky tape) on a specially marked 30mm diameter aluminium SEM stubs so that individual grains could be recognised from a reference diagram. The grains were manipulated from sample bottle to SEM stub using a low powered binocular microscope and a "needle" spatula. Once all of the grains had been mounted, and their position on the stub recorded, the grains were then sputter coated, under vacuum, with a thin film (approx. 200Å) of carbon to aid conduction between the SEM stub and the gold grains. During SEM examination the following observations and analyses were undertaken:

- (i) at least two electron micrographs were taken, so that there was a permanent record of the morphological characteristics of each grain.
- (ii) A semi-quantitative analysis for gold and silver on a suitable area of the grain (usually on an area 40X40 μ m), using a counting time of 100s.
- (iii) An energy dispersive spectrum was acquired to see if any other elements other than gold or silver were present.

A2.1. Preparation of the Southern Uplands placer gold for EPMA analysis.

After all of the SEM observations and analyses had been completed on an individual SEM stub the gold grains were very carefully removed from the SEM stub using a low powered binocular microscope and a "needle" spatula onto a specially prepared 2x1 inch glass slide. The slide was first gridded using indelible ink, clear double sided sticky tape was then placed over the grid, the gold grains were then mounted onto the grid using a "needle" spatula and a low powered binocular microscope, and the grid position of each grain recorded. The surface of the slide was then covered with a layer (1-2mm thick) of epoxy resin. When the epoxy resin had set the gold grains were then erupted by very careful grinding with 600 mesh carborundum grit on

a glass plate. The final polish was achieved using 6, 1, and 1/4 μ m diamond paste on a paper lap, after further grinding using 800 and 1200 mesh carborundum grit.

Prior to EPMA the section was sputter coated, under vacuum, with a thin (250Å) layer of carbon.

APPENDIX 3.

METHOD EMPLOYED FOR THE CALCULATION OF THE ANNEALING HISTORY LIMITS FOR HETEROGENEOUS PLACER GOLD.

The method for calculation of the annealing history limits of heterogeneous placer gold has been described by Czamanske et al. (1973). The method, as described here, is a direct quote from their original paper.

Diffusion coefficients in two-component, alloy systems that exhibit concentration-dependant diffusion are readily calculated using the Boltzmann-Matano method. [this method assumes an initial step discontinuity]...The requirement that Boltzmann-Matano solution be applied to systems where there is no volume change on mixing is fulfilled for electrum. The equation relevant to the Boltzmann-Matano solution is

$$D(c') = -1/2t \frac{dx}{dt} c' \int_0^{c'} X dc \quad (1)$$

where

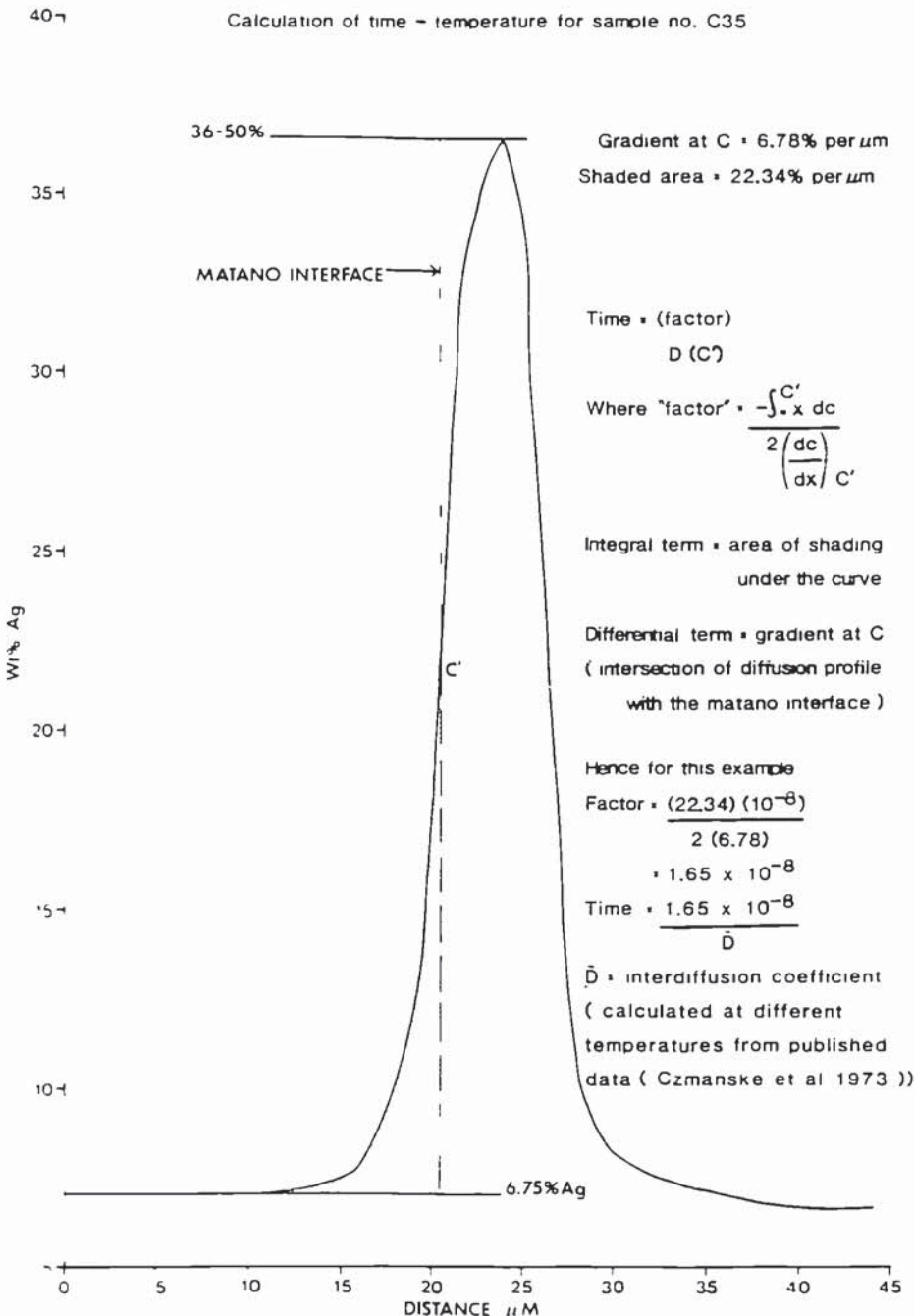
$D(c')$ = diffusion coefficient in cm²/sec at concentration c'
 c = concentration in any consistent units
 t = time in secs
 X = distance in cm
 \int = integral sign

This equation is usually solved using graphical methods by determining the matano interface which provides a reference point for calculation of the integral term. This is the plane that makes equal the two graphic areas bounded by itself and the diffusion profile.....By algebraic rearrangement of equation (1), one may obtain

$$t = (\text{factor})/D(c'), \text{ where 'factor'} = [-\int_0^{c'} X dc]/[2(dc/dx)c'] \quad (2)$$

In their study Czmanske et al. (1973) use a worked example to show how annealing history limits can be established from the above equation. Here a worked example (using a heterogeneous gold grain from pan concentrate C35) is also presented using the same method of calculation. The line concentration profile illustrated in figure A3.1 may be considered to represent the diffusion profile that could result in time if there were initially a steplike change in composition at approximately the line labelled "Matano interface". The point c' (eq.2) at which the diffusion coefficient is to be evaluated was taken at C' the intersection of the profile with the Matano interface. With this designation, the integral term (eq. 2) is equivalent to the stippled area in figure A3.1 and has units of microns x weight percent. Similarly the differential term (dc/dx) in equation (2) can be approximated as the slope of the profile at the Matano interface; the slope has the units of weight percent / micron. Specifically for the diffusion profile illustrated (fig A2.1) the area (integral term) involved is 22.34 microns x weight percent and the slope (derivative) is 6.78 weight percent per micron.

Figure A3.1 Diffusion profile across a heterogeneous placer gold grain illustrating the method of calculation of annealing history limits



Hence

$$\text{'Factor'} = (22.34) (10^{-8}) / 2 (6.78) = 1.65 \times 10^{-8}$$

and:

$$t = 1.65 \times 10^{-8} / D \sim$$

where 10^{-8} is a conversion factor for square microns to square centimetres, t is the time in seconds and $D \sim$ is the interdiffusion coefficient. Because values of the interdiffusion coefficient are temperature dependant a range of values were selected over the temperature range 350-100°C and used to calculate the annealing history limits for the Southern Uplands placer gold (cf fig. 9.13).

APPENDIX 4a.

SAMPLE DETAILS FOR CLOGAU MINE AND THE DOLGELLAU GOLD-BELT.

<u>SAMPLE NUMBER</u>	<u>SAMPLE DETAILS</u>	<u>SAMPLE LOCALITY</u>
BMNH Kingsbury Clogau Mine (K2)	Native gold in quartz with shale ribbons	Locality in the mine workings unknown
BMNH Kingsbury Clogau Mine (K2b)	Gold in Clogau shale	Locality in the mine workings not known
BMNH Kingsbury Clogau Mine (K2c)	Native gold in quartz with inclusions of black shale	Locality in the mine workings not known
BMNH Kingsbury Clogau Mine (K2d)	Native gold in quartz with inclusions of black shale	Locality in the mine workings not known
BMNH Kingsbury Clogau Mine (K3)	Native gold in galena	Location in the mine workings not known
BMNH Kingsbury Clogau Mine (K5)	Bismuth tellurides in quartz	Locality in the mine workings is unknown.
BMNH Kingsbury Clogau Mine (K5b)	Bismuth tellurides in quartz	Locality in the mine workings not known
BMNH Kingsbury Clogau Mine (K5c)	Bismuth tellurides in quartz with minor amounts of native gold.	Locality in the mine workings not known
Clogau Mine Level 4	Galena in quartz with shale wallrock material	Locality 2
CMC 1	Mill concentrate with abundant native gold	Locality 1
CMC 2	Mill concentrate containing abundant gold from clogau mine	Locality 1
D. Au 4/78	Pyrite in Clogau Shale	unknown
JN 1	Bismuth tellurides in quartz	Locality 1
JN 2	Bismuth tellurides in quartz	Locality 1
JN 3a	Bismuth tellurides in quartz	Locality 1
JN 3b	Galena with cobaltite, plus minor native bismuth and bismuthtellurides in quartz	Locality 1

<u>SAMPLE NUMBER</u>	<u>SAMPLE DETAILS</u>	<u>SAMPLE LOCALITY</u>
JN 4	Bismuth tellurides in quartz	Locality 1
JN 5	Bismuth tellurides in quartz	Locality 1
JN 6	Galena in quartz with shale wallrock material	Locality 2
JN 12	Galena with cobaltite, plus minor native bismuth and bismuth tellurides in quartz	Locality 1
JN 13	Bismuth telluride concentrate	Locality 1
JN 14	Galena,pyrite, pyrrhotine and chalcopyrite in quartz with shale wallrock material	Locality 2
JN 15	Pyrrhotine, chalcopyrite and galena in quartz with shale inclusions	Locality 2
JN 16	Bismuth tellurides in quartz with chalcopyrite and galena	Locality 1
JN 17	Quartz veins in shale with pyrrhotine	Locality 2
JN 19	Bismuth telluride concentrate obtained by dissolving the quatz in HF	Locality 1
JN 29	Bismuth telluride concentrate obtained by dissolving the quartz in HF	Locality 1
JN 30	Galena in quartz with shale wallrock material	Locality 2
JN 31a	Galena in quartz with shale wallrock material	Locality 2
JN 31b	Pyrrhotine, chalcopyrite and Galena in quartz with shale wallrock material	Locality 2
JN 31c	Pyrrhotine, chalcopyrite and Galena in quartz with shale wallrock material	Locality 2
JN 32	Galena in quartz with shale wallrock material	Locality 2

<u>SAMPLE NUMBER</u>	<u>SAMPLE DETAILS</u>	<u>SAMPLE LOCALITY</u>
JN 34	Galena in quartz with shale wallrock material	Locality 2
JN 35	Galena in quartz with shale wallrock material	Locality 2
JN 36	Placer gold from the Hirgwm river	
JN 37	Chalcopyrite and pyrrhotine with minor Bismuth tellurides in quartz	Locality 1
JN 39	Vein of cobaltite in quartz	Locality 1
JN 40	Shale inclusions in quartz	Locality 2
JN 41	Pyrrhotine, chalcopyrite and Galena in quartz with shale wallrock material	Locality 2
SB 4.6	Chalcopyrite and pyrrhotine in 'barren' quartz	Locality 1
SB 128 C/2	Chalcopyrite in 'barren' quartz	Locality 1
SB 128B	Pyrrhotine and chalcopyrite associated with a shale inclusion in vein quartz	Locality 1
SB 128C	Pyrrhotine and chalcopyrite associated with a shale inclusion in vein quartz	Locality 1
SB 128D	Galena in quartz	Locality 1
SB 128F	Pyrrhotine and chalcopyrite associated with a shale inclusion in vein quartz	Locality 1
SB BiTe	Bismuth telluride concentrate	Locality 1
SB COB 128	Cobaltite in quartz	Locality 1
SB JH 1	Galena and chalcopyrite in mineralised quartz from the John Hughes lode, Clogau Mine	

SAMPLE NUMBERSAMPLE DETAILSSAMPLE
LOCALITY

SB JH2

Galena and chalcopyrite in mineralised
quartz from the John Hugh's Lode, Clogau
Mine

APPENDIX 4b.

MINERAL CHEMISTRY DATA FOR CHAPTER 4.

TABLE A4.1 Cobaltite analyses from sample JN 12. The top line of each analysis is the proportions of the elements in weight percent, and the bottom line the proportions of the elements in mol percent. The column titled "distance μm " give the distance between each quantitative analysis of the line concentration profile and the column titled "analysis" indicates whether an analysis is part of a line concentration profile ("Line profile") or a random spot analysis ("Random").

Fe	Cu	As	Ni	Co	S	Ag	Sb	Total	Distance (μm)	Mineral	Analysis
5.71	tr	44.61	9.66	19.64	19.91	tr	tr	99.58			
5.63	tr	32.77	9.06	18.32	34.17	.03	tr	100	1	Cobaltite	Line profile
6.21	tr	44.92	9.81	19.03	20.12	nd	nd	100.1			
6.08	tr	32.8	9.14	17.65	34.33	nd	nd	100.01	71	Cobaltite	Line profile
6.34	.06	44.98	8.12	19.85	20.12	.04	nd	99.51			
6.24	.05	33.02	7.61	18.51	34.51	.07	nd	100.01	142	Cobaltite	Line profile
7.75	nd	44.91	10.77	15.27	20.15	.03	tr	98.9			
7.67	nd	33.12	10.14	14.3	34.72	.05	tr	100.01	213	Cobaltite	Line profile
33.01	nd	45	.04	1.26	21	.03	.04	100.38			
31.61	nd	32.12	.04	1.14	35.02	.05	tr	100	284	Arsenopyrite	Line profile
32.95	nd	45.99	.16	.7	19.94	nd	.05	99.79			
32.05	nd	33.35	.15	.65	33.78	nd	tr	100	355	Arsenopyrite	Line profile
33.01	nd	46.41	.14	.64	19.81	tr	.06	100.08			
32.08	nd	33.62	.13	.59	33.53	tr	.03	100	426	Arsenopyrite	Line profile
31.39	tr	46.98	.16	2.42	19.4	tr	.04	100.42			
30.56	tr	34.1	.15	2.23	32.9	.03	tr	100	497	Arsenopyrite	Line profile
26.6	nd	47.55	.35	6.72	18.9	nd	.05	100.17			
26.16	nd	34.86	.33	6.26	32.38	nd	tr	100.01	568	Arsenopyrite	Line profile
29.16	tr	46.82	.3	4.56	18.94	nd	.06	99.85			
28.68	tr	34.32	.28	4.24	32.44	nd	.03	100	639	Arsenopyrite	Line profile
29.23	tr	47.59	.12	4.55	18.68	nd	.04	100.23			
28.74	tr	34.88	.11	4.24	31.99	nd	tr	100	710	Arsenopyrite	Line profile
30.87	nd	46.46	.07	3.52	19.66	.04	tr	100.64			
29.91	nd	33.55	.06	3.23	33.17	.07	tr	100	781	Arsenopyrite	Line profile
32.19	tr	45.57	tr	1.85	19.64	nd	.04	99.31			
31.51	tr	33.25	tr	1.71	33.49	nd	tr	100	852	Arsenopyrite	Line profile
4.61	.12	43.95	6.65	16.25	20.2	.28	.07	92.13			
4.86	.11	34.53	6.67	16.21	37.08	.52	.03	100.01	923	Cobaltite	Line profile
4.39	nd	44.8	2.92	28.06	18.98	nd	nd	99.15			
4.38	nd	33.33	2.77	26.51	33	nd	nd	99.99	*	Cobaltite	Random
5.02	nd	44.71	3.36	26.65	19.26	nd	.77	99.77			
4.99	nd	33.1	3.17	25.06	33.32	nd	.35	99.99	*	Cobaltite	Random
3.84	nd	44.44	3.56	27.65	19.29	nd	.96	99.74			
3.82	nd	32.94	3.37	26.03	33.41	nd	.44	100.01	*	Cobaltite	Random

TABLE A4.1 CONTINUED

Fe	Cu	As	Ni	Co	S	Ag	Sb	Total	Distance (μm)	Mineral	Analysis
7.5	nd	46.27	10.75	17.03	18.56	nd	nd	100.11			
7.45	nd	34.26	10.16	16.02	32.11	nd	nd	100	•	Cobaltite	Random
5.18	nd	44.85	4.71	26.47	19.47	nd	nd	100.68			
5.08	nd	32.76	4.39	24.55	33.23	nd	nd	100.01	•	Cobaltite	Random
5.16	nd	45.03	4.21	25.48	19.15	nd	nd	99.03			
5.15	nd	33.5	4	24.07	33.28	nd	nd	100	•	Cobaltite	Random
5.98	nd	44.79	4.74	25.05	19.73	nd	nd	100.29			
5.87	nd	32.75	4.42	23.26	33.71	nd	nd	100.01	•	Cobaltite	Random

Table A4.2 Line concentration profiles of the telluride intergrowths. The top line of each analysis is the proportions of the elements in weight percent, and the bottom line the proportions of the elements in mol percent. The column titled "distance μm " give the distance between each quantitative analysis of the line concentration profile and the column titled "Mineral" indicates the mineral being analysed (Tellurbismuth, Tetradyomite, the fingerprint intergrowth ("Fingerprint") or galena.

SCAN 1 Line concentration profile across a Tellurbismut-Galena intergrowth (Sample No. JN 13)

Pb	Bi	S	Te	Sb	Cd	Ag	Total	Distance (μm)	Mineral
.38 .29	49.48 38.47	tr .03	46.57 59.29	.8 1.06	.41 .59	.18 .27	97.81 100	6	Tellurbismuth
nd nd	50.15 38.79	.04 .18	47.06 59.63	.71 .94	.28 .4	.04 .06	98.27 100	12	Tellurbismuth
nd nd	49.86 38.77	nd tr	46.81 59.62	.67 .9	.48 .7	nd nd	97.82 100	18	Tellurbismuth
nd nd	49.46 38.62	nd nd	46.82 59.87	.78 1.04	.31 .45	tr tr	97.37 100	24	Tellurbismuth
nd nd	50.57 39.24	nd nd	46.65 59.27	.73 .97	.34 .5	tr tr	98.31 100	30	Tellurbismuth
85.63 49.65	.8 .46	13.29 49.82	nd nd	tr tr	.05 .05	nd nd	99.79 100	36	Galena
nd nd	50.7 39.16	tr .04	46.88 59.3	.79 1.04	.3 .44	tr .03	98.69 100	42	Tellurbismuth
nd nd	49.66 38.67	tr .03	46.85 59.76	.8 1.07	.32 .46	nd nd	97.64 100	48	Tellurbismuth
nd nd	49.79 38.51	nd nd	47.26 59.86	.84 1.12	.29 .42	.06 .09	98.25 100	54	Tellurbismuth
nd nd	50.34 39.17	.04 .19	46.4 59.13	.79 1.06	.32 .46	nd nd	97.88 100	60	Tellurbismuth
nd nd	49.04 38.47	.04 .19	46.58 59.84	.81 1.09	.27 .39	tr tr	96.74 100	66	Tellurbismuth
nd nd	50.71 38.9	tr .06	47.31 59.44	.77 1.01	.38 .54	.04 .05	99.21 100	72	Tellurbismuth
nd nd	49.89 38.73	.03 .13	46.76 59.45	.75 1	.47 .68	tr tr	97.9 100	78	Tellurbismuth
nd nd	48.6 37.9	.03 .16	47.22 60.32	.8 1.07	.34 .5	.04 .05	97.02 100	84	Tellurbismuth
58.54 40.02	1.01 .69	13.23 58.44	.51 .56	.06 .07	.12 .15	.05 .06	73.52 100	90	Tellurbismuth
84.43 48.69	1.04 .59	13.47 50.2	.35 .33	nd nd	.09 .09	.08 .09	99.46 100	96	Tellurbismuth
nd nd	50.04 39	nd nd	46.66 59.56	.8 1.07	.24 .35	tr tr	97.76 100	102.....	Tellurbismuth

Table A4.2 Continued

Pb	Bi	S	Te	Sb	Cd	Ag	Total Distance (μm)	Mineral
nd	50.6	nd	46.02	.78	.36	nd	97.77	
nd	39.54	nd	58.89	1.05	.52	nd	100	108.....Tellurbismuth
nd	50.71	nd	47	.89	.25	nd	98.85	
nd	39.11	nd	59.36	1.18	.35	nd	100	114.....Tellurbismuth
nd	50.04	nd	47.03	.85	.4	nd	98.32	
nd	38.71	nd	59.59	1.13	.57	nd	100	120.....Tellurbismuth
nd	50.16	nd	46.37	.81	.36	.04	97.75	
nd	39.11	nd	59.22	1.09	.52	.07	100	126.....Tellurbismuth
85.23	1.12	13.34	nd	.1	.03	.14	99.95	
49.26	.64	49.82	nd	.1	.03	.16	100	132.....Tellurbismuth
85.71	.95	13.4	.36	.06	nd	nd	100.48	
49.28	.54	49.78	.34	.06	nd	nd	100	138.....Tellurbismuth
nd	50.28	nd	46.49	.84	.34	.03	97.98	
nd	39.11	nd	59.23	1.12	.49	.05	100	144.....Tellurbismuth
85.67	.85	13.19	nd	.09	.03	tr	99.84	
49.81	.49	49.55	nd	.09	.03	tr	100	150.....Tellurbismuth
85.85	.97	13.23	nd	.04	.14	nd	100.25	
49.71	.56	49.53	nd	.04	.15	nd	100	156.....Tellurbismuth
nd	50.07	nd	46.83	.74	.41	.07	98.12	
nd	38.83	nd	59.48	.99	.6	.11	100	162.....Tellurbismuth
nd	50.15	nd	46.35	.73	.36	.06	97.64	
nd	39.14	tr	59.25	.98	.53	.08	100	168.....Tellurbismuth
.06	50.21	nd	46.1	.71	.23	tr	97.32	
.05	39.4	nd	59.25	.96	.33	tr	100	174.....Tellurbismuth
nd	49.71	nd	46.66	.66	.51	.04	97.58	
nd	38.75	nd	59.57	.88	.74	.06	100	180.....Tellurbismuth

Table A4.3 Scan 2, line concentration profile across a tetradyomite-fingerprint intergrowth (Sample No. JN 13).

Pb	Bi	S	Te	Sb	Cd	Ag	Total	Distance (μm)	Mineral
11.42 42.3	51.41 9.48	1.19 6.37	30.35 40.9	.43 .6	.23 .35	nd nd	95.02 100	6	Fingerprint
9.09 34.95	51.48 6.22	5.13 22.71	31.35 34.85	.75 .87	.3 .38	nd nd	98.11 100	12	Tetradyomite
13.78 34.16	48.73 9.74	4.57 20.89	29.73 34.14	.55 .67	.21 .27	.1 .13	97.67 100	18	Fingerprint
28.77 27.41	38.2 20.82	4.42 20.68	25.89 30.42	.28 .34	.22 .29	.03 .04	97.79 100	24	Fingerprint
29.77 27.85	39.21 21.33	4.46 20.64	25.29 29.43	.33 .41	.26 .35	nd nd	99.33 100	30	Fingerprint
33.48 25.42	36.03 23.82	5.05 23.22	23.13 26.73	.37 .45	.27 .35	tr tr	98.33 100	36	Fingerprint
7.09 35.38	52.24 4.84	5.18 22.86	32.16 35.67	.81 .94	.25 .31	nd nd	97.73 100	42	Tetradyomite
7.73 35.32	52.11 5.29	5.08 22.46	32.15 35.69	.73 .85	.31 .39	nd nd	98.11 100	48	Tetradyomite
7.63 35.16	52.49 5.16	5.28 23.05	32.34 35.46	.79 .91	.22 .27	nd nd	98.75 100	54	Tetradyomite
7.12 35.66	52.51 4.88	5.07 22.46	32.17 35.78	.75 .87	.28 .36	nd nd	97.9 100	60	Tetradyomite
7.21 35.58	52.07 4.96	4.98 22.18	32.19 36.02	.82 .97	.23 .3	nd nd	97.51 100	66	Tetradyomite
7.52 35.08	50.44 5.27	4.87 22.09	31.83 36.26	.8 .96	.24 .32	tr tr	95.72 100	72	Tetradyomite
7.45 35.53	52.52 5.09	5.05 22.29	32.26 35.75	.77 .89	.36 .45	nd nd	98.42 100	78	Tetradyomite
7.06 35.74	52.06 4.89	4.99 22.33	31.82 35.77	.74 .88	.3 .38	nd nd	96.97 100	84	Tetradyomite
7.23 35.26	51.04 5.04	4.9 22.07	32.01 36.21	.78 .93	.38 .49	nd nd	96.34 100	90	Tetradyomite
6.9 35.57	52.16 4.74	4.99 22.19	32.16 35.92	.88 1.03	.34 .43	.09 .12	97.51 100	96	Tetradyomite
6.93 35.35	51.64 4.79	5.03 22.44	32.19 36.09	.82 .96	.29 .37	nd nd	96.89 100	102	Tetradyomite
6.97 36.28	52.28 4.88	4.63 20.96	32.29 36.69	.73 .87	.25 .33	nd nd	97.15 100	108	Tetradyomite
6.38 35.48	51.94 4.4	4.93 21.96	32.79 36.69	.82 .96	.39 .5	tr tr	97.28 100	114	Tetradyomite
6.39 35.36	52.6 4.34	5.21 22.83	32.76 36.07	.78 .9	.41 .51	nd nd	98.15 100	126	Tetradyomite

Table A4.3 Continued

Pb	Bi	S	Te	Sb	Cd	Ag	Total Distance (μm)	Mineral
6.39 35.41	52.7 4.33	5.17 22.64	33.01 36.32	.76 .87	.34 .43	nd nd	98.37 100	132.....Tetradymite
6.93 35.13	51.55 4.76	5.07 22.53	32.6 36.39	.72 .85	.27 .34	nd nd	97.14 100	138.....Tetradymite
6.93 35.39	52.28 4.73	5.14 22.7	32.24 35.74	.77 .89	.44 .55	nd nd	97.8 100	144.....Tetradymite
7.08 35.24	51.74 4.86	5.16 22.89	31.96 35.65	.77 .9	.34 .43	tr tr	97.05 100	150.....Tetradymite
7.75 34.74	51.42 5.28	5.27 23.2	32.05 35.47	.75 .87	.35 .44	nd nd	97.58 100	156.....Tetradymite
7.24 34.79	51.17 4.96	5.14 22.77	32.48 36.17	.8 .93	.3 .38	nd tr	97.13 100	162.....Tetradymite
7.14 35.19	52.06 4.87	5.2 22.92	32.27 35.73	.75 .88	.33 .41	nd nd	97.75 100	168.....Tetradymite
7.76 34.18	50.2 5.33	5.25 23.29	32.13 35.82	.8 .94	.34 .43	tr tr	96.49 100	174.....Tetradymite
7.96 34.98	51.44 5.46	5.18 22.97	31.63 35.23	.81 .94	.34 .42	nd nd	97.35 100	180.....Tetradymite
7.64 35.06	50.72 5.32	4.93 22.24	31.8 36	.8 .94	.31 .4	.03 .04	96.23 100	186.....Tetradymite
8.02 34.79	51.86 5.43	5.32 23.24	32.08 35.25	.75 .87	.34 .42	nd nd	98.36 100	192.....Tetradymite
7.86 34.89	51.14 5.4	5.16 22.95	31.74 35.47	.8 .93	.28 .36	nd nd	96.98 100	198.....Tetradymite
7.87 34.98	51.95 5.34	5.24 22.98	32.13 35.43	.78 .9	.29 .37	nd nd	98.25 100	204.....Tetradymite
7.93 35.16	52.18 5.39	5.2 22.84	32.1 35.42	.81 .94	.2 .26	nd nd	98.43 100	210.....Tetradymite
7.91 35.2	51.93 5.41	5.12 22.64	31.95 35.47	.72 .84	.35 .45	nd nd	97.99 100	216.....Tetradymite
7.64 5.17	51.72 5.24	5.12 22.67	31.89 35.52	.78 .91	.31 .4	.07 .09	97.53 100	222.....Tetradymite
7.87 34.6	51.16 5.37	5.25 23.13	32.01 35.45	.82 .95	.39 .49	tr tr	97.5 100	228.....Tetradymite
7.82 34.74	51.31 5.34	5.26 23.2	31.86 35.33	.75 .87	.38 .48	tr tr	97.4 100	234.....Tetradymite
7.68 35.14	51.8 5.26	5.12 22.63	32.1 35.66	.76 .88	.31 .39	.04 .05	97.8 100	240.....Tetradymite
7.87 34.16	50.15 5.41	5.22 23.19	32.17 35.88	.78 .91	.36 .45	nd nd	96.55 100	246.....Tetradymite
7.98 34.79	51.24 5.46	5.2 23.01	31.86 35.43	.77 .9	.31 .39	tr tr	97.38 100	252.....Tetradymite

Table A4.3 Continued

Pb	Bi	S	Te	Sb	Cd	Ag	Total Distance (μm)	Mineral
7.6 34.8	51.17 5.21	5.19 23	32.06 35.72	.76 .89	.3 .38	nd nd	97.08 100	258.....Tetradymite
8.08 34.3	50.8 5.5	5.33 23.45	32.13 35.53	.74 .86	.29 .36	nd nd	97.38 100	264.....Tetradymite
7.81 34.56	51.73 5.26	5.34 23.27	32.39 35.44	.74 .85	.47 .58	.03 .04	98.51 100	270.....Tetradymite
7.5 35.11	51.68 5.14	5.09 22.55	32.14 35.76	.84 .98	.36 .46	nd nd	97.62 100	276.....Tetradymite
8.11 34.62	51.12 5.54	5.18 22.86	32.14 35.65	.77 .9	.32 .4	tr .03	97.66 100	282.....Tetradymite
7.72 34.74	51.57 5.25	5.25 23.07	32.3 35.64	.76 .87	.34 .43	nd nd	97.94 100	288.....Tetradymite
7.92 34.01	49.81 5.45	5.18 23.06	32.13 35.93	.73 .86	.49 .62	.05 .06	96.31 100	294.....Tetradymite
7.96 34.43	50.72 5.45	5.19 22.95	32.42 36.05	.7 .81	.24 .3	nd nd	97.22 100	300.....Tetradymite
4.38 37.32	48.75 3.38	1.26 6.27	41.05 51.47	.72 .95	.37 .53	.05 .07	96.59 100	306.....Tetradymite
nd 38.58	49.13 nd	nd nd	46.62 59.96	.74 1	.32 .46	nd nd	96.81 100	312.....Tellurbismuth

Table A4.4 Scan 3, line concentration profile across a tellurbismuth-galena intergrowth (Sample No. JN 13).

Pb	Bi	S	Te	Sb	Cd	Ag	Total	Distance (μm)	Mineral
.38	49.48	tr	46.57	.8	.41	.18	97.81		
.29	38.47	.03	59.29	1.06	.59	.27	100	6	Tellurbismuth
nd	50.15	.04	47.06	.71	.28	.04	98.27		
nd	38.79	.18	59.63	.94	.4	.06	100	12	Tellurbismuth
nd	49.86	nd	46.81	.67	.48	nd	97.82		
nd	38.77	tr	59.62	.9	.7	nd	100	18	Tellurbismuth
nd	49.46	nd	46.82	.78	.31	tr	97.37		
nd	38.62	nd	59.87	1.04	.45	tr	100	24	Tellurbismuth
nd	50.57	nd	46.65	.73	.34	tr	98.31		
nd	39.24	nd	59.27	.97	.5	tr	100	30	Tellurbismuth
85.63	.8	13.29	nd	tr	.05	nd	99.79		
49.65	.46	49.82	nd	tr	.05	nd	100	36	Galena
nd	50.7	tr	46.88	.79	.3	tr	98.69		
nd	39.16	.04	59.3	1.04	.44	.03	100	42	Tellurbismuth
nd	49.66	tr	46.85	.8	.32	nd	97.64		
nd	38.67	.03	59.76	1.07	.46	nd	100	48	Tellurbismuth
nd	49.79	nd	47.26	.84	.29	.06	98.25		
nd	38.51	nd	59.86	1.12	.42	.09	100	54	Tellurbismuth
nd	50.34	.04	46.4	.79	.32	nd	97.88		
nd	39.17	.19	59.13	1.06	.46	nd	100	60	Tellurbismuth
nd	49.04	.04	46.58	.81	.27	tr	96.74		
nd	38.47	.19	59.84	1.09	.39	tr	100	66	Tellurbismuth
nd	50.71	tr	47.31	.77	.38	.04	99.21		
nd	38.9	.06	59.44	1.01	.54	.05	100	72	Tellurbismuth
nd	49.89	.03	46.76	.75	.47	tr	97.9		
nd	38.73	.13	59.45	1	.68	tr	100	78	Tellurbismuth
nd	48.6	.03	47.22	.8	.34	.04	97.02		
nd	37.9	.16	60.32	1.07	.5	.05	100	84	Tellurbismuth
85.54	1.01	13.23	.51	.06	.12	.05	73.52		
40.02	.69	58.44	.56	.07	.15	.06	100	90	Galena
84.43	1.04	13.47	.35	nd	.09	.08	99.46		
48.69	.59	50.2	.33	nd	.09	.09	100	96	Galena
nd	50.04	nd	46.66	.8	.24	tr	97.76		
nd	39	nd	59.56	1.07	.35	tr	100	102	Tellurbismuth
nd	50.6	nd	46.02	.78	.36	nd	97.77		
nd	39.54	nd	58.89	1.05	.52	nd	100	108	Tellurbismuth
nd	50.71	nd	47	.89	.25	nd	98.85		
nd	39.11	nd	59.36	1.18	.35	nd	100	114	Tellurbismuth
nd	50.04	nd	47.03	.85	.4	nd	98.32		
nd	38.71	nd	59.59	1.13	.57	nd	100	120	Tellurbismuth

Table A4.3 Continued

Pb	Bi	S	Te	Sb	Cd	Ag	Total Distance (μm)	Mineral
nd	50.16	nd	46.37	.81	.36	.04	97.75	
nd	39.11	nd	59.22	1.09	.52	.07	100	126.....Tellurbismuth
85.23	1.12	13.34	nd	.1	.03	.14	99.95	
49.26	.64	49.82	nd	.1	.03	.16	100	132.....Galena
85.71	.95	13.4	.36	.06	nd	nd	100.48	
49.28	.54	49.78	.34	.06	nd	nd	100	138.....Galena
nd	50.28	nd	46.49	.84	.34	.03	97.98	
nd	39.11	nd	59.23	1.12	.49	.05	100	144.....Tellurbismuth
85.67	.85	13.19	nd	.09	.03	tr	99.84	
49.81	.49	49.55	nd	.09	.03	tr	100	150.....Galena
85.85	.97	13.23	nd	.04	.14	nd	100.25	
49.71	.56	49.53	nd	.04	.15	nd	100	156.....Galena
nd	50.07	nd	46.83	.74	.41	.07	98.12	
nd	38.83	nd	59.48	.99	.6	.11	100	162.....Tellurbismuth
nd	50.15	nd	46.35	.73	.36	.06	97.64	
nd	39.14	tr	59.25	.98	.53	.08	100	168.....Tellurbismuth
.06	50.21	nd	46.1	.71	.23	tr	97.32	
.05	39.4	nd	59.25	.96	.33	tr	100	174.....Tellurbismuth
nd	49.71	nd	46.66	.66	.51	.04	97.58	
nd	38.75	nd	59.57	.88	.74	.06	100	180.....Tellurbismuth

Table A4.4 Scan 4, line concentration profile across a tellurbismuth-galena-tetradymite intergrowth (Sample No. JN 13).

Pb	Bi	S	Te	Sb	Cd	Ag	Total	Distance (μm)	Mineral
nd	51.81	nd	43.7	.7	.28	nd	96.49		
nd	41.41	nd	57.21	.96	.42	nd	100	7	Tellurbismuth
nd	51.95	nd	46.44	.68	.37	.11	99.55		
nd	39.94	nd	58.48	.9	.53	.16	100	14	Tellurbismuth
nd	50.45	tr	46.92	.71	.39	tr	98.51		
nd	39	.06	59.41	.95	.56	tr	100	21	Tellurbismuth
nd	50.99	tr	46.53	.77	.49	nd	98.79		
nd	39.38	.04	58.86	1.02	.7	nd	100	28	Tellurbismuth
nd	50.26	nd	46.67	.69	.41	nd	98.03		
nd	39.07	nd	59.42	.92	.6	nd	100	35	Tellurbismuth
nd	50.39	nd	46.82	.67	.4	nd	98.27		
nd	39.07	nd	59.46	.89	.58	nd	100	42	Tellurbismuth
7.82	52.29	5.29	31.93	.73	.55	.03	98.64		
5.28	35.03	23.09	35.03	.84	.69	.03	100	56	Tetradymite
8.19	52.61	5.41	31.77	.72	.23	nd	98.93		
5.51	35.11	23.54	34.73	.83	.28	nd	100	63	Tetradymite
7.54	51.56	5.12	32.23	.74	.41	nd	97.6		
5.16	34.98	22.66	35.82	.86	.51	nd	100	70	Tetradymite
8.15	51.26	5.26	31.75	.72	.31	tr	97.47		
5.57	34.72	23.24	35.23	.84	.39	tr	100	77	Tetradymite
8.42	52.39	5.34	31.93	.7	.29	nd	99.08		
5.67	34.98	23.26	34.93	.81	.36	nd	100	84	Tetradymite
8.29	52.11	5.35	32.23	.75	.25	nd	98.97		
5.58	34.77	23.25	35.22	.86	.32	nd	100	91	Tetradymite
9.97	49.69	5.08	30.16	.72	.29	nd	95.92		
6.98	34.5	23	34.29	.86	.37	nd	100	98	Tetradymite
8.34	50.95	5.25	31.94	.72	.57	nd	97.76		
5.68	34.38	23.08	35.3	.84	.72	nd	100	105	Tetradymite
8.39	52.73	5.32	31.78	.73	.28	.05	99.29		
5.65	35.2	23.16	34.75	.83	.34	.07	100	112	Tetradymite
8.86	51.94	5.35	31.85	.75	.31	nd	99.06		
5.96	34.68	23.28	34.83	.86	.39	nd	100	119	Tetradymite
9.15	52.34	5.48	32.14	.69	.32	nd	100.13		
6.08	34.5	23.55	34.7	.79	.39	nd	100	126	Tetradymite
8.58	52.38	5.34	32.7	.71	.21	tr	99.95		
5.73	34.67	23.06	35.45	.81	.26	tr	100	133	Tetradymite
8.54	51.93	5.29	32.3	.71	.35	nd	99.12		
5.75	34.67	23.03	35.31	.81	.43	nd	100	140	Tetradymite
8.58	51.77	5.29	32.36	.71	.39	nd	99.11		
5.78	34.55	23	35.37	.81	.49	nd	100	147	Tetradymite

Table A4.4 Continued

Pb	Bi	S	Te	Sb	Cd	Ag	Total Distance (μm)	Mineral
8.57	51.61	5.42	31.73	.65	.38	nd	98.36	
5.79	34.55	23.64	34.79	.75	.47	nd	100	154.....Tetradymite
10.33	51.18	5.56	31.3	.67	.34	tr	99.39	
6.9	33.91	24.03	33.96	.76	.41	tr	100	161.....Tetradymite
8.57	51.06	5.41	31.68	.76	.35	.04	97.87	
5.8	34.29	23.69	34.85	.87	.44	.06	100	168.....Tetradymite
8.22	52.13	5.17	31.54	.79	.22	.05	98.12	
5.61	35.31	22.84	34.98	.92	.28	.06	100	175.....Tetradymite
85.9	.68	13.68	nd	.1	.05	nd	100.41	
49.01	.39	50.46	nd	.1	.05	nd	100	182.....Galena
nd	50.01	nd	47.12	.7	.34	nd	98.18	
nd	38.76	nd	59.81	.94	.49	nd	100	189.....Tellurbismuth
85.57	.81	13.17	nd	.05	.24	nd	99.83	
49.75	.46	49.49	nd	.05	.26	nd	100	196.....Galena
85.84	.71	13.46	nd	nd	.12	nd	100.13	
49.41	.41	50.06	nd	nd	.13	nd	100	203.....Galena
85.51	.75	13.6	.32	.09	tr	nd	100.29	
48.91	.43	50.26	.3	.09	tr	nd	100	210.....Galena
85.07	.84	13.41	.24	.11	.16	nd	99.83	
49.05	.48	49.97	.22	.11	.17	nd	100	217.....Galena
nd	50.14	tr	46.2	.78	.21	tr	97.36	
nd	39.27	.08	59.26	1.05	.31	.03	100	224.....Tellurbismuth
nd	50.58	nd	47	.8	.34	tr	98.72	
nd	39.04	nd	59.4	1.06	.49	tr	100	231.....Tellurbismuth
nd	49.48	nd	47.24	.73	.42	nd	97.88	
nd	38.39	nd	60.03	.98	.61	nd	100	238.....Tellurbismuth

Table A4.5 Random spot analyses of Tellurbismuth from a telluride concentrate (Sample No. JN 13)

Pb	Bi	S	Te	Sb	Cd	Ag	Total
nd	50.71	tr	47.31	.77	.38	.04	99.22
nd	38.9	.06	59.44	1.01	.54	.05	100
nd	50.26	nd	46.67	.69	.41	nd	98.03
nd	39.07	nd	59.42	.92	.6	nd	100.01
nd	49.71	nd	46.66	.66	.51	.04	97.58
nd	38.75	nd	59.57	.88	.74	.06	100
nd	50.15	nd	46.35	.73	.36	.06	97.65
nd	39.15	tr	59.25	.98	.53	.08	100.01
nd	51.95	nd	46.44	.68	.37	.11	99.55
nd	39.94	nd	58.48	.9	.53	.16	100.01
nd	49.48	nd	47.24	.73	.42	nd	97.87
nd	38.39	nd	60.03	.98	.61	nd	100.01
1.05 .83	48.61 37.84	tr .09	46.17 58.87	.8 1.07	.44 .64	.45 .67	97.54 100.01
nd	50.7	tr	46.88	.79	.3	tr	98.7
nd	39.16	.04	59.3	1.04	.44	.03	100.01
nd	50.6	nd	46.02	.78	.36	nd	97.76
nd	39.54	nd	58.89	1.05	.52	nd	100
1.54 1.21	48.52 37.87	nd tr	45.84 58.59	.81 1.09	.37 .54	.45 .68	97.53 100
.69 .54	48.55 38.13	nd nd	46.09 59.27	.74 1	.32 .47	.39 .59	96.78 100
nd	49.79	nd	47.26	.84	.29	.06	98.24
nd	38.51	nd	59.86	1.12	.42	.09	100
nd	50.04	nd	46.66	.8	.24	tr	97.75
nd	39	nd	59.56	1.07	.36	tr	100.01
nd	49.04	.04	46.58	.81	.27	tr	96.75
nd	38.47	.19	59.84	1.09	.39	tr	100
.82 .65	48.56 38.1	nd tr	45.97 59.07	.75 1.01	.48 .69	.3 .45	96.88 99.99
nd	49.72	nd	47.01	.69	.29	tr	97.73
nd	38.7	nd	59.93	.92	.41	.03	99.99
6.53 5.09	43.8 33.88	tr .08	45.9 58.15	.82 1.09	.36 .52	.79 1.18	98.22 99.99
2.01 1.57	47.81 36.97	nd tr	46.53 58.93	.73 .97	.33 .47	.71 1.07	98.12 100
nd	49.89	.03	46.76	.75	.47	tr	97.91
nd	38.73	.13	59.45	1	.68	tr	100
.91 .71	48.95 38.09	nd nd	46.37 59.1	.67 .89	.37 .54	.44 .66	97.71 99.99

Table A4.5 Continued

Pb	Bi	S	Te	Sb	Cd	Ag	Total
nd	49.09	nd	46.2	.71	.23	.12	96.35
nd	38.76	nd	59.76	.96	.33	.19	100
.69	48.53	nd	46.82	.65	.21	.17	97.07
.55	37.99	tr	60.02	.87	.3	.26	100.01
nd	50.07	nd	46.83	.74	.41	.07	98.12
nd	38.83	nd	59.48	.99	.6	.11	100.01
1.94	46.79	.08	44.45	.71	.34	.53	94.84
1.56	37.45	.43	58.26	.98	.5	.81	99.99
nd	50.99	tr	46.53	.77	.49	nd	98.79
nd	39.38	.04	58.86	1.02	.7	nd	100
nd	50.16	nd	46.37	.81	.36	.04	97.74
nd	39.11	nd	59.22	1.09	.52	.07	100.01
nd	50.56	nd	46.74	.76	.45	nd	98.51
nd	39.12	nd	59.23	1	.65	nd	100
nd	49.66	tr	46.85	.8	.32	nd	97.64
nd	38.67	.03	59.76	1.07	.46	nd	99.99
nd	49.26	nd	47	.84	.36	nd	97.46
nd	38.38	nd	59.97	1.12	.52	nd	99.99
nd	50.45	tr	46.92	.71	.39	tr	98.49
nd	39	.06	59.41	.95	.56	tr	99.99
.38	49.48	tr	46.57	.8	.41	.18	97.83
.29	38.47	.03	59.29	1.06	.59	.27	100
.8	48	nd	46.34	.67	.3	.34	96.45
.64	37.77	nd	59.73	.9	.44	.52	100
nd	48.23	nd	46.08	.73	.37	nd	95.41
nd	38.38	nd	60.07	1	.55	nd	100
nd	49.72	nd	47.01	.69	.29	tr	97.73
nd	38.7	nd	59.93	.92	.41	.03	99.99
nd	48.11	.03	45.26	.69	.43	nd	94.52
nd	38.67	.15	59.59	.95	.64	nd	100
.74	48.95	nd	46.03	.64	.33	.45	97.14
.59	38.34	tr	59.04	.86	.48	.68	100.00
1.95	47.44	tr	45.78	.69	.26	.56	96.69
1.54	37.3	.04	58.96	.93	.37	.85	99.99
nd	50.04	nd	47.03	.85	.4	nd	98.32
nd	38.71	nd	59.59	1.13	.57	nd	100
.75	49.04	nd	46.47	.77	.39	.43	97.85
.59	38.08	nd	59.1	1.02	.56	.65	100
nd	49.86	nd	46.81	.67	.48	nd	97.82
nd	38.77	tr	59.62	.9	.7	nd	100
nd	50.71	nd	47	.89	.25	nd	98.85
nd	39.11	nd	59.36	1.18	.35	nd	100

Table A4.6 Random spot analyses of galena from the sulphide-dominated assemblage.

Pb	Bi	S	Te	Sb	Cd	Ag	Total	Sample No.
nd	51.81	nd	43.7	.7	.28	nd	96.49	
nd	41.41	nd	57.21	.96	.42	nd	100	
82.59	3.3	13.21	nd	.07	.11	.77	100.05	JN 12
86.15	.82	12.48	nd	.09	.06	nd	99.6	JN 12
83.75	1.61	13.12	nd	.1	.19	.38	99.15	JN 12
85.9	.86	12.87	nd	.1	.17	nd	99.9	JN 12
85.74	.68	12.87	nd	.11	nd	nd	99.4	JN 12
86.51	.71	12.88	nd	.08	.09	nd	100.27	JN 12
86.38	.87	12.61	nd	.08	.07	nd	100.01	JN 12
86.94	.7	12.96	nd	.08	.13	nd	100.81	JN 12
85.62	.88	12.78	nd	.1	.1	nd	99.48	JN 12
85.43	.75	12.78	nd	.07	.04	nd	99.07	JN 12
83.25	3.22	12.83	nd	.08	.1	.53	100.01	JN 14
82.34	2.41	13.26	.34	.07	.05	.64	99.11	JN 14
85.95	.8	12.91	nd	.1	.08	nd	99.84	JN 14
85.96	.91	12.77	nd	.05	.12	nd	99.81	JN 14
84.96	.88	12.89	nd	.05	.1	nd	98.88	JN 14
85.79	.79	13.17	nd	.06	.1	nd	99.91	JN 14
85.78	.61	12.82	nd	.1	nd	nd	99.31	JN 14
85.71	.69	12.56	nd	.1	.08	nd	99.14	JN 14
86.05	.8	12.81	nd	.07	.08	nd	99.81	JN 14
86.76	.85	12.79	nd	.09	.04	nd	100.53	JN 14
85.88	.79	12.89	nd	.07	.07	nd	99.7	JN 14
86.76	.73	12.98	nd	.08	.1	nd	100.65	JN 14
85.11	.79	13.02	nd	.07	.09	nd	99.08	JN 14
83.44	13.69	nd	nd	.09	.09	.87	98.18	JN 14
84.47	2.25	13.4	nd	.06	.08	.51	100.77	JN 30
86.7	.65	13.09	.37	.03	nd	nd	100.84	JN 30
86.91	.77	13	.11	.1	.1	nd	100.99	JN 30
86.27	.75	12.82	nd	.06	.06	nd	99.96	JN 30
85.1	.77	12.44	.44	.11	.1	nd	98.96	JN 30
85.35	.85	12.87	nd	.1	.04	nd	99.21	JN 30
85.4	.74	12.76	nd	.06	.11	nd	99.07	JN 30
86.19	.76	12.8	nd	.11	.07	nd	99.93	JN 30
86.86	.69	12.99	nd	.08	.11	nd	100.73	JN 30
86.23	.75	12.86	.47	.08	.11	nd	100.5	JN 30
85.6	.69	12.67	nd	.09	.13	nd	99.18	JN 30
86.17	.79	12.61	nd	.7	.1	nd	100.37	JN 30

Table A4.6 Continued.

Pb	Bi	S	Te	Sb	Cd	Ag	Total	Sample No.
83.08	2.85	13.08	nd	.04	.15	.82	100.02	JN 30
86.02	.71	12.88	nd	.1	.06	nd	99.77	JN 30
85.56	.73	12.92	.32	.09	.04	nd	99.66	JN 31
84.13	2.2	13.25	nd	.08	.07	.58	100.31	JN 31
85.8	.75	13.1	nd	.04	nd	nd	99.69	JN 31
84.46	1.65	13.17	nd	.09	.04	.36	99.77	JN 31
85.48	.82	12.51	nd	.08	.1	nd	98.99	JN 31
85.85	.9	12.9	nd	.09	.3	nd	100.04	JN 31
86.58	.74	12.79	.45	.09	.1	nd	100.75	JN 31
84.86	2.24	13.17	.4	.08	.05	.63	101.43	JN 31
84.76	1.85	13.42	nd	.06	nd	.38	100.47	JN 31
86.08	.78	12.93	.34	.11	.1	nd	100.34	JN 31
84.69	.69	12.72	nd	.04	.11	nd	98.25	JN 32
83.14	2.68	13.37	nd	.07	.18	.97	100.41	JN 32
81.98	2.36	12.94	nd	.11	.2	1.23	98.82	JN 32
85.97	.73	12.8	nd	.11	.06	nd	99.67	JN 32
85.75	.69	12.73	.33	.05	.08	nd	99.63	JN 32
83.96	2.56	13.15	nd	.04	.06	.81	100.58	JN 32
87.31	.83	12.91	nd	.07	.14	nd	101.26	JN 32
84.88	.76	12.98	.4	.08	.05	nd	99.15	JN 32
86.93	.67	12.77	.54	.04	.05	nd	101	JN 32
85.76	.72	12.73	nd	.05	nd	nd	99.26	JN 32
85.78	.71	12.92	nd	.08	.07	nd	99.56	JN 32
85.84	.75	12.9	nd	.05	.05	nd	99.59	JN 32
85.74	.78	13.05	.41	.07	.06	nd	100.11	JN 32
86.05	.84	12.91	nd	.1	.06	nd	99.96	JN 32
85.73	.63	12.7	.34	.11	.05	nd	99.56	JN 32
86.64	.73	12.85	nd	.07	.03	nd	100.32	JN 33
85.73	.85	12.87	.41	.11	.16	nd	100.13	JN 33
83.96	2.62	13.34	nd	.07	.06	.74	100.79	JN 33
86.09	12.93	nd	nd	.09	.08	nd	99.19	JN 33
85.82	.87	12.8	nd	.11	.07	nd	99.67	JN 33
84.69	2.68	13.54	nd	.05	.06	.66	101.68	JN 33
86.19	.7	12.71	nd	.06	.04	nd	99.7	JN 33
86.72	.82	12.76	nd	.09	.09	nd	100.48	JN 33
83.87	2.58	13.39	nd	.06	nd	.58	100.48	JN 33
85.34	.89	12.88	nd	.06	.09	nd	99.26	JN 33
85.32	.78	12.25	.34	.06	.1	nd	98.85	JN 33

Table A4.6 Continued.

Pb	Bi	S	Te	Sb	Cd	Ag	Total	Sample No.
85.74	.68	12.98	nd	.06	.03	nd	99.49	JN 33
85.94	.89	12.84	nd	.07	.04	nd	99.78	JN 33
82.6	2.75	13.01	nd	.12	.3	.7	99.48	JN 34
86.1	.8	12.65	nd	.12	.04	nd	99.71	JN 34
85.43	.83	13.22	nd	.04	.14	nd	99.66	JN 34
84.67	.68	12.88	nd	.1	.07	nd	98.4	JN 34
85.31	.74	12.8	nd	.09	.05	nd	98.99	JN 34
84.77	.85	12.87	.37	.06	.08	nd	99	JN 34
83.25	2.69	13.37	nd	.07	.18	.97	100.53	JN 34
85.67	2.3	13.5	nd	.1	.06	.45	102.08	JN 34
84.73	.85	12.96	nd	.07	.03	nd	98.64	JN 34
85.06	.63	12.73	.43	.09	.04	nd	98.98	JN 34
86.07	.86	12.68	nd	.07	.06	nd	99.74	JN 34
81.72	2.66	13.16	.42	.09	.21	1.28	99.54	JN 34
83.57	2.86	13.46	nd	.06	.14	.77	100.86	JN 35
86.21	.8	12.71	nd	.08	tr	nd	99.82	JN 35
86.56	.91	12.81	.45	.1	.05	nd	100.88	JN 35
86.22	.77	12.74	nd	.09	.07	nd	99.89	JN 35
87.03	.9	12.9	nd	.09	.09	nd	101.01	JN 35
85.19	.84	12.66	.38	.07	.05	nd	99.19	JN 35
2.45	77.86	6.92	nd	.14	.45	9.52	97.34	JN 35
86.48	.82	12.82	nd	.08	nd	nd	100.2	JN 35
85.86	.82	12.62	nd	.04	.07	nd	99.41	JN 35
85.44	.82	12.88	nd	.13	.04	nd	99.31	JN 35
4.09	nd	.69	nd	nd	nd	nd	4.78	JN 41
85.09	.72	12.88	nd	.07	.06	nd	98.82	JN 41
85.7	.69	12.87	nd	.1	.07	nd	99.43	JN 41
85	.71	12.73	nd	.12	.1	nd	98.66	JN 41
87.39	.77	12.79	nd	.07	.1	nd	101.12	JN 41
84.06	2.58	13.14	nd	.1	nd	.76	100.64	JN 41
83.57	2.51	13.45	nd	.09	.08	.69	100.39	JN 41
85.19	.82	12.52	nd	.08	.07	nd	98.68	JN 41
85.94	.78	12.86	nd	.06	.07	nd	99.71	JN 41
85.1	.81	13.09	.34	.08	.12	nd	99.54	JN 41
86.48	.8	12.77	nd	.04	.08	nd	100.17	JN 41
85.3	.8	12.94	.34	.09	.09	nd	99.56	JN 41
85.02	.82	12.91	nd	.08	.1	nd	98.93	JN 41
85.39	.79	12.53	.34	.1	nd	nd	99.15	JN 41

Table A4.6 Continued.

Pb	Bi	S	Te	Sb	Cd	Ag	Total	Sample No.
85.81	.69	12.92	.35	.08	.06	nd	99.91	JN 6
85.95	.79	12.69	nd	.09	.05	nd	99.57	JN 6
85.05	.82	12.61	nd	.08	.07	nd	98.63	JN 6
83.5	2.32	13.12	nd	.08	.11	.62	99.75	JN 6
82.82	3.01	13.15	.37	.09	.09	.86	100.39	JN 6
85.59	.78	12.91	nd	.07	.03	nd	99.38	JN 6
85.99	.09	12.93	nd	.08	.17	nd	99.25	JN 6
86.98	.9	12.81	nd	.07	.05	nd	100.81	JN 6
86.27	.76	12.94	nd	.06	.05	nd	100.08	JN 6
85.77	.83	13.07	nd	.1	.06	nd	99.83	JN 6
86.35	.76	12.73	nd	.1	.09	nd	100.03	JN 6
87.1	.82	13	nd	.07	.12	nd	101.11	JN 6
83.6	3.14	13.67	nd	.05	.05	.93	101.44	JN 6
84.9	.8	12.97	nd	.07	.08	nd	98.82	K3
86.25	.8	12.74	nd	.08	.09	nd	99.96	K3
84.02	2.27	12.99	nd	.11	.03	.57	99.99	K3
85.6	.8	12.62	nd	.07	tr	nd	99.11	K3
85.6	.79	12.73	nd	.13	nd	nd	99.25	K3
85.79	.72	12.77	.44	.09	.03	nd	99.84	K3
84.66	.81	12.89	nd	.07	.08	nd	98.51	K3

Table A4.7 Analyses of mill concentrate gold form No. 4 Level (Sample Nos. CMC1 and CMC2).

Au	Hg	Ag	Ir	Cu	Fineness	Total
92.21	nd	5.16	.11	nd	947	97.5
89.1	nd	8.66	.11	nd	911	97.88
90.11	nd	8.45	.14	nd	914	98.7
89.29	nd	8.19	.08	nd	916	97.57
93.09	nd	5.2	.12	nd	947	98.41
94.32	nd	4.89	tr	nd	951	99.26
94.72	nd	4.76	.08	nd	952	99.56
81.64	nd	15.52	nd	nd	840	97.16
86.43	nd	11.28	.06	nd	885	97.77
91.39	nd	6.43	.09	nd	934	97.91
80.24	nd	15.29	nd	nd	840	95.53
90.92	nd	6.94	.06	nd	929	97.93
91.81	nd	6.05	.06	nd	938	97.92
90.16	nd	6.21	.07	nd	936	96.44
92.14	nd	6.05	.11	nd	938	98.31
89.93	nd	6.75	tr	nd	930	96.7
81.2	nd	15.82	.3	nd	837	97.32
87.37	nd	10.83	.21	nd	890	98.41
81.65	nd	16.23	.29	nd	834	98.17
82.95	nd	15.02	.26	nd	847	98.23
93.78	nd	5.37	.3	nd	946	99.52
93.28	nd	5.27	.38	nd	946	98.93
90.66	nd	7.41	.25	nd	924	98.32
91.02	nd	7.62	.22	nd	923	98.86
92.35	nd	6.74	.35	nd	932	99.44
92.03	nd	6.87	.26	nd	931	99.18
92.65	nd	5.9	.33	nd	940	98.89
94.17	nd	5.17	.31	nd	948	99.67
80.35	nd	15.38	.2	nd	839	95.93
93.88	nd	5.38	.2	nd	946	99.49
93.01	nd	5.18	.32	nd	947	98.51
92.15	nd	6.49	.34	nd	934	99.08
91.97	nd	7.24	.32	nd	927	99.57
91.43	nd	6.37	.31	nd	935	98.14
94.69	nd	3.49	.35	nd	964	98.53
92.08	nd	6.28	.31	nd	936	98.67
91.59	nd	6.47	.32	nd	934	98.38

Table A4.7 Continued.

Au	Hg	Ag	Ir	Cu	Fineness	Total
93.05	nd	6.61	.37	nd	934	100.1
92.35	nd	6.73	.28	nd	932	99.36
93.16	nd	6.08	.27	nd	939	99.51
92.15	nd	6.5	.3	nd	934	98.95
92.18	nd	6.5	.37	nd	934	99.05
93.8	nd	5.13	.36	nd	948	99.33
95.44	nd	4.84	.34	nd	952	100.62
94.11	nd	4.94	.28	nd	950	99.37
91.23	nd	8.23	.3	nd	917	99.76
93.61	nd	5.69	.27	nd	943	99.59
94.25	nd	5.32	.23	nd	947	99.9
92.94	nd	5.98	.29	nd	940	99.21
92.52	nd	5.97	.38	nd	939	98.87
93.3	nd	5.83	.34	nd	941	99.51
93.2	nd	5.78	.29	nd	942	99.27
89.75	nd	7.35	.13	nd	924	97.33
93.24	nd	4.51	.13	nd	954	97.97
91.38	nd	4.95	.15	nd	949	96.49
92.98	nd	3.86	.14	nd	960	96.98
93.25	nd	4.72	.17	nd	952	98.19
90.05	nd	6.46	.13	nd	933	96.68
92.59	nd	5	.09	nd	949	97.7
96.35	nd	3.16	.17	nd	968	99.68
95.53	nd	3.06	.22	nd	969	98.81
92.59	nd	5.92	.13	nd	940	98.69
93.47	nd	4.8	.2	nd	951	98.51
92.51	nd	5.07	.31	nd	948	97.93
93.35	nd	4.6	.13	nd	953	98.16
89.54	nd	7.14	.15	nd	926	96.84
91.35	nd	6.19	.16	nd	937	97.7
92.24	nd	5.88	.22	nd	940	98.34
81.44	nd	15.17	.08	nd	843	96.69
80.68	nd	15.3	.06	nd	841	96.04
93.64	nd	4.22	.23	nd	957	98.1
90.59	nd	5.95	.19	nd	938	96.73
79.46	nd	15.04	.14	nd	841	94.66
78.99	nd	17.04	.15	nd	823	96.18
90.14	nd	5.6	.19	nd	942	95.93

Table A4.7 Continued.

Au	Hg	Ag	Ir	Cu	Fineness	Total
90.75	nd	6.2	.23	nd	936	97.18
91.81	nd	5.24	.22	nd	946	97.31
90.41	nd	4.81	.19	nd	950	95.41
90.54	nd	5.96	.2	nd	938	96.7
92.07	nd	5.74	.18	.43	941	98.48
96.11	nd	3.45	.2	nd	965	99.82
93.47	nd	4.87	.12	nd	950	98.49
86.16	nd	10.18	.18	nd	894	96.52
93.78	nd	5.53	.15	nd	944	99.53
93.49	nd	3.68	.25	nd	962	97.42
91.94	nd	6.19	.04	nd	937	98.17
93.77	nd	4.87	.12	nd	951	98.77
91.34	nd	6.28	.16	nd	936	97.78
92.19	nd	6.17	.14	nd	937	98.5
92.95	nd	5.92	.23	nd	940	99.18
92.42	nd	5.92	.16	nd	940	98.5
91.65	nd	6.3	.14	nd	936	98.09
93.61	nd	5.01	.12	.44	949	99.2
90.27	nd	7.35	.04	.49	925	98.15
92.27	nd	5.57	.12	nd	943	97.96
93.72	nd	5.32	.23	nd	946	99.27
93.28	nd	4.86	.11	nd	950	98.25
94.24	nd	4.96	.23	nd	950	99.5
92.42	nd	5.57	.23	nd	943	98.25
91.7	nd	6.28	.04	nd	936	98.02

Table A4.8 Analyses of placer gold from the Hirgwm river (Sample No. JN 36)

Au	Hg	Ag	Ir	wt %	Fineness
94.13	nd	3.79	.2	97.93	961
94.4	nd	3.9	.08	98.3	960
89.5	nd	8.55	nd	98.06	913
85.98	nd	12.21	nd	98.19	876
91.85	nd	7.06	nd	98.92	929
90.84	nd	7.06	.06	97.9	928
90.7	nd	7.21	nd	97.9	926
89.61	nd	8.86	nd	98.47	910
89.21	nd	9	nd	98.21	908
92.28	nd	5.77	.09	98.05	941
88.06	nd	10.37	.05	98.43	895
91.53	nd	6	nd	97.54	938
92.27	nd	5.71	.06	97.97	942
86.5	nd	11.71	nd	98.22	881
85.13	nd	10.54	nd	95.67	890
88.75	nd	9.16	.03	97.91	906
93.44	nd	5.45	tr	98.9	945
93.46	nd	5.31	.09	98.77	946
92.8	nd	6.53	nd	99.33	934
90.91	nd	5.16	nd	96.07	946
90.07	nd	8.84	nd	98.91	911
90.01	nd	8.71	nd	98.72	912
95.13	nd	3.89	tr	99.02	961
82.11	nd	15.51	tr	97.61	841
91.09	nd	5.43	.04	96.52	944
93.38	nd	5.12	.06	98.5	948
95.01	nd	3.17	.04	98.18	968
72.34	20.64	4.25	nd	76.59	944
89.77	nd	8.12	nd	97.89	917
76.92	4.6	2.96	nd	79.88	963
88.24	nd	8.44	.1	96.68	913
76.52	5.05	1.04	nd	77.56	987
92.31	nd	5.65	nd	97.96	942
39.1	14.06	2.07	nd	41.17	950
92.83	nd	5.32	.05	98.15	946
93.91	nd	5.08	.03	98.99	949
96.72	nd	2.4	.08	99.12	976
77.1	19.7	2.53	nd	79.63	968

Table A4.8 Continued.

Au	Hg	Ag	Ir	wt %	Fineness
88.03	nd	11.19	nd	99.22	887
85.32	nd	10.85	tr	96.17	887
88.69	nd	9.33	.06	98.03	905
82.14	nd	15.28	nd	97.42	843
60.17	2.6	33.06	nd	93.23	645
89.3	nd	6.45	.05	95.74	933
89.1	nd	8.17	.03	97.27	916
95.15	nd	3.56	.04	98.71	964
95.86	nd	3.2	.06	99.06	968
65.92	25.52	3.2	nd	69.12	954
81.18	nd	16.36	nd	97.54	832
89.93	nd	8.75	.04	98.68	911
91.03	nd	7.5	tr	98.53	924
94.61	nd	4.56	.04	99.16	954
89.81	nd	8	tr	97.81	918

APPENDIX 5.

SOUTHERN UPLANDS PLACER GOLD DATA.

Table A5.1 Analytical data for the Southern Uplands placer gold. The sample number refers to the pan concentrate number in the two Mineral Reconnaissance reports for the Loch Doon-Glenkens and Abington-Biggar-Moffat areas by Dawson *et al.* (1977) and Dawson *et al.* (1979). The initials HET in the core fineness column refer to placer gold grains that are heterogeneous.

Sample Number	Morphological Characteristics	S.E.M Fineness	Core Fineness	Grid ref. (X)	Grid ref. (Y)
11a	2 4 9 11 •	994	•	6069	7727
11b	4 12 14 • •	994	•	6069	7727
11c	7 10 18 • •	933	•	6069	7727
16	11 3 7 • •	949	•	5989	7936
18	4 18 • • •	996	HET	5909	7915
21a	4 5 11 • •	927	886	5823	7930
21b	6 3 11 • •	939	886	5823	7930
22	13 14 4 • •	992	HET	5814	7870
27a	4 3 11 16 •	995	992	5880	7760
27b	4 3 16 • •	984	913	5880	7760
35	1 2 9 • •	785	HET	5624	8063
37a	4 10 14 • •	922	864	5677	8080
37b	4 11 • • •	947	690	5677	8080
48	4 14 10 • •	992	882	5989	7774
51	3 11 • • •	972	922	5616	8415
73	4 14 18 • •	968	882	5327	8577
83	3 18 10 • •	996	969	5254	8723
95	1 9 8 • •	1000	969	4850	8583
108	4 14 • • •	993	870	5284	9147
111	3 9 11 • •	998	988	5012	9018
132	3 4 11 12 •	972	937	5465	10095
136	5 16 • • •	982	910	6088	9418
138	1 7 14 • •	820	785	6235	9911
139	4 13 11 • •	852	511	6268	9830
140	1 2 4 9 •	987	910	6125	9747
141a	4 5 12 14 15	995	•	6108	9816
141b	7 14 15 • •	980	937	6108	9816
143	7 13 • • •	967	•	6131	9719
146	2 4 11 • •	943	909	6061	9554
157	12 4 • • •	759	903	5917	10069
158	6 14 15 • •	998	•	5958	9993
159	7 9 18 • •	989	976	6059	10002

Table A5.1 Continued.

Sample Number	Morphological Characteristics	S.E.M Fineness	Core Fineness	Grid ref. (X)	Grid ref. (Y)
163	1 3 9 • •	975	800	6137	10105
176	2 11 • • •	1000	990	5010	10425
178	8 15 18 • •	1000	988	5214	9688
199	3 6 10 11 •	963	893	4735	9540
276	7 15 18 • •	994	•	4022	8825
300	8 16 • • •	982	922	3986	8086
301	7 14 • • •	968	•	4032	8092
317	6 14 • • •	996	976	4181	7620
324	2 3 9 • •	885	726	4156	7733
340	6 14 18 • •	983	•	3820	7359
345	• • • • •	964	864	4820	7339
349	4 11 14 • •	979	894	3769	7491
365	• • • • •	777	799	4423	7565
415a	6 11 • • •	998	987	12041	2349
415b	18 • • • •	988	954	12041	2349
415c	5 6 14 • •	985	•	12041	2349
415d	3 6 9 14 15	1000	•	12041	2349
415e	6 3 13 • •	989	976	12041	2349
415f	7 13 • • •	999	987	12041	2349
415g	• • • • •	964	945	12041	2349
415h	• • • • •	977	•	12041	2349
415i	7 14 15 • •	982	967	12041	2349
415j	6 14 15 • •	998	•	12041	2349
415k	• • • • •	996	•	12041	2349
421	4 5 9 11 •	977	854	11828	1821
430	4 11 • • •	996	•	10818	1124
433	4 11 • • •	991	•	•	•
435a	8 14 15 • •	987	•	10843	994
435b	8 14 15 • •	1000	1000	10843	994
444a	8 18 • • •	990	•	9513	2208
444b	8 18 • • •	1000	985	9513	2208
444c	6 14 18 • •	999	904	9513	2208
444d	5 11 • • •	998	962	9513	2208
444e	11 4 • • •	997	964	9513	2208
444f	4 13 • • •	998	•	9513	2208
444h	7 14 15 18 •	997	•	9513	2208

Table A5.1 Continued.

Sample Number	Morphological Characteristics	S.E.M Fineness	Core Fineness	Grid ref. (X)	Grid ref. (Y)
444g	4 11 • • •	1000	1000	9513	2208
444i	6 14 18 • •	1000	995	9513	2208
444j	8 14 15 18 •	996	•	9513	2208
444k	7 14 • • •	1000	1000	9513	2208
426	8 14 18 • •	1000	854	10794	1238
453	4 14 • • •	993	990	10341	1552
455	7 14 • • •	974	•	10062	2174
463	1 9 • • •	987	949	9946	1840
472	4 11 • • •	993	945	10082	2017
475	14 7 • • •	996	892	9927	2066
476	4 11 • • •	979	•	9731	1890
489	7 14 11 • •	996	990	9808	2588
495	3 4 9 • •	993	990	10478	1734
505	8 14 • • •	1000	954	10910	1252
510a	6 13 • • •	1000	925	10533	1629
510b	7 14 • • •	1000	937	10533	1629
515	8 14 15 • •	946	928	10344	1813
535a	6 9 14 15 •	1000	941	10548	2198
535b	6 14 • • •	998	887	10548	2198
537	6 13 • • •	974	906	10578	2270
539	3 11 • • •	1000	999	•	•
540	7 14 • • •	993	923	11135	900
544	4 11 • • •	994	921	10791	1864
545	4 11 • • •	997	•	10830	1846
546a	7 14 • • •	1000	1000	10795	1984
546b	4 11 • • •	997	969	10795	1984
546c	4 11 • • •	986	•	10795	1984
546d	16 14 • • •	992	931	10795	1984
547	11 • • • •	985	•	11028	2046
557	• • • • •	985	•	10084	2710
566	• • • • •	977	923	10207	3091
568	• • • • •	987	•	10387	2690
585a	7 14 18 • •	970	•	9930	2817
585b	7 14 • • •	986	954	9930	2817
585c	7 14 • • •	976	891	9930	2817
588a	4 9 • • •	1000	940	9541	2811

Table A5.1 Continued.

Sample Number	Morphological Characteristics	S.E.M Fineness	Core Fineness	Grid ref. (X)	Grid ref. (Y)
588b	7 14 18 • •	1000	1000	9541	2811
588c	7 18 • • •	1000	1000	9541	2811
591	7 14 18 • •	941	•	11090	2130
596	7 14 18 • •	987	908	11077	2980
600	6 18 • • •	1000	990	10551	2404